Thermodynamics of Turbulence

Boye Ahlborn[1], Frank Curzon[1], Bernd R. Noack[2], Michael Schlegel[2] & Gilead Tadmor[3]

[1]*Department of Physics and Astronomoy, University of British Columbia, Vancouver, Canada*
[2]*Dept. of Fluid Dynamics and Engineering Acoustics, Berlin Institute of Technology, Germany*
[3]*Communications & Digital Signal Proc. Center, Northeastern University, Boston, MA, USA*
ahlborn@phas.ubc.ca

Abstract

Turbulence displays a rich caleidoscope of phenomena reminiscent of a new thermodynamic phase of fluid flows. The kinetic theory of gases inspired, for instance, Prandtl's mixing layer theory for the estimation of the eddy viscosity. Intriguingly, fully developed grid turbulence is experimentally observed to give rise to vortices following a Maxwell-Boltzmann distribution. In addition, the onset of turbulence has features of a phase transition. In this talk, we recapitulate and elaborate the analogy of turbulence as a thermodynamic phase of fluid motion in order to motivate open research questions.

1) Temperatures and energy distributions in thermodynamics

Thermodynamics describes how matter can appear in different phases, like solid, liquid, gaseous, and plasma. Transition from one phase to another occurs when the temperature T is increased and the phase change energy ΔL is introduced. For instance, water turns into steam when the heat of vaporization $L_V = 2257$kJ/kg is added to water at $T = 373\text{K}^\circ$. Temperature is a macroscopic expression of the microscopic random motion of the atoms or molecules (mass m) that fly around and interact by collisions. These random velocities of the molecules can be described in many cases (called thermal equilibrium) by the famous Maxwell-Boltzmann distribution. The random velocities imply a distribution of random kinetic energies, so that a velocity distribution can also be converted into an energy distribution, as illustrated in Fig.1a for two different temperatures.

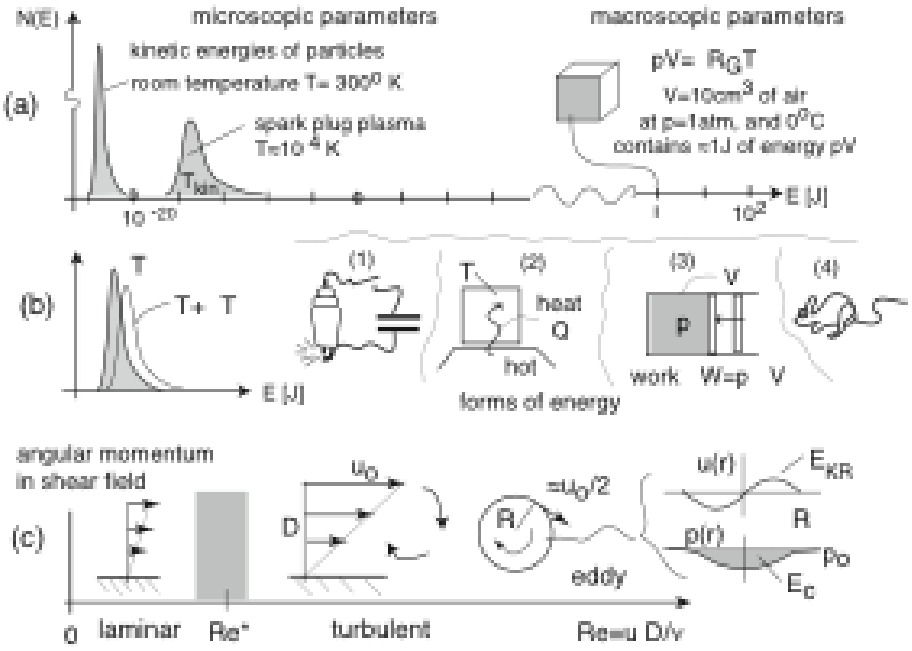

Figure 1: Molecular energy distributions for gases at 2 different temperatures, and thermal energy of air; (b) Temperature change due to (1) input from electrical sparc, (2) heat Q, (3) work W, or (4) eating; (c) Shear fields at $Re < Re^*$ (laminar), and $Re > Re^*$ (turbulent) eddy with rotation induced p.

Generally speaking the temperature T is a measure for the average kinetic energy of the molecules, and T can be increased by some amount ΔT through the input of work ΔW, or by the injection of heat ΔQ, when an object

is brought into thermal contact to a hotter object, as indicated in Fig. 1b. Thus, the temperature is a macroscopic parameter measuring the energy of the microscopic random motion.

2) New internal energies and energy distributions in turbulent fluid — the features of a new phase

Matter in all phases possesses internal energies, U, partly related to the energies of the microscopic molecular motion, and partly hidden as structural energies. In addition, some macroscopic segments of matter of mass m, like a cloud moving through the sky, or water flowing in a river also can have macroscopic velocities $\mathbf{u}(\mathbf{x}, t)$ that give each volume element of mass m the macroscopic kinetic energy $E_K = m\|\mathbf{u}\|^2/2$. For such motion, one must always specify the reference system in which the motion is measured. So, for instance, a glass of water of mass m_W sitting in a train that moves at the speed u_T , carries no kinetic energy for an experiment performed in the train, but will dump the kinetic energy $m_W u_T/2$ onto a spectator seeing the train pass by when the water is tossed out of the window.

In contrast, the internal energy U of a medium does not depend on the reference system in which the matter is observed. When the temperature of a medium is raised by the input of energy, its internal energy increases. There are additional components to the internal energy, namely (a) the *phase change* energy [1], or (b) — of particular concern here — the energies residing in the structures of turbulent flow. These components are neither associated with a change of temperature ΔT , nor the speed of the reference system against which the flow is measured, and must be counted as a part of the internal energy — thus giving individual phases their unique identities.

Laminar flow carries translational kinetic energy, but when the flow turns turbulent at $Re > Re^*$, it acquires eddies which carry two new forms of internal energy: *rotational kinetic energy* , E_{KR}, which resides in every newly formed eddy, and an equal amount of *coherence energy* [2], E_C residing in the pressure defect-volume work of every eddy, see Fig.1c. Both forms of energy are extracted out of the kinetic energy from the parent laminar flow in which the turbulence evolved.

While the translational kinetic energy E_{KT} of the parent laminar flow depends on the velocity $U_{\rm ref}$ of the reference system against which the flow was measured, neither E_{KR} nor E_C is a function of the speed of $U_{\rm ref}$. Therefore $E_{\rm KR}$ and E_C must be counted as part of the internal energy, giving turbulent fluid the distinct *features of a new phase*. Thus, we consider the turbulent "state" as the dynamic phase of fluid motion. However, due to friction, this internal energy leaks gradually into the thermal background and is only temporarily "parked" in the mesoscopic energy range, between the microscopic molecular motion, and the macroscopic pressure - volume work. The macroscopic thermodynamic parameters like p and T have their roots in the microscopic energy distribution of their constituent molecules, e.g. a Maxwell-Boltzmann distribution. We noted many years ago [3] that the "mesoscopic" eddies of turbulence, also possess energy distributions, reminding of a Maxwell-Boltzmann distribution. These results are repeated here, showing the apparatus (Fig. 1a), eddy energy distributions for different distances from the grid, as extracted from photo sequences like Fig. 2c,d. At the grid speed $U = 20$cm/sec, the distance $X = 190$cm corresponds to $\Delta t = 9.5$sec after starting the turbulence. Clearly, the eddies "cool" as they lose energy into the thermal background.

(a)

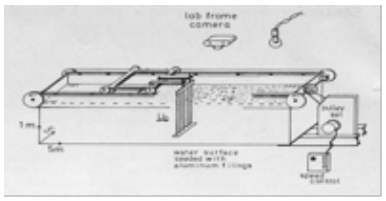

(b)

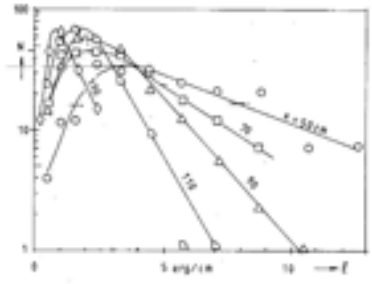

(c,d)

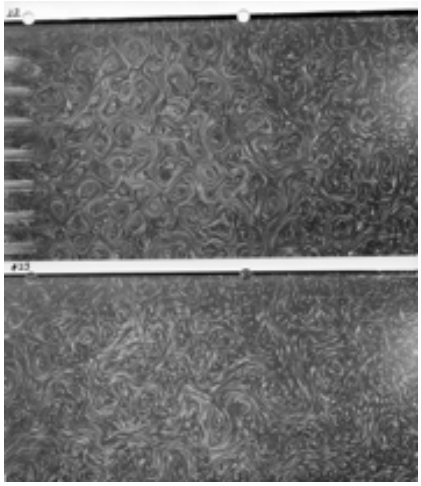

Figure 2 (a) Apparatus Grid bar diameter $d = 1.26$cm, spacing 5.08cm, moving through tank at 20cm/s. (b) Number of eddies of radius R, as function of distance x from the grid. (c) Surface streaks exposure time $\Delta t = 1$sec, and (d) same surface area 3sec later.

The new internal energies in turbulent flow may be broken up into spatial modes of a Galerkin method, generalizing spectral methods [4]. Energy modes, are well known in spectroscopy and thermodynamic, for instance electronic excitation, or angular momentum modes in molecules. Subsequent to the excitation of such modes they revert back to the lower energy state upon the emission of photons, which move some energy out of the system. The Galerkin modes are originally excited by momentum input from the macroscopic range, they interact among themselves via triadic interactions and the eventually loose all heir energy into the thermal background, thereby increasing the entropy of the system.

3) From thermodynamics energies to questions about turbulence

Energy can show up in thermodynamics on very different scales: (a) As particle energy inside atomic nuclei, (b) as atomic excitation in atoms or molecules, (c) as microscopic kinetic energy of the random motion in gases, or (d) as pressure volume work via $pV = \mu R_G T$, and (e) macroscopic kinetic residing in flow fields. Turbulent flow with its "self organized" coherent structures adds additional *mesoscopic* internal energy on a scale that falls between the *microscopic* and the *macroscopic* energy ranges. Numerical calculations of turbulent flows [4] show that the eddy energy distribution is raised for the larger eddies by input from the macroscopic inhomogeneous flow field, and is reduced on the small energy side by dissipative energy losses to the thermal background, see Fig. 3c.

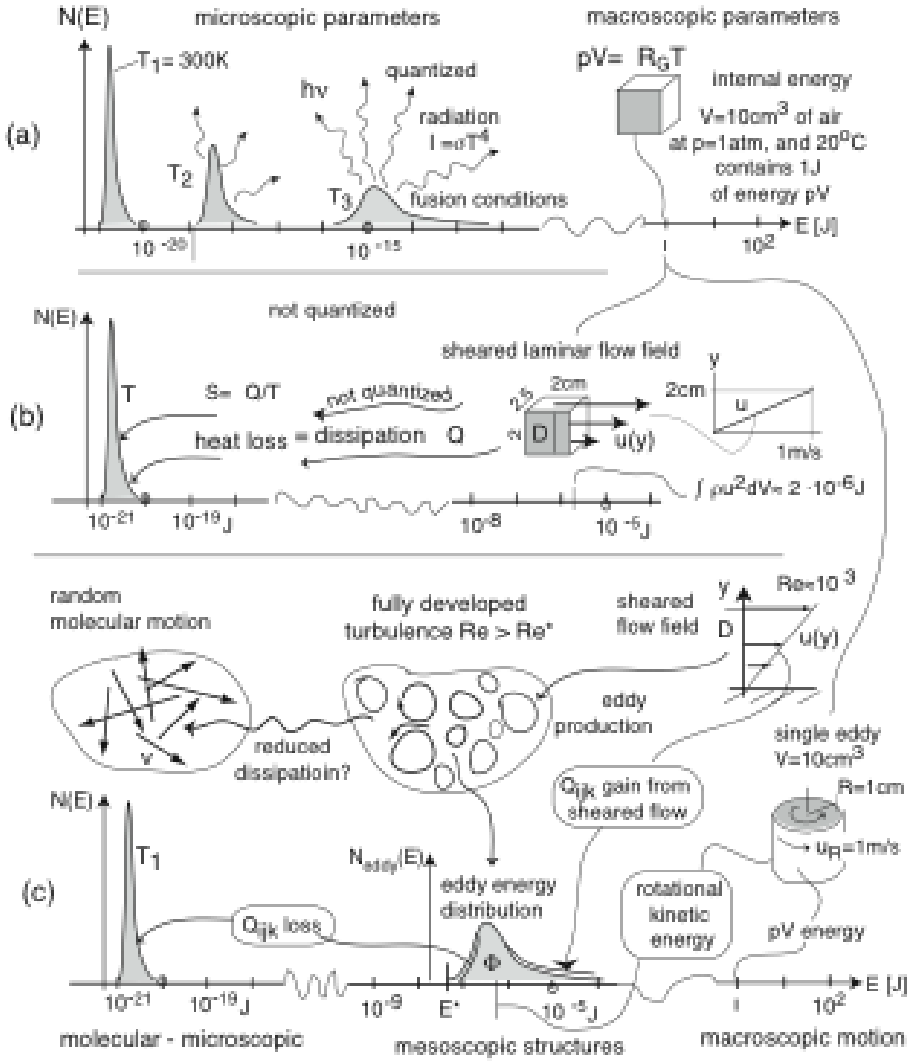

Figure 3: Energy scales and fluxes (a) from particle energies to pressure p, and temperature T, (b) "Laminar" shear flow field with viscous dissipation, (c) shear flow leading to fully developed turbulence, with eddy energy distributions in the mesoscopic energy range between microscopic kinetic energies, and macroscopic pdV.

However turbulence internal energy is not "static" like the heat of evaporation of a medium, because the energy of the turbulent eddies is continuously degraded into heat by the actions of viscosity, that gradually increases the entropy of the medium. We suspect that in turning turbulent shear flows reduce or even minimize their entropy production rate β.

Fig. 3c shows turbulent flow structures in relation to the molecular and macroscopic parameters and energy scales. Hot structures, like sparks, loose energy by radiation, and thermal conduction into other regions of space, while turbulent fluid dissipates its energy locally into the molecular motion of its background fluid.

Here we like to explore what new insight could be gained for thermodynamics as well as for fluid flow by looking at the thermodynamic aspects of turbulence. A number of intriguing research questions can be pursued:

1. Turbulence arising in shear flows at $Re = DU/\nu > Re^{\star}$ adds the new energy modes $E_{\rm TURB} = E_{\rm KR} + E_C$ to the spectrum of atomic/molecular energy modes $E_{A/M}$ (random kinetic energies, dissociation energies, electronic excitation -, and ionization energies). While the $E_{A/M}$ modes convey energy through "photons" (transversal E-M waves), the $E_{\rm TURB}$ modes dump heat through friction into the thermal background, thereby gradually dissipating the turbulence energies.
2. What are the thermodynamic roots of the Reynolds number Re, and what fundamental new physics occurs at the critical Reynolds number Re^*? Is there some similarity to the boiling temperature T_B, where a liquid turns into a gas, albeit that the Reynolds number deals with angular momentum, while the temperature is an energy parameter (fluid dynamics boiling)?
3. Describe the complete energy content of eddies (and rivers as seen in grid turbulence [3] using the mode picture, with mode life-times, and possibly using the energy distribution half width parameter F of the eddy spectrum (similar to the kinetic energy-defined temperature T. It should include a function of the Reynolds number.
4. Separate the power flux terms Q_i of [4] into energy input from macroscopic flow and heat loss terms to the microscopic regime —- like the induced absorption B_{nm}, and spontaneous transition A_{mn} probabilities of spectroscopy.
5. Can the energy dissipation rate for eddies $\Gamma = dP/dt = aM^b$ [Watt] be expressed as function of only the eddy mass/unit length M [kg/m], and 2 unique constants a, and b, similar to the famous "allometric" metabolic rate of animals [5], known as the "mouse to elephant" curve Γ [Watt] $\approx 4M$ [kg]$^{3/4}$, which describes the energy dissipation of animals? (Further comment: the slope $b = 3/4$ holds over 18 orders of magnitude: for unicellular organisms, ectotherms, and warm blooded, only the constant differs: It is $a_W \approx 4$ for warm blooded, and $a_C \approx 0.3$ for ectotherms!
6. Turbulence "parks" energy temporarily in the mesoscopic range. Does it thereby also reduce (or even minimize) the entropy production rate?
7. Heat engines convert temperature differences (reservoirs of temperatures T_H and T_C) into macroscopic mechanical work. Can one similarly regain macroscopic (angular) momentum out of two different reservoirs (characterized by Φ_1 and Φ_2 of angular momentum, and can one derive an efficiency H_{mp} for this process (possibly in the form $H_{mp} = 1 - \sqrt{\Phi_1/\Phi_2}$) similar to the thermodynamic maximum power efficiency?

References

[1] For instance a 1kg block of ice at $T = 273\text{K}^\circ$ turns into water at the same temperature when the heat of fusion $L_F = 333.5$kJ/kg is added, and boiling water at $T = 373\text{K}^\circ$ turns into water vapor when the heat of vaporization $L_V = 2257$kg/kJ is added)

[2] B. Ahlborn, N. Kevlahan, and M. Lefranǫis: "Coherence energies of turbulent flow". Physics Essays 4, pp. 406-416 (1991)

[3] S. Loewen, B. Ahlborn, and A.B. Filuk: "Statistics of surface flow structures on decaying grid turbulence". Phys. Fluids 29, pp. 2388-2397 (1986).

[4] B.R. Noack, M. Schlegel, B. Ahlborn, G. Mutschke, M. Morzyński, P. Comte, and G. Tadmor: "A Finite Time Thermodynamics of Unsteady Fluid Flows?. J.Non. Equilibr.Thermodyn, 2008, 33, pp.

[5] e.g. K. Schmidt-Nielsen: "Scaling: Why is animal size so important?" (Cambridge University Press, 1993, pp.123), or B. Ahlborn: "Zoological Physics", Springer Verlag 2006, pp.12.

Limit possibilities of controlled temperature's fields.

Andrei Akhremenkov, Anatoly Tsirlin
Program Systems Institute of RAS
andrei@svp.polnet.botik.ru

Novikov-Curzon-Ahlburn discovered that the power of an internally reversible heat engine with two heat reservoirs and linear (irreversible) heat exchange between the working body and reservoirs can not exceed some given maximal power, and if an engine operates at this maximal power then the ratio of its working body's temperatures during contacts with reservoirs must be equal to the square root of the ratio of reservoirs' temperatures. We proved that this result also holds for an internally irreversible heat engine operating within inhomogeneous thermodynamic system of the general type (which includes multiple heat reservoirs, multiple subsystems with finite heat capacity and arbitrary contacts between them). This proof follows from our solution of the general problem of the maximal extend of heat into work and work into heat transformation permitted by thermodynamics. It also obtain the conditions which determine temperature distributions within the systems that can only be maintained if an external energy is supplied to the system and the optimal temperature lows that are required to maintain the given distribution of temperatures in a part of the system.

Introduction

The problem of obtaining the maximal work in a nonequilibrium thermodynamic system is one of the fundamental problems of thermodynamics. If process' duration and its objective low's rate (engine's power) are not constrained then the solution is a reversible process. In many cases the problem of maximal-possible power of a heat engine arises ([1], [2]). This problem is meaningless when heat engine operates reversibly. It this paper we extend it to a heat engine operating in a general type stationary thermodynamic system with multiple reservoirs and multiple finite-capacity subsystems. If heat transfer laws and heat transfer coefficients are given then such a system will reach a stationary state and remain in it. This state is described by distribution of temperatures between subsystems, that is, by a discrete temperature field within the system. We assume first that each subsystem (reservoir with constant a temperature, finite-capacity ubsystems, transformer – heat engine or heat pump) be internally-reversible. Thus, irreversible effects occur only on the boundaries between the subsystems. This assumption is necessary to guarantee the validity of thermodynamic description for each subsystem.

Various constraints on the subsystems' temperatures may cause the maximal power N in such a system to be positive or negative. If there is no transformer in the system then some, usually unique, distribution of temperatures will be reached. We shall call this self-settled temperature field in the system. If the system includes a transformer then different configurations of temperature fields

are possible depending on the temperatures of its working body during contacts with the subsystems (control variables) and heat transfer coefficients. For some temperatures the maximal power generated by transformer will be positive and for others it will be negative.

The maximal power problem for two reservoirs and linear heat transfer has been studied in details. The optimal thermostatting problem has been formulated and solved for a system that consists of sequentially connected subsystems ([3], [4], [5]). To the best of our knowledge the problem of constructing the set of realizable temperature fields and its division into generating and consuming power subsets has not been considered in the literature.

In this paper is considers these problems for a general type system with arbitrary structure. The general solutions are then specified for Newton laws of heat transfer. In many cases it turns out that the extremal conditions are reduced to the requirements that some function has the same value during every contact between the heat engine (heat pump) and every subsystem. This allows us to construct a control system to maintain maximal power when external conditions change. In the sequel we will refer to the heat engine and heat pump as transformers. All these problems can be extended into the systems which are non-homogeneous with respect to pressure or to other intensive variables. We limited the scope to temperature non-homogeneous systems to keep results in a compact form.

Transformer's maximal power

We consider a stationary thermodynamic system which consists of (n - m) reservoirs with constant temperatures, m finite-capacity subsystems, whose temperatures are determined by their internal energies and the transformer. We denote the heat exchange lows between subsystems as q_{ij} . These lows are caused by the temperature differences between subsystems. The transformer generates power by contacting the subsystems when it receives heat from them or rejects heat into them. It is required to find such temperatures ui for the contact between the transformer and each of the subsystems that the power N is maximal. If the maximal power is negative then it corresponds to the minimum of the external power consumed by the system.

Problem formulation and conditions of optimality We denote the temperature of the i-th subsystem as T_i, the heat low between the i-th and the j-th subsystems as $q_{ij}(T_i, T_j)$, and the temperature of the working body when it contacts the i-th subsystem as u_i, the heat low between the i-th subsystem and the transformer as $q_i(T_i, u_i)$ and the power of the transformer as N. We define the low entering each subsystem as positive. When T_i increases, q_{ij} decreases monotonically, and when T_j increases, the low increases monotonically. If $T_i = T_j$ then $q_{ij} = 0$. If there is contact between subsystems then $q_{ij} = 0$. We assume that functions $q_{ij}(T_i, T_j)$ are continuously-differentiable and that the working body is internally reversible and the entropy production in it is equal zero. The maximal power problem takes the form

$$N = \sum_{i=1}^{n} q_i(T_i, u_i) \to \max_{u_i} \tag{1}$$

subject to

$$\sum_{i=1}^{n} \frac{q_i(T_i, u_i)}{u_i} = 0 \tag{2}$$

$$\sum_{i=1}^{n} q_{ij}(T_i, T_j) = q_j(T_j, u_j), j = 1, ..., m \tag{3}$$

The optimal contacts' temperatures obey the condition

$$\frac{u_i^2 \partial q_i/\partial u_i}{u_i \partial q_i/\partial u_i - q_i} = \Lambda, i = m+1, ..., n \tag{4}$$

We shall call the left-hand side of this equation (which has the dimension of temperature) the *reduced contact temperature*. Thus, the following Statement holds:
In order to obtain the maximal power the reduced contacts' temperatures for contacts with all reservoirs of the transnformer must be equal. The optimal contact temperature for a contact with a finite-capacity subsystem is

$$\frac{u_i^2 \partial q_i/\partial u_i}{u_i \partial q_i/\partial u_i - q_i} = \frac{\Lambda}{1+\lambda_i}, i = 1, ..., m. \tag{5}$$

The condition (5) relates the reduced contact temperature for contact with the i-th subsystem with the reduced contact temperature with reservoirs Λ and λ_i multipliers . These general conditions can be significantly simplified for particular systems.

Conclusion

The limited possibilities of energy transformation in a thermodynamic system with given structure and given exchange kinetics were studied. The results obtained include maximal power and the formula which determines the boundary between temperature fields in the system can be maintained only if power is generated (maximal power is positive) or if energy is spent (maximal power is negative). The minimal energy required to maintain given field of temperatures in a multi-chamber system and the corresponding heat flows and temperatures of chambers with free temperatures have been obtained.

References

[1] *Novikov I.I., J.Nucl.* Energy II (USSR) 7, 125 (1958).

[2] *Curzon F.L., Ahlborn B.*, Amer. J. Phys., 43, 22 (1975).

[3] *Sofiev, M.A.*, Theor. Bas. Chem. Tech., 3, 150 (1988).

[4] *Martinovskii V.S.* Cycles, schemes and characteristics of the thermotransformators. Moscow, Energia, (1979). [in Russian].

[5] *Tsirlin A.M., SoЇev M.A., Kazakov V.*, J. Phys. D, Appl. Phys., 31, 2264 (1998).

Thermodynamic approach to modeling of a firm: economic interactions and technology

Sergey Amelkin[1]
Program System Institute of Russian Academy of Sciences
sam@sam.botik.ru

An industrial firm is an important element of an economic system. In economic theory the firm is considered as a peculiar case of economic agents. Its specific features are following:

- The firm fixes prices for both sides of the system: factors of production and output goods, if the firm has got monopolistic power at corresponding markets.
- The firm extracts money from the economic system; intensity of this money flux is the firm's profit and it is an objective function for the firm.

The firm as a subject of the economic theory is investigated well including application of thermodynamic approach [1–3]. But all economic models use only one tool namely production function to describe features of manufacturing method. Production function is a dependency between yield and inputs. It is assumed that regime of processing line operation have been chosen to be optimal for any set of factors of production before the economic analysis.

The similar assumption is made by engineers. During the analysis of the manufacturing method they assume all prices to be constant. It means that as for economic researches we suppose that economic policy of the firm is optimal for any regime of manufacturing equipment.

In this report a problem of optimal control of the firm is formulized as a complex problem of cost-performance choice. Problem statement: *to determine process-dependent parameters, prices of yield and inputs, intensities of resources fluxes to maximize a vector of performance indices of the firm*. Note that the vector of performance indices includes both engineering and economic components.

[1] This work is supported by Russian Foundation for Basic Research (grant No. 08-06-00141).

In a simple case of separable factors of production we can introduce analogs of COP as ratio of intensities of yield flux and the *i*-th factor flux. Thermoeconomic investigations [4, 5] bring to significant results but some sufficient troubles occur because of different interpretation of "cost" notion. Here are some questions without an unambiguous answer:

- Which kinds of costs should be accounted during the economic analysis of the firm?
- Which economic criteria should be chosen as the objective function?
- Which intensive variables do determine intensities of the resources fluxes in the system?

Results of the investigation depend on answers of these questions; that is why these results are different.

Here we consider a generalized model of the firm. Otherwise this model would be one more solution in a row. So, let us consider the firm consisting of the manufacturing equipment. The firm can exchange resources with its environment. Production process depends on both exogenous potentials $\mu_0 = (\mu_{01}, \dots, \mu_{0N})$ and endogenous potentials $\mu = (\mu_1, \dots, \mu_N)$. These two kinds of potentials determine values of driving forces. Driving forces determine in turn intensities of fluxes $g = (g_1, \dots, g_M)$ of production factors. One can use equations of material balances to calculate yield flux intensity n as a dependency of vector g. The performance vector $\eta = (\eta_1, \dots, \eta_M)$, where $\eta_i = n/g_i$, can be found now.

To optimize engineering part of the model of the firm one need to solve the following problem:

$$\eta \to \max_{\mu}, \quad \text{subject to} \quad n\big(g(\mu_0, \mu)\big) = \text{fix}. \tag{1}$$

To describe economic interactions we use the thermodynamic approach [6]. Objective for the firm is the profit π and the performance index is the profitability $\eta_e = \pi/(pg)$. Here p is prices vector. Prices p determine intensities of factors of production fluxes according to demand functions (kinetic equations of the economic processes). These fluxes g determine values of exogenous potentials μ_0. So, optimization problem for economic part has the form

$$\eta_e \to \max_{\mu_0}, \quad \text{subject to} \quad \pi\big(n, g, p(g, \mu_0)\big) = \text{fix}. \tag{2}$$

Fluxes of factors of production are determined by process-dependent parameters on the one hand and economic potentials on the other hand.

These fluxes are irreversible and we can introduce a measure of irreversibility of exchange processes. Let us call it traditionally: dissipation of the resources. In our model dissipation is a vector.

The following statement is proved in the report: *Considered problem on performance maximization is dual to the problem on minimization of dissipation vector*. For both the problems the optimal solution can be found in Pareto set. It means that the solution is not uniquely dependent.

List of references

[1] Mirowski P. More heat than light. Economics as Social Physics, Physics as Nature's Economics. – Cambridge, UK: Cambridge University Press, 1989.

[2] Martinás K. Irreversible microeconomics. // In K. Martinás, M. Moreau (eds.) Complex Systems in Natural and Economic Sciences, Matrafüred, 1995.

[3] Amelkin S.A., Martinás K., Tsirlin A.M. Optimal Processes in Irreversible Thermodymamic and Microeconomic Systems. // Avtomatika i Telemekhanika, 4, 2002, p. 3–25.

[4] De Vos A. Endoreversible Thermoeconomics. // Energy Conversion Management, 36 (1), 1995, p. 1–5.

[5] Thermodynamics and Thermoeconomics. S. Sieniutycz, P. Salomon (eds.), Advances in thermodynamics, v.4, N.Y. Taylor & Francis, 1990.

[6] Tsirlin A.M., Amelkin S.A. Dissipation and Conditions of Equilibrium for an Open Microeconomic System // Open Systems & Information Dynamics, 8, 2001, p. 157–168.

Thermodynamic foundations of evolutionary theory

Arto Annila[1,2,3,*]

[1]Department of Physics, [2]Institute of Biotechnology and [3]Department of Biosciences, FI-00014 University of Helsinki, Finland; [*]Email: arto.annila@helsinki.fi

The theory of evolution by natural selection (1) is undoubtedly the most general and holistic description of the living nature. However, from the cross-disciplinary perspective of biophysics, it is relevant to ask: What is the fundamental law of nature that evolution follows? How to express the evolutionary theory in thermodynamic terms?

It is, of course, no new thought that evolution is a manifestation of the 2nd law of thermodynamics (2). On the contrary, it seems that already a century ago Ludwig Boltzmann aimed at deriving an equation of motion for evolution from the first principles. Boltzmann understood evolution as a probable process, a likely sequence of events, far from being a miracle. Therefore he defined a concept, known as probability P, to summarize the state of a many-body system. Logarithmic probability, known as entropy $S = k_B \ln P$, is the additive measure for the status of a system in evolution from one state to another, more probable one. This directional process is thus understood to follow the principle of increasing entropy $dS/dt > 0$.

Apparently Boltzmann failed to complete his agenda since statistical physics, *i.e.*, the foundation of thermodynamics, has remained limited to closed systems whereas biological systems are unmistakably open to their surroundings. Consequently, thermodynamics has had difficulties in understanding what life is. The lack of understanding is reflected in many puzzling questions. For example, why life emerged? Why natural amino acids in proteins display a consensus of chirality? Why the genetic code is ubiquitous? Why our genomes are loaded with non-phenotypic DNA? Why protein folding is so difficult to predict? Why distributions of animals and plants are skewed, nearly log-normal? Why cumulative curves of natural distributions are on log-log plots mostly straight lines, *i.e.*, power-laws such as the species-area relationship? What drives ecological succession and gives rise to diversity in general? Why the entire biosphere behaves as a homeostatic system? Why nature organizes itself in a nested hierarchy of functional systems within systems? Of course there are many other related perplexing questions in the fields where Darwin's theory has found supporters. For example, where do the laws of economy, such as the law of supply and demand as well as the law of diminishing returns come from?

These questions are addressed using the 2nd law of thermodynamics written as an equation of motion derived from statistical physics of open systems (3,4,5). Thermodynamics pictures everything in terms of energy. The holistic theory is independent of scale and mechanisms of energy transduction and dispersal. While the description of evolution to hierarchical organizations by the natural law is by no means new (6), the value of the mathematical formulation of natural processes is that evolution at any scale and irrespective of its mechanisms can be analyzed rigorously. The analysis reveals that evolution is a non-deterministic process that consumes free energy in the quest to level off energy density differences. However, evolutionary trajectories are inherently intractable, *i.e.*, unpredictable because the flows of energy are inseparable from their driving forces in non-Hamiltonian systems with degrees of freedom.

1. Darwin, C. *On the Origin of Species*. John Murray, London, UK, 1859.
2. Salthe, S. N. *Development and evolution: Complexity and change in biology*. MIT Press, Cambridge, MA, 1993.
3. Sharma, V. & Annila, A. Natural process – Natural selection. *Biophys. Chem.* 2007, 127, 123–128.
4. Annila, A. & Annila, E. Why did life emerge? *Int. J. Astrobiol.* 2008, 7, 293–300.
5. Tuisku, P., Pernu, T. K. & Annila, A. In the light of time. *Proc. R. Soc. A.* 2009, 465, 1173–1198.
6. Salthe, S. N. *Evolving hierarchical systems: Their structure and representation*. Columbia University Press, New York, NY, 1985.

On the Teaching of Entropy

A. Özer Arnas
Professor of Mechanical Engineering
United States Military Academy at West Point
ozer.arnas@usma.edu

SUMMARY

In Thermodynamics education, *precise* teaching and learning the laws of thermodynamics is of utmost importance. Unfortunately, both have deteriorated in the last couple of decades and are still on a negative slope. There are various reasons for it the most important being the fact that the instructors of thermodynamics are no longer thermodynamicists but rather people who have doctoral degrees in computational heat transfer, fluid mechanics and the like. Also, although the page numbers in textbooks have increased, the quality of content has decreased. Thus the fundamental understanding of thermodynamics is lacking as well as advanced knowledge. Here a method to present entropy to the undergraduates is discussed in the hope that a better job can be done in the classroom.

THE CARNOT CYCLE

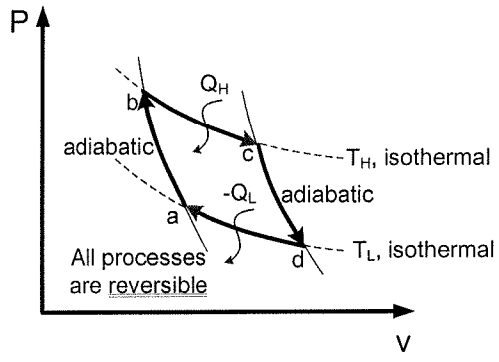

A *thermodynamic cycle* is defined as a series of thermodynamic processes that return to the initial state. A *thermodynamic thermal reservoir* is defined as a system that stays at its temperature, a constant, no matter how much energy is transferred into it or out of it. An example would be a large body of water or air, such as a river or ocean or the atmosphere. Strictly speaking there are none in nature. A *reversible* process is one in which the *system* ***and*** the *surroundings* can be returned to their original state after certain changes have been made without leaving any trace in its path. Again, of course, in nature there are none. All *natural* processes are *irreversible.* However, in thermodynamics these assumptions are freely made to determine the limits of performance for systems, devices and cycles. One such cycle is the *CARNOT* cycle. It is made of two reversible adiabatic processes and two constant temperature heat reservoirs. If the working fluid is considered to be an ideal gas, for simplicity of algebra, then the energy added as heat at T_H is given by, since $\{dU = mc_v dT = 0\}$ and $(\delta Q = pdV)$ which for process b-c and an ideal gas gives $\left\{Q_{bc} = \frac{mR}{M} T_H \ln \frac{V_c}{V_b}\right\}$. Similarly an equivalent relationship can easily be obtained for the process (d-a) as $\left\{Q_{da} = \frac{mR}{M} T_L \ln \frac{V_a}{V_d}\right\}$. Thus the ratio of these two becomes $\left\{\frac{Q_{da}}{Q_{bc}} = \frac{T_L}{T_H}\left(\frac{\ln \frac{V_a}{V_d}}{\ln \frac{V_c}{V_b}}\right)\right\}$. Since the process (a-b) is reversible and adiabatic, then from the first law of thermodynamics $\{-mc_v dT = pdV\}$ or $\left\{-mc_v dT = \frac{mR}{M} T \frac{dV}{V}\right\}$. This relationship integrates to give for the process

(a-b) $\left\{-\frac{M}{R}\int_{T_L}^{T_H} c_v \frac{dT}{T} = \ln\frac{V_b}{V_a}\right\}$. Similarly, for the process (c-d) the result becomes $\left\{-\frac{M}{R}\int_{T_H}^{T_L} c_v \frac{dT}{T} = \ln\frac{V_d}{V_c}\right\}$.

Therefore, since the limits of integration are reversed, the equivalence gives $\left\{\ln\frac{V_a}{V_b} = \ln\frac{V_d}{V_c}\right\}$ or $\left\{\frac{\ln\frac{V_c}{V_b}}{\ln\frac{V_a}{V_d}} = -1\right\}$. This upon substitution results in $\left\{\frac{-Q_L}{Q_H} = \frac{T_L}{T_H}\right\}$ which permits one to substitute temperatures for heat quantities in the determination of Carnot performance criteria which quickly give performance values for the actual efficiency of an engine $\left\{\eta = \frac{Q_{in} + Q_{out}}{Q_{in}}\right\}$ and for Carnot $\left\{\eta_{CARNOT} = 1 - \frac{T_L}{T_H}\right\}$, as well as coefficient of performance for a refrigerator, $\left\{\beta = \frac{-Q_L}{-W_{in}}\right\}$ and for Carnot $\left\{\beta_{CARNOT} = \frac{T_L}{T_H - T_L}\right\}$ since $\{-W_{in} = Q_H + Q_L\}$, and for a heat pump, $\left\{\gamma = \frac{Q_H}{-W_{in}}\right\}$ and for Carnot $\left\{\gamma = \frac{T_H}{T_H - T_L}\right\}$. It must be remembered that one of the heat quantities is negative, *out* of a system, as it should be since the ratio of absolute temperatures is always positive. The sign convention, whatever it is assumed to be, must be followed strictly and without compromise within a given problem [1] in spite of the fact that some textbooks would rather use absolute values and suggest that "...a relaxed sign convention will be followed", [2]. No such thing is acceptable in the *precise* teaching of thermodynamics.

ENTROPY

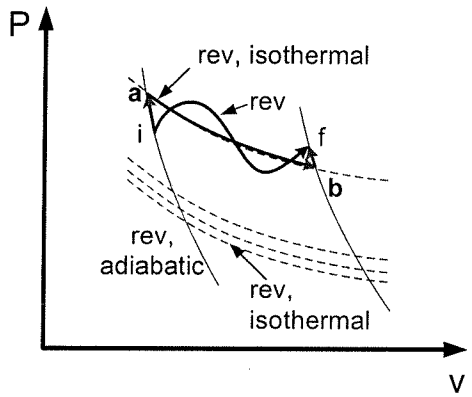

Entropy is a thermodynamic property which comes about as a result of the second law of thermodynamics. To demonstrate its existence, consider a reversible process from an initial state i to a final state f and use the first law to give $\{Q_{if} - W_{if} = (U_f - U_i)\}$. From i and f draw two reversible adiabatic lines. Then construct a reversible isotherm a-b so that the area above and below the isotherm and between the original process i-f and the adiabatic lines are equal. Thus we obtain that $\{W_{if} = W_{iabf}\}$. Therefore, now the heat terms give $\{Q_{if} = Q_{iabf}\}$ since ($U_f - U_i$) does not change because of the general character of a thermodynamic property. Also Q_{ia} and Q_{bf} are equal to zero since they are adiabatic processes resulting in $(W_{if}) = (W_{iabf}) = \{W_{ia} + W_{ab} + W_{bf}\}$. Therefore, the result becomes $\{Q_{ab} - W_{if} = (U_f - U_i)\}$ giving the final result that $\{Q_{ab} = Q_{if}\}$. In general, therefore, an arbitrary reversible process can always be replaced by a zigzag path between the same state points consisting of a reversible adiabatic line, a reversible isotherm, and another reversible adiabatic line, such that $\{Q_{originalprocess} = Q_{isotherm}\}$. Now, to reach the definition of thermodynamic quantity entropy, consider a smooth reversible cycle as shown below. On it inscribe reversible adiabatic lines of thickness Δ. For each slice or arc, which is a reversible process, inscribe an isotherm so that the condition given above is satisfied. The cycles thus

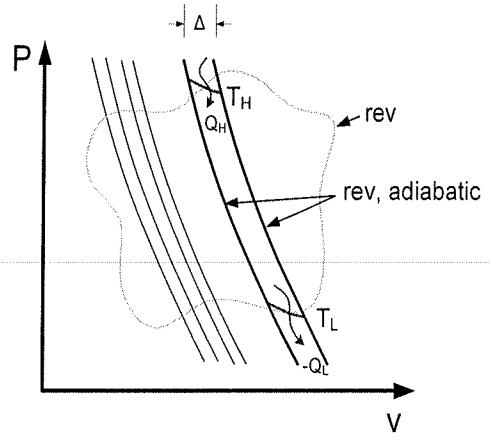

formed are all Carnot cycles with the characteristic relationship obtained between heat transfer and absolute temperature ratios. Thus for the first cycle drawn, $\left\{\frac{Q_{H_1}}{-Q_{L_1}}=\frac{T_{H_1}}{T_{L_1}}\right\}$ or $\left\{\frac{Q_{H_1}}{T_{H_1}}+\frac{Q_{L_1}}{T_{L_1}}=0\right\}$. In a similar fashion, for the second cycle we have $\left\{\frac{Q_{H_2}}{T_{H_2}}+\frac{Q_{L_2}}{T_{L_2}}=0\right\}$. Adding these two results and generalizing for the sum of all such cycles, then $\left\{\sum_i \frac{Q_i}{T_i}=0\right\}$. In the limit as $\Delta \rightarrow 0$, the adiabatic lines come closer thus making the heat quantities infinitesimal resulting in $\left\{\oint_{rev}\frac{\delta Q}{T}=0\right\}$ which is the important CLAUSIUS THEOREM. Now consider two reversible processes R_1 and R_2 starting from the initial state i and ending at the final state f. Since they are reversible, it is possible to change the sense of R_2. Since R_1 and R_2 now form a reversible cycle, then $\left\{\oint_{R_1R_2}\frac{\delta Q}{T}=0\right\}$ and $\left\{\int_{i_{R_1}}^{f}\frac{\delta Q}{T}+\int_{f_{R_2}}^{i}\frac{\delta Q}{T}=0\right\}$. This results in the general relation $\left\{\int_{i_{R_1}}^{f}\frac{\delta Q}{T}\right\}=\left\{\int_{i_{R_2}}^{f}\frac{\delta Q}{T}\right\}=\ldots=\left\{\int_{i_R}^{f}\frac{\delta Q}{T}\right\}$ which says

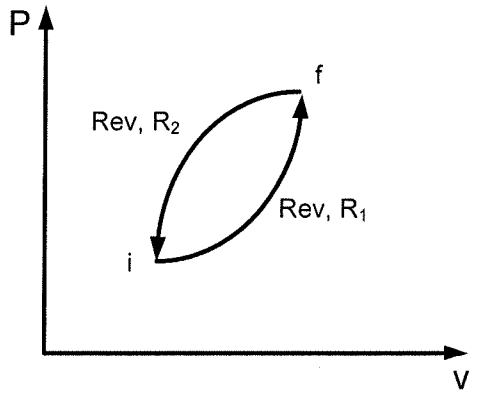

that if a reversible path is chosen, the path itself is not important so long as the process starts at i and ends at f. The quantity is, therefore, given by the end states and not the path. As is the case in the first law of thermodynamics, $\left\{\oint\delta Q-\oint\delta W=\oint dU\right\}$ and $\left\{\oint dU=0\right\}$ since internal energy is a thermodynamic property, then $\left\{\oint_{rev}\frac{\delta Q}{T}=0\right\}$ is a thermodynamic property and is called entropy, S. Therefore, $\left\{\int_{i_{REV}}^{f}dS=\left(S_f-S_i\right)\right\}$ or for an infinitesimal process, $\left\{\frac{\delta Q_{rev}}{T}=dS\right\}$ that forms the mathematical formulation of the second law of thermodynamics. It is, therefore, seen that there is a similarity between the two laws of thermodynamics and their definitions of internal energy and entropy. To further extend this discussion to the inequality of Clausius, consider the fact that all heat engines operating between a given high temperature source and a lower temperature sink none can have a higher efficiency than the Carnot engine. Thus using the figure above, but this time having the process at T_H to be irreversible, then $\left(1+\frac{Q_{L_{REV}}}{Q_{H_{IRREV}}}\right)\leq\left(1+\frac{Q_L}{Q_H}\right)_{REV}$. Using the fact that $\left\{\frac{-Q_L}{Q_H}=\frac{T_L}{T_H}\right\}$ for reversible energy transfers,

$\left(\frac{Q_{L_{REV}}}{Q_{H_{IRREV}}}\right) \leq \left(1 - \frac{T_L}{T_H}\right)$. Transposing and keeping in mind that there is a negative sign, the result becomes $\left(\frac{\delta Q_{L_{REV}}}{T_L}\right) \geq \left(\frac{\delta Q_{H_{IRREV}}}{T_H}\right)$. Using the definition of entropy as given above, $dS \geq \left(\frac{\delta Q_{H_{IRREV}}}{T_H}\right)$ or $\oint dS \geq \left(\frac{\delta Q}{T}\right)_{IRREV}$ which states that in all real processes entropy increases and the equality is only for the reversible process. This further reduces the result to what is expected, the inequality of Clausius, the fact that $\oint\left(\frac{\delta Q}{T}\right)_{IRREV} \leq 0$.

CONCLUSION

The explanation given above for the second law and entropy was attempted in [3] and [4] although to no complete conclusion. What happened in the decades after is that this explanation was abandoned in the hope of "making things clear". Discussing entropy in this context, with the correct sign convention of heat in positive and work in negative, HIP-WIN, although all energy in is positive and all energy out is negative could also be used [5], clearly explains what entropy is, a *thermodynamic property*, and how it can be derived simply at the level of the novice undergraduate student. The mystery about it should really not exist and its value in practice is enhanced.

ACKNOWLEDGEMENT

The views expressed herein are those of the author and do not purport to reflect the position of the United States Military Academy at West Point, The Department of the Army, or the Department of Defense.

REFERENCES

[1] A. Özer Arnas, Daisie D. Boettner and Margaret B. Bailey, (2003), "On the sign convention in thermodynamics – An asset or an evil", *Proceedings of ASME-IMECE2003,* IMECE2003-41048. Also, Daisie D. Boettner, Margaret B. Bailey and A. Özer Arnas, (2006), "On the Consistent Use of Sign Convention in Thermodynamics," *International Journal of Mechanical Engineering Education*, **34/4**, 330-348.

[2] Yunus A. Çengel and Michael E. Boles, (2008), *Thermodynamics-An Engineering Approach*, 6th Edition, McGraw-Hill.

[3] M. W. Zemansky, (1943), *Heat and Thermodynamics,* Wiley.

[4] David A. Mooney, (1953), *Mechanical Engineering Thermodynamics*, Prentice-Hall.

[5] H. B. Callen, (1960), *Thermodynamics*, Wiley.

Intramolecular Association within the SAFT framework

Ane S. Avlund [a], Georgios M. Kontogeorgis [a], Michael L. Michelsen [a]
and Walter G. Chapman [b]
[a] DTU Chemical Engineering, Technical University of Denmark,
[b] Chemical and Biomolecular Engineering, Rice University
asa@kt.dtu.dk

Intramolecular association (association internal to the molecule) has been shown to have a significant effect on the phase behavior of glycol ethers (a green solvent) [1] and of telechelic polymers [2]. Brinkley and Gupta [1] measured the extent of intramolecular association in systems containing glycolethers using spectroscopy (FTIR). The influence of intermolecular and intramolecular association on the phase behavior of telechelic polymers was shown by Gregg, Stein and Radosz [2].

When the SAFT equation of state was originally developed in the late 1980's [3] it only included intermolecular association to form chain or tree-like structures, while the formation of rings was neglected. Around 1994-1995 two groups (Sear & Jackson [4] and Chapman & coworkers [5-6]) independently extended the SAFT theory to include ring formation from chains with one attractive site on each terminal segment. Using different approaches, the two groups developed equivalent expressions for the contribution to the Helmholtz free energy for this specific type of intramolecular association. Although the theories were eventually applied to mixtures, a general solution for mixtures of molecules with multiple association sites was not obtained.

In this work the theory has been extended to provide a general expression for the free energy of mixtures of molecules with multiple associating sites that can form intermolecular and intramolecular bonds (even multiple intramolecular bonds within the same molecule are possible).The equations have been rewritten using the approach of Michelsen and Hendriks [7] in order to simplify the calculations.

The theory will be applied to different systems of interest, such as systems containing glycol, glycolether, or other compounds with multiple functional (associating) groups, using the PC-SAFT equation of state [8-9], and the results will be compared to the results with PC-SAFT without accounting for intramolecular association.

[1] R.L. Brinkley, R.B. Gupta, Ind. Eng. Chem. Res. 37 (1998) 4823-4827
[2] C.J. Gregg, F.P. Stein, M. Radosz, Macromolecules, 27 (1994) 4972-4980
[3] W.G. Chapman, G. Jackson, K.E. Gubbins, Molec. Phys. 65 (1988) 1057-1079.
[4] R.P. Sear, G. Jackson, Phys. Rev. E, 50 (1994) 386-394
[5] D. Ghonasgi, V. Perez, W.G. Chapman, J. Chem. Phys. 101 (1994) 6880-6887
[6] D. Ghonasgi, W.G. Chapman, J. Chem. Phys. 102 (1994) 2585-2592
[7] M.L. Michelsen, E.M. Hendriks, Fluid Phase Equil. 180 (2001) 165-174
[8] J. Gross, G. Sadowski, Ind. Eng. Chem. Res. 40 (2001) 1244-1260
[9] N. Von Solms. M.L. Michelsen, G.M. Kontogeorgis, Ind. Eng. Chem. Res. 42 (2003) 1098-1105

Thermosize effects and thermodynamic analysis of a thermosize power cycle

Babac G and Sisman A

Energy Institute, Istanbul Technical University, 34469 Maslak, Istanbul, Turkey.
babac@itu.edu.tr

Abstract

A rectangular box filled by an ideal monatomic gas and separated into two parts, namely macro and nano, is considered. Under temperature gradient, it is shown that thermosize effects, similar to thermoelectric effects, arise due to changes of thermodynamic and transport characteristics of gases in small scaled systems. A possibly new thermodynamic power cycle based on thermosize effects is analyzed. Expressions for specific work, heat and efficiency of a possible thermosize power cycle are derived and the cycle is thermodynamically examined. The results can be useful to design some new devices.

1. Introduction

In recent years, micro/nano systems constitute a new research area in literature. In addition to a great number of experimental inventions and practical applications, also the theoretical predictions about the new effects, which can appear just in micro/nano systems, provoke rapid developments in nanotechnology [1-7]. In nano scale, thermodynamic and transport properties of gases differ from those in macro scale [8-15]. These differences introduce some new effects and make the realization of new devices possible. Thermosize effects are the new effects, which arise due to changes of thermodynamic and transport characteristics of gases in small scaled systems. Physical mechanisms of thermosize effects are similar to those of thermoelectric effects although they do not exactly match up with each other in mathematical representation. In this study, a rectangular box divided into two parts, namely macro and nano, is considered. The box is assumed to be under a temperature gradient and filled by a monatomic gas. Macro and nano parts are connected to each other by a channel at low temperature side while they are disconnected at high temperature side. Under steady state conditions, pressure gradient is zero in macro part. On the other hand, the particle flux is zero in nano part since the domain size is smaller than the mean free path of particles, l. It is shown that these different regimes cause different chemical potential gradient under the same temperature gradient. Therefore, a chemical potential difference occurs at the high temperature side of the box. This chemical potential difference can drive the particle transport if the disconnected parts at high temperature side are connected to each other by a hole smaller than l. Consequently, temperature gradient causes a gas flow, which is able to produce work. This constitutes a possibly new thermodynamic power cycle which can be observed in case of the combination of macro and nano structures. These effects are called here thermosize effects and the cycle constitutes a thermosize power cycle which is similar to thermoelectric power cycle. Expressions for specific work, heat and efficiency of a possible thermosize power cycle are derived and the cycle is thermodynamically analyzed. The results obtained here can be useful to design a new device based on thermosize effects.

2. Thermosize effects

A rectangular box filled by a monatomic gas and separated into nano and macro parts in one direction is seen in figure 1. The box is under temperature gradient. Macro and nano parts are connected to each other by a channel at low temperature side while they are disconnected at high temperature side. At the beginning, gas flow is not allowed since macro and nano parts are disconnected at high temperature side. Under steady state conditions, zero

net particle flux corresponds to zero pressure gradient, $\vec{\nabla}p = 0$, in macro part since the size of the domain is much bigger than the mean free path of particles and the hydrodynamic regime is built in this part [16]. On the other hand, zero net particle flux corresponds to the condition of $\vec{\nabla}\left(p/\sqrt{T}\right) = 0$ since the size of the domain is smaller than the mean free path of particles and the free molecular regime is built in nano part [16]. Therefore, chemical potential gradients are different in macro and nano parts although the temperature gradients are the same.

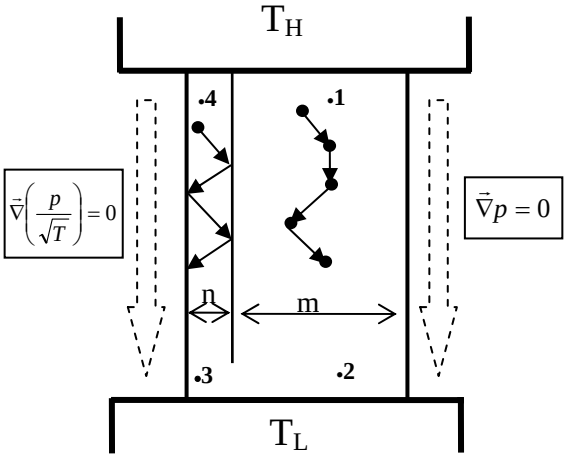

Figure 1: Thermosize effects.

Chemical potential of a monatomic ideal gas is given as [14]

$$\mu = -kT\ln\left(\frac{cT^{3/2}}{n}\right) \tag{1}$$

where T is temperature, k is the Boltzmann's constant, n is particle density, c is a constant defined by $c = (2\pi mk)^{3/2}/h^3$, m is the atomic mass and h is the Planck's constant. By considering Eq.(1) and the conditions of $\vec{\nabla}p = 0$ and $\vec{\nabla}\left(p/\sqrt{T}\right) = 0$, the derivations of chemical potential with respect to temperature for macro and nano domains can be determined as follows respectively,

$$\left(\frac{d\mu}{dT}\right)_m = \left(\frac{d\mu}{dT}\right)_{\vec{\nabla}p=0} = \frac{\mu(T,n_m)}{T} - \frac{5}{2}k \tag{2}$$

$$\left(\frac{d\mu}{dT}\right)_n = \left(\frac{d\mu}{dT}\right)_{\vec{\nabla}\left(p/\sqrt{T}\right)=0} = \frac{\mu(T,n_n)}{T} - 2k\,. \tag{3}$$

Since $\mu_2 = \mu_3$, net chemical potential difference, $\Delta\mu = \mu_4 - \mu_1$, can be obtained as

$$\Delta\mu = \mu_4 - \mu_1 = (\mu_4 - \mu_3) - (\mu_1 - \mu_2) = \int_{T_L}^{T_H}\left(\frac{d\mu}{dT}\right)_n - \int_{T_L}^{T_H}\left(\frac{d\mu}{dT}\right)_m = \int_{T_L}^{T_H}\left(\frac{\mu_n - \mu_m}{T}\right)dT + \frac{k}{2}(T_H - T_L)\,. \tag{4}$$

By use of ideal gas equation of state, $p = nkT$, and the conditions of $\vec{\nabla}p = 0$ and $\vec{\nabla}\left(p/\sqrt{T}\right) = 0$, the variations of densities in macro and nano parts can be given as respectively,

$$n_m(T) = n_2 T_L/T \tag{5}$$

$$n_n(T) = n_2(T_L/T)^{1/2} \tag{6}$$

It should be noted that $n_2 = n_3$ since $\mu_2 = \mu_3$ and $T_2 = T_3 = T_L$. Therefore, net chemical potential difference, $\Delta\mu = \mu_4 - \mu_1$, can be determined by using Eqs.(1), (4)-(6) as

$$\Delta\mu = \mu_4 - \mu_1 = \int_{T_L}^{T_H} \left(\frac{\mu_n - \mu_m}{T} \right) dT + \frac{k}{2}(T_H - T_L) = \frac{k}{2} T_H \ln\left(\frac{T_H}{T_L} \right). \tag{7}$$

Therefore, in this kind of configuration, temperature gradient causes a driving force for particle (or mass) transport from region 1 to region 4. Particle transport causes also heat exchange during isothermal process 4-1. Isothermal heat exchange per transferred particle can be calculated as

$$q_{41} = \int_4^1 T ds = T_H (s_1 - s_4) \tag{8}$$

For an ideal Maxwell gas, the relation between entropy per particle and chemical potential is given by

$$s = \frac{5}{2} k - \frac{\mu}{T}. \tag{9}$$

By using Eq.(9) in Eq.(8), q_{41} is obtained as follows,

$$q_{41} = (\mu_4 - \mu_1) = \frac{k}{2} T_H \ln\left(\frac{T_H}{T_L} \right). \tag{10}$$

It should be noted that both chemical potential difference due to temperature gradient, Eq.(7), and isothermal heat exchange, Eq.(10), are similar to the Seebeck and Peltier effects in thermoelectric processes. These effects here are called thermosize effects since they result from both temperature and size difference together.

3. Thermodynamic analysis of a thermosize power cycle

If the regions (4) and (1) are connected to each other by a hole smaller than *l*, a gas flow begins and a thermodynamic cycle occurs. Figure (2a) represents this cycle. T-s diagram of the cycle is given in Figure (2b). Exchanged heats during the processes (1-2), (2-3) and (3-4) can be calculated as

$$q_{12} = \int_1^2 T ds = -\int_{T_H}^{T_L} T d\left(\frac{\mu}{T} \right) = \frac{5}{2} k (T_L - T_H) \tag{11}$$

$$q_{23} = 0 \tag{12}$$

$$q_{34} = \int_3^4 T ds = -\int_{T_L}^{T_H} T d\left(\frac{\mu}{T} \right) = 2k(T_H - T_L). \tag{13}$$

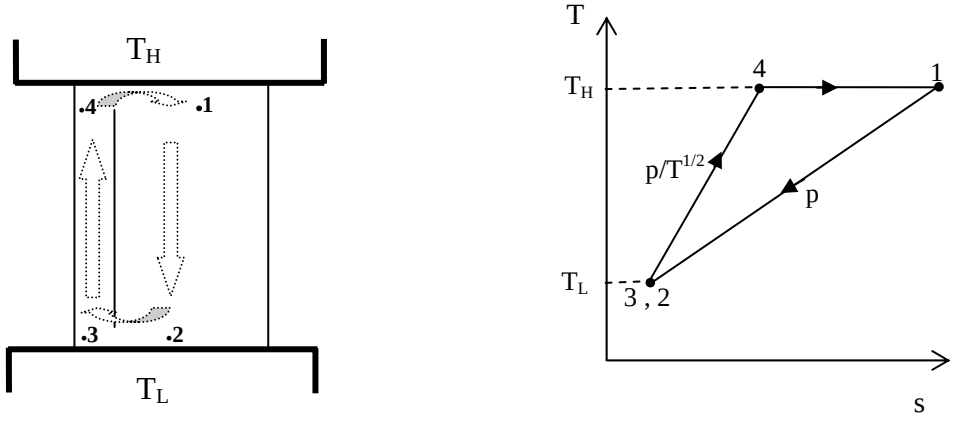

Figure 2: Thermosize power cycle.

Net specific work output is

$$w = q_{12} + q_{23} + q_{34} + q_{41} = \frac{k}{2} T_H \ln\left(\frac{T_H}{T_L}\right) - \frac{k}{2}\left(T_H - T_L\right), \tag{14}$$

While the net specific heat input is q_{41} given by Eq.(10). Therefore efficiency of this cycle is

$$\eta = 1 + \frac{1-\tau}{\ln \tau}. \tag{15}$$

where τ is the temperature ratio defined by $\tau = T_L / T_H$. Efficiency and the Carnot efficiency versus to temperature ratio are shown in figure 3a. It is seen that the difference between the efficiency of the cycle and that of Carnot reaches its maximum value of 0.3 when τ=0.2. Variation of the dimensionless specific work with the temperature ratio is given in figure 3b. It is understood that specific work is less than the thermal energy of particles in the wide range of τ.

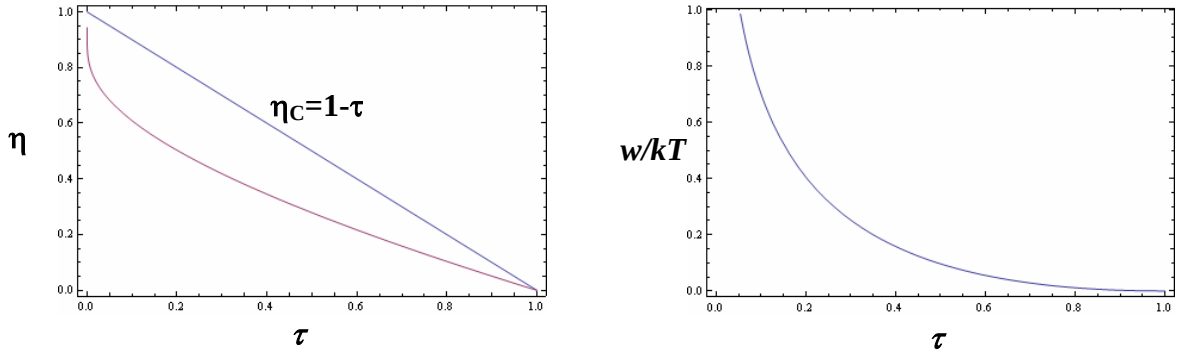

Figure 3: (a) Variation of efficiency with temperature ratio, (b) Dimensionless specific work vs τ.

Conclusion

Combination of macro and nano channels filled by an ideal gas under temperature gradient constitutes a thermodynamic cycles based on thermosize effects. This possibly new effects and the cycle can be used to convert heat energy to mechanical energy in micro/nano devices. A more detailed investigation of this kind of cycles using ideal quantum gases is also an undergoing work.

References

[1] Goddard, W.A., Brenner, D.W., Lyshevski, S.E. and Iafrate, G.J., (Editors) 2003, *Handbook of Nanoscience, Engineering, and Technology*, Boca Raton: CRC Press.
[2] Wolf, E.L., 2004, *Nanophysics and Nanotechnology*, Weinheim: WILEY-VCH.
[3] Kang, J.W. and Hwang, H.J., 2004, *Nanotechnology*, 15, 1633-38.
[4] Li, Z. and Ling, H., 2007, *The Journal of Chemical Physics*, 127, 0747706/1-5.
[5] Schöll, E.,1998, *Theory of Transport Properties of Semiconductor Nanostructures*, Chapman & Hall.
[6] Roldughin, V.I. and Zhdanov, M.V., 2003, *Colloid Journal*, 65, 598-601.
[7] Skoulidas, A.I., Ackerman, D.M., Johnson, J.K. and Sholl, D.S., 2002, *Physical Review Letters*, 89, 185901/1-4.
[8] Sisman, A., Ozturk, Z.F. and Firat, C., 2007, *Phys. Lett.* A, 362, 16-20.
[9] Dai, W.S. and Xie, M., 2007, *J. Math. Phys.*, 48, 123302.
[10] Pang, H., Dai, W.S. and Xie, M., 2006, *J. Phys.* A*: Math. Gen.*, 39, 2563-71.
[11] Sisman, A., 2004, *J.Phys.* A: *Math. Gen.*, 37, 11353-61.
[12] Sisman, A. and Müller, I., 2004, *Phys. Lett.* A, 320, 360-6.
[13] Dai, W.S. and Xie, M., 2004, *Phys. Rev.* E, 70, 016103-1.
[14] Pathria, R.K., 1998, *Am. J. Phys*., 66, 1080-85.
[15] Molina, M.I., 1996, *Am. J. Phys*., 64, 503-5.
[16] Reif, F., 1965, *Fundamentals of statistical and thermal physics*, McGraw-Hill, New York.

Optimal Control Methods Used During the Design and Utilization of Solar Energy Collection Systems

Viorel Badescu
Candida Oancea Institute, Polytechnic University of Bucharest,
Spl. Independentei 313, Bucharest 060042, Romania
email: badescu@theta.termo.pub.ro

This paper shows how the classical methods of optimal control can be used by the solar energy engineer. A number of applications were selected to give a broad idea about the usefulness of these optimization procedures.

1. Sizing solar collection area

As a first example, we refer to the optimum size and structure of the solar energy collection systems [1]. Several procedures for sizing and optimizing the structure of solar collection systems are proposed. Four economical indices, including net present value and internal return rate, are given as examples of objective functions. Three solar energy applications were considered. A rather involved but still simple flat-plate solar collector model is used in calculations. The implementation was made for a specific geographical location with a detailed meteorological database available. In the case of solar collectors with uniformly distributed parameters, the procedure allows one to select the best devices from a given set of solar collectors. For every selected device the optimum range of the operation temperature is also determined. The best solution corresponds to systems with optimal non-uniformly distributed parameters (Fig. 1).

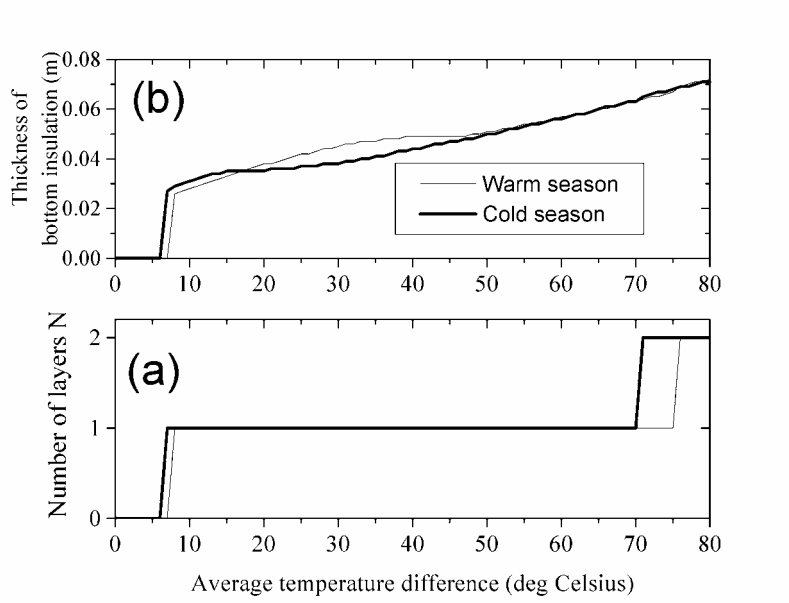

Fig. 1. (a) The number of transparent layers N and (b) the thickness of the bottom thermal insulation L_b for a solar collector system with non-uniform optimally distributed parameters.

The general theorem proposed here shows how the modified optical efficiency and heat loss coefficient should be distributed for cost minimization. One finds that unglazed, single-glazed and double-glazed

collectors should be used on the same collection area in order to obtain the best performance. Also, the bottom insulation thickness should be changed accordingly.

2. Sizing solar collectors

As a second example, we refer to the optimum fin geometry in flat-plate solar collector systems [2]. The width and thickness of fins is optimized by minimizing the cost per unit useful heat flux. The proposed procedure allows computation of the necessary collection surface area. A rather involved but still simple flat-plate solar collector model is used in calculations. Model implementation requires a specific geographical location with a detailed meteorological database available. Both fins of uniform and variable thickness were considered. In case of fins with uniform thickness, the optimum distance between tube centre decreases by increasing the operation temperature, while the optimum fin thickness is relatively the same, whatever the operation temperature and meteorological factors. The optimized width of the collection surface decreases when the operation temperature increases. The best economical performance is obtained in case of fins with optimized space variable thickness (Fig. 2).

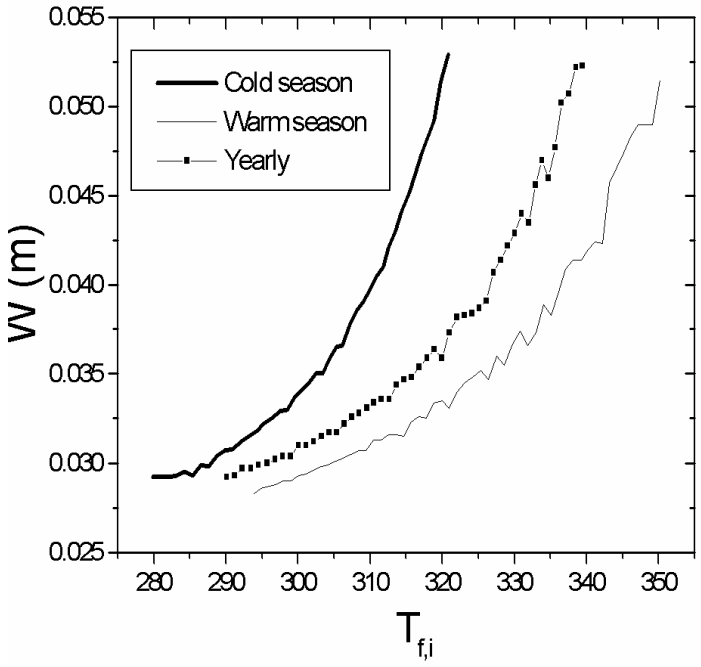

Fig. 2. Optimum distance W between two adjacent tubes centers for a fin of variable thickness as a function of fluid inlet temperature $T_{f,i}$. Operation during the cold and warm season as well as during the whole year was considered. Meteorological data for the whole year 1961 in Bucharest were used.

Optimal control techniques are used in this case. The optimum fin cross-section is very close to an isosceles triangle. The fin width is shorter and the seasonal influence is weaker at lower operation temperatures. Fin width and thickness at base depend on season. The optimum distance between the tubes increases by increasing the inlet fluid temperature and it is larger in the cold season than in the warm season.

3. Optimal operation - systems with water storage tanks

As a third example, we refer to the optimal control of flow in solar collector systems with fully mixed water storage tanks [3]. Closed loop flat-plate solar collector systems are considered. The water storage

tank operates in fully mixed regime. Two design configurations were considered: (A) one serpentine in the tank (for the secondary circuit) and (B) two serpentines in the tank (for both primary and secondary circuits). An indirect optimal control technique based on Pontryagin's maximum principle was implemented. A detailed collector model and realistic meteorological data from both cold and warm seasons were used in applications. Configuration (A) gives better performance than configuration (B) but cannot be used during the cold season at higher geographical latitudes. The optimal operation strategy involves two-step up and down jumps between zero and a maximum allowable fluid flow rate in the primary circuit. During days with overcast sky the pump in the primary circuit operates almost continuously. During days with cloudy or clear sky the pump often stops. The heat provided to the user increases when the maximum fluid flow rate increases. This applies to both configurations (A) and (B). In case of configuration (B) the heat provided to the user becomes rather constant at higher flow rates.

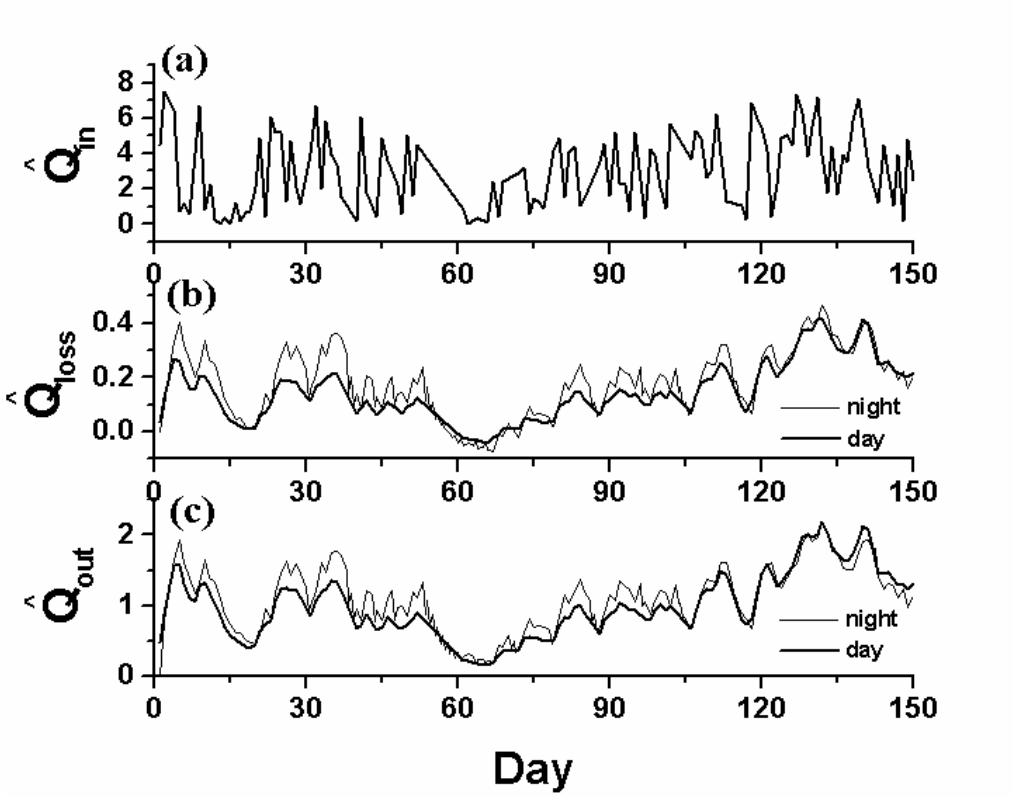

Fig. 3. Dependence on day during cold season of: (a) thermal energy $\hat{Q}_{in}$ [kWh] accumulated during a day in the water storage tank, (b) thermal energy lost through the walls of the water storage tank, $\hat{Q}_{loss}$ [kWh] and (c) thermal energy $\hat{Q}_{out}$ [kWh] supplied to the user. Results for day-time and night-time are presented separately in cases (b) and (c).

Figure 3 shows some results. When a constant flow rate strategy is adopted, there is an optimum ratio between the volume of the storage tank and the area of the solar energy collection surface: $V_s / A \approx 33.3\ L/m^2$. The optimal control strategy does not exhibit such an optimum: the thermal energy supply to the user (slightly) decreases by increasing the ratio V_s / A.

4. Optimal operation - maximum exergy extraction

As a fourth example, we refer to optimal control of flow in solar collectors for maximum exergy extraction [4]. The best operation strategies for open loop flat-plate solar collector systems are considered. A direct optimal control method (the TOMP algorithm) is implemented. A detailed

collector model and realistic meteorological data from both cold and warm seasons are used in applications. The maximum exergetic efficiency is low (usually less than 3 %), in good agreement with experimental measurements reported in literature.

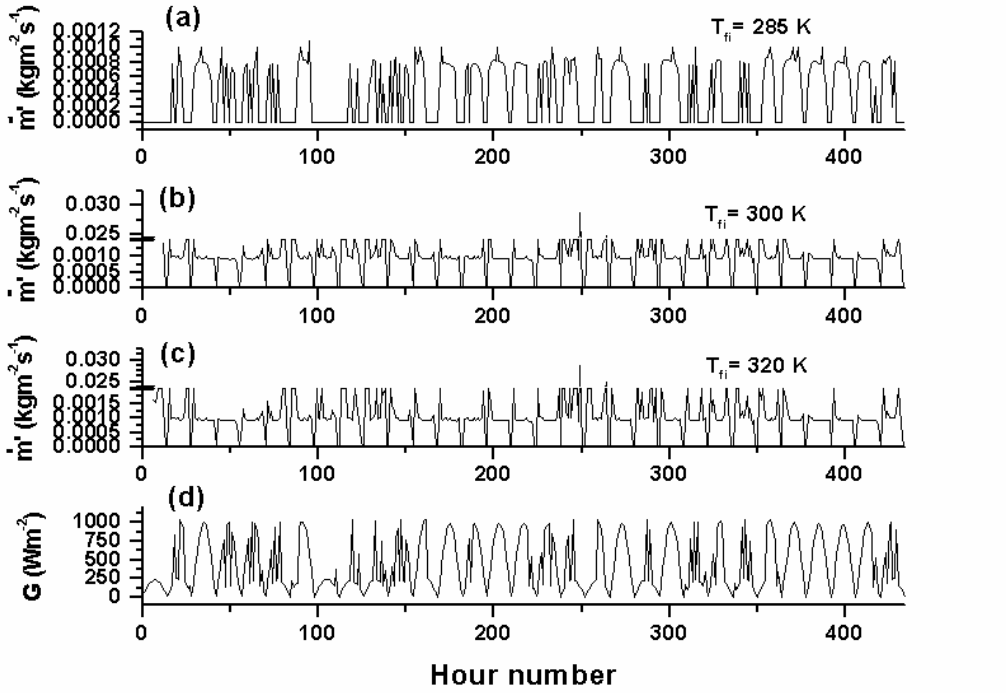

Fig. 5. Dependence of the optimum mass flow rate $\dot{m}'$ per unit collector surface area on hour number in July for different values of the inlet fluid temperature. (a) $T_{fi} = 285$ K ; (b) $T_{fi} = 300$ K (c) $T_{fi} = 320$ K . The dependence of the incident solar global irradiance on the hour number is also shown in (d). Only hours during the daylight time are represented.

The optimum mass flow rate increases near sunrise and sunset and by increasing the fluid inlet temperature. The optimum mass flow rate is well correlated with global solar irradiance during the warm season (Fig. 4). Also, operation at a properly defined constant mass flow rate may be close to the optimal operation.

References

[1] V Badescu, Optimum size and structure for solar energy collection systems, Energy 31 (2006) 1483-1499

[2] V Badescu, Optimum fin geometry in flat plate solar collector systems, Energy Conversion and Management, 47 (2006) 2397-2413

[3] V Badescu, Optimal control of flow in solar collector systems with fully mixed water storage tanks, Energy Conversion and Management 49 (2008) 169–184

[4] V Badescu, Optimal control of flow in solar collectors, for maximum exergy extraction, International Journal of Heat and Mass Transfer 50 (2007) 4311–4322

Critical Discharge from Flash Boiling Atomizer

T. Bar-Kohany (kahany@bgu.ac.il) and E. Sher (sher@bgu.ac.il)

The Sir Bargit Professor, The Pearlstone center for Aeronautical Studies, Department of Mechanical Engineering, Ben-Gurion University of the Negev, Beer-Sheva, Israel

Abstract

Flash-boiling atomization is one of the most effective means of generating a fine and narrow (size)-dispersed spray. It consists of an inlet and discharge orifices, connected by an expansion chamber. Employing a special designed injector**,** lead to optimized spray properties for lower injection pressures.

A mixture of liquids flows through the inlet orifice into the expansion chamber. The solute, usually the propellant, is characterized by a high vapour pressure. Flash boiling of the propellant occurs within the inlet orifice, after which the bubbles grow along the expansion chamber. The growth process continues until the solvent, the liquid to be sprayed, is no longer a continuous medium, but rather large droplets, separated by the propellant's vapour. The mixture than exits through the discharge orifice, and further atomizes, usually by shear mechanisms.

The higher the number of the vapour nuclei created during the flash boiling process, the smaller the droplets that will be created just prior to discharging. If so, than one must strive to design an atomizer in which the metastable degree of the propellant will be the highest possible, i.e. phase change at the spinodal limit.

However, it was found that the optimal discharge occurs when the 2Phase mixture discharges in a critical regime, at high volume fraction, according to the ***Slip Frozen Model*** (**SFM**). Namely, when the vapour discharge at sound velocity, maximal slip prevail, thus enhancing the shear atomization, outside the atomizer.

Rigorous and General Definition of Thermodynamic Entropy. Part II: Temperature of a Thermal Reservoir and Entropy

Gian Paolo Beretta* and Enzo Zanchini†

Assumption 1: **restriction to normal system**. We call *normal system* any system A that, starting from every state, can be changed to a non-equilibrium state with higher energy by means of a weight process for A in which the regions of space $\boldsymbol{R}^A$ occupied by the constituents of A have no net change. From here on, we consider only normal systems.

Comment. In traditional treatments of thermodynamics, Assumption 1 is *not stated explicitly, but it is used*, for example when one states that any amount of work can be transferred to a thermal reservoir by a stirrer.

Theorem 1. Impossibility of a PMM2. If a normal system A is in a stable equilibrium state, it is impossible to lower its energy by means of a weight process for A in which the regions of space $\boldsymbol{R}^A$ occupied by the constituents of A have no net change.

Proof. (Figure 1) Suppose that, starting from a stable equilibrium state A_{se} of A, by means of a weight process Π_1 with positive work $W^{A\rightarrow} = W > 0$, the energy of A is lowered and the regions of space $\boldsymbol{R}^A$ occupied by the constituents of A have no net change. On account of Assumption 1, it would be possible to perform a weight process Π_2 for A in which the regions of space $\boldsymbol{R}^A$ occupied by the constituents of A have no net change, the weight M is restored to its initial state so that the positive amount of energy $W^{A\leftarrow} = W > 0$ is supplied back to A, and the final state of A is a nonequilibrium state, namely, a state clearly different from A_{se}. Thus, the zero-work sequence of weight processes (Π_1, Π_2) would violate the definition of stable equilibrium state.

Second Law. Among all the states of a system A such that the constituents of A are contained in a given set of regions of space $\boldsymbol{R}^A$, there is a unique stable equilibrium state for every value of the energy E^A.

Lemma 1. Any stable equilibrium state A_s of a system A is accessible via an irreversible zero-work weight process from any other state A_1 with the same regions of space $\boldsymbol{R}^A$ and the same value of the energy E^A.

Proof. By the first law and the definition of energy, A_s and A_1 can be interconnected by a zero-work weight process for A. However, a zero-work weight process from A_s to A_1 would violate the definition of stable equilibrium state. Therefore, the process must be in the direction from A_1 to A_s. The absence of a zero-work weight process in the opposite direction, implies that any zero-work weight process from A_1 to A_s is irreversible.

Mutual stable equilibrium states. We say that two stable equilibrium states $A_{\rm se}$ and $B_{\rm se}$ are *mutual stable equilibrium states* if, when A is in state $A_{\rm se}$ and B in state $B_{\rm se}$, the composite system AB is in a stable equilibrium state. The definition holds also for a pair of states of the same system: in this case, system AB is composed of A and of a duplicate of A.

Thermal reservoir. We call *thermal reservoir* a closed and always separable system R with a single constituent, contained in a fixed region of space, with a vanishing external force field, and with values of the energy restricted to a finite range such that all the stable equilibrium states of R are mutual stable equilibrium states.

Comment. Every single-constituent system without internal boundaries and applied external fields, and with a number of particles of the order of one mole (so that the *simple system* approximation as defined in Ref. [1, p.263] applies), when restricted to a fixed region of space of appropriate volume and to the range of energy values corresponding to the so-called *triple-point* stable equilibrium states, is a thermal reservoir.

Assumption 2. Equivalent thermal reservoirs. If R' and R'' are thermal reservoirs with the same constituent, then every stable equilibrium state of R' is in mutual stable equilibrium with any stable equilibrium state of R''. Then, R' and R'' are called *equivalent thermal reservoirs*.

*Università di Brescia, Italy, beretta@ing.unibs.it
†Università di Bologna, Italy, enzo.zanchini@unibo.it

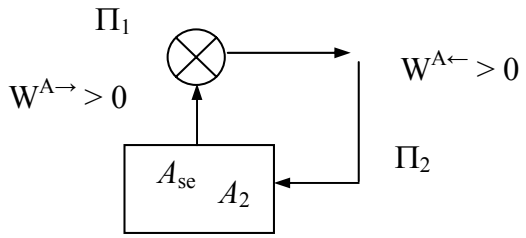

Figure 1: Schematic illustration of the proof of Theorem 1.

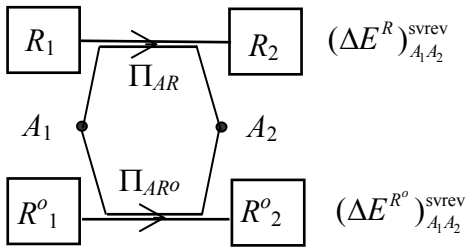

Figure 2: Schematic illustration of the processes used to define the temperature of a thermal reservoir.

Reference thermal reservoir. A thermal reservoir with a constituent chosen once and for all, will be called a *reference thermal reservoir*. To fix ideas, we will choose water as the constituent of our reference thermal reservoir.

Standard weight process. Given a pair of states (A_1, A_2) of a system A and a thermal reservoir R, we call *standard weight process* for AR from A_1 to A_2 a weight process for the composite system AR in which the end states of R are stable equilibrium states. We denote by $(A_1R_1 \rightarrow A_2R_2)^{\rm sw}$ a standard weight process for AR from A_1 to A_2 and by $(\Delta E^R)^{\rm sw}_{A_1A_2}$ the corresponding energy change of the thermal reservoir R.

Assumption 3. Every pair of states $(A_1,\ A_2)$ of a system A can be interconnected by a reversible standard weight process for AR, where R is an arbitrarily chosen thermal reservoir.

Theorem 2. For a given system A and a given reservoir R, among all the standard weight processes for AR between a given pair of states $(A_1,\ A_2)$ of A, the energy change $(\Delta E^R)^{\rm sw}_{A_1A_2}$ of the thermal reservoir R has a lower bound which is reached if and only if the process is reversible.

The proof of Theorem 2 is omitted here, for brevity.

Theorem 3. Let R' and R'' be any two thermal reservoirs and consider the energy changes, $(\Delta E^{R'})^{\rm swrev}_{A_1A_2}$ and $(\Delta E^{R''})^{\rm swrev}_{A_1A_2}$ respectively, in the reversible standard weight processes $\Pi_{AR'} = (A_1R'_1 \rightarrow A_2R'_2)^{\rm swrev}$ and $\Pi_{AR''} = (A_1R''_1 \rightarrow A_2R''_2)^{\rm swrev}$, where $(A_1,\ A_2)$ is an arbitrarily chosen pair of states of any closed system A. Then the ratio $(\Delta E^{R'})^{\rm swrev}_{A_1A_2}/(\Delta E^{R''})^{\rm swrev}_{A_1A_2}$:
a) is positive;
b) depends only on R' and R'', *i.e.*, it is independent of *(i)* the initial stable equilibrium states of R' and R'', *(ii)* the choice of system A, and *(iii)* the choice of states A_1 and A_2;
c) is unity if R' and R'' are equivalent thermal reservoirs.

The proof of Theorem 3 is omitted here, for brevity.

Temperature of a thermal reservoir. (Figure 2) Let R be a given thermal reservoir and R^o a reference thermal reservoir. Select an arbitrary pair of states $(A_1,\ A_2)$ of a system A and consider the energy changes $(\Delta E^R)^{\rm swrev}_{A_1A_2}$ and $(\Delta E^{R^o})^{\rm swrev}_{A_1A_2}$ in two reversible standard weight processes from A_1 to A_2, one for AR and the other for AR^o, respectively. We call *temperature* of R the positive quantity

$$T_R = T_{R^o}\ \frac{(\Delta E^R)^{\rm swrev}_{A_1A_2}}{(\Delta E^{R^o})^{\rm swrev}_{A_1A_2}}\ , \tag{1}$$

where T_{R^o} is a positive constant associated arbitrarily with the reference thermal reservoir R^o. If for R^o we select a thermal reservoir having water as constituent and we set $T_{R^o} = 273.16$ K, we obtain the Kelvin temperature scale. Clearly, the temperature T_R of R is defined only up to an arbitrary multiplicative constant.

Corollary 2. The ratio of the temperatures of two thermal reservoirs, R' and R'', is independent of the choice of the reference thermal reservoir and can be measured directly as

$$\frac{T_{R'}}{T_{R''}} = \frac{(\Delta E^{R'})^{\rm swrev}_{A_1A_2}}{(\Delta E^{R''})^{\rm swrev}_{A_1A_2}}\ , \tag{2}$$

where $(\Delta E^{R'})^{\rm swrev}_{A_1A_2}$ and $(\Delta E^{R''})^{\rm swrev}_{A_1A_2}$ are the energy changes of R' and R'' in two reversible standard weight processes, one for AR' and the other for AR'', which interconnect the same pair of states $(A_1,\ A_2)$.

Proof. Let $(\Delta E^{R^o})^{\rm swrev}_{A_1A_2}$ be the energy change of the reference thermal reservoir R^o in any reversible standard

weight process for AR^o which interconnects the same states (A_1, A_2) of A. From Eq. (1) we have

$$T_{R'} = T_{R^o} \frac{(\Delta E^{R'})^{\rm swrev}_{A_1A_2}}{(\Delta E^{R^o})^{\rm swrev}_{A_1A_2}} \quad , \quad T_{R''} = T_{R^o} \frac{(\Delta E^{R''})^{\rm swrev}_{A_1A_2}}{(\Delta E^{R^o})^{\rm swrev}_{A_1A_2}} \quad , \tag{3}$$

so that the ratio $T_{R'}/T_{R''}$ is given by Eq. (2).

Corollary 3. Let (A_1, A_2) be any pair of states of system A, and let $(\Delta E^R)^{\rm swrev}_{A_1A_2}$ be the energy change of a thermal reservoir R with temperature T_R, in any reversible standard weight process for AR from A_1 to A_2. Then, for the given system A, the ratio $(\Delta E^R)^{\rm swrev}_{A_1A_2}/T_R$ depends only on the pair of states (A_1, A_2), *i.e.*, it is independent of the choice of reservoir R and of its initial stable equilibrium state R_1.

Proof. Let us consider two reversible standard weight processes from A_1 to A_2, one for AR' and the other for AR'', where R' is a thermal reservoir with temperature $T_{R'}$ and R'' is a thermal reservoir with temperature $T_{R''}$. Then, equation (2) yields

$$\frac{(\Delta E^{R'})^{\rm swrev}_{A_1A_2}}{T_{R'}} = \frac{(\Delta E^{R''})^{\rm swrev}_{A_1A_2}}{T_{R''}} \quad . \tag{4}$$

Definition of (thermodynamic) entropy, proof that it is a property. Let (A_1 , A_2) be any pair of states of a system A, and let R be an arbitrarily chosen thermal reservoir placed in the environment B of A. We call *entropy difference* between A_2 and A_1 the quantity

$$S^A_2 - S^A_1 = -\frac{(\Delta E^R)^{\rm swrev}_{A_1A_2}}{T_R} \tag{5}$$

where $(\Delta E^R)^{\rm swrev}_{A_1A_2}$ is the energy change of R in any reversible standard weight process for AR from A_1 to A_2, and T_R is the temperature of R. On account of Corollary 3, the right hand side of Eq. (5) is determined uniquely by states A_1 and A_2; therefore, entropy is a property of A.
Let A_0 be a reference state of A, to which we assign an arbitrarily chosen value of entropy S^A_0. Then, the value of the entropy of A in any other state A_1 of A is determined uniquely by the equation

$$S^A_1 = S^A_0 - \frac{(\Delta E^R)^{\rm swrev}_{A_1A_0}}{T_R} \quad , \tag{6}$$

where $(\Delta E^R)^{\rm swrev}_{A_1A_0}$ is the energy change of R in any reversible standard weight process for AR from A_0 to A_1, and T_R is the temperature of R. Such a process exists for every state A_1, on account of Assumption 3.

Theorem 4. Additivity of entropy differences. Consider the pairs of states ($C_1 = A_1B_1, C_2 = A_2B_2$) of the composite system $C = AB$. Then,

$$S^{AB}_{A_2B_2} - S^{AB}_{A_1B_1} = S^A_2 - S^A_1 + S^B_2 - S^B_1 \quad . \tag{7}$$

Proof. Let us choose a thermal reservoir R, with temperature T_R, and consider the sequence (Π_{AR}, Π_{BR}) where Π_{AR} is a reversible standard weight process for AR from A_1 to A_2, while Π_{BR} is a reversible standard weight process for BR from B_1 to B_2. The sequence (Π_{AR}, Π_{BR}) is a reversible standard weight process for CR from C_1 to C_2, in which the energy change of R is the sum of the energy changes in the constituent processes Π_{AR} and Π_{BR}, *i.e.*, $(\Delta E^R)^{\rm swrev}_{C_1C_2} = (\Delta E^R)^{\rm swrev}_{A_1A_2} + (\Delta E^R)^{\rm swrev}_{B_1B_2}$. Therefore:

$$\frac{(\Delta E^R)^{\rm swrev}_{C_1C_2}}{T_R} = \frac{(\Delta E^R)^{\rm swrev}_{A_1A_2}}{T_R} + \frac{(\Delta E^R)^{\rm swrev}_{B_1B_2}}{T_R} \quad . \tag{8}$$

Equation (8) and the definition of entropy (5) yield Eq. (7).

Comment. As a consequence of Theorem 4, if the values of entropy are chosen so that they are additive in the reference states, entropy results as an additive property.

Theorem 5. Let (A_1, A_2) be any pair of states of a system A and let R be a thermal reservoir with temperature T_R. Let $\Pi_{AR\rm irr}$ be any irreversible standard weight process for AR from A_1 to A_2 and let $(\Delta E^R)^{\rm swirr}_{A_1A_2}$ be the energy change of R in this process. Then

$$-\frac{(\Delta E^R)^{\rm swirr}_{A_1A_2}}{T_R} < S^A_2 - S^A_1 \quad . \tag{9}$$

Proof. Let $\Pi_{AR\rm rev}$ be any reversible standard weight process for AR from A_1 to A_2 and let $(\Delta E^R)^{\rm swrev}_{A_1A_2}$ be the energy change of R in this process. On account of Theorem 2,

$$(\Delta E^R)^{\rm swrev}_{A_1A_2} < (\Delta E^R)^{\rm swirr}_{A_1A_2} \quad . \tag{10}$$

Since T_R is positive, from Eqs. (10) and (5) one obtains

$$-\frac{(\Delta E^R)^{\rm swirr}_{A_1A_2}}{T_R} < -\frac{(\Delta E^R)^{\rm swrev}_{A_1A_2}}{T_R} = S_2^A - S_1^A \quad . \tag{11}$$

Theorem 6. Principle of entropy nondecrease. Let (A_1, A_2) be a pair of states of a system A and let $(A_1 \to A_2)_W$ be any weight process for A from A_1 to A_2. Then, the entropy difference $S_2^A - S_1^A$ is equal to zero if and only if the weight process is reversible; it is strictly positive if and only if the weight process is irreversible.

Proof. If $(A_1 \to A_2)_W$ is reversible, then it is a special case of a reversible standard weight process for AR in which the initial stable equilibrium state of R does not change. Therefore, $(\Delta E^R)^{\rm swrev}_{A_1A_2} = 0$ and by applying the definition of entropy, Eq. (5), one obtains

$$S_2^A - S_1^A = -\frac{(\Delta E^R)^{\rm swrev}_{A_1A_2}}{T_R} = 0 \quad . \tag{12}$$

If $(A_1 \to A_2)_W$ is irreversible, then it is a special case of an irreversible standard weight process for AR in which the initial stable equilibrium state of R does not change. Therefore, $(\Delta E^R)^{\rm swirr}_{A_1A_2} = 0$ and Equation (9) yields

$$S_2^A - S_1^A > -\frac{(\Delta E^R)^{\rm swirr}_{A_1A_2}}{T_R} = 0 \quad . \tag{13}$$

Moreover: if a weight process $(A_1 \to A_2)_W$ for A is such that $S_2^A - S_1^A = 0$, then the process must be reversible, because we just proved that for any irreversible weight process $S_2^A - S_1^A > 0$; if a weight process $(A_1 \to A_2)_W$ for A is such that $S_2^A - S_1^A > 0$, then the process must be irreversible, because we just proved that for any reversible weight process $S_2^A - S_1^A = 0$.

CONCLUSIONS

A general definition of thermodynamic entropy [2] is presented, based on operative definitions of all the concepts employed in the treatment, designed to provide a clarifying and useful, complete and coherent, minimal but general, rigorous logical framework suitable for unambiguous fundamental discussions on Second Law implications.

Operative definitions of system, state, isolated system, environment of a system, process, separable system, and system uncorrelated from its environment are stated, which are valid also in the presence of internal semipermeable walls and reaction mechanisms. The concepts of heat and of quasistatic process are never mentioned, so that the treatment holds also for nonequilibrium states, both for macroscopic and few particles systems.

A definition of thermal reservoir less restrictive than in previous treatments is adopted: it is fulfilled by any single-constituent simple system contained in a fixed region of space, provided that the energy values are restricted to a suitable finite range. The proof that entropy is a property of the system is completed by a new explicit proof that the entropy difference between two states of a system is independent of the initial state of the thermal reservoir chosen to measure it.

The definition of a reversible process is given with reference to a given *scenario*, *i.e.*, the largest isolated system whose subsystems are available for interaction; thus, the operativity of the definition is improved and the treatment becomes compatible also with old [3] and recent [4] interpretations of irreversibility in the quantum theoretical framework.

References

[1] E.P. Gyftopoulos and G.P. Beretta, *Thermodynamics. Foundations and Applications*, Dover, Mineola, 2005 (first edition, Macmillan, 1991).

[2] For the criteria which identify the *entropy of thermodynamics* among the many other concepts also called *entropy*, see E.P. Gyftopoulos and E. Cubukcu, Entropy: Thermodynamic definition and quantum expression, *Phys. Rev. E*, **55**, 3851 (1997).

[3] See, *e.g.*, G.N. Hatsopoulos and G.P. Beretta, Where is the entropy challenge?, in *Meeting the Entropy Challenge*, AIP Conf. Proc. Series, Vol. **1033**, 2008, p. 34; G.P. Beretta et al., Quantum thermodynamics: a new equation of motion for a single constituent of matter, *Nuovo Cimento B*, **82**, 169 (1984).

[4] See, *e.g.*, C.H. Bennett, The second law and quantum physics, p. 66, and S. Lloyd, The once and future second law of thermodynamics, p. 143, in *Meeting the Entropy Challenge*, AIP Conf. Proc. Series, Vol. **1033**, 2008; S. Goldstein et al., Canonical typicality, *Phys. Rev. Lett.*, **96**, 050403 (2006); L. Maccone, A quantum solution to the arrow-of-time dilemma, arXiv:quant-ph 0802.0438.

Thermal Diffusion Coefficients in Multicomponent Mixtures: Comparison between experimental and empirical values.

Pablo Blanco[1,2], David A. de Mezquia[2], M. Mounir Bou-Ali[2], Jose A. Madariaga[3], Carlos Santamaria[3] and J. Karl Platten[2,4]

[1]Forschungszentrum Juelich GmbH, IFF-Weiche Materie, D-52428 Juelich, Germany

[2]MGEP Mondragon Goi Eskola Politeknikoa, Loramendi 4, 20500 Mondragon, Spain

[3]UPV University of Basque Country, Apdo. 644, 48080 Bilbao, Spain

[4]University of Mons-Hainaut, 7000 Mons, Belgium

p.blanco@fz-juelich.de

Introduction

Larre *et al.*[1] proposed an empirical additive rule to predict the thermal diffusion coefficient of a component in a ternary mixture from the combination of the corresponding thermal diffusion coefficients of the binary mixtures. More recently, Bou-Ali and Platten[2] determined the thermal diffusion coefficients of the three components in the ternary mixture 1,2,3,4-tetrahydronaphthalene (THN), isobutylbenzene (IBB) and normal dodecane (nC12) with mass fraction ratio 1:1:1 at 25ºC. They verified the empirical additive rule and the results showed that this additive rule[1] was "not too bad" at least for the only case that was investigated. Leahy-Dios *et al.*[3] have provided the thermal diffusion coefficients of the components in the ternary mixtures composed of normal octane (nC$_8$), normal decane (nC$_{10}$) and 1-methylnaphthalene (MN) with mass fraction ratios 1:1:1 and 1:1:4 at 22.5ºC, using the same experimental technique as in Ref. [2]. They pointed out that for the mixture with mass fraction ratio 1:1:4 the additive rule[1] does not work. Therefore, the main goal of this study is to extend the previous studies to more ternary mixtures, especially with different mass fraction ratios, in order to verify the empirical additive rule[1].

Summary

In this study, we present a comparison between experimental results with ternary mixtures obtained from two different configurations of thermogravitational columns, cylindrical and parallelepiped or flat. Thermal diffusion coefficients of six ternary mixtures composed of 1,2,3,4-Tetrahydronaphthalene-Isobutylbenzene-

nDodecane and 1,2,3,4-Tetrahydronaphthalene-Isobutylbenzene-nDecane with different mass concentrations are determined at 25 ºC. Thermal diffusion coefficients of thirteen binary mixtures composed of various combinations and mass fractions of these four liquids were also determined at 25 ºC. The experimental results show that the thermal diffusion coefficients of the components in ternary mixtures can be determined reasonably accurately from a suitable combination of their corresponding thermal diffusion coefficients in binaries with specific concentration of the components[1]. Additionally, we propose new correlations that improve the prediction of the ternary thermal diffusion coefficients:

$$\left(D_T^i\right)_{ijk}\frac{\mu_{ijk}}{\alpha_{ijk}}=\left(D_T^i\right)_{ij}c_i c_j\frac{\mu_{ij}}{\alpha_{ij}}+\left(D_T^i\right)_{ik}c_i c_k\frac{\mu_{ik}}{\alpha_{ik}}$$

D_T^i is the thermal diffusion coefficient of *i* component in the mixture. α is the thermal expansion coefficient and μ is the dynamic viscosity. The subscripts of α and μ indicate the components of the binary or ternary mixtures.

References

[1]J. Larre, J.K. Platten and G. Chavepeyer, *Int. J. Heat Mass Transfer*, **1997**, *40*, 545.

[2]M.M. Bou-Ali and J.K. Platten, *J Non-Equilibrium Thermod*. **2005**, *30*, 385.

[3]A. Leahy-Dios, M.M. Bou-Ali, J.K. Platten and A. Firoozabadi, *J. Chem. Phys*. **2005**, *122* 234502-1.

Thermoosmotic transfer of ferrocolloids through a capillary porous layer in the presence of uniform magnetic field

Blums E., Kronkalns G., Mezulis A., Sints V.
Institute of Physics, University of Latvia, Salaspils, LV-2169, Latvia
eblums@sal.lv

Magnetic nanoparticles and ferrocolloids have interesting medical application possibilities. One the most popular novel idea is magnetic hyperthermia of tissues, particularly for cancer treatment. Unsteady magnetic field of relatively low amplitude and of median frequency (20 – 80 kHz) may cause energy dissipation in colloidal particles of up to 1 – 2 W/g. Such a heating intensity is quite enough to realize the medical hyperthermia treatment. However, besides the heating measurements it is important to investigate the dynamics of particle transfer in tissues because their heating intensity depends on the particle concentration.

The present paper is devoted to studying the ferroparticle transfer in non-isothermal capillary porous layer in the presence of a steady uniform magnetic field. The mass transfer experiments are performed employing two equal cylindrical volumes kept at different temperatures and united by chemically stable wide-pore capillary layer. The examined ferrofluid consists of magnetite nanoparticles coated with oleic acid and suspended in tetradecane. First experiments [1] showed that the measured thermoosmotic pressure difference is directed toward the temperature gradient. The unsteady pressure difference primarily grows and after reaching a maximum starts to decrease exponentially. Homogeneous magnetic field, directed normally to the membrane, causes a remarkable growth of the pressure difference. If the magnetic field is aligned parallel to the membrane, the observed pressure changes are significantly less.

The experimental results are interpreted in frame of linear theory of irreversible thermodynamics [2]. Three fluxes j_i (the flow of solvent j_1, the particle flux j_2 and the heat flux j_3) contain three summands which are proportional to thermodynamic driving forces $\nabla\varphi_i$ (gradients of pressure P, particle chemical potential φ_c and temperature T). In long time experiments the unsteady pressure difference relaxes to a zero. This concedes assuming that the mass transfer through the porous layer is influenced mostly by osmotic processes whereas the particle transport (convective, diffusion and thermodiffusion) is small. Under such simplification there arises a possibility to calculate from pressure measurements the filtration coefficient α_{11}, the coefficient of osmosis α_{12} and that of thermoosmosis α_{13}. The Onsager relations $\alpha_{ik}= \alpha_{ki}$ allow evaluating also the coefficient of convective particle transfer α_{21}. Obtained values of these coefficients confirm the assumption of predomination of filtration and osmosis in the examined system. External magnetic field induces an additional pressure difference across the porous layer and evokes an increase in the chemical potential of particles [3]. Due to dependence of fluid magnetization on both the particle concentration and the temperature, the normal field effects manifest themselves as an increase in thermoosmotic pressure and some reduction of solutal osmosis. Longitudinal magnetic field causes only small changes in particle mass diffusion transfer. The calculation results agree relatively well with experiments.

References:

[1] E. Blums, G. Kronkalns, M. Maiorov, In: Lecture notes of the 8th International Meeting on Thermodiffusion, Thermal Nonequilibrium, Eds. S. Wiegand, W. Kohler, J. K. G. Dhont, Forshungscentrum Julich, 2008, **3**, 169 – 174.

[2] N. V. Churaev. Physical Chemistry of Heat and Mass Transfer Processes in Porous Media, Moscow, Himiya, 1990.

[3] E. Blums, A. Cebers and M. M. Maiorov. Magnetic Fluids, Walter de Gryuter & Co., Berlin - New-York, 1997.

On Optimal Reconstruction of Constitutive Relations

V. Bukshtynov[a], O. Volkov[b], and B. Protas[b]

[a]School of Computational Engineering and Science, McMaster University
Hamilton, Ontario L8S 4K1, Canada
[b]Department of Mathematics and Statistics, McMaster University
Hamilton, Ontario L8S 4K1, Canada
Emails: bukshtu@math.mcmaster.ca, ovolkov@math.mcmaster.ca, bprotas@mcmaster.ca

In this investigation we develop a computational framework for optimal reconstruction of isotropic constitutive relationships between thermodynamic variables based on measurements obtained in a spatially–extended system. In other words, assuming the constitutive relation in the following general form

$$\begin{bmatrix}\text{thermodynamic}\\ \text{flux}\end{bmatrix} = k\,(\text{state variables})\begin{bmatrix}\text{thermodynamic}\\ \text{“force”}\end{bmatrix}, \tag{1}$$

our approach allows us to reconstruct the dependence of the transport coefficient k on the state variables consistent with the assumed governing equation(s). Constitutive relations in the form (1) arise in many areas of nonequilibrium thermodynamics and continuum mechanics. To fix attention, but without loss of generality, in the present investigation we focus on a heat conduction problem in which the heat flux $\mathbf{q}$ represents the thermodynamic flux, whereas the temperature gradient ∇T is the thermodynamic "force", so that relation (1) takes the specific form

$$\mathbf{q}(\mathbf{x}) = k(T)\,\nabla T, \qquad \mathbf{x}\in\Omega, \tag{2}$$

where $\Omega\in\mathbb{R}^n$, $n=1,2,3$ is the spatial domain on which the problem is formulated. We note that by assuming the function $k:\mathbb{R}\to\mathbb{R}$ to be given by a constant, we recover the well–known linear Fourier law of heat conduction. While expressions for the transport coefficients such as $k(T)$ are typically derived using methods of statistical thermodynamics, in the present investigation we will show how to reconstruct the function $k(T)$ based on some available measurements of the spatial distribution of the state variable T combined with the relevant conservation law. Such a technique could be useful to systematically adjust the form of the constitutive relationship derived theoretically to better match actual experimental data. Combining constitutive relation (2) with the conservation of energy, we obtain a partial differential equation (PDE) describing the distribution of the temperature T in the domain Ω corresponding to the distribution of heat sources $g:\Omega\to\mathbb{R}$ and suitable boundary conditions (for example, of the Dirichlet type)

$$-\nabla\cdot[k(T)\,\nabla T] = g \qquad \text{in } \Omega, \tag{3a}$$

$$T = T_b \qquad \text{on } \partial\Omega, \tag{3b}$$

where T_b denotes the boundary temperature. We note that, for all values of T, we should have $k(T)>0$ which follows from the second principle of thermodynamics, but is also required for the mathematical well–posedness of elliptic boundary value problem (3). The specific problem we address in this investigation is formulated as follows. Given a set of "measurements" $\{\tilde{T}_i\}_{i=1}^M$ of the state variable (temperature) T at a number of points $\{\mathbf{x}_i\}_{i=1}^M$ in the domain Ω, we seek to reconstruct the constitutive relation $k(T)$ such that solutions of problem (3) obtained with this reconstructed function will fit best the available measurements. This is in fact an example of an "inverse problem" i.e., one in which one tries to determine the cause (i.e., the constitutive relation) corresponding to some known effects (i.e., pointwise measurements of the temperature field). An approach commonly used to solve inverse problems consists in reformulating them as minimization problems. This is done by defining the cost functional $\mathcal{J}:\mathbb{R}\to\mathbb{R}$ as

$$\mathcal{J}(k) \triangleq \frac{1}{2}\sum_{i=1}^{M}\left[\tilde{T}_i - T(\mathbf{x}_i;k)\right]^2, \tag{4}$$

where the dependence of the temperature field $T(\cdot;k)$ on the form of the constitutive relation $k=k(T)$ is given by governing equation (3). Assuming that the functions $k(T)$ characterizing the constitutive relation belong to a Hilbert (function) space $\mathcal{X}$, the optimal reconstruction $\hat{k}$ is obtained as the minimizer of cost functional (4), i.e.,

$$\hat{k} = \operatorname{argmin}_{k\in\mathcal{X}}\mathcal{J}(k). \tag{5}$$

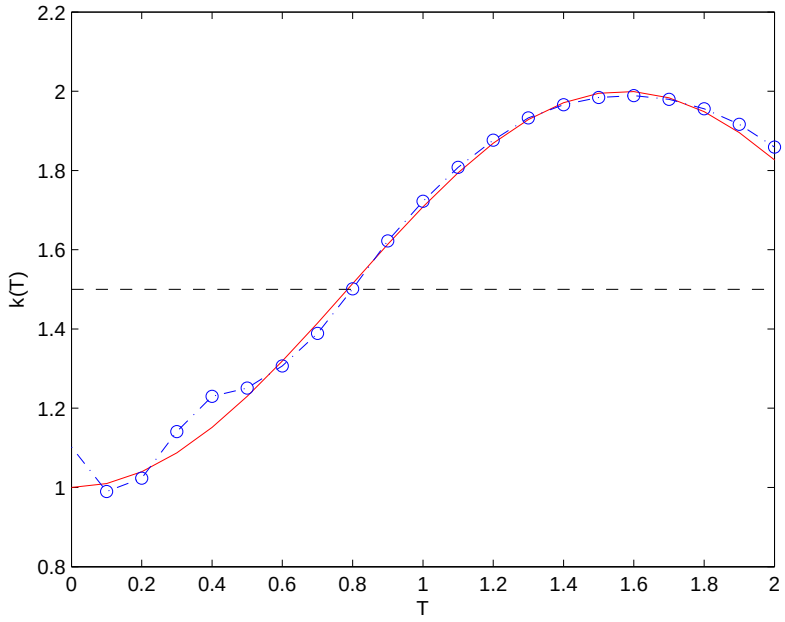

Figure 1: The figure represents (solid line) the actual constitutive relation $k(T)$ and (dotted line with symbols) its optimal reconstruction $\hat{k}(T)$ obtained using the proposed algorithm starting from (dashed line) a constant value k_0 as the initial guess. The measurements $\{\tilde{T}_i\}_{i=1}^M$ were obtained at $M = 10$ points uniformly distributed in over the domain $\Omega = [-1,1]$.

The minimizer $\hat{k}$ is characterized by the first–order optimality conditions which require the Gâteaux differential of cost functional (4), defined as $\mathcal{J}'(k;k') = \lim_{\varepsilon\to 0}\varepsilon^{-1}[\mathcal{J}(k+\varepsilon k') - \mathcal{J}(k)]$ to vanish for all perturbations $k' \in \mathcal{X}$, i.e.,

$$\mathcal{J}'(k;k') = 0. \tag{6}$$

The minimizer $\hat{k}$ can be computed with the following gradient descent algorithm as $\hat{k} = \lim_{n\to\infty} k^{(n)}$, where

$$\begin{cases} k^{(n+1)} = k^{(n)} - \tau^{(n)}\nabla_k \mathcal{J}(k^{(n)}), & n = 1,\dots, \\ k^{(1)} \quad\;\; = k_0, \end{cases} \tag{7}$$

in which $\nabla_k \mathcal{J}(k)$ represents the *gradient* of cost functional $\mathcal{J}(k)$ with respect to the control variable k, $\tau^{(n)}$ is the length of the jump along the descent direction at the n–th iteration, whereas k_0 is the initial guess taken, for instance, as a constant corresponding to a linear constitutive relation (2), or some other approximate theoretical prediction. For the sake of clarity, formulation (7) represents the steepest–descent algorithm, however in practice one typically uses more advanced minimization techniques, such as the conjugate gradient method, or one of the quasi–Newton techniques [1]. We note that, since minimization problem (4)–(5) is in general nonconvex, condition (6) characterizes only a *local*, rather than *global*, minimizer.

The key ingredient of minimization algorithm (7) is computation of the cost functional gradient $\nabla_k \mathcal{J}(k)$. We emphasize that, since $k = k(T)$ is a continuous variable, the gradient $\nabla_k \mathcal{J}(k)$ represents in fact an infinite–dimensional sensitivity of $\mathcal{J}(k)$ to perturbations of $k(T)$. In our presentation we will show that the gradient can be obtained from the Gâteaux differential using the Riesz representation theorem

$$\mathcal{J}'(k;k') = \left\langle \nabla_k \mathcal{J}(k), k' \right\rangle_{\mathcal{X}}, \tag{8}$$

where $\langle\cdot,\cdot\rangle_{\mathcal{X}}$ represents the inner product in the Hilbert space $\mathcal{X}$, and suitably defined *adjoint variables* [2]. These adjoint variables (Lagrange multipliers) are obtained from the solution of the corresponding *adjoint system* which is at the heart of the proposed reconstruction algorithm. Since in general inverse problems often tend to be ill–posed, care must be taken to perform suitable regularization. We add that problems in which the transport coefficient k is a function of the space variable

x, rather than the state variable T, i.e., $k = k(\mathbf{x})$, have received some attention in the literature [3], and are now relatively well understood. The originality of our contribution consists in that, in contrast to such "parameter estimation" problems, we address estimation of state–dependent, and therefore nonlinear, constitutive relations. We demonstrate that, as a matter of fact, the mathematical structure of this new problem is quite different from the structure of the parameter estimation problem. In Figure 1 we present some sample results obtained with our approach in which we were able to reconstruct the actual constitutive relation $k(T)$ that was used to obtain the initial measurements. Our future work will focus on generalizing our approach to more complex systems arising in fluid mechanics and nonequilibrium thermodynamics. This will include problems governed by time–dependent equations expressing the conservation of mass, momentum and energy, and involving also constitutive relations with anisotropic transport coefficients.

References

[1] J. Nocedal and S. Wright, "Numerical Optimization", Springer, (2002).

[2] M. D. Gunzburger, "Perspectives in flow control and optimization", SIAM, Philadelphia, (2003).

[3] A. Tarantola, "Inverse Problem Theory and Methods for Model Parameter Estimation", SIAM, (2005).

Critical behaviour of non-equilibrium nanoemitter radiation in a percolation material at the mesoscopic level

G. Burlak[1], A. Díaz-de-Anda[1], Yu. Karlovich[2], and A.B. Klimov[3]

[1]Centro de Investigación en Ingeniería y Ciencias Aplicadas, [2]Facultad de Ciencias. Universidad Autónoma del Estado de Morelos, Cuernavaca, Mor. México. [3]Departamento de Física, Universidad de Guadalajara, Revolución 1500, Guadalajara, Jalisco, 44420, México.
gburlak@uaem.mx

The nonequilibrium radiation of photons by disordered nanoemitters incorporated into three-dimensional (3D) clusters in percolation solids is an area of active research. If the concentration of clusters exceeds a certain threshold value, then in the system it is formed spanning (infinite) cluster, penetrating the entire volume. This cluster qualitatively changes the dynamic properties of the medium and produces a generalized conductivity in the system which originally does not possess such a property. In such geometry, the spanning cluster serves as the "backbone", or a set of bonds, through which the field radiation of nanosources can flow.

The percolation problem is concerned with elementary geometrical objects (spheres, sticks, sites, bonds, etc.) placed randomly in a d-dimensional lattice or continuum. The objects have a well-defined connectivity radius, and two objects are said to communicate if the distance between them is less than this radius. One is interested in how many objects can form a cluster of communication, and especially, when and how the clusters become infinite.

The order parameter **Ps** in such a medium is defined as the ratio of the number of pores belonging to the spanning cluster to the general number of pores. It is obvious that **Ps** is distinct from zero only when exceeding the threshold concentration (0.31 for *3D* case).

After formation of the spanning cluster, the opportunity to incorporate the nanoemitters through such the opened cluster structure becomes possible. It is important that the cross-section of clusters normally exceeds the field wavelength; therefore, such a network forms the open waveguide system by means of which the passage of an intensive laser short pulse behaves as the field pump. As a result, the two-level nanoemitters incorporated into such a cluster can be raised to the excited state. For simplification of the problem, we have used the natural assumption that nanosources are incorporated only in those clusters which have a connection with the entrance (input for laser pump) side of the sample. Since the spatial cluster structure in the medium does not change with time, the corresponding order parameter Ps is a static property of the system. However, the situation becomes more complicated for the case of nonequilibrium radiating nanoemitters incorporated in such disordered structure.

The analysis of such a system consists of two steps, and in general it requires quite long computations. The first step deals with identification of the spanning cluster **Ps** as a function of probability occupation **p**. In the second step, the field properties of radiating nanoemitters incorporated into the percolation structure (known from the first step) are calculated with the use of technique *FDTD*.

We studied the field radiation of disordered nanoemitters incorporated in three-dimensional spanning clusters in a percolation material. If the concentration of defects exceeds the threshold value, in the system a spanning cluster penetrating the entire medium is formed. The intensity of the radiated field plays the role of the dynamic field order parameter at the percolation phase transition. The subcritical clusters with nanoemitters represent a low-density statistically disordered phase. However, at the supercritical state with the spanning cluster fulfilled by nanoemitters occurs the raise of field intensity that allows to generate a high-density coherent field state (statistically ordered phase). In such a situation, the result is different for lossless and lossy mediums. For material with small losses, the long-term coherence arises in the supercritical area close to the percolation threshold. As a result, the dynamic non-monotonic behaviour of the field order parameter is formed. We found that such a property can be predicted from a simple 1D model that allows us to conclude that such a nonequilibrium behaviour emerges due to high contribution of the coherent nanoemitters in the area closely to the threshold of percolation.

As a result of numerical experiments, we have found that at the supercritical concentration of disordered nanosources the intensity of the field radiation increases sharply. In the lossy medium, or for emitters with random phases, the field order parameter **Pe** has well known equilibrium behaviour. However, the situation changes essentially for the coherent radiated nanoemitters in materials with small losses due to arising of field long-term coherence. As a result, the dynamic non-monotonic behaviour of the field order parameter raises that allows to reach the optimal field intensity already at **p** near 0.5.

This effect can allow the use of the disordered optical nanostructures with incorporated radiating nanoemitters in various applications of information technology. Since the position of the maximum field order parameter depends on the value of the source phases, it also allows the measurement of the level of coherency photons in disordered nanostructures.

Stationary droplet evaporation in the diffusive regime: diffusive flow, entropy production, Onsager's coefficients evaluation.

Cherevko K.V., Gavryushenko D.A., Sysoev V.M.

Physics Department, Kiev National University, 2(1) Glushkova av., Kiev, Ukraine, 03127
Kostia_Cherevko@univ.kiev.ua

Abstract
The diffusive regime of the drop evaporation process is investigated in the work on the basics of the fundamental equations of the linear irreversible processes thermodynamics. Therefore the full diffusion equation is used to take into account all the peculiarities of the investigated system on the very beginning of the investigation process. As the result the equation that describes the temperature distribution around the droplet is obtained. Mechanisms to explain the absence of the buffer gas diffusion towards the evaporating drop while the concentration gradient exists are found. The method to find Onsager's phenomenological coefficients from the drop evaporation experiments is proposed.

Introduction

Droplet aerosols are widely used in the different fields such as chemistry, medicine, and atmosphere physics. In many situations the evaporation of the drops from the substrate surface is of great interest [1]. Such systems require a lot of different factors to be taken into account [2, 3], but in any case the basics for the understanding the whole process is the model of the free drop evaporation in the buffer gas. The usual way to describe that process is to use the Fick's law with the constant diffusion coefficient and in such a way to calculate the diffusive flow. For the system in the thermostat this law is represented by the next equation:

$$J = -4\pi\rho^2 \frac{\partial n}{\partial \rho} D, \qquad (1)$$

where ρ is the radius in the spherical coordinates, D is the diffusion coefficient and n is the vapor concentration. It should be emphasized that in that case the diffusion coefficient is thought to be constant and is calculated by the means of the kinetic theory [5]. The classical Maxwell's formula could be obtained from that equation that gives the result for the diffusive flow:

$$J = 4\pi D r \left(n_0 - n_\infty \right), \qquad (2)$$

where $n_0 = n(r)$ - concentration in of the evaporating substance close to the drop, and n_∞ - is the concentration on the infinity. In the same time for the description of the real processes it is necessary to take into account a great number of the different corrections to the equation (2). They are the Stefan's flow correction, correctional terms that appear from the drop temperature variations and so on [4]. The very important thing that is to be emphasized is that all the correctional terms are introduced to the final result (2) but not to the original equation (1). Therefore, the particular problem is solved and the result is being modified for the common problem. Such an approach could not be called fundamental. Should be also mentioned that even consideration of all the correctional terms in some cases is not enough to describe the experimental data [6].

In such a way we can make a conclusion that the problem of finding the exact thermodynamic theory of the evaporation process, based on the fundamental equations of the linear irreversible process thermodynamics seems to be of high importance. That means that the common diffusion equation that includes addends connected with all the existing gradients should be solved and in such a way the characteristics of the process are to be found.

Model Description

The problem that is investigated in the work is the problem of the stationary drop evaporation process in the diffusive regime. The buffer gas is thought to be not able to dissolve in the droplet. This condition gives us a possibility to state that all the flows in the direction of the droplet are to be equal to zero. We assume that while evaporating the droplet doesn't change its shape and during all the process it stays ideally spherical. All the system is treated as being in the thermostat and all the external fields are neglected.

The system of differential [7] equations that fully describes the suggested model is based on the fundamental phenomenological law of the irreversible processes thermodynamics [8].

$$\begin{cases} J_1 = -\dfrac{4\pi r^2 L_1}{T}\cdot\left(\left(\dfrac{\partial\mu_1}{\partial n_1}\right)\cdot\nabla(n_1)+\left(\dfrac{\partial\mu_1}{\partial n_2}\right)\cdot\nabla(n_2)+\left(\dfrac{\partial\mu_{10}}{\partial T}\right)\cdot\nabla T-\left(\dfrac{\mu_{10}}{T}\right)\cdot\nabla T\right) \\ 0 = -\dfrac{4\pi r^2 L_2}{T}\cdot\left(\left(\dfrac{\partial\mu_2}{\partial n_1}\right)\cdot\nabla(n_1)+\left(\dfrac{\partial\mu_2}{\partial n_2}\right)\cdot\nabla(n_2)+\left(\dfrac{\partial\mu_{20}}{\partial T}\right)\cdot\nabla T-\left(\dfrac{\mu_{20}}{T}\right)\cdot\nabla T\right) \\ 0 = \nabla(n_1)+\nabla(n_2) \end{cases} \quad (3)$$

Temperature gradient in the drop evaporation process and entropy production function

The system of differential equations (3) gives the possibility to find the temperature gradient that is to appear due to the diffusion of the evaporating substance. We obtained the following result:

$$\frac{dT}{d\rho} = -2\frac{\dfrac{\partial\mu_2}{\partial n_1}}{\dfrac{\partial\mu_2}{\partial T}-\dfrac{\mu_2}{T}}\frac{dn_1}{d\rho} \quad (4)$$

As for the substance flow in contradiction to the classical approach the nonlinear flow dependence on concentration difference near the drop and on the infinity is found (fig. 1)

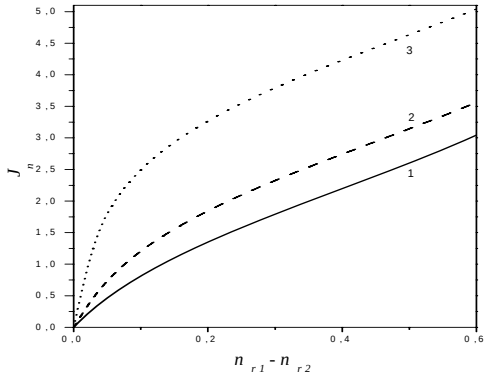

Fig. 1 Flow dependence $J_n = -\dfrac{J_1}{2kL_1}\dfrac{\rho_2-\rho_1}{\rho_1\rho_2}\rho^2$ on the concentration difference $n_{\rho_1} - n_{\rho_2}$ for the different n_{ρ_1}: 1 – 10^{-1}, 2 – $5\cdot10^{-2}$, 3 – 10^{-2}; n_{ρ_1} $7\cdot10^{-1}$

For the entropy production function the next equation is obtained:

$$\sigma = \langle 2k\rangle^2 L_1\left(\frac{r_1 r_2}{r_2-r_1}\right)^2\frac{1}{r^4}\left[\ln\frac{x_{r_2}}{x_{r_1}}-\ln\frac{1-x_{r_2}}{1-x_{r_1}}\right]^2 \quad (5)$$

On fig.2 the entropy production function dependence on the concentration difference is shown.

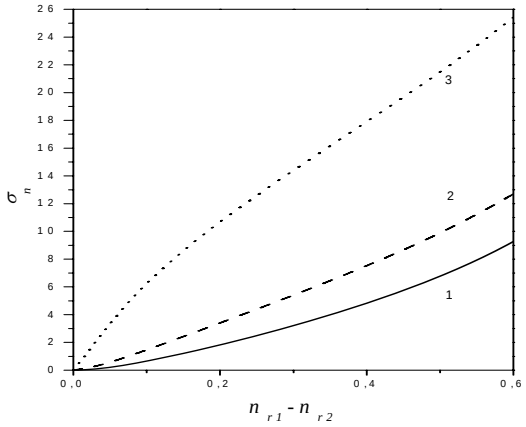

Fig. 2 Entropy production function $\sigma_n = \frac{\sigma}{\langle 2k \rangle^2 L_1}\left(\frac{r_2 - r_1}{r_1 r_2}\right)^2 r^4$ dependence on the concentration difference $n_{\rho_1} - n_{\rho_2}$ for the different n_{r_2} values: 1 – 10^{-1}, 2 – $5 \cdot 10^{-2}$, 3 – 10^{-2}; n_{ρ_1} $7 \cdot 10^{-1}$

One may see that the dependence differs from the quadratic one. Therefore, Entropy effects consideration in the mixture thermodynamic potentials leads to the quite strong difference of the obtained results from the classical one with the constant diffusion coefficient.

Conclusions

From the obtained results one can make a conclusion that in the case of the diffusive regime of the drop evaporation process the temperature gradient arises in the surrounding matter. The obtained results are in good correspondence with the results for the methanol and ethanol drops evaporation [9]. The existence of such a gradient allows explaining the absence of the buffer gas flow in the direction of the droplet when the concentration gradient exists.

The suggested approach shows the strong stabilizing effect in the flow dependence on concentration difference. For the simplest model of the mixture the entropy production function is very different from those obtained for the constant diffusion coefficient model in classical approach.

Te method to evaluate Onsager's kinetic coefficients from the drop evaporation experiments is proposed in the work.

The obtained results show that not in all cases it is possible to use the Fick's law with the constant diffusion coefficient. In some cases it is necessary to take into account its dependence on all the local parameters.

References

[1] S.P. Bugaev et al.: Plasma Chem. Plasma Proces Vol. 18(2) (1998), p. 247

[2] M. Cachile, O. Benichou, A.-M. Cazabat: Langmuir Vol. 18 (2002), p. 7985

[3] R.D. Deegan, O. Bakajin, T.F. Dupont, et al.: Nature Vol. 389 (1997), p. 827

[4] N.A. Fooks: Evaporation and grow of the droplets in the gas media, russian (publ. AS USSR, Moscow, 1954)

[5] J.O. Hirschfelder, Ch.F. Curtiss, R.B. Bird: *Molecular theory of gases and liquids* (Champman and Hall, London, 1954)

[6] V.N. Malnev, V.M. Nuzhnyi, O.A. Zagorodnya *J. Phys.: Condens. Matter* Vol. 14 (2002), p. 9469

[7] Cherevko K., Gavryushenko D., Sysoev V. *Ukrainian Physical Journal* V.52, I. 1 (2007), p.31-34.

[8] S.R. de Groot, P. Mazur: *Nonequilibrium thermodynamics* (NorthHolland, Amsterdam, 1962)

[9] R.J. Hopkins, J. Reid *J. Phys. Chem.* B Vol. 110 (2006), p. 3239

A new perspective on the form of first and second law in weakly nonlocal thermodynamics*

V. A. Cimmelli
Department of Mathematics and Computer Science,
University of Basilicata, 85100, Potenza, Italy
e-mail:vito.cimmelli@unibas.it

Properties of complex materials are not always localizable, since features as singularities interact with one another at a distance which can become relevant at a convenient scale [1]. Nonlocal effects become also important in miniaturized systems, such as various kinds of nano-wires and nano-tubes, since even a small difference of temperature, or electrical potential, over a small scale length may generate very high temperature gradients [2–4].

A simple way to take into account nonlocal effects is to introduce the gradients of the basic thermodynamic fields into the constitutive equations describing the material behavior. In such a case one is facing with weakly nonlocal continuum theories [5]. The classical formulation of second law of thermodynamics [6], which restricts the form of the constitutive functions, requires that the dissipation inequality

$$\varrho s_{,t} + \varrho s_{,i} v_i + \left(\frac{q_i}{\vartheta}\right)_{,i} \geq \varrho \frac{r}{\vartheta}, \tag{1}$$

with ϱ as the mass density, s as the specific entropy, ϑ as the absolute temperature, r as the radiative heat supply, $v_i, i = 1, 2, 3$, as the components of the velocity, q_i as the components of the heat flux, must be satisfied in any thermodynamic process, namely by any solution of the local balances of mass, linear and angular momentum and energy and, eventually, of additional governing equations (not necessarily in the balance form) ruling the evolution of some other thermodynamical parameters representing internal degrees of freedom of the system [7].

The most celebrated techniques for deriving the restrictions placed by second law of thermodynamics on the constitutive functions are the Coleman-Noll [8] and Liu [9] procedures. In the absence of any modification of the local form of first or second law of thermodynamics, both procedures lead to the conclusion that only the fluxes are nonlocal while the entropy and the absolute temperature may depend only on the unknown fields. Such a conclusion may generate serious discrepancies, because it renders some important classes of nonlocal materials, such as the Korteweg fluids, incompatible with second law [10, 11].

In order to circumvent these problems, and still remain in the framework of weakly nonlocal thermodynamics,[1], two different approaches can be found in the literature.

The first one modifies the local balance of energy, by supposing the existence of an energy extra-flux $\mathbf{u}$, due to the matter diffusion [15] or to the interstitial working of long range interactions [10, 16], such that it reads

$$\varrho \varepsilon_{,t} + \varrho \varepsilon_{,i} v_i - T_{ij} v_{i,j} + q_{i,i} - u_{i,i} = \varrho r, \tag{2}$$

with ε as the specific internal energy and $T_{ij} = T_{ji}, i, j = 1, 2, 3$, as the components of the Cauchy stress tensor .

The second one modifies the entropy inequality [17], by postulating the existence of an entropy extra-flux $\mathbf{k}$ such that Eq. (1) becomes

*In this talk we present some recent results obtained in cooperation with D. Jou (Barcelona), A. Sellitto (Potenza) and V. Triani (Potenza).

[1]It is worth noticing that a different theory, namely rational extended thermodynamics [12], postulates a local state space and regards the fluxes as independent thermodynamic variables. In such a case problems arise in dealing with some results from kinetic theory which would require a nonlocal state space, such as the celebrated Guyer-Krumhansl [13, 14] heat transport equation.

$$\varrho s_{,t} + \varrho s_{,i} v_i + \left(\frac{q_i}{\vartheta}\right)_{,i} + k_{i,i} \geq \varrho \frac{r}{\vartheta}. \tag{3}$$

Since the two modifications above are not equivalent and lead to different sets of thermodynamic restrictions, the choice of one of the two options should be decided on the base of additional information, either from experiments or from kinetic theory. Furthermore, even if we assume one of the two points of view above, problems arise in dealing with first order nonlocal constitutive equations, i.e. with the main part of the nonlocal continuum theories. This is due to the fact that the classical procedures allow the entropy to depend on the gradients of order n of the unknown fields if and only if the constitutive functions depend on the gradients of order $n + 1$. It is clear that this leads again to a local entropy in the case of first order non-locality [10, 15, 17].

The considerations above prove that in weakly nonlocal thermodynamics the form of the constitutive equations for the energy and entropy fluxes, is an open problem which deserves consideration.

The aim of this presentation is to illustrate an alternative approach to the problem above, which does not need to modify the basic thermodynamics represented by the classical balances of energy and entropy, because a different method of exploitation of second law is applied. The basic idea is to consider as additional constraints for the entropy inequality the gradient extensions of the governing equations up to the order of the gradients appearing into the constitutive equations [11, 18, 19]. That way, the number of the independent equations which constrain the entropy inequality is always equal to the number of independent thermodynamic variables. The method yields a nonlocal entropy even in the case of only first order non-locality.

As an application, we present some recent results concerning nonlinear heat conduction in miniaturized systems and in crystalline dielectrics [20]. In this case a nonlocal entropy is particularly interesting, since the nonlocal terms contribute important nonlinear terms in the heat transport equation. Modelling heat transport in solids, we use the concept of non-equilibrium semi-empirical temperature [21–23]. Such a concept is inspired by the essential idea that the heat flux is given by

$$q_i = -\kappa \beta_i, \tag{4}$$

with κ a suitable function of the thermodynamic state variables, representing the thermal conductivity, and β a dynamical non-equilibrium temperature. According to Fourier law, the equation (4) preserves the heat flux in the inverted direction of the gradient of temperature, but in contrast with it, the temperature differs from thermodynamic absolute temperature θ.

In the presence of first order nonlocal constitutive equations, such an approach is capable to reproduce the lagging behavior, which is expected in heat conduction in small systems. Also, it leads to nonlinear generalizations of the celebrated Maxwell-Cattaneo [24] and Guyer-Krumhansl [13, 14] equations, describing, respectively, the hyperbolic and diffusive-hyperbolic regime during heat conduction in crystalline solids.

As a further example, a nonlocal thermodynamic model of helium II is presented.

As the conclusion, we present some applications of a new method of exploitation of second law of thermodynamics, which allows the entropy to be nonlocal also in the absence of an extra-flux of energy or entropy. Of course, our result does not mean that these extra-fluxes do not exist. For instance, it is well known that in the the movement of a mixture, the effects of matter diffusion manifest themselves in the appearance of an additional energy flux related to the chemical potential and to the relative mass flux of each constituent [15]. We simply claim that, according to the generalized method of exploitation, they are not essential to the end of conserving nonlocal terms into the constitutive equation of the entropy. Hence, their effective presence should be decided only on the base of suitable experimental results. Moreover, to our opinion, new experiments are necessary in order to decide what is the most well-suited modification of the basic laws of thermodynamics in the presence of extra-fluxes.

References

[1] Z. P. Bazant and G. Pijauder-Cabot. *Nonlocal damage theory.* J. Eng. Mech. ASCE, **113** (1987), 1512-1533.

[2] F. X. Alvarez and D. Jou. *Memory and nonlocal effects in heat transport.* Appl. Phys. Lett., **90** (2007), 083109 (3 pages).

[3] D. Jou, J. Casas-Vázquez, G. Lebon and M. Grmela. *A phenomenological scaling approach for heat transport in nano-systems*. **18** (2005), 963-967.

[4] D. Jou, J. Casas-Vázquez, G. Lebon. *Extended Irreversible Thermodynamics*. 3rd revised edition, Springer Verlag, Berlin, 2001.

[5] P. Ván. *Weakly nonlocal irreversible thermodynamics*. Annalen der Physik, **12** (2003), 142-169.

[6] C. Truesdell. *Rational thermodynamics*. 2nd edition, Springer Verlag, Berlin, 1984.

[7] W. Muschik, C. Papenfuss and H. Ehrentraut. *A sketch of continuum thermodynamics*. J. Non–Newtonian Fluid Mech., **96** (2001), 255–290.

[8] B. D. Coleman, W. Noll. *The thermodynamics of elastic materials with heat conduction and viscosity*. Arch. Ration. Mech. Anal., **13** (1963), 167-178.

[9] I–Shih Liu. *Method of Lagrange multipliers for exploitation of the entropy principle*. Arch. Ration. Mech. Anal., **46** (1972), 131–148.

[10] J. E. Dunn and J. Serrin. *On the thermomechanics of the interstitial working*. Arch. Ration. Mech. Anal., **88** (1985), 95–133.

[11] V. A. Cimmelli, A. Sellitto and V. Triani. *A new thermodynamic framework for second grade Korteweg type viscous fluids*. (2009), submitted.

[12] I. Müller and T. Ruggeri. *Rational Extended Thermodynamics*. 2nd edition, Springer Tracts in Natural Philosophy, **37**. Springer Verlag, New York, 1998.

[13] R. A. Guyer, J. A. Krumhansl. *Solution of the linearized phonon Boltzmann equation*. Phys. Rev., **148** (1966), 766–778.

[14] R. A. Guyer, J. A. Krumhansl. *Thermal conductivity, second sound and phonon hydrodynamic phenomena in nonmetallic crystals*. Phys. Rev., **148** (1966), 778-788.

[15] M. E. Gurtin and A. S. Vargas, *On the classical theory of reacting fluid mixtures*, Arch. Ration. Mech. Anal., **43** (1971), 179-197.

[16] J. E. Dunn. *Interstitial working and a nonclassical continuum thermodynamics*. In: New Perspectives in Thermodynamics. J. Serrin Ed., Ch. 11, 187–222, Springer Verlag, Berlin, 1986.

[17] I. Müller. *On the Entropy Inequality*. Arch. Ration. Mech. Anal., **26** (1967), 118-141.

[18] V. A. Cimmelli. *An extension of Liu procedure in weakly nonlocal thermodynamics*. J. Math. Phys., **48** (2007), 113510 (13 pages).

[19] V. A. Cimmelli, A. Sellitto and V. Triani. *A generalized Coleman-Noll procedure for the exploitation of the entropy principle*. (2009), forthcoming.

[20] V. A. Cimmelli, A. Sellitto and D. Jou. *Nonlocal effects and second sound in a nonequilibrium steady state*. Phys. Rev. B, **79** (2009), 014303 (13 pages).

[21] V. A. Cimmelli, W. Kosiński. *Nonequilibrium semi-empirical temperature in materials with thermal relaxation*. Arch. Mech., **43** (1991), 753-767.

[22] K. Frischmuth, V. A. Cimmelli. *Numerical reconstruction of heat pulse experiments*. Int. J. Engng. Sci., **33** (1994), 209-215.

[23] V. A. Cimmelli, K. Frischmuth. *Nonlinear effects in thermal wave propagation near zero absolute temperature*. Physica B, **355** (2005), 147-157.

[24] C. Cattaneo. *Sulla conduzione del calore*. Atti Sem. Mat. Fis. Univ. Modena. **3** (1948), 83–101.

The influence of the Yarkovsky effect on the global temperature

by Alexis De Vos
Universiteit Gent
B - 9000 Gent
alex@elis.UGent.be

and Anna Kaplar
Politechnika Łódzka
PL - 90 924 Łódz

Ivan Yarkovsky (1844–1902) was a Polish engineer working in Russia [1]. In his spare time, he was an amateur physicist, searching for a fundamental theory of gravity [2]. In this framework, Yarkovsky discovered 'his effect'. His discovery fell into oblivion, until it was rediscovered about 1950. Today the scientific literature has the tendency to investigate ever more detailed influences on the Y effect. In contrast, the present paper aims at presenting a model as simple as possible, in order to give basic properties of the Y effect.

The sun is assumed to be a spherical black body with radius R_s and surface temperature T_s. At the sun's surface a power density σT_s^4 is emitted. Here σ is the Stefan–Boltzmann constant. During its way to a planet, the total power is distributed over an ever increasing surface area, until the power density is decreased by a factor $f = R_s^2/r^2$. Here r is the radius of the planet's (circular) orbit around the sun.

The planet is assumed to be a spherical black body with radius R_p. In first approximation, we may assume that the planet has a uniform surface temperature T_p. Writing the planet's energy balance [3]

$$f\sigma T_s^4 \ \pi R_p^2 = \sigma T_p^4 \ 4\pi R_p^2 \ , \tag{1}$$

yields the planet's temperature:

$$T_p = \sqrt[4]{\frac{f}{4}} \ T_s \ . \tag{2}$$

This result is thus obtained from the law of conservation of energy. One could remark that the law of conservation of momentum is equally fundamental. Therefore, the question arises how conservation of momentum influences the radiation equilibrium of the planet. It is clear that the spherical shape and uniform temperature of the planet results in a spherical symmetry of its (infrared) emitted radiation. The resulting sum of all photon momenta is zero.

The Yarkovsky effect is caused by the fact that the temperature (and thus the emitted radiation) of the planet is <u>not</u> uniform. Therefore we introduce a

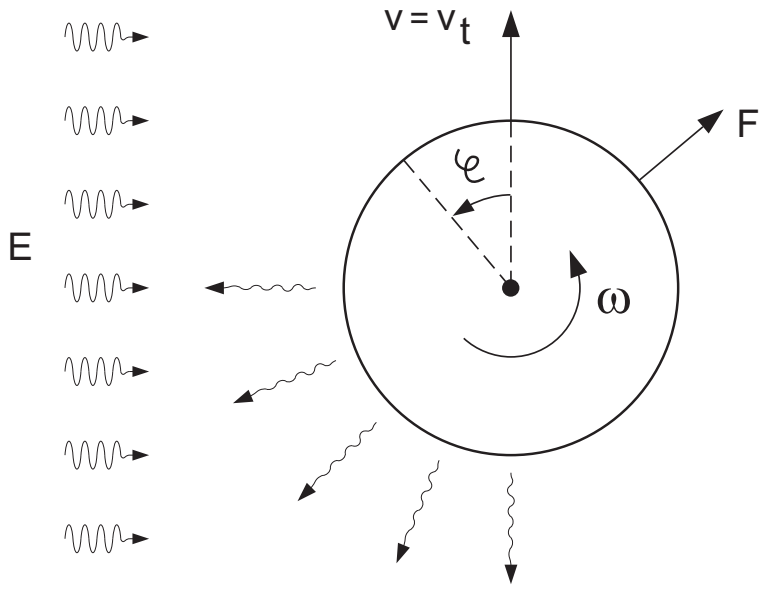

Figure 1: A planet illuminated by the solar constant E and emitting infrared radiation, which causes a rebound force F.

place-dependent temperature T. In order to make the mathematics transparent, we assume that the local T is only dependent on the longitude φ and not on the latitude ϑ of the place. See Figure 1.

We replace the global equilibrium (1) by a local balance. Choosing $\varphi = 0$ for the sunrise meridian (i.e. the meridian with 6 o'clock a.m. time), we get:

$$\begin{aligned} T(\varphi) &= T_p \sqrt[4]{\pi \sin(\varphi)} && \text{if } \varphi < \pi \\ &= 0 && \text{if } \varphi > \pi \ , \end{aligned} \tag{3}$$

where T_p is the temperature (2) from the uniform-temperature model. The curve $\Phi = 0$ in Figure 2 shows the resulting temperature profile $T(\varphi)$. The reader may easily verify that the average $\frac{1}{S} \iint_S T^4 dS = \frac{1}{2\pi} \int T^4 d\varphi$ equals T_p^4. Here S is the surface area of the planet: $dS = R_p^2 \cos(\vartheta) d\vartheta d\varphi$. The average $(\frac{1}{S} \iint_S T^4 dS)^{1/4}$ is denoted as $\mathcal{R}_4$ by Essex et al. [4].

A non-uniform emission of photons causes a non-zero rebound force F felt by the planet. This force is directed away from the sun. No mechanical energy is transferred to the planet: $\vec{v}.\vec{F} = v_r F_r + v_t F_t = 0 F_r + v_t 0 = 0$.

Whereas the uniform temperature (2) is not realistic (nights and days on earth showing a same temperature), the result (3) is even less realistic. The latter correctly predicts high day temperatures and low night temperatures, but greatly exaggerates these temperature fluctuations.

There thus is need for a third, better model. It acknowledges that, on real planets, temperatures are smoothed out. By heat storage, combined with

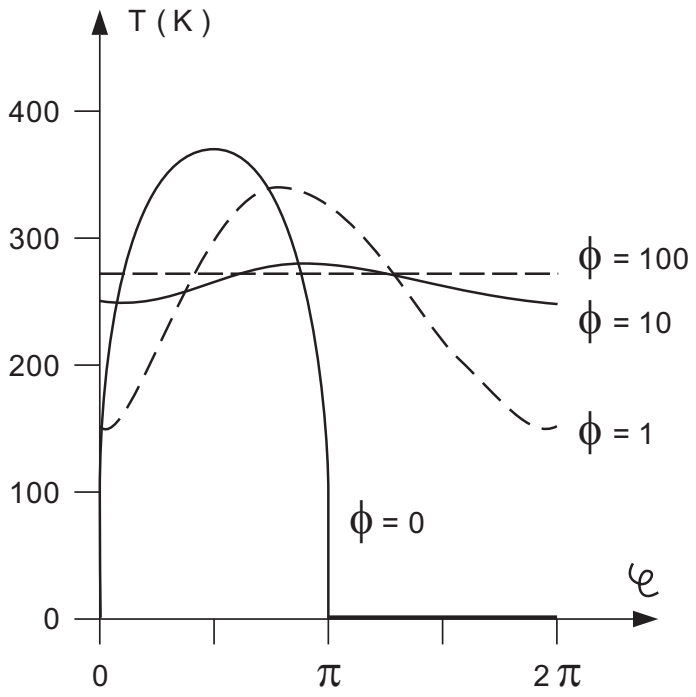

Figure 2: A planet's surface temperature T, as a function of longitude φ.

rotation around the planet's axis, heat is transported from the day side to the night side. Therefore, we add to the energy balance a capacitive term. Moreover, merely for mathematical convenience, we replace the linear capacitive heat current by a non-linear one: $K\frac{dT^4}{dt}$. Assuming the north-south axis is perpendicular to the ecliptic, we thus obtain the linear differential equation in the unknown $T^4(\varphi)$:

$$\begin{aligned} \Phi\ \frac{dT^4}{d\varphi} + T^4 &= \pi\, T_p^4 \sin(\varphi) && \text{if } \varphi < \pi \\ &= 0 && \text{if } \varphi > \pi\ . \end{aligned}$$

Here, the angle Φ is a short-hand notation for $K\omega/\sigma$, where ω is the angular velocity of the planet spinning around its own axis. One finds the following periodic solution:

$$\begin{aligned} T^4 &= \pi\ \frac{1}{\Phi^2+1}\ [\ \frac{X}{X-1}\ \Phi\ \exp(-\varphi/\Phi) - \Phi\ \cos(\varphi) + \sin(\varphi)\ ]\ T_p^4 \quad \text{for } \varphi < \pi \\ &= \pi\ \frac{\Phi}{\Phi^2+1}\ \frac{X^2}{X-1}\ \exp(-\varphi/\Phi)\ T_p^4 \qquad\qquad\qquad\qquad\qquad\qquad \text{for } \varphi > \pi\ , \end{aligned}$$

where X is a short-hand notation for $\exp(\pi/\Phi)$. The reader may check that again the property $\frac{1}{S}\iint_S T^4 dS = T_p^4$ and thus $\mathcal{R}_4(T) = T_p$ holds. Figure 2

shows curves $T(\varphi)$. The curves $T(\varphi)$ display a maximum in the afternoon side of the planet. In spite of the simplicity of our model, our curves are very similar to the graphs published by Lorenz and Spitale [5] [6] and by Vokrouhlický [7]. We note that now the tangential force $F_t(\Phi) = \frac{\pi}{3}\ \frac{\sigma}{c}\ R_p^2\ \int\ T^4 \cos(\varphi)\, d\varphi$ is non-zero.

Thus, because a planet with thermal inertia has its hottest side oriented away from the sun, the net rebound caused by the emission of (infrared) radiation has a component F_t along the orbit of the planet around the sun. Therefore, mechanical power is transferred:

$$\vec{v}.\vec{F} = v_t F_t = \frac{\pi^3}{6}\ \frac{v}{c}\ \frac{\Phi}{\Phi^2+1}\ \sigma R_p^2 T_p^4\ ,$$

with a maximum for $\Phi = 1$. Thus (1) is replaced by

$$f\sigma T_s^4\ \pi R_p^2 = \sigma T_p^4\ 4\pi R_p^2 + \sigma T_p^4\ \frac{\pi^3}{6}\ R_p^2\ \frac{\Phi}{\Phi^2+1}\ \frac{v}{c}\ .$$

In first-order, we obtain the following average planet temperature:

$$\mathcal{R}_4(T) = \sqrt[4]{\frac{f}{4}}\ T_s\ \left(1 + \frac{\pi^2}{96}\ \frac{\Phi}{\Phi^2+1}\ \frac{v}{c}\right)\ ,$$

The relative correction x is small. E.g. for the earth we find a number of the order of -10^{-5}. The absolute Yarkovsky correction xT_p is thus of the order of -1 millikelvin.

[1] G. Beekman : " I. O. Yarkovsky and the discovery of 'his' effect ", *J. Astronomy* **37** (2006), pp. 71-86.

[2] I. Yarkovsky : " Kinetic theory of universal gravitation in relation with the generation of ponderable matter within celestial bodies ", Moscow, in French (1888) and in Russian (1889).

[3] A. De Vos : " Thermodynamics of solar energy conversion ", Wiley–VCH, Weinheim (2008).

[4] C. Essex, R. McKitrick, and B. Andresen : " Does a global temperature exist? ", *J. Non-Equilibrium Therm.* **32** (2007), pp. 1-27.

[5] R. Lorenz and J. Spitale : " Entropy and the Yarkovsky effect ", *Book of Abstracts of the 5 th Lunar and Planetary Lab. Conf.*, Tuczon, 22-23 May 2002.

[6] R. Lorenz and J. Spitale : " The Yarkovsky effect as a heat engine ", *Icarus* **170** (2004), pp. 229-233.

[7] D. Vokrouhlický : " Diurnal Yarkovsky effect as a source of mobility of meter-sized asteroidal fragments ", *Astronomy and Astrophysics* **335** (1998), pp. 1093-1100, and **338** (1998), pp. 353-363.

A MATHEMATICAL MODEL FOR CLONE EXPANSION OF T CELLS DURING VACCINATION

DOLFIN, M.* AND CRIACO, D.*

*Department of Mathematics, University of Messina, It.
E-mail: dolfin@dipmat.unime.it

Abstract. In this communication a mathematical model is presented trying to look insight the dynamic of immunitary response to antigen attack.
In particular the dynamic of a single clone of lymphocites T repertoire is considered during the two phase of first and second meeting with the antigen; a dynamic typically involved in T cell base vaccination.
We have used a macroscopic approach considering the continuum as a mixture. Local balances are then introduced for the density of the mixture and the density of memory T cells together with the related momenta and involving the effect of chemotaxis.

References

[1] Dolfin M.,*A mathematical model for the dynamic of cytotoxic T cells*, Oral communication to VII simai congress , BaiaSamuele(Ragusa)22-26 maggio 2006.
[2] Bellomo, N., De Angelis, E., Preziosi, L. *Multiscale Modeling and Mathematical Problems related to tumor evolution and medical therapy*, J. of Theoretical Medicine 2 (2003) 11-136.
[3] Murray, J.D. *Mathematical Biology. I: An introduction*, Springer (2002), pp.405-407.
[4] Sprent, J., Surh, C.D. *T cell Memory*, Annu. Rev.Immunol., 20 (2002), 551-579.
[5] Gouin, H., Ruggeri, T. *Identification of an average temperature and a dynamical pressure in a multitemperature mixture of fluids*, Physical Review E 78 (2008).
[6] Jansen, V.A.A., Korthals Altes, H., Funk, GA.,Wodarz, D. *Contrasting B cell- and T cell-based protective vaccines*, J. of Theoretical Biology 234 (2005) 39-48.
[7] De Boer, R.J., Perelson, A.S.*T cell repertoires and competitive exclusion*, Journal of Theoretical Biology 169 (1994) 375-390.
[8] Ritter, L.R. *A short course in the modeling of chemotaxis*, Research experience for undergraduates, Summer Course 2004, Texas A M University, College Station Texas.
[9] Perelson, A.S., Weisbuch G. *Immunology for physicists*, Reviews of Modern Physics 69 n.4(1997) 1219-1267.

Gibbs-Bogoliubov Variational Procedure with the Square-Well Reference System

N.E. Dubinin
Institute of Metallurgy of the Ural Division of the Russian Academy of Sciences
ned67@mail.ru

The variational method based on the Gibbs-Bogoliubov inequality is widely used for thermodynamic calculations of liquid metals. As a rule, the hard-sphere (HS) reference system is used for this purpose. There are a number of attempts to use other reference systems: the one-component-plasma system [1], the charged-hard-sphere system [2], and the hard-sphere Yukawa one [3]. Here, we perform variational calculations with the square-well (SW) reference system. The analytical expression for the SW structure factor is taken in the framework of the random phase approximation. The Helmholtz free energy is minimized with respect to the core diameter, the SW width, and the SW depth. This approach is applied to the liquid Na and liquid K at 373K. The Animalu-Heine model pseudopotential and the Vashishta-Singwi exchange-correlation function are used. Obtained results are compared with results of works [1-3] and with our HS-reference-system results.

We are grateful to the Russian Foundation for Basic Research for the financial support (grant N 08-03-00992).

1. K.K. Mon, R. Gann, D. Stroud, *Phys. Rev. A.*, 1981, v. 24, p. 2145.
2. S.K. Lai, *Phys. Rev. A.*, 1985, v. 31, p. 3886.
3. C. Hausleitner, J. Hafner, *J. Phys. F: Met.Phys.*, 1988, v. 18, p. 1013.

The principal equations of state for classical particles, photons, and neutrinos

Christopher Essex[1] and Bjarne Andresen[2]

[1]Department of Applied Mathematics, The University of Western Ontario
London, Ontario N6A 5B7, Canada

[2]Niels Bohr Institute, University of Copenhagen
Universitetsparken 5, DK-2100 Copenhagen Ø, Denmark

essex@uwo.ca, andresen@fys.ku.dk

Functions, not differential equations, are the definitive mathematical objects of equilibrium thermodynamics. They are described as "the equation of state" suggesting only one exists, but such equations take many forms for any particular physical system. Often the relationships between the forms are obscure, unexplored, or even wrongly depicted as external to thermodynamics.

Here we explore classical equations of state for ideal particles, photons, and neutrinos. The usual equations of state are interpreted here as partial differential equations, which lead to a unique, fully extensive equation of state. These forms are rarely, if ever, expressed explicitly. They are designated as the *principal equation of state*. The principal equation of state is a unique form that acts as a generator for all other forms of the equation of state. Moreover, certain obscure properties, such as zero chemical potential for photons, become plain to see. Despite their diverse physical contexts they have certain distinctive properties in common, some of which are not fully understood.

The traditional equations of state for an ideal gas of different species are

$$U = NC_V T$$

$$PV = NkT$$

$$\mu_i = kT\left[\ln\left(\frac{N_i}{V}\right) - \frac{C_V}{k}\ln(m_i kT) + g\right]$$

with the number N_i of species i, summing to a total of N particles. The mass of a particle of species i is m_i, and g is a constant collecting a number of basic constants of nature. These equations, involving intensive as well as extensive variables, are just different projections of the principal equation of state $U(S, V, \{N_i\})$, where the intensive variables come in as coefficients in the total differential

$$dU = TdS - PdV + \sum_i \mu_i dN_i$$

The full principal equation of state for the multi-component ideal gas reads

$$U = \frac{h^2 C_V}{2\pi k} \exp\left(-1 - \frac{k}{C_V}\right) N \prod_i \left[\left(\frac{N_i}{V}\right)^{\frac{k}{C_V}} \left(\frac{1}{\varsigma_i m_i}\right)^{\frac{C_i}{C_V}} \right]^{\frac{N_i}{N}} \exp\left(\frac{S}{NC_V}\right)$$

where ζ_i accounts for internal degrees of freedom of species *i* while C_i is the heat capacity per particle for the species. This equation acts as a generator for all the usual equations through differentiation and possibly keeping one of the variables constant. It is also the starting point for calculating the Hessian or metric in thermodynamic geometry,

$$\mathbf{M} = D^2 U = \left\{ \frac{\partial^2 U}{\partial X_i \partial X_j} \right\}$$

where $\boldsymbol{X}$ is the full set of extensive arguments for *U*: *S*, *V*, $\{N_i\}$.

For a single-component monatomic ideal gas this principal equation of state reduces to

$$U = \frac{3}{4} \frac{h^2}{\pi} \exp\left(-\frac{5}{3}\right) \frac{N}{m} \left(\frac{N}{V}\right)^{2/3} \exp\left(\frac{2}{3} \frac{S}{Nk}\right)$$

which has a striking resemblance to the expression for a van der Waals gas,

$$U = \frac{3}{4} \frac{h^2}{\pi} \exp\left(-\frac{5}{3}\right) \frac{N}{m} \left(\frac{N}{V - bN}\right)^{2/3} \exp\left(\frac{2}{3} \frac{S}{Nk}\right) - \frac{aN^2}{V}$$

in which *a* and *b* are the van der Waals coefficients.

The principal equation of state for photons is

$$U = \frac{3}{16} \left(\frac{12c}{\sigma V}\right)^{1/3} S^{4/3}$$

and for neutrinos

$$U = \frac{3}{56} \left(\frac{588c}{\sigma V}\right)^{1/3} S^{4/3}$$

In both cases *c* is the speed of light and σ the radiation constant. The small numerical difference arises because photons are bosons and neutrinos are fermions. Note that these latter two equations do not depend on the particle number *N*, and consequently their chemical potential $\mu = \partial U / \partial N = 0$. Furthermore, we note that the classical equation of state *P*=(*U*/*V*)/3, often depicted as external to thermodynamics, also occurs for neutrinos, and it arises directly from these equations. They also yield something less well-known but entirely analogous for entropy: *P*/*T*=(*S*/*V*)/4.

The Hessians indicate that all principal equations of state considered here are convex functions, but they also are all singular. Why? Is this a necessary property for all thermodynamic systems?

QUANTUM REFRIGERATORS

Tova Feldmann and Ronnie Kosloff
Institute of Chemistry the Hebrew University, Jerusalem 91904, Israel
tovaf@fh.huji.ac.il

A first principle reciprocating quantum refrigerator approaching absolute zero Reciprocating refrigerators operate by a working medium shuttling heat from the cold to the hot reservoir. This requires external control of the temperature of the working medium. At very low temperatures a quantum description of the working medium is required where the control of temperature is governed by manipulating the energy levels of the system. A generic working medium possesses a Hamiltonian that is only partially controlled externally:

$$\hat{\mathbf{H}} \quad = \quad \hat{\mathbf{H}}_{int} + \hat{\mathbf{H}}_{ext}(\omega) \tag{1}$$

where $\omega = \omega(t)$ is the time dependent external control field. Typically, the internal and external parts do not commute $[\hat{\mathbf{H}}_{int}, \hat{\mathbf{H}}_{ext}] \neq 0$. Therefore, in general, the evolution operator $\hat{\mathbf{U}}$ of the system's operator algebra also does not commute with $\hat{\mathbf{H}}(t)$. As a result a state diagonal in the temporary energy eigenstates cannot follow adiabatically. This fact, which is the source of quantum friction, has a profound effect on the performance of the heat pump(engine) [1–4, 6].

Limitations of cooling toward absolute zero for systems with finite energy gap above ground state Almost perfect adiabaticity is the key to low temperature refrigeration. Typically, the internal interaction leads to an uncontrollable finite gap J in the energy level spectrum between the ground and first excited state. It is shown in the study that this gap combined with unavoidable quantum friction leads to a finite minimal temperature, termed T_c^{min} above zero. The reason is that such a gap, combined with a negligible amount of noise, prevents adiabatic following during the expansion stage which is the necessary condition for reaching $T_c \to 0$. Theoretically the effect of the noise can be described by a double commutator with the relevant operator associated with the noise [5]. The dynamics on the expansion adiabat is analysed to reveal the deviation δ from adiabatic following. A constant adiabatic parameter allows to solve the equations of motion analytically. The solution shows a periodical alternation between frictionless solutions to ones with profound friction [7].

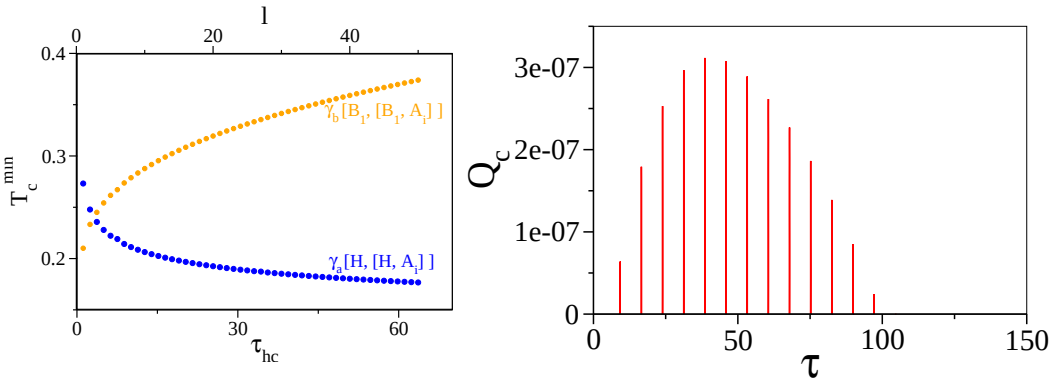

FIG. 1: Left: The minimum temperature as a function of the time allocated to the expansion *adiabat* τ_{hc} (bottom scale) and l, number of times the system's trajectory circles around the energy vector (the winding number -upper scale), for the two noise models. The phase noise has a monotonic decrease of $T_c(min)$ reaching saturation as $\tau_{hc} \to \infty$ where $T_c(min) = \frac{\hbar J}{-2k_B \log(\gamma_a \Phi_{hc}/2)}$. $(\Phi_{hc} = [arcsin(\frac{\omega_c}{\Omega_c}) - arcsin(\frac{\omega_h}{\Omega_h})])$. $T_c(min)$ of the amplitude noise is monotonically increasing function of time which means that short expansion times lead to the minimum temperature. If both amplitude and phase noise operate simultaneously the minimum temperature will be obtained at the crossing point. Right: The heat drawn from the cold bath, Q_c, as a function of cycle time with the time scheduling, $\omega(t)$ resulting from the analytical solution on the *adiabats* . The decrease of Q_c both for short and long times is seen.

The coupled spin system model The model refrigerator is based on a working medium consisting of quantum systems composed of an ensemble of two coupled spins. The performance of this model resembles a refrigerator with intrinsic

friction. We find that the optimal average cooling rate per cycle is exponentially decreasing when approaching absolute zero, independently of the functional time dependence (scheduling) of the control field. It is shown, that T_c^{min} is limited by the zero field splitting.

There are two families of refrigerator cycles; the "normal" cycles whose cycle times are much larger than period determined by the energy splitting $2\pi/\Omega$, and the "sudden" cycles which are short relative to this period.

Normal cycles The trajectories in the space of the expectation values of the relevant operators are quantized, according to the number of revolutions the trajectory traverses in that space The inverse minimal temperature $1/T_c^{min}$ is approximately linear in the allocated cycle time determined by the maximal cooling rate. The cycles show non-isoentropic approach to absolute zero, which is to some extent a violation of one of Nernst's interpretation of the third law.

Sudden cycles These cycles have no classical analogues. Their energy entropy is much higher than their Von Neumann entropy, which indicates large off diagonal elements in the density operators in the energy representation. There is no time even on the *isochores* to equllibrate. The sudden cycles are far from the adiabaticity condition.

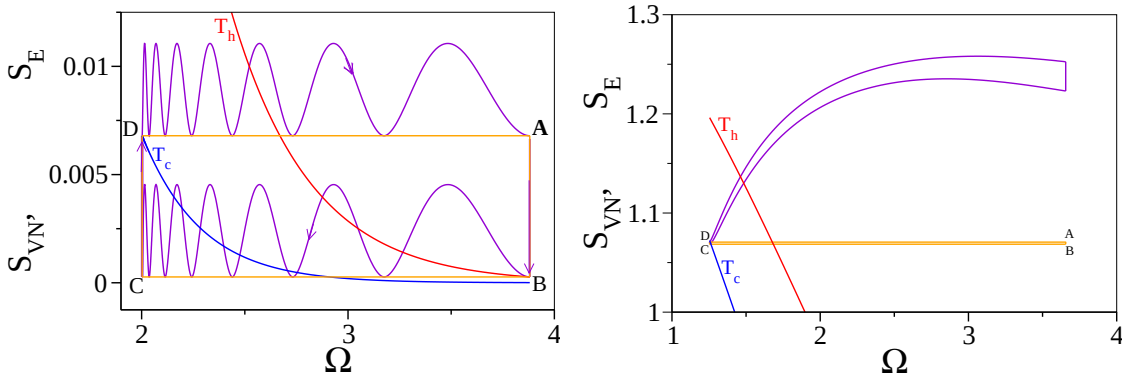

FIG. 2: Refrigerator cycles in the frequency entropy plane. The Von Neumann entropy $\mathcal{S}_{VN} = -tr\{\hat{\boldsymbol{\rho}} \log \hat{\boldsymbol{\rho}}\}$ (**ABCD** rectangle) as well as the energy entropy $\mathcal{S}_E = -\sum p_i \log p_i$ are shown (p_i is the population of energy level i). The hot and cold isotherms are also indicated. Left: *normal cycle* , both the expansion *adibat* and the compression *adibat* revolve exactly seven periods. Right: *sudden cycle*

[1] T. Feldmann and R. Kosloff, Phys. Rev. E **61**, 4774 (2000).
[2] R. Kosloff and T. Feldmann, Phys. Rev. E **65**, 055102 (2002).
[3] T. Feldmann and R. Kosloff, Phys. Rev. E **68**, 016101 (2003).
[4] T. Feldmann and R. Kosloff, Phys. Rev. E **70**, 046110 (2004).
[5] T. Feldmann and R. Kosloff, Phys. Rev. E **73**, 025107(R) (2006).
[6] Y Rezek, P Salamon, K H Hoffmann and R Kosloff, Eur. Phys. Lett. **85** 30008 (2009).
[7] Tova Feldmann and Ronnie Kosloff, arXiv **[phys.chem-ph]**, 0902.0326v1 (2009).

Thermodynamics of irreversible processes enhanced by mixed solvent electrolyte activity coefficient models

Philip Loldrup Fosbøl*, Kaj Thomsen*, and Erling H. Stenby*

(*) IVC-SEP, DTU Chemical Engineering, Søltofts Plads, Building 229, Technical University of Denmark, DK-2800 Kongens Lyngby, Denmark.
e-mail: plf@kt.dtu.dk

Introduction

The calculation of the diffusion process is performed by setting up a discretized partial differential equation (PDE) mass balance of the form:

$$\frac{\partial c_i}{\partial t} = -\frac{\partial N_i}{\partial z} + R_i \tag{1}$$

Here shown for the one dimensional case. R_i is the reaction term, $\partial c_i / \partial t$ is the accumulation tem, and $\partial N_i / \partial z$ is the flux term. The molar flux, N_i, can be calculated by diffusion theory of Fick also know as Fick's law:

$$N_i = -Đ_{is}^{\infty} \frac{dc_i}{dz} \tag{2}$$

Which states that the flux is a linear function of concentration profile. Or the molar flux may be calculated by the Nernst-Planck (NP) equation:

$$\frac{N_i}{c_t} = \underbrace{-Đ_{is}^{\infty} \frac{\partial x_i}{\partial z}}_{Diffusion} \underbrace{- Đ_{is}^{\infty} \frac{x_i z_i F}{RT} \frac{\partial \phi}{\partial z}}_{Migration} + \underbrace{x_i u_s}_{Convection} \tag{3}$$

Where $Đ_{is}^{\infty}$ is the diffusivity between component *i* and the solvent *s* at infinite dilution, also known as the diffusion coefficient. c_t is the total concentration, z_i the ionic charge, z the length, ϕ the electrical potential, x_i the mol fraction, and u_s the solvent velocity towards the wall.

The advantage of using the NP equation relative to Fick's law is the term related to the electrical potential $\partial\phi/\partial z$ also known as the migration term. This term is central in electrolyte diffusion where the charges of ions become important. One ion will influence the diffusion of other ions due to charge interaction. The slower ions drag the faster due to the pulling/pushing force from the ionic charge difference. For example a big slow diffusing negative ion will drag smaller positive ions and the small positive ions will pull the slow negative ion.

Improving the theory

The molal ionic strength (I) in mol/kg H_2O is high in a number of engineering diffusion relevant cases, eg. CO_2 corrosion and CO_2 capture and storage (CCS). The ionic strength indicates that the solutions behave thermodynamically non-ideally. Using the Fick's law and the NP equations may be inaccurate since ideality is assumed and they are therefore only strictly valid at I<0.001 mol/kg H_2O. In many cases both equations are used outside the valid operation window. The NP equation can be extended to include activity coefficients by the following as shown by Fosbøl[1]

$$\frac{N_i}{c_t} = -Đ_{is}^{\infty}\frac{1}{x_s}\Gamma_{ii}\frac{\partial x_i}{\partial z} - Đ_{is}^{\infty}\frac{x_i z_i F}{x_s RT}\frac{\partial \phi}{\partial z} + x_i u_s \tag{4}$$

Where x_s is the solvent concentration and Γ_{ii} is the thermodynamic factor or the thermodynamic correction factor, e.g. discussed by Taylor and Krishna[2] for non-electrolyte mixtures. It represents the deviation from ideal diffusion behaviour. Comparing the above equation to (3) shows that it requires minor extensions to improve the calculation. A more complete but more complex diffusion equation can be written as discussed by Fosbøl[1]. The thermodynamic correction factor (TCF) Γ_{ii} is calculated by

$$\Gamma_{ii} = 1 + x_i\frac{\partial \ln\left(\gamma_i\left(T,P,\mathbf{n}\right)\right)}{\partial x_i} \tag{5}$$

which is a function of the activity coefficient γ_i derived with respect to composition. In this work the electrolytic Extended UNIQUAC (UNIversal QUAsi-Chemical) model by Thomsen *et al.*[3-5] is used in the calculation of the activity coefficient. It has previously proven to be acceptable for predicting activities of mixed solvent electrolyte systems up high ionic strengths.

It should be noticed that incorporating an activity coefficient model in the diffusion equations may still impose limitation of the ionic strength, i.e. the Debye-Hückel limiting law activity coefficient model is only valid at I≤0.01 mol/kg H_2O and the extended Debye-Hückel law is valid at I≤0.1 mol/kg H_2O. The applicable window can be extended slightly by using the Davies rule[6,7] instead, which is valid at I≤0.3 mol/kg H_2O. The Pitzer equation is typically valid up to I=6 mol/kg H_2O. None of these models are by default useable for mixed solvent systems.

Several fluid effects are not discussed in this study which needs to be considered in full diffusion calculations. This is the case even though activity coefficients are used in the diffusion equations or not. The effects refer to the concentration dependency of the diffusivities and not to the actual flux. These are the electrophoretic effect as discussed by Harned and Owen[8] and Robinson and Stokes[9], the viscosity, the porosity, and the direct diffusivity concentration dependency discussed by Newman *et al.*[10], Vignes[11], and Umino and Newman[12].

An example system CO_2-NaOH-MEG-H_2O

In this work example calculations of TCF for the mixed solvent electrolyte system CO_2-NaOH-Mono ethylene Glycol(MEG)-H_2O will be shown. Results will be based on the Extended UNIQUAC model given by Fosbøl *et al.*[1]. With the aim of showing how large an effect the TCF may have on diffusion. This is done in order to illustrate the deviation between the original Nernst-Planck formulation (3) and the improvements by using (4). The TCF gives the difference between the two equations. A Γ_{ii} of 1.5 indicates that the flux of the component would be 50% higher in the real non-ideal system compared to infinite dilution. The calculation of Γ_{ii} requires a thermodynamic activity coefficient model and a speciation routine. The speciation routine calculates the equilibrium composition from the given T, P, and concentrations. The thermodynamic model calculates Γ_{ii} as function of T, P, and equilibrium composition.

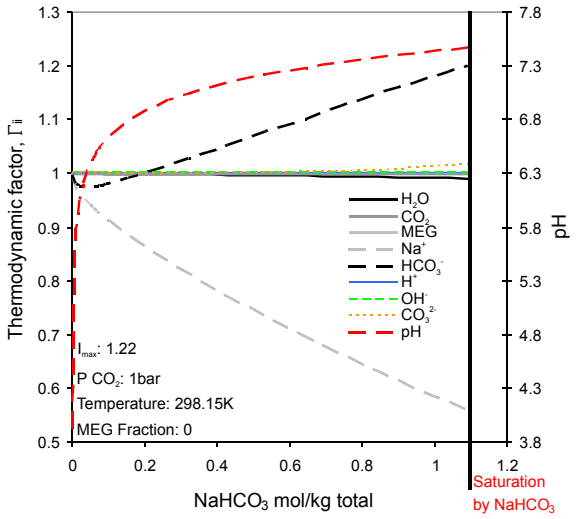

FIGURE 1. Thermodynamic factors, Γ_{ii}, as function of added $NaHCO_3$ salt. Saturation by $NaHCO_3$ is reached at the vertical black line. I_{max} indicates the maximum ionic strength obtained at saturation.

Figure 1 shows an example calculation of TCF for sodium bicarbonate in water. Results will be shown for the mixed solvent case and comparison between the cases will be made. A number of important conclusions may be drawn for the mixed solvent calculations which will be revealed by the results of this work. The figure shows that the ionic strength of the systems, I_{max}, is approximately 1.2 mol/kg H_2O at saturation. This is an indication that the solutions behave non-ideal. The thermodynamic factors, Γ_{ii}, of i=HCO_3^- is approximately 1 below 0.3 mol $NaHCO_3$/kg total. It illustrates that above this concentration the effective diffusion coefficient is considerable different from 1. It is 20 % higher at saturation compared to infinite dilution. Γ_{ii} of i=Na^+ is 0.55 at saturation which indicates the effective diffusivity is 55 % of the value at infinite dilution. Consequently the diffusion of Na^+ is lower at saturation compared to infinite dilution. The concentration of CO_3^{2-} is low in this solution, 0.01 molal, and Γ_{ii} of i=CO_3^{2-} is consequently also

close to one, here 1.02. The concentrations of the remaining components are close to infinite dilution and Γ_{ii} of these compounds are consequently $\Gamma_{ii} \approx 1$.

Cited literature

[1] Fosbøl, P. L. Carbon Dioxide Corrosion: Modelling and Experimental Work Applied to Natural Gas Pipelines. Ph.D. Thesis, IVC-SEP, Technical University of Denmark, Kongens Lyngby, Denmark, 2008.

[2] Taylor, Ross; Kooijman, Hendrik A. Composition derivatives of activity coefficient models (for the estimation of thermodynamic factors in diffusion). Chemical Engineering Communications 102, 87-106, 1991.

[3] Thomsen, K.; Rasmussen, P.; Gani, R. Correlation and prediction of thermal properties and phase behaviour for a class of electrolyte systems. J. Chem. Eng. Science 51, 3675-83, 1996.

[4] Thomsen, K. Aqueous Electrolytes, model parameters and process simulation. Ph.D. Thesis, IVC-SEP, Technical University of Denmark, Kongens Lyngby, Denmark, 1997.

[5] Iliuta, M; Thomsen, K.; Rasmussen, P. Extended UNIQUAC model for correlation and prediction of vapor-liquid-solid equilibria in aqueous salt systems containing non-electrolytes. Part A. Methanol-water-salt systems. Chemical Engineering Science 55, 2673-2686, 2000.

[6] Davies, C. W. The extent of dissociation of salts in water. VIII. An equation for the mean ionic activity coefficient of an electrolyte in water, and a revision of the dissociation constants of some sulfates. Journal of the Chemical Society 2, 2093-8, 1938.

[7] Davies, C. W. Ion Association. Butterworths, London, 1962.

[8] Harned, H. S.; Owen, B. B. The physical chemistry of electrolytic solutions. Reinhold Publishing Corporation, New York, third edition, 1964.

[9] Robinson, R. A.; Stokes, R. H. Electrolyte solutions. Butterworths, London, 1965.

[10] Newman, J.; Bennion, D.; Tobias, C. W. Mass transfer in concentrated binary electrolytes. Berichte der Bunsengesellschaft für Physikalische Chemie 69, 608-612, 1965.

[11] Vignes, A. Diffusion in Binary Solutions. Variation of Diffusion Coefficient with Composition. Ind. Eng. Chem. Fund. 5, 189-199, 1966.

[12] Umino, S.; Newman, J. Diffusion of sulfuric acid in concentrated solutions. J. Electrochem. Soc. (1993) 140(8), 2217-2221.

On the Experimental Verification of the Onsager Reciprocal Relation in Thermoelectric Processes

Javier Garrido
Departamento de Física de la Tierra y Termodinámica, Universitat de Valencia
E-46100 Burjassot (Valencia), España
javier.garrido@uv.es

INTRODUCTION

Four transport coefficients characterize the thermoelectric properties of materials: the thermal conductivity κ, the thermoelectric power or Seebeck coefficient S, the electric conductivity σ, and the Peltier coefficient π. The first three are profusely measured and studied: dozens of papers are published every year. Nevertheless from the last coefficient the number of references are very limited: they do not reach a paper for year. In this unequal result the Onsager reciprocal relation (ORR) $\pi = TS$ has a decisive influence. In fact the easiness and accuracy of the techniques which measure the Seebeck coefficient obviates the need for Peltier coefficient measurements. But the ORR which is founded in statistical mechanics needs to be experimentally checked in a few cases at least [1]. Therefore the experimental confirmation of this relation depends on the preciseness and accuracy of Peltier coefficient measurements. A review of this subject has been developed in this work.

In order to describe the thermoelectric processes in an advantageous way, the observable formulation has been used [2-4]. This is characterized by the electric potential measured at the probe terminals $\Delta\psi$ and for the heat flux which the conductor laterally dissipates J_Q (figure 1). In this formulation both the electrochemical potential of the electrons and the energy flux play the central role. The energy balance provides the basic relationships among the observables and the Peltier and Thomson coefficients.

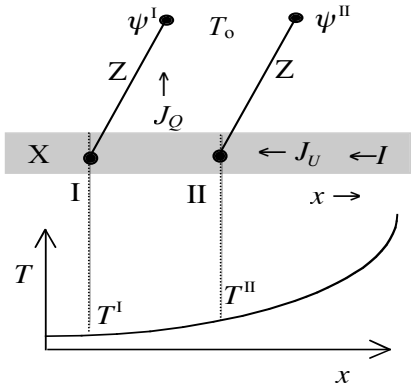

Figure 1. Observables $\Delta\psi = \psi^{\mathrm{II}} - \psi^{\mathrm{I}}$ and J_Q in the conductor X. The terminals of probes Z are at the same temperature T_{o}.

The interest for studying the Peltier coefficient is also due to this coefficient forms part of the expressions which define both the Thomson coefficient τ and the figure of merit ZT. The first combines the effect of two basic coefficients $\tau = \mathrm{d}\pi/\mathrm{d}T - S$. And the second relates three of them $ZT = \sigma\pi^2/T\kappa$. When one applies the ORR, we deduce the well-known expressions $\tau = T(\mathrm{d}S/\mathrm{d}T)$ y $ZT = \sigma S^2 T/\kappa$. The first provides the bases to evaluate $\mathrm{d}S/\mathrm{d}T$ from measurements of Thomson's coefficient. And the second is relevant to technological questions of great importance, such as the construction of solid state energy

conversion devices. Materials with high thermoelectric figure of merit are promising candidates for use in thermoelectric power generation.

THEORY

Transport equations

The evaluation of the transport coefficients is carried out in filiform systems from the measurement of several observables. In these wires all the flows and forces are parallel to the *x*-direction. The transport equations of the thermoelectric phenomena are usually expressed in a local formulation

$$J_U = \kappa A \frac{\mathrm{d}T}{\mathrm{d}x} + \left(\pi - \frac{\tilde{\mu}_\mathrm{e}}{e} \right) I \tag{1}$$

$$\frac{\mathrm{d}\left(\tilde{\mu}_\mathrm{e}/e\right)}{\mathrm{d}x} = S \frac{\mathrm{d}T}{\mathrm{d}x} - \frac{1}{\sigma A} I \tag{2}$$

where J_U is the energy flux, A is the cross-section area, $\tilde{\mu}_\mathrm{e}$ is the electrochemical potential of the electron, $e > 0$ is the magnitude of the electron charge, and I is the electric current. Here, the positive direction of the fluxes J_U and I is the opposite of the coordinate x (Figure 1).

To evaluate the transport coefficients of a material we need to know the local values of the following quantities J_U, T, $\tilde{\mu}_\mathrm{e}$ and I. Some of them can be directly measured, i.e. T and I. The other quantities need to be determined from the observable electric potential $\Delta\psi = \psi^\mathrm{II} - \psi^\mathrm{I}$ measured between the terminals of probes Z connected to sections I and II, and the heat flux J_Q which laterally departs from the conductor towards the surroundings between the sections I and II (Figure 1). These two observables are defined next.

Observable electric potential

The observable electric potential ψ measured at the terminals of probes Z at the temperature T_o is closely related to the distribution of the electrochemical potential $\tilde{\mu}_\mathrm{e}$ of the electrons along the conductor.[2-4]

$$\mathrm{d}\left(\tilde{\mu}_\mathrm{e}/e\right) = S_\mathrm{Z}\mathrm{d}T - \mathrm{d}\psi, \tag{3}$$

Then the second transport equation, equation (2), can be transformed to

$$\frac{\mathrm{d}\psi}{\mathrm{d}x} = \left(S_\mathrm{Z} - S_\mathrm{X}\right)\frac{\mathrm{d}T}{\mathrm{d}x} + \frac{1}{\sigma A} I\,. \tag{4}$$

When the probes are of the same material as the conductor, that is $\mathrm{Z} \equiv \mathrm{X}$, equation (4) simplifies to $\mathrm{d}\psi = I\mathrm{d}R$, where $\mathrm{d}R = \mathrm{d}x/\sigma A$ is the electric resistance of the element $\mathrm{d}x$ of conductor X. That is, when $\mathrm{Z} \equiv \mathrm{X}$ the observable electric potential difference measures the ohmic drop independently of the actual temperature distribution in the conductor.

Energy balance

Under steady-state conditions, and for the wire geometry here considered, the energy balance in the wire between two cross-sections I and II is presented as $J_U^\mathrm{II} - J_U^\mathrm{I} = J_Q$, where J_Q is the heat flux that laterally departs between the sections I and II from the wire to the surroundings (Figure 1). From the result $J_U^\mathrm{II} - J_U^\mathrm{I} = J_Q$ and equation (1) we obtain

$$\Delta\left(\kappa A \frac{\mathrm{d}T}{\mathrm{d}x}\right) + I\Delta\pi - I\Delta\left(\frac{\tilde{\mu}_\mathrm{e}}{e}\right) = J_Q\,, \tag{5}$$

which can be used to evaluate the Peltier and Thomson coefficients.

Single wire

When $I = 0$, from equation (4) we have

$$S_{\mathrm{Z}} - S_{\mathrm{X}} = \left(\frac{\partial \Delta\psi}{\partial T^{\mathrm{II}}}\right)_{T^{\mathrm{I}}, I=0}. \tag{6}$$

This expression is commonly used to evaluate $S_{\mathrm{Z}} - S_{\mathrm{X}}$. Note that only differences can be determined but not their absolute values. In these measurements four leads are attached to the sample in order to provide the values of $\Delta\psi$, T^{I} and T^{II}.

To evaluate the Thomson coefficient $\tau = \mathrm{d}\pi/\mathrm{d}T - S$ we consider two sections I and II in a conductor X at different temperatures $T^{\mathrm{I}} \neq T^{\mathrm{II}}$ (Figure 1). If the probes and wire are of the same material, $\mathrm{Z} \equiv \mathrm{X}$, equation (4) can be integrated as $\Delta\tilde{\mu}_{\mathrm{e}}/e = \int_{T^{\mathrm{I}}}^{T^{\mathrm{II}}} S\mathrm{d}T - \Delta\psi$. Combining this result and equation (5) we find the energy balance

$$\Delta\left(\kappa A \frac{\mathrm{d}T}{\mathrm{d}x}\right) + I\int_{T^{\mathrm{I}}}^{T^{\mathrm{II}}} \tau \mathrm{d}T + I\Delta\psi = J_Q, \tag{7}$$

that allows us to evaluate the Thomson coefficient from the observables $\mathrm{d}T^{\mathrm{I}}/\mathrm{d}x$, $\mathrm{d}T^{\mathrm{II}}/\mathrm{d}x$, $\Delta\psi = RI$ and J_Q.

Couple X/Y: Peltier's coefficient measurements

Consider a couple X/Y (Figure 2) where an electric current I is flowing. The temperature distribution evolves towards a steady-state with a maximum (or a minimum) at the junction. The energy balance at the junction is expressed by $(J_U)_{\mathrm{X}} \equiv (J_U)_{\mathrm{Y}}$ where the subscripts X and Y denote each one of the two wires. The equilibrium for distribution of matter at the junction is expressed by $(\tilde{\mu}_{\mathrm{e}})_{\mathrm{X}} = (\tilde{\mu}_{\mathrm{e}})_{\mathrm{Y}}$. Then, from equation (1) we deduce $(\pi_{\mathrm{Y}} - \pi_{\mathrm{X}})I = A\left[\kappa_{\mathrm{X}}(\mathrm{d}T_{\mathrm{X}}/\mathrm{d}x) - \kappa_{\mathrm{Y}}(\mathrm{d}T_{\mathrm{Y}}/\mathrm{d}x)\right]$ and we can evaluate the Peltier coefficient from the measurement of the two temperature gradients in the junction region. As far as we know, the difference of Peltier coefficients has never been measured using this equation.

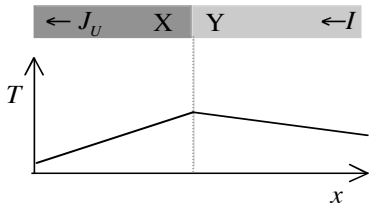

Figure 2. Peltier's effect refers to the temperature profile along a couple X/Y. At the steady-state the junction temperature reaches a maximum (or a minimum).

The usual way of determining $\Delta\pi = \pi_{\mathrm{Y}} - \pi_{\mathrm{X}}$ considers the couple at a steady-state while an electric current I is flowing (Figure 3). Let I and II be two sections at the same temperature $T = T^{\mathrm{I}} = T^{\mathrm{II}}$. Then as $\Delta(\tilde{\mu}_{\mathrm{e}}/e) = -\Delta\psi$, equation (5) can be written

$$\Delta\left(\kappa A \frac{\mathrm{d}T}{\mathrm{d}x}\right) + I\Delta\pi + I\Delta\psi = J_Q. \tag{8}$$

Therefore from the observables $\mathrm{d}T^{\mathrm{I}}/\mathrm{d}x$, $\mathrm{d}T^{\mathrm{II}}/\mathrm{d}x$, $\Delta\psi$ and J_Q we can calculate $\Delta\pi = \pi_{\mathrm{Y}} - \pi_{\mathrm{X}}$. This energy balance can also be expressed in terms of the electric resistance

$$\Delta\left(\kappa A \frac{\mathrm{d}T}{\mathrm{d}x}\right) + I\Delta\pi + RI^2 + I\int_{T^{\mathrm{I}}}^{T^{\mathrm{II}}} \left(S_{\mathrm{Y}} - S_{\mathrm{X}}\right)\mathrm{d}T = J_Q\,, \tag{9}$$

where $R = R_{\mathrm{X}} + R_{\mathrm{Y}}$, $R_{\mathrm{X}} = \int_{x^{\mathrm{I}}}^{x^{\mathrm{III}}} \mathrm{d}x/\sigma_{\mathrm{X}} A_{\mathrm{X}}$ and $R_{\mathrm{Y}} = \int_{x^{\mathrm{III}}}^{x^{\mathrm{II}}} \mathrm{d}x/\sigma_{\mathrm{Y}} A_{\mathrm{Y}}$.

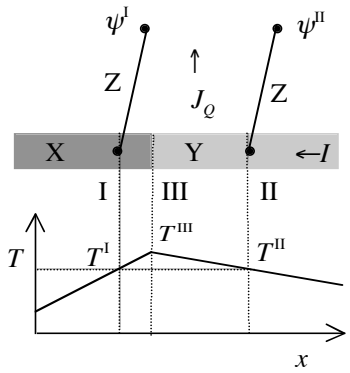

Figure 3. To determine $\pi_{\mathrm{Y}} - \pi_{\mathrm{X}}$ the observables $\mathrm{d}T^{\mathrm{I}}/\mathrm{d}x$, $\mathrm{d}T^{\mathrm{II}}/\mathrm{d}x$, $\Delta\psi$, and J_Q need to be measured. The sections I and II have the same temperature $T^{\mathrm{I}} = T^{\mathrm{II}}$.

REVIEW OF EXPERIMENTAL WORKS

In the previous section several expressions that relate the transport coefficients with the observables $\Delta\psi$ and J_Q have been deduced. Some of them are well-known and have been successfully applied for evaluating transport coefficients, as in thermal conductivity κ, thermoelectric power S and electric conductivity σ. However we cannot say the same when we refer to Peltier and Thomson coefficients. In the literature we find works where other energy balances have been applied. This subject will be discussed in a review of several selected papers [5-8].

The direct measurements of the Peltier coefficient are usually based on energy balances. This makes them difficult and rare. In fact we find very few works with measurements on this coefficient. Some of these papers use couples X/Y and apply the energy balance under steady-state isothermal conditions. Then, the Fourier term $\Delta\left[\kappa A\left(\mathrm{d}T/\mathrm{d}x\right)\right]$ and the Seebeck term $I\int_{T^{\mathrm{I}}}^{T^{\mathrm{II}}} \left(S_{\mathrm{Y}} - S_{\mathrm{X}}\right)\mathrm{d}T$ of equation (9) disappear. But this temperature distribution does not seem to be possible because at the junction $\mathrm{d}T_{\mathrm{X}}/\mathrm{d}x \neq \mathrm{d}T_{\mathrm{Y}}/\mathrm{d}x$ due to $\pi_{\mathrm{X}} \neq \pi_{\mathrm{Y}}$ (see figure 2).

Finally, from the lack of confidence in the values of the Peltier coefficient we conclude that the Onsager reciprocal relation still needs to be experimentally confirmed.

REFERENCES

1 Miller D G 1960 *Chem. Rev*. **60**, 15
2 Garrido J 2002 *J. Phys. Chem*. B **106**, 10722
3 Garrido J 2004 *J. Phys. Chem*. B **108**, 18336
4 Garrido J 2009 *J. Phys.: Condens. Matter* accepted.
5 Caswell A E 1911 *Phys. Rev*. **33**, 379
6 Rötzer G, Lockwood L and Gil J L 1977 *J. Appl. Phys*. **48**, 750
7 Jiménez J, Rojas E and Zamora M, 1984 *J. Appl. Phys*. **56**, 3250
8 Fukushima A, Kubota H and Yamamoto A 2006 *J. Appl. Phys*. **99**, 08H706

The Ternary Thermodynamic System CuSnP- Experimental and Computational Investigation

M. Grasser, A. Ludwig, J. Riedle
Christian-Doppler Laboratory for Multiphase Modelling of Metallurgical Processes
Department of Metallurgy, University of Leoben
Wieland-Werke AG, Research & Development, Ulm, Germany

Technical bronzes tend to form both macrosegregation and microsegregation during DC-casting due to the particular phase diagram situation, kinetics of phase transformation, and relative velocity between liquid and solid. As a result a heterogeneous cast microstructure forms. This can be observed after casting even in wrought alloys with a tin content from 4 to 8 wt.% Sn. Since the tin rich phases are brittle at room temperature as well as at hot working temperature, workability deteriorates. To describe solidification of these alloys, the ternary system Cu-Sn-P in the Cu-rich corner is investigated. For that, experimental investigations have been performed to define on the one hand the liquidus surface in detail and, besides, to confirm the ternary eutectic point in this region of the phase diagram. This is of special interest for industry, because the ternary eutectic point it is thought to be responsible for specific rigidity changes in technical bronze alloys.

In the presented work, the thermodynamics of the system Cu-Sn-P in the Cu-rich corner has been studied by computational thermodynamics and experimental investigations. Figure1 shows a 3D projection of the liquidus surface of the Cu-rich part of the ternary phase diagram Cu-Sn-P where the front view displays the binary Cu-Sn phase diagram up to 35 wt.% Sn. The isothermal lines (black fine lines) and mono variant lines (colored lines) of the liquidus surface are drawn based on the calculations performed with Thermo-Calc.

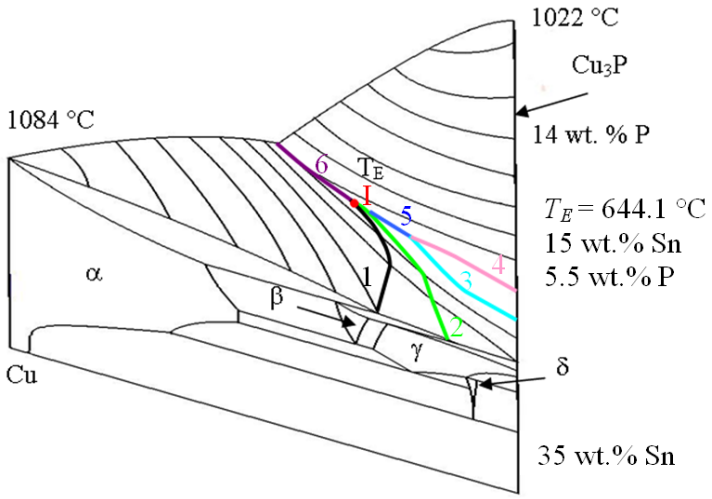

Figure 1: 3D liquidus surface of the ternary phase diagram Cu-Sn-P in the Cu rich-corner up to 35 wt.% Sn and 14 wt.% P based on calculations with Thermo-Calc (database CuSnII [THERMOCALC 05]*). The colored lines show the monovariant lines of the liquidus surface and the front view the binary system Cu-Sn. Monovariant lines corresponding to the (1) peritectic reaction* $L + \alpha \rightarrow \beta$ *(black line), (2) peritectic reaction* $L + \beta \rightarrow \gamma$ *(green line), (3) peritectic reaction* $\gamma + L \rightarrow \varepsilon$ *(bright blue line), (4) eutectic reaction* $L \rightarrow Cu_3P + \varepsilon$ *(pink line), (5) eutectic reaction* $L \rightarrow Cu_3P + \gamma$ *(blue line), (6) eutectic reaction* $L \rightarrow Cu_3P + \alpha$ *(purple line), (I) the ternary eutectic point (red point).* α *= Cu (max. Sn 15.8 wt.%, P 2 wt.%);* $\beta \sim Cu_{17}Sn_3$*;* $\gamma \sim Cu_3Sn$*;* $\delta \sim Cu_{41}Sn_{11}$*;* $\varepsilon \sim Cu_3Sn$*;* $\xi \sim Cu_{10}Sn_3$ *(nomenclation taken from* [EFFENBERG 07]*).*

DSC (Differential Scanning Calorimetrie) –measurements, annealing and diffusion experiments have been performed for the binary, Cu-Sn and Cu-P, and the ternary, Cu-Sn-P,

systems. Phase concentrations and phase regions where detected by SEM micrographs, LM-micrographs, and microprobe measurements.

For the binary systems, the performed DSC measurements confirm the published phase diagrams so far. It was possible to obtain all expected phase transformations by DSC measurement for CuSn4, CuSn20, CuP2, and CuP5, except for the ε phase. But it has to be mentioned that there are some discrepancies observed between different statements in literature [MASSALSKY 86], Thermo-Calc calculations, and the performed experiments. For example the liquidus temperature in the thermodynamic calculation is partly underestimated compared to both, literature and the obtained DSC measurements.

In addition, annealing experiments have been performed. Since P tends to evaporate at high temperature, a closed cylindrical geometry was used. For the ternary samples, a core of CuSn20P6 was combined with a pure copper casing and a combination of CuSn20 (as casing) and CuP8.3 (as core) was investigated. The sample shows a fine structured matrix consisting of α–δ eutectoid and dendrites of Cu_3P which is consistent with the expected phases based on literature. As published phase diagram data proposes, δ does not contain any P and Cu_3P no Sn. The temperature range and sample concentrations for the experimental study were chosen to lie in the area close to the ternary eutectic point to prove already published data and to gain more information about the ternary eutectic point. After annealing, the samples were quenched in cold water and prepared for SEM investigations.

Figure 2 shows a sample with a core of CuSn20P6 combined with a pure copper casing after annealing at 648 °C for 6 days and subsequently quenching. The sample got liquid at least in the centre (6, 5).

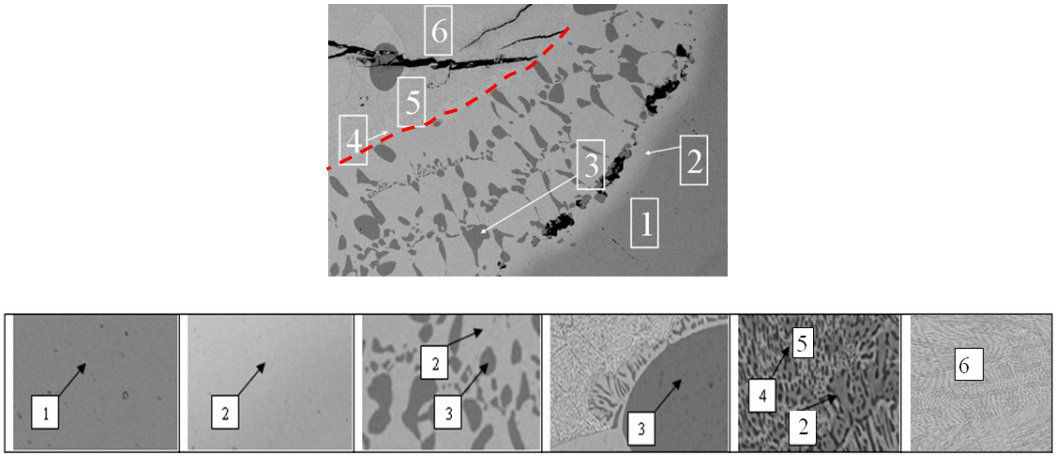

Figure 2: The upper picture shows a SEM picture of the diffusion sample at 648 °C. The numbers indicate the position of the different phase regions displayed in the phase sequence at the bottom of the figure. The observed phases are: (1) Cu, (2) α, (3) Cu_3P, (4) β. (5) indicates the three phase region $Cu_3P+\alpha+\beta$ showing the concentration of CuSn14.7P4.6, and (6) the three phase region $Cu_3P+\alpha+\beta$ showing the concentration of CuSn16.5P4.4. The red broken line marks the expected boundary of the liquid region.

In principle, the obtained results show good agreement with published and assessed data for the binary phase diagram as well as the ternary one. The diffusion experiments performed indicate that there is a ternary eutectic point in the Cu-rich corner of the Cu-Sn-P system at approximately CuSn15P5. Thermo-Calc (database CuSnII) and Miettinen [MIETTINEN 01] propose this point to be at around 644 °C. Based on the observed phase distributions up to

now, this point can be confirmed to lie between 648 °C and 642 °C. In addition, the γ phase was detected in a ternary sample in the presented study although former experimental work performed for the ternary system by Takemoto [TAKEMOTO 87] did not mention the occurrence of the γ phase. The ε phase was not observed in the presented study, neither in the DSC measurements nor in the diffusion experiments. According to literature and industry, this phase occurs after a very long transformation time. Due to this fact it is reasonable to ignore it for technical applications.

References:

[EFFENBERG 07] G. Effenberg, S. Ilyenko, Landolt-Börnstein-Group IV Physical Chemisty, 2007, 355-367.

[MASSALSKY 86] T.B. Massalsky, J.L. Murray, L.H. Bennet, H. Baker, American Society for Metals, Ohio, 1, 1986.

[MIETTINEN 01] J. Miettinen, Calphad, 25, 1, 2001, 67-78.

[TAKEMOTO 87] T. Takemoto, I. Okamoto, J. Matusumura, Trans. JWRI 16, 301, 1987, 73-79.

[THERMOCALC 05] ThermoCalc, “CuSnII Database“, 2005.

Understanding the first and second laws of thermodynamics: the microscopic/macroscopic duality

Bernard GUY
Ecole nationale supérieure des mines de Saint-Etienne
42023 Saint-Etienne cedex 2, France
guy@emse.fr

There remains a large variety of ways of presenting thermodynamics, associated with a large variety of understanding its foundations. This is another way to say that these foundations are still not clear, or at the very least not interpreted in a uniform way by the scientific community. This situation may cause confusion. The difficulties which arise are the differences in exposure between the phenomenological approach and the statistical approach, the definition of the new quantities (Q, U, S), the understanding of a privileged direction of evolution and the relations of the whole with standard mechanics.

It seems to us that *the duality between the two microscopic and macroscopic points of view is the key to seize in a unified way the two pillars of thermodynamics* that are: - new quantities as compared to mechanics (first law), and - the existence of a privileged direction of evolution (second law). We present the broad outline of this analysis, useful for the understanding of what is thermodynamics, and not usually exposed in all its generality. This is for us at the moment in good part a physical understanding in the meaning of Feynmann: “it is a completely un-mathematical, imprecise and inexact thing, but absolutely necessary for a physicist”! This presentation may also be useful to discuss some current trends in thermodynamics.

- definition of the new quantities
It rests on a distinction between two scales. *If the system is reduced to one or a few particles, one cannot make the difference between heat and work.* For a system made up of a great number of particles, one makes a separation between the macroscopic level (as summarized for example by the position of the barycentre of the system and its contours) and the microscopic level (position of the individual particles). In this separation, one admits that the movements of the individual particles are negligible with respect to the overall movement or do not affect it. One can thus to define heat (transfer of energy that does not affect the position of the barycentre of the system - nor its contours), in opposition to work (transfer that modifies them), internal energy (sum of the kinetic and potential energies of the particles referred to the barycentre; it equilibrates the energy balance when one takes into account the positions and movements at microscopic scale), and the entropy (a measurement of energy which is not associated to work), normalized to temperature (“energy” of a unit system, in correspondence with the system considered, with no interactions between its components, i.e. with no energy effect of its arrangement). By dividing dQ (that includes both position- and velocity- related energy) by T, one mostly restricts dS to the energy properties associated to the microscopic arrangement of the system (a higher Q exchange at a higher T will result in the same change in arrangement). There remain the vibrational and rotational energies that are not of a purely combinatorial character; but cannot be computed in the macroscopic work, in agreement with the above definition of entropy. Thus, two correlated definitions of entropy may be given: measurement of energy that is not associated to work, or, equivalently, energy associated to microscopic arrangement of the system, plus vibration and rotation terms.

- understanding of a privileged direction of evolution
The microscopic level also corresponds to the level where one cannot control (neither practically nor within one’s mind) the parameters of the system (positions of the individual particles). The possible evolutions are in correspondence with the most probable initial conditions. If these were finely controlled, one could generate evolutions that would be contrary to the second law. The practical resolution of the equations of mechanics for systems with a great number of particles leads to irreversibility (loss of the link with the initial conditions, effect of instabilities, sensitivity to the initial conditions that are known with a limited precision, influences of various types etc).

- consequences
It will be said that entropy is not intrinsic (it is not attached to a particle as its mass is for example), and that heat transfers are actually connected to a change of the combinatorial arrangement of the system. The definition and

properties of entropy can be understood but within a single package comprising both the first and second laws of thermodynamics.

In short, concepts of *heat, internal energy, entropy, privileged direction of evolution (and all the construction that follows, i.e. "a" thermodynamics), appear each time that, for a mechanical system, one makes a division between two levels of scale and a division of our knowledge (and our ignorance) between these two levels.* The transition from one scale to another cannot avoid in general making some assumptions of statistical nature in addition to the axioms of the mechanical starting level. *The separation can be made everywhere one wants* (one can build several "thermodynamics" according to the place where one cuts between various scales). For instance, one can decide to observe the overall movement of a mountain (the author is a also geologist!) with respect to which small movements at local scale (even macroscopic on a human scale!) are "heat transfers", and define thermodynamic quantities for the entire mountain.

Ways of research are proposed. At the conceptual and mathematical level: - it is necessary to wonder first: where do we put a limit, when do we decide to neglect the movement of a "microscopic" entity as compared to a "macroscopic" movement? - it is necessary to properly write the distinction between heat and work, and all that follows, as a function of the increase in the size of the system, for the various possible cases. Does this approach give an understanding of the non-equilibrium states? At the practical level: we have a method to rigorously define the quantities adapted to such new field (nano-materials?). Without forgetting the teaching level!

References

GP Beretta (2007) Axiomatic definition of entropy for non-equilibrium states, in: B. Guy and D. Tondeur, eds *Joint European Thermodynamics Conference IX*, Proceedings, Ecole n.s. des mines de Saint-Etienne, 24-29.

B. Guy (2008) Particles, scale, time construction and the second law of thermodynamics, *Meeting the entropy challenge, an international thermodynamics symposium*, GP Beretta, AF Ghoniem and GN Hatsopoulos eds., American Institute of Physics, 174-179.

One will compare with interest the definitions of the principal concepts of thermodynamics and their order of exposure for authors like: Balian, Beretta, Callen, Fargue, Fer, Gibbs, Keenan et al., Lemarchand et al., Perrot, Prigogine, Richet, Tisza etc.

Balance of Spin from the point of view of Mesoscopic Continuum Physics

Heiko Herrmann
Centre for Non-Linear Studies
TTÜ Küberneetika Instituut, Tallinn
hh@cens.ioc.ee

Mesoscopic Continuum Physics introduces variables describing the microstructure – like orientation of crystals – into the domain of the fields, thus treating them equivalently to space. The theory of Mesoscopic Continuum Physics has been reformulated, resulting in more compact equations, which are easier to understand. In this new formulation the balance of spin shows up naturally as component equations of the balance of momentum, this is an advantage over the standard formulation, in which it is postulated separately.

Thermodynamic Properties of Gaseous Plasmas in the Zero-Temperature Limit

Igor Iosilevskiy
Moscow Institute of Physics and Technology (State University)
ilios@orc.ru

Limiting structure of thermodynamic functions of gaseous plasmas is under consideration in the limit of extremely low temperature and density. Remarkable tendency, which was claimed previously [1-3], is carried to extreme. The point is that the discussed limit ($T \to 0$; $n \to 0$) is carried out at fixed value for chemical potential of electrons ($\mu_{el} = const$) or "atoms" ($\mu_a = Z\mu_e + \mu_i = const$) or "molecule" ($\mu_{m \leftrightarrow 2a} = 2\mu_a = const$) *etc*. In this limit both equations of state (EOS) thermal and caloric ones, obtain almost identical *stepped* structure ("ionization stairs" [3]) when one uses special forms for exposition of these EOS as a function of electron chemical potential: i.e. PV/RT for thermal EOS and $U - (3/2)PV$ for caloric EOS *vs.* μ_{el}. Examples of this limiting structure are exposed at figures 1 and 2 for thermal and caloric EOS of lithium and helium plasmas [4-6]. For rigorous theoretical proof of existing the limit, which is under discussion (Saha-limit) in the case of hydrogen see [7,8] and references therein.

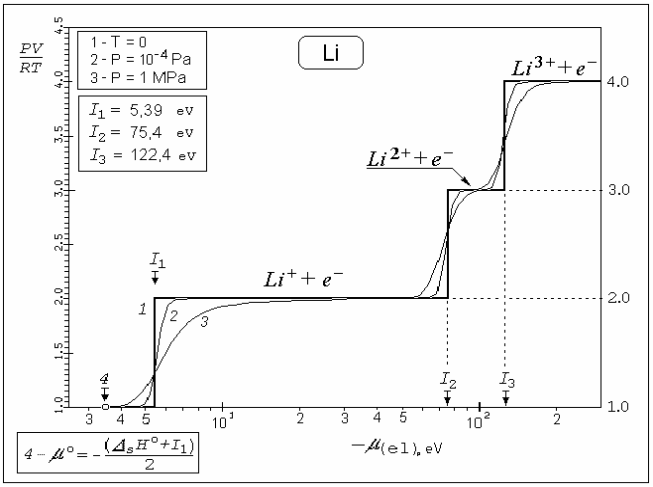

Figure 1. Thermal EOS of lithium plasma in quasi-chemical limit (figure from [4,6]). Compressibility factor $PV/RT \equiv P/(n_{Li}kT)$ as a function of (negative) value of electron chemical potential. *Notations*: *1* – isotherm $T = 0$; *2, 3* – isobars ($P = const$); *arrows* – elements of "*intrinsic energy scale*" for lithium: I_1, I_2, I_3 – lithium ionization potentials; *4* – saturation vapour boundary $\{(\mu_e)^0 = -(\Delta_s H^0 + I_1)/2\}$. (Isobars *2, 3* are calculated via code SAHA-IV [9] with neglecting of equilibrium radiation contribution)

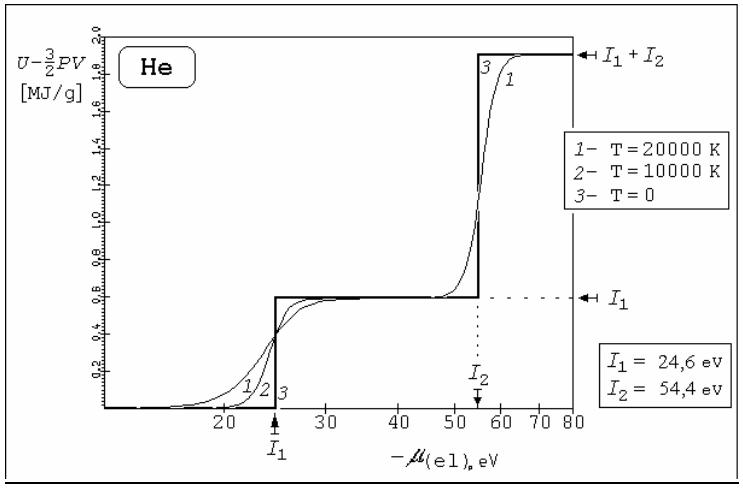

Figure 2. Caloric EOS of helium plasma in quasi-chemical limit (figure from [6,10]. Complex $U - (3/2)PV$ as a function of (negative) value of electron chemical potential. *Notations*: *1* – isotherm $T = 20\ 000$ K; *2* – $T = 10\ 000$ K; *3* – $T = 0$ K; *arrows* – elements of helium "*intrinsic energy scale*": I_1, I_2 – helium ionization potentials; (Isotherms *1, 2* are calculated via code SAHA-IV [9] with neglecting of equilibrium radiation contribution)

The same *stepped* structure appears in the zero-temperature limit in any molecular gases, for example hydrogen [4][6].

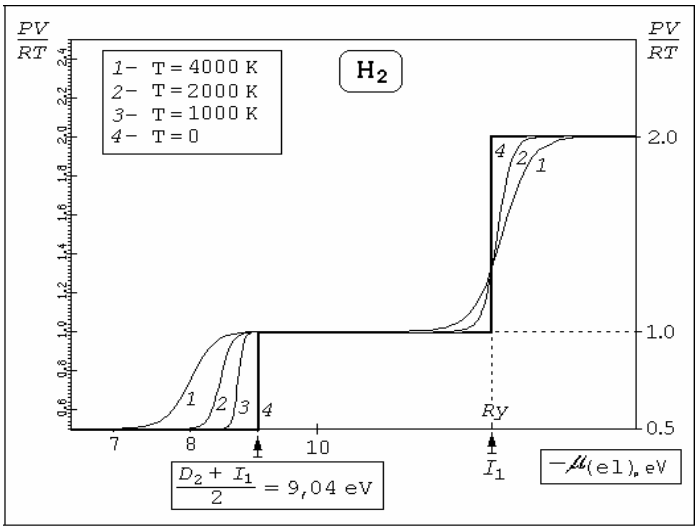

Figure 3. Thermal EOS of hydrogen plasma in quasi-chemical limit (figure from [4]) Compressibility factor $PV/RT \equiv P/(n_{Li}kT)$ as a function of (negative) value of electron chemical potential. *Notations*: *1,2,3,4* – isotherms T = 4000, 2000, 1000, 0 K correspondingly. I_1 = Ry – hydrogen ionization potential. $(D_2 + I)/2$ – position of "dissociation step" at electron chemical potential scale. Isotherms *1-3* are calculated via code SAHA [11] with neglecting of equilibrium radiation contribution.

This limiting structure appears within a fixed (negative) range of μ_{el} ($\mu_{el}^{**} \geq \mu_{el} \geq \mu_{el}^{*}$). It is bounded below by value of major ionization potential ($\mu_{el}^{*} = -I_Z = -Z^2Ry$) and above by the value depending on ionization potential and sublimation energy of substance $\{\mu_{el}^{**} = -(\Delta_o H^S + I_1)/2\}$. Binding energies of all possible bound complexes (atomic, molecular, ionic and clustered) in its *ground state* are the *only* quantities that manifest itself in meaningful details of this limiting picture as location and value of every step. The energy of *macroscopic* binding – the heat of condensation at $T = 0$ – supplement this collection. At the same time there are *no* such *steps* for *exited states* of such bounded complexes (ions, atoms, molecules and clusters). Altogether, all energies mentioned above form "*intrinsic energy scale*" [3][10] for any substance.

In the zero-temperature limit all thermodynamic differential parameters (heat capacity, compressibility, *etc.*) obtain their remarkable δ-like structures ("thermodynamic spectrum" [3][10]). Both kinds of such "spectrum" became apparent: i.e. "emission-like spectrum" for heat capacity (fig. 3) and "absorption-like spectrum" for the isentropic coefficient $-(\partial \ln P/\partial \ln V)_S$ (fig. 4). It should be stressed again that all "lines" of these "thermodynamic spectrum" are centralized just at the elements of the "*intrinsic energy scale*" – binding energies of ground states for all bound complexes in the system.

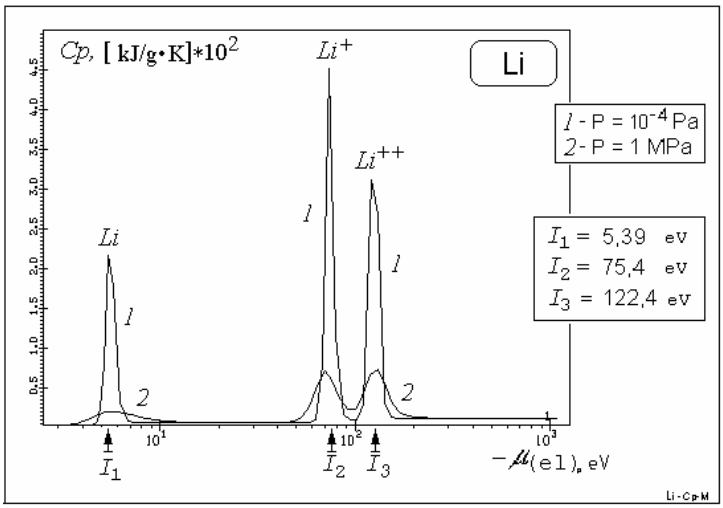

Figure 3. Limiting structure for differential thermodynamic quantities ("thermodynamic spectrum") in quasi-chemical limit $T \to 0$ (figure from [4,6]). Isobaric heat capacity of lithium plasma as a function of (negative) value of electron chemical potential. *Notations*: *1, 2* – isobars (10^{-4} Pa and 1 MPa)*; arrows* – elements of "*intrinsic energy scale*" for lithium: I_1, I_2, I_3 – lithium ionization potentials. (Isobars *1,2* are calculated via code SAHA-IV [9] with neglecting of equilibrium radiation contribution)

The limiting EOS stepped structure ("ionization stairs") of gaseous zero-Kelvin isotherm is generic prototype of well-known "shell oscillations" in EOS of gaseous plasmas at low, but finite temperatures and non-idealities [2]. At the same time this limiting form of plasma thermodynamics could be used as a natural basis for rigorous deduction of well-known quasi-chemical approach ("chemical picture") in frames of asymptotic expansion around this reference system. The point is that this expansion must be provided on temperature at fixed chemical potential, in contrast to the standard procedure of expansion on density at constant temperature [12,1].

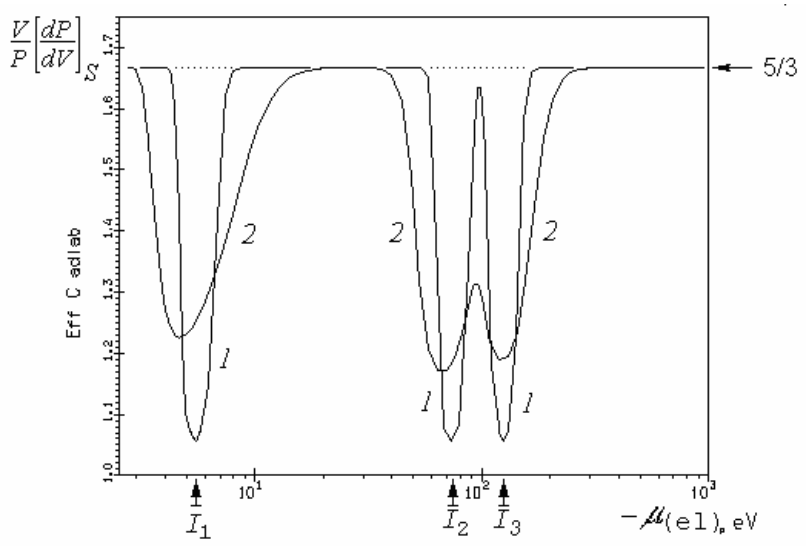

Figure 4. Limiting structure for differential thermodynamic quantities ("thermodynamic spectrum") in quasi-chemical limit $T \to 0$ (figure from [4,6,10]). Isentropic coefficient of lithium plasma $(\partial \ln P/\partial \ln V)_S$ as a function of (negative) value of electron chemical potential. *Notations*: – as at figure 3. Ideal-gas value $(\partial \ln P/\partial \ln V)_S = 5/3$ is noted.

The *gaseous branch* of zero-Kelvin isotherm $U_0^{gas}(\boldsymbol{\mu})$ could be naturally conjugated with associated *condensed branch* $U_0^{crystal}(\boldsymbol{\mu})$. Due to the choice of chemical potential as a ruling parameter this combination creates complete and *totally meaningful* non-standard "cold curve" for any substance $\{U_0(\boldsymbol{\mu})$ instead of $U_0(\rho)\}$. The point is the appearance of stable thermodynamic gaseous branch for this "cold curve", which reflects schematically *all reactions* (ionization, dissociation etc.) and phase transitions which are realized at the system. Besides, the stable part of new combined "cold curve" it could be supplemented with additional *metatstable* branches, corresponding to overcooled vapour from gaseous part, and extended crystal from condensed part (figure 5) [13]. Another advantage of new representation for cold curve is natural identity of all transformations mentioned above (ionization, dissociation and phase transitions). It approve widely used interpretation of finite temperature ionization and dissociation as a "smoothed" phase transitions [10].

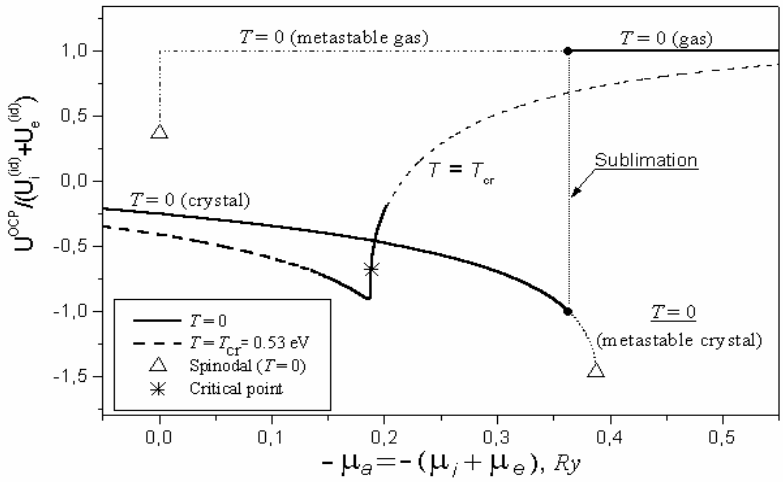

Figure 5. Modified "cold curve" (isotherm $T = 0$) and critical isotherm ($kT_{cr} \approx 0.53$ eV) in modified one-component plasma model on *uniformly-compressible* compensating background {OCP(~)} [14]. Dimensionless internal energy, $U^{OCP}/(U_i^{(id)} + U_e^{(id)})$, as function of "atomic" chemical potential (electroneutral combination of chemical potentials for ion and electrons (background)). Two metatstable branches are exposed: *overcompressed* vapour and *extended* solid completed by spinodal points (figure from [3,10]).

Remarkable limiting structure of thermodynamics for real substances, which is under discussion, could manifest itself also in simplified classical models. Similar "ionization stairs", "thermodynamic spectrum" and modified "cold curve" was predicted [3,13,10] for modified one-component ionic model on uniformly-compressible compensating background OCP(~) [14,15] and for two-component classical ionic model with Glauberman's [16] potential $\{V_{ij}(r) \equiv Z_i Z_j e^2[1 - \exp(-r/\sigma)]/r\}$ [4] and for classical charged hard- and soft-spheres models. In the first model OCP(~) there is no electron-ionic associations on definition. The only transformations permitted in the model are three 1st-order phase transitions between solid, liquid and gas-like states. Non-standard cold curve of OCP(~) with sublimation jump and metatstable portions are shown at fig. 5.

All present statements about remarkable limiting structure of thermodynamic functions in zero-temperature limit for single substances are valid also in application to the chemical compounds. In this case one-dimensional structures: "ionization stairs", modified "cold curve" and "thermodynamic spectrums" turn into more complicated two-dimensional figures composed from discontinuities (steps) and ideal-gas planes. Features and properties of such limiting structures are non-investigated at the moment.

New representation for cold curve (isotherm $T = 0$), which is introduced in present paper, has advantage for solution of theoretical problem of correct deducing of quasi-chemical representation (so-called "chemical picture" – ensemble of "free" simple and complex particles, atoms, molecules, ions and electrons with weak effective interaction) from rigorous physical representation (ensemble of nuclei and electrons with strong Coulomb interaction). Both "ionization stairs" in thermal and caloric EOS are natural zero-order terms in systematic asymptotic expansion for thermodynamic functions in the limit $T \to 0$ by the small parameter $\lambda \sim \exp\{-const/T\}$ at constant value of chemical potential [3,4,10]. It should be noted that well-known presently accepted traditional theoretical approach uses asymptotic expansion in terms of *activities* at *constant temperature* (for example [12]). Rigorous asymptotic expansion by functions of *temperature* in the limit $T \to 0$ (SAHA-limit) is developed for hydrogen in papers [7,8] et al. for the region of atomic chemical potential corresponding to the case of electron-ion-atomic plasma. It should be stressed that desirable approach should develop asymptotic expansion in the limit $T \to 0$ simultaneously for *all values* of chemical potential within mentioned above "energy scale" from the state of full ionization ($\mu_{el} \sim -I_Z$) up to the saturation point and including the regions of *all stages* of ionization and atoms and molecules formation.

Acknowledgments

The work was supported by Grants: ISTC 3755 and by RAS Scientific Programs "Research of matter under extreme conditions" and "Physics of high pressure and interiors of planets"

References

[1] Iosilevski I. *High Temperature* **19** 494 (1981).
[2] Iosilevski I. and Gryaznov V. *High Temperature* **19** 799 (1981).
[3] Iosilevskiy I. *Plasma Thermodynamics in Zero-Temperature Limit* / Int. Conference "Physics of Non-Ideal Plasmas", Greifswald, Germany, 2000.
[4] Iosilevskiy I. / in *Encyclopedia of low-temperature plasma physics,* Supplement III-1 /eds. A. Starostin and I. Iosilevskiy, FIZMATLIT: Moscow, 2004, PP 349-428 (in Russian)
[5] Iosilevskiy I. / *Thermodynamic properties of low-temperature plasmas,* in: "*Encyclopedia of low--temperature plasma physics*" /ed. V. Fortov, Moscow: NAUKA, 2000, V.1, P.284 (in Russian).
[6] Iosilevskiy I. *Thermodynamics of gaseous plasmas at the zero-temperature limit* / in "Physics of matter under extreme conditions" /ed. V. Fortov, IPCP RAS: Moscow, 2002, P.157 (in Russian).
[7] Brydges C. and Martin P. *J. Stat. Phys.* **96** 1163 (1999).
[8] Alastuey A., Ballenegger V. *J. Phys. A: Math. & Theor.* **42** (2009) (in press).
[9] Gryaznov V., Iosilevskiy I., Fortov V. *Thermodynamic properties of shock-compressed plasmas* / in: "*Encyclopedia of Low-Temperature Plasma Physics",* Supplement III-1 /eds. A. Starostin and I. Iosilevskiy, FIZMATLIT: Moscow, 2004, PP. 111-139 (in Russian)
[10] Iosilevskiy I., Krasnikov Yu., Son E., Fortov V. *Thermodynamic properties of non-ideal plasmas* / in "*Thermodynamics and Transport in Non-Ideal Plasmas*", MIPT Publishing: Moscow, 2000, PP.120-138 (in Russian); FIZMATLIT: Moscow, 2009, (in press).
[11] Gryaznov V., Iosilevskiy I., Krasnikov Yu., Kuznetsova N., Kucherenko V., Lappo G., Lomakin B., Pavlov G., Son E., Fortov V. // *Thermophysics of Gas-Core Nuclear Engine* / ed. V.M. Ievlev, ATOMIZDAT: Moscow, 1980 (in Russian)
[12] Ebeling W., Kraeft W.D., Kremp D. *Theory of Bound States and Ionization Equilibrium in Plasmas and Solids,* Akademic–Verlag: Berlin, 1976.
[13] Iosilevskiy I. *Generalized "cold curve" and thermodynamics of a substance at the zero-temperature limit* // in "Physics of matter under extreme conditions" /Ed. V. Fortov, IPCP RAS: Moscow (2001) p.116 (in Russian).
[14] Iosilevskiy I. *High Temperature* **23** 807 (1985) arXiv:0901.3535
[15] Iosilevski I. and Chigvintsev A. /in "*Physics of Non-Ideal Plasmas"*// eds. W. Ebeling and A. Forster /Teubner: Stuttgart-Leipzig, 1992, PP. 87-94, arXiv:physics/0612113
[16] Glauberman A.E. *Doklady of Soviet Academy of Science,* **78**, 883 (1951)

Predicting with accuracy the phase equilibria of synthetic petroleum fluids with the purely predictive PPR78 approach.

Jean-Noël JAUBERT, Romain PRIVAT and Fabrice MUTELET
Institut National Polytechnique de Lorraine, Ecole Nationale Supérieure des Industries Chimiques, Laboratoire de Thermodynamique des Milieux Polyphasés, 1, rue Grandville, F54000 Nancy.
e-mail: jean-noel.jaubert@ensic.inpl-nancy.fr

The thermodynamic modelling of petroleum fluids is a highly challenging task for engineers. Indeed, such mixtures contain a huge number of various compounds, such as paraffins, naphthenes, aromatics, gases (CO_2, H_2S, N_2, …), mercaptans and so on. A proper representation involves to accurately quantifying the interactions between each pair of molecules, which is obviously becoming increasingly difficult if not impossible as the number of molecules is growing. To avoid such a fastidious work, an alternative solution lies in using a predictive model, able to estimate the interactions from mere knowledge of the structure of molecules within the petroleum blend. To build such a model, we have combined the 1978 version of the Peng-Robinson (PR) equation of state (EOS) [1] with a group contribution (GC) method [2-10] allowing the estimation of the interactions between molecules:

$$\begin{cases} P = \dfrac{RT}{v-b} - \dfrac{a(T)}{v(v+b)+b(v-b)} \\ a(T) = \displaystyle\sum_{i=1}^{N}\sum_{j=1}^{N} z_i z_j \sqrt{a_i(T)\,a_j(T)}\left[1-k_{ij}(T)\right] \\ b = \displaystyle\sum_{i=1}^{N} z_i b_i \end{cases}$$

P is the pressure of the N component-mixture, v is its molar volume, T is its temperature and **z** is the molar fractions vector. $a_i(T)$ and b_i are specific parameters for pure component i. $k_{ij}(T)$, whose choice is difficult even for the simplest systems, is the so-called binary interaction parameter characterizing molecular interactions between molecules "i" and "j". The common practice is to fit k_{ij} so as to represent the vapor-liquid equilibrium data of the mixture under consideration. Such a solution works well for binary systems but can not be applied to a petroleum fluid containing hundreds of compounds and therefore thousands of binary interaction parameters. In this study, in order to obtain a predictive model and to define the PPR78 (predictive, 1978 PR EOS) approach, k_{ij}, which depends on temperature, is expressed in terms of group contributions, through the following expression:

$$k_{ij}(T) = \frac{-\dfrac{1}{2}\displaystyle\sum_{k=1}^{N_g}\sum_{l=1}^{N_g}(\alpha_{ik}-\alpha_{jk})(\alpha_{il}-\alpha_{jl})A_{kl}\cdot\left(\frac{298.15}{T}\right)^{\left(\frac{B_{kl}}{A_{kl}}-1\right)} - \left(\dfrac{\sqrt{a_i(T)}}{b_i}-\dfrac{\sqrt{a_j(T)}}{b_j}\right)^2}{2\sqrt{a_i(T)\cdot a_j(T)}\Big/\left(b_i\cdot b_j\right)}$$

N_g is the number of different groups defined by the method (for the time being, 16 groups are defined and $N_g = 16$). α_{ik} is the fraction of molecule i occupied by group k (occurrence of group k in molecule i divided by the total number of groups present in molecule i). $A_{kl} = A_{lk}$ and $B_{kl} = B_{lk}$ (where k and l are two different groups) are constant parameters ($A_{kk} = B_{kk} = 0$). These parameters have been determined in order to minimize the deviations between calculated and experimental fluid phase equilibrium data (liquid-vapour, liquid-liquid, azeotropic and critical data) from a huge binary data base (nearly all the available fluid phase equilibrium data of binary systems available in the open literature have been collected) using a well-chosen optimization procedure.

As a general rule, the restitution of these experimental data points is quite satisfactory for a predictive model [10]. The following table gives an overview of the absolute and relative average deviations (respectively AAD and RAD) for the 66016 binary data points considered:

Table 1. Deviations between experimental phase equilibrium data of binary systems and their estimation by the PPR78 model.

	AAD	RAD	Number of experimental data
Liquid molar fractions	0.018	6.3 %	36797
Vapour molar fractions	0.011	6.9 %	28152
Critical molar fractions	0.016	5.8 %	1067
Critical pressure	6.3 bar	3.4 %	1067

Once the group contributions i.e. the A_{kl} and B_{kl} parameters estimated, the PPR78 model can be used as a purely predictive approach, to model the fluid phase behaviours of petroleum fluids. In that way, we have tested out the capacity of PPR78 on many synthetic fluids found in the literature and we have got quite accurate results in most of the cases [10]. Figure 1 here below, shows predicted phase envelopes of some natural gases and oils.

Figure 1. Phase envelopes of three synthetic petroleum fluids (crude oils and condensate gas) predicted by the PPR78 model. (+) experimental bubble or dew pressures, (□), experimental critical point, (○), predicted critical point. Line: predicted bubble and dew curves.

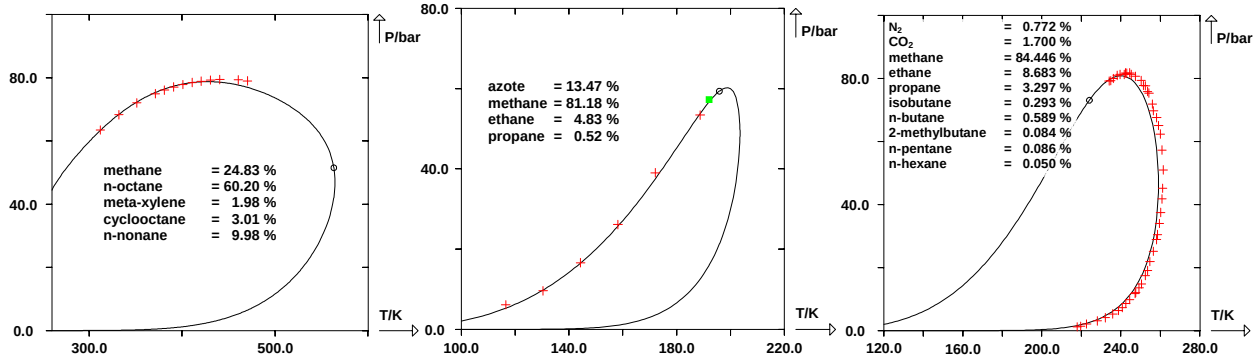

In addition, satisfactory predictions of swelling experiments (see figure 2) and accurate estimation of the MMP (minimum miscibility pressures) can be obtained from PPR78.

Figure 2. Swelling of a crude oil by pure CO_2 at two different temperatures. (□), experimental bubble or dew point, (○), predicted critical point. (∗), predicted first contact miscibility pressure. Line: predicted bubble and dew curves.

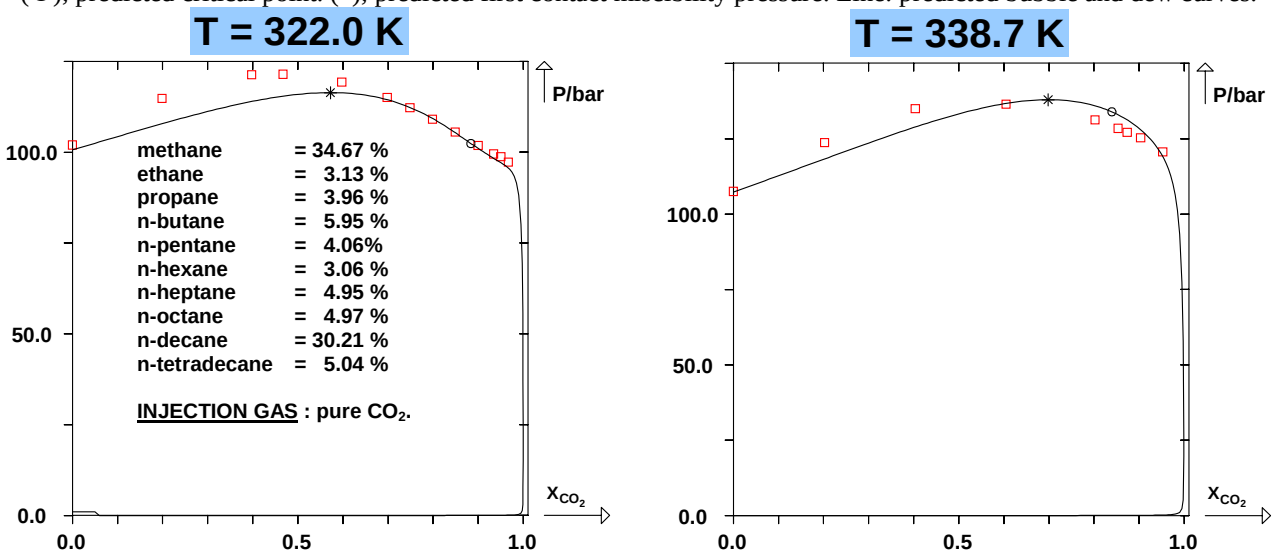

References.

[1] Robinson, D.B., Peng, D.Y., Gas Processors Association, Research Report RR-28, 1978.
[2] Jaubert, J.-N., Mutelet, F., Fluid Phase Equilibria, (2004), 224(2), 285-304.
[3] Jaubert, J.-N.; Vitu, S.; Mutelet, F.; Corriou, J. P. Fluid Phase Equilib. 2005, 237(1-2), 193-211.
[4] Vitu, S.; Jaubert, J.-N.; Mutelet, F. Fluid Phase Equilib. 2006, 243, 9-28.
[5] Vitu, S.; Privat, R.; Jaubert, J.-N.; Mutelet, F. J. Supercrit. Fluids. 2008, 45(1), 1-26.
[6] Privat, R.; Jaubert, J.-N.; Mutelet, F. Ind. Eng. Chem. Res. 2008, 47(6), 2033-2048.
[7] Privat, R.; Jaubert, J.-N.; Mutelet, F. J. Chem. Thermodynamics, 2008, 40, 1331-1341.
[8] Privat, R.; Jaubert, J.-N.; Mutelet, F. Ind. Eng. Chem. Res. 2008, 47, 7483-7489.
[9] Privat, R.; Jaubert, J.-N.; Mutelet, F. Ind. Eng. Chem. Res. 2008, 47, 10041-10052.
[10] Privat, R.; PhD thesis, Nancy Université - INPL, France, 2008.

Superstatistics paradigm and path-integral calculus

Petr Jizba[1,2] and Hagen Kleinert[2]

[1]FNSPE, Czech Technical University, Břehová 7, 115 19, Praha 1, Czech Republic
[2]ITP, Freie Universität Berlin, Arnimallee 14 D-14195, Berlin, Germany

jizba@physik.fu-berlin.de

Abstract

Probability distributions which can be obtained from superpositions of Gaussian distributions of different variances $v = 2$ play presently a favored role in quantum mechanics and in theory financial markets [1]. In general, such superpositions do not necessarily obey the Chapman–Kolmogorov semigroup relation for Markovian processes because they often introduce memory effects. In this talk we derive the general form of the smearing distributions in v which do not destroy the semigroup property. The presented smearing technique has two immediate applications which we wisch to discuss [2,3].

Firstly, our approach permits simplifying the system of Kramers–Moyal (and Fokker–Planck) equations for smeared and unsmeared conditional probabilities. In the latter case the dynamics of the smearing distribution is explicitly separated from the dynamics of the transitional amplitude which a desirable starting point, for instance, in quantum optics or in superstatistics.

Secondly, our smearing technique can be conveniently implemented in the path integral calculus. This is because in many cases, the superposition of path integrals can be evaluated much easier than the initial path integral. To put some flesh on the bar bones we will present three simple examples [2,3]; "microcanonical" smearing, Heston's stochastic volatility model and relativistic scalar particle. We will also briefly comment on the possibility of extension of the presented technique to quantum mechanics and quantum field theory. Finally, some comments will be also added on a natural appearance of the Tsallis distribution in the scheme.

---

[1] P. Jizba, H. Kleinert and P. Haener, [arXiv:0708.3012]; will apper in Physica A

[2] P. Jizba and H. Kleinert, [arXiv:0712.0083]

[3] P. Jizba and H. Kleinert, [arXiv:0802.0695]; Phys. Rev. E **78** (2008) 031122

The Universal Effectiveness of Topological Thermodynamics

R. M. Kiehn
University of Houston (retired)
http://www.cartan.pair.com
rkiehn2352@ aol.com

Continuous Topological Evolution and its application to non-equilibrium Thermodynamic Systems and Irreversible processes, was conceived using Cartan's methods of exterior differential forms, evaluated on partially ordered differentiable varieties - not the diffeomorphic geometric equivalences of tensor analysis. Topological non-equilibrium thermodynamic *systems* are encoded in terms exterior differential 1-forms with topological properties dependent upon the Pfaff Topological (not geometrical) Dimension (PTD). The *process* direction fields (for both reversible and irreversible processes) are defined in terms of the coefficients of exterior differential 3-forms, or currents, on 4D pre-geometric (no metric) space-time. Unlike the Amperian currents of electromagnetism, it was discovered that there are two 3-form currents that exist only in non-equilibrium systems where PTD > 2. These currents do not necessarily obey conservation laws. The first 3-form (1969) was called the 3-form of Topological Spin. The second 3-form (1976) was called the 3-form of Topological Torsion. This Torsion current (when PTD=4) is inextrincably linked with Turbulence and irreversible decay in fluid flow; hydrodynamic wakes are evidence of when the PTD=3. Examples of emergence of systems with PTD=3 in dissipative systems of PTD=4 give formal credence to Prigogine's conjectures. In 1964, the concept of a (topological) Spin Current was an exotic idea, but now, the concept of a Spin Current has entered the practical world of nanometer physics called "Spintronics".

The Torsion current is an artifact of processes in non-equilibrium systems, and can contain components that have been described by E. Cartan as isotropic (macroscopic) spinors, or complex vectors of null amplitude and complex eigenvalues. The fact that the root structure (1 positive, 2 complex) above the Critical Isotherm for a van der Waals gas is evidence of such spinors. The existence of processes with spinor components implies the existence of anti-symmetries, and are the cause of (topological) fluctuations and irreversible dissipation.

The use of Cartan's magic formula in terms of the Lie differential with respect to a process acting on a thermodynamic systems encodes the idea of Continuous Topological Evolution as a cohomological statement of dynamics: the result is a dynamical-topological-universal representation of the First Law of Thermodynamics.

This perspective of Continuous Topological Evolution leads to a number of significant results:

1. Topological change is a necessary condition for thermodynamic irreversibility.
2. Continuous Topological Evolution establishes a logical basis for thermodynamic irreversibility and the arrow of time without the use of statistics. Evolution from a disconnected KCT_0 topology to a connected topology can be continuous and irreversible, but evolution from a connected topology to a disconnected topology cannot be continuous.

3. An irreversible process requires that the Heat current 3-form is not zero: $Q \hat{} dQ \neq 0$. Smooth C2 processes can be irreversible, $Q \hat{} dQ \neq 0$, while segmented C1 approximations to C2 smooth processes can be reversible.

4. Adiabatic processes are transverse to the Heat 1-form, $(i(\rho \mathbf{V}_4)Q) = 0$. Adiabatic processes need not be quasi-static, and can be reversible or irreversible.

5. A fundamental difference between Work and Heat is that Work always is transversal to the processes, such that $i(\rho \mathbf{V}_4)W = 0$; but it is not true that $i(\rho \mathbf{V}_4)Q = 0$, unless the process is adiabatic.

6. For non-equilibrium systems, the 3-form of Topological Torsion (an N-1=3-form current) is not zero: $A \hat{} dA = i(\mathbf{T}_4)dx \hat{} dy \hat{} dz \hat{} dt \neq 0$. The Topological Torsion vector, $\mathbf{T}_4$, is deduced intrinsically from the 1-form that encodes the thermodynamic system. It can be used as a direction field for an irreversible process current, $\rho \mathbf{T}$, if the divergence of the process current is not zero.

7. For PTD=3 "closed" thermodynamic systems, the process current $\rho \mathbf{V}_4$ has zero divergence, and the 4D volume element is a conformal invariant (any ρ). This result is the space-time extension of the Liouville theorem that preserves the phase-space volume element in classical theory

8. For a PTD=4 "open" thermodynamic systems, the Topological Torsion Current is not conserved. This result is the extension of the Vlasov equation; the 4D differential volume element is expanding or contracting. Such processes in the direction of $\mathbf{T}_4$ are irreversible and dissipative.

9. In electromagnetic systems, the dissipation coefficient is proportional to $\mathbf{E} \circ \mathbf{B}$; in hydrodynamics, the dissipation coefficient is called "Bulk viscosity" and equals (a$\circ$curl v).

10. Examples of thermodynamic systems can be given to demonstrate that the conjectured format of the London Current of superconductivity, where $\mathbf{J} = \chi \mathbf{A}$, can be deduced as a consequence of the Topological Theory of Thermodynamics.

11. For the Spin Current 3-form, examples can demonstrate that, formally, the Spin current is proportional to the Lorentz force (the space-time components of the Work 1-form, W). This is a new interpretation of an old result, $\mathbf{J} = \sigma(\mathbf{E} + \mathbf{VxB})$, which is Ohm's law. The new part is due to the idea that the dissipation is due to Spin Currents and the transport of collective spins, $A \hat{} G$.

12. The Kolmogorov-Cartan T_0 topological structure for equilibrium domains of PTD ≤ 2 creates a connected, but not necessarily simply connected, topology. Evolutionary predictive solution uniqueness is possible, as the Frobenius theorem is satisfied, and the problem can be reduced to two independent functions (a two body problem).

13. The Kolmogorov-Cartan T_0 topological structure for non-equilibrium domains of PTD ≥ 2 creates a disconnected topology of multiple components. If solutions to a particular evolutionary problem exist, then the solutions are not unique. Envelope solutions, such as Huygen wavelets and propagating tangential discontinuities (called signals, or wakes) are classic examples.

14. All Hamiltonian, Symplectic-Bernoulli and Helmholtz processes are thermodynamically reversible. In particular, the work 1-form, W, created by Hamiltonian processes is of Pfaff Topological Dimension 1 or less. In all reversible cases the Work 1-form is closed, $dW = 0$.

15. In the PTD=4 case, there exist density distributions, ρ, such that the divergence of the process current is zero. There exist an infinite number of such integrating factors, that define "stationary states" far from equilibrium. It can be demonstrated in terms of continuous topological evolution that a density dis-

tribution which defines a "stationary" state can emerge as a topological defect,or soliton, in a PTD=4 system, by dissipative processes. Such a result gives formal credence to Prigogine's conjectures.

16. The assumption of uniqueness of evolutionary solutions (which implies the Pfaff Topological Dimension of the thermodynamic system be equal to 2 or less), or the assumption of homeomorphic evolution, have imposed constraints upon classical mechanics that eliminate any time asymmetry.

17. The Lie differential can encode both non-adiabatic or adiabatic processes. The ubiquitous affine covariant differential of tensor analysis can *always* be cast into a form representing an *adiabatic* process.

18. On spaces of PTD=4, the Jacobian of the components of the 1-form of Action, A, define a correlation matrix, which has a four order characteristic polynomial that defines an equation of state in terms of Cayley-Hamilton similarity invariants. The Cayley-Hamilton theorem produces an implicit hypersurface function that can have envelopes and edges of regression in the format of the Gibbs function for a (universal and deformable) van der Waals gas. The method yields analytic expressions for the critical point, and the binodal and spinodal lines, in terms of the similarity invariants. The same technique can be applied to dynamical systems.

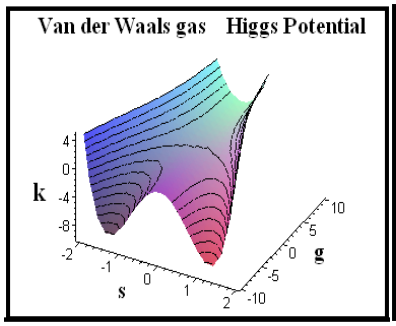

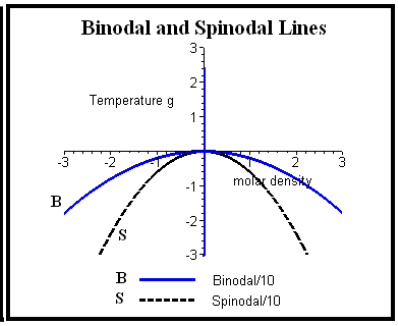

19. Cartan's Magic formula, in terms of the Lie differential acting on exterior differential 1-forms, establishes the long sought for combination of dynamics and thermodynamics, enabling non-equilibrium systems, and many irreversible processes, to be computed in terms of continuous topological evolution, without resort to probability theory and statistics.

20. Topological fluctuations can be induced by processes that have components in terms of thermodynamic macroscopic Spinors. Thermodynamic Macroscopic Spinors are non-zero complex eigenvectors with complex eigenvalues (and zero quadratic form) of the antisymmetric 2-form (or matrix) representing the "Limit Points", dA, of the 1-form of Action, A. Such Macroscopic Spinors are capable of representing minimal surface conjugate pairs.

21. A conjecture of a turbulent non-equilibrium thermodynamic cosmology can be constructed in terms of a dilute van der Waals gas near its critical point. The conjecture yields an explanation for:

a. The granularity of the night sky as exhibited by stars and galaxies due to density fluctuation near the critical point, and the Newtonian law of gravitational attraction proportional to $1/r^2$ as a correlation between fluctuations (Lev Landau).

b. The conformal expansion of the universe as an irreversible phenomenon-associated with Quartic similarity invariants in the thermodynamic phase function, and conformally related to dissipative effects.

c. The possibility of domains of *negative pressure* (explaining what has recently been called "*dark energy*") are due to a *classical* "Higgs" mechanism for aggregates below the critical temperature

d. The possibility of domains of *negative temperature* (explaining what has recently been called "*dark matter*") due to macroscopic collective states of ordered spins. The conjecture is that Positive temperature radiates, Negative temperature does not. The conjecture is that black holes could be negative temperature states of collective spins.

e. The possibility of domains where gravitational effects (quadratic similarity invariants, or 2nd order Gauss curvature effects) appear to be related to entropy and temperature properties of the thermodynamic system, and where cubic curvature effects could impede gravitational collapse.

f. Black Holes (generated by Petrov Type D solutions in gravitational theory) are to be related to Minimal Surface solutions to the Universal thermodynamic 4th order Phase function.

22. The Kolmogorov T0 topology of thermodynamics is based upon a specialization partial order of closure. Every Open set is an upper (Up) set $\uparrow$ and every closed set is a lower (Down) set $\downarrow$. The T0 topological structure for thermodynamics is deduced from any 1-form on a specialization order of differential varieties. The T0 topology admits a dual topology, T*0. The closure condition is inherent in the concept of Continuous Topological Evolution of T0 and T*0 topologies and CONTINUOUS FIELDS. Both Kolmogorov topologies are partitions of a DISCRETE Alexandroff T1 topology. The T1 topology is inherent in the concept of DISCRETE PARTICLES. Hence, there is an intimately relationship among the three topological structures, but in thermodynamics there are three important 1-forms, A, W, and Q. Hence there is a plethora of *triple* relationships between T1, T0 and T*0 for each 1-form. Is this the Universal Effectiveness of Topological Thermodynamics acting as the foundation for Quarks?

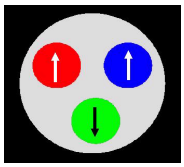

http://www22.pair.com/csdc/download/dean.pdf

COSMO-RS: From Quantum Chemistry to Liquid Phase Thermodynamics

Andreas Klamt
COSMOlogic GmbH&CoKG, Leverkusen, Germany and
Inst. of Physical and Theoretical Chmistry, University of Regensburg, Germany
klamt@cosmologic.de

COSMO-RS [1,2] is a novel method for the *a priori* prediction of chemical potentials, activity coefficients and vapor pressures of almost arbitrary chemical compounds in pure liquid solvents and mixtures. In contrast to the widely used group contribution methods COSMO-RS gets the information about the intermolecular interactions from uni-molecular quantum chemical calculations on the compounds and thus it is far less dependent on experimental data. Hence COSMO-RS is an efficient alternative to group contribution methods on the one hand and to the Monte-Carlo and Molecular Dynamics simulations on the other side. Aside from a few disadvantages it has a lot of systematic advantages. The greatest strengths are the broad applicability and extrapolation power of the method, and the systematic physical insight into the mixture behavior of the systems, which COSMO-RS opens by its sound physical basis. Thus complicated or rare compounds can be treated and differences between isomers can be resolved.

Beyond the basic features regarding activity coefficients, vapor pressures, and enthalpies of fluid systems, COSMO-RS can be applied to solid-liquid equilibria, to solubility in polymers, to ionic liquids and electrolytes, to pKa-prediction, to adsorption phenomena and physiological partitioning, reaction thermodynamics, micelle and biomembrane binding, chromatographic retention times, crystal face polarities, and many other problems of physical chemistry which have to do with liquid phase equilibria. Due to its broad predictive capabilities it has become a widely used method in chemical engineering thermodynamics.

The lecture will give an introduction to the COSMO-RS theory and an overview of its application area.

[1] A. Klamt, Conductor-like Screening Model for Real Solvents: A New Approach to the Quantitative Calculation of Solvation Phenomena, J. Phys. Chem., 99, 2224-2235 (1995)
[2] A. Klamt, From Quantum Chemistry to Fluid Phase Equilibria and Drug Design, Elsevier, 2005

The Soret Effect in Polymer Solutions: Search for the Effective Segment

W. Köhler[1] and D. Stadelmaier
Physikalisches Institut, Universität Bayreuth, Germany
werner.koehler@uni-bayreuth.de

The purpose of the present work is the investigation of the Soret effect in dilute polymer solutions, especially the crossover from small molecule to high polymer behaviour. Whereas monomers and short oligomers behave as 'erratic and unpredictable' as other small molecules, the thermal diffusion coefficient of many high polymers behaves surprisingly simple: it is independent of the chain length and, apparently, depends only on the solvent viscosity. The crossover from monomer- to polymer-type behavior occurs at a certain chain length that defines an *effective segment*, which we have been able to identify in our experiments.

A temperature gradient induces a diffusive mass current $\vec{j}_T = -\rho D_T c(1-c)\nabla T$ in a binary fluid mixture due to the Soret effect. ρ is the density of the mixture, c the mass fraction of component one and D_T the so-called thermal diffusion coefficient. $\vec{j}_T$ leads to the build-up of a concentration gradient and an accompanying Fickian mass diffusion current $\vec{j}_D = -\rho D \nabla c$. D is the mutual mass diffusion coefficient. Eventually a stationary concentration gradient

$$\nabla c = -S_T c(1-c)\nabla T$$

is reached, where the total current vanishes ($\vec{j}_T + \vec{j}_D = 0$). Typical Soret coefficients $S_T = D_T/D$ of ordinary liquid mixtures far away from a phase transition are of the order of 10^{-3} K^{-1}, but values up to 100 K^{-1} are reached close to a critical point.

The isothermal diffusion coefficient in dilute polymer solutions shows a well-known scaling law $D \propto N^{-\nu}$ with the Flory-exponent $\nu \approx 0.6$ in case of good solvents. The thermal diffusion coefficient D_T and, hence, the thermophoretic drift velocity $\vec{v}_T = -D_T \nabla T$ are independent of the degree of polymerization N of the polymer. Nevertheless, D_T is not a monomer property. The different molar mass dependencies of these two diffusion coefficients can be rationalized in terms of different hydrodynamic flow fields around the segments. Isothermal diffusion is described by a stick boundary condition and long-ranged flow fields with hydrodynamic coupling between the segments of the polymer chain. Thermal diffusion belongs to the problem class of phoretic motion with slip boundary condition between the surface of a segment and the solvent. The corresponding flow field is short ranged without hydrodynamic coupling of the segments [3, 4].

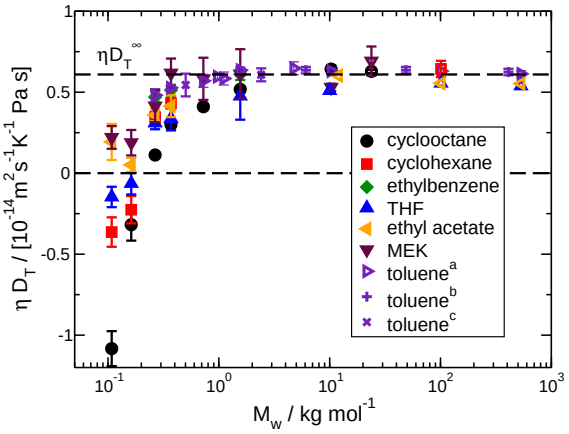

Figure 1: ηD_T as function of molar mass for PS in different solvents at $T = 295$ K [1, 2].

We have studied the crossover from small-molecule to polymer behavior in the Soret effect of dilute solutions of polystyrene in seven different solvents. The molar masses range from the monomer to $M \approx 10^6$ g/mol. The thermal diffusion coefficient D_T is molar mass independent in the high polymer regime and the quantity ηD_T is approximately constant and, surprisingly, independent of the solvent (Fig. 1) [1, 5].

[1] presenting author

For shorter chains below $M \approx 10\,\mathrm{kg/mol}$, D_T decreases monotonously with M and ηD_T does no longer follow a common master curve. For the two 'monomers' ethylbenzene and 3,3'-dimethylbutylbenzene there is even a sign change in several solvents, corresponding to a reversal of the direction of the thermophoretic motion. We conclude that the thermal diffusion coefficient, albeit being molar mass independent in the high polymer limit, is not a property of the monomer but rather of correlated segments of the order of the Kuhn segment (Fig. 2).

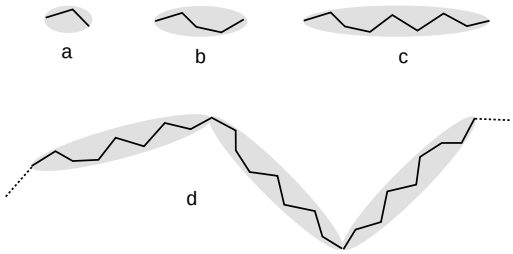

Figure 2: Increasing size of the effective (cooperative) unit with increasing degree of polymerization, starting from the monomer (a) over short oligomers (b) until the *effective segment* (c) is reached. Longer chains are composed of such effective segments (d) that act independently.

In order to test the influence of the size of the *effective segment*, we have investigated seven different polymers (PE, PI, PDMS, PMMA, PS, pαMS, tBMA) in various solvents (Fig. 3). As a measure for the extent of correlation along the chain we have resorted to the concept of the Kuhn statistical segment, whose molar mass is approximately $C_\infty M_m$, with M_m being the monomer molar mass and C_∞ the so-called characteristic ratio. The results of these experiments show that D_T always increases and then becomes molar mass independent for long chains. Polymer-typical behavior with a solvent-independent plateau value of ηD_T is only reached for sufficiently stiff polymers with high values of $C_\infty M_m$, where the size and/or mass of the *effective segment* significantly exceeds the corresponding quantity of the solvent molecules. Highly flexible polymers, such as poly(ethylene), with short and light effective segments do not reach a solvent-independent plateau value of ηD_T.

Besides the thermal diffusion coefficient D_T we will also address the properties of the Soret coefficient S_T. We will show that hydrodynamic interactions dominate the behavior of S_T for sufficiently long chains, where swelling due to excluded volume interactions becomes important. For a given molar mass the Soret coefficient depends only on the effective hydrodynamic radius of the polymer coil and, hence, on the solvent quality.

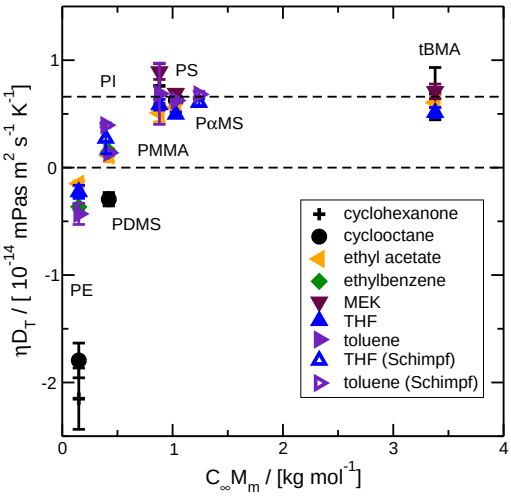

Figure 3: Plateau value ($M \to \infty$) of ηD_T for different polymer/solvent combinations as function of the molar mass of the Kuhn segment. $T = 295\,\mathrm{K}$.

References

[1] D. Stadelmaier and W. Köhler, Macromolecules **41**, 6205 (2008).

[2] J. Rauch and W. Köhler, Macromolecules **38**, 3571 (2005).

[3] F. Brochard and P.-G. de Gennes, C. R. Acad. Sc. Paris, Ser. 2 **293**, 1025 (1981).

[4] A. Würger, Phys. Rev. Lett. **98**, 138301 (2007).

[5] M. Hartung, J. Rauch, and W. Köhler, J. Chem. Phys. **125**, 214904 (2006).

Capabilities and Limitations of Association Models

Georgios M. Kontogeorgis, Amra Tihic, Georgios Folas[1], Ioannis Tsivintzelis, Andreas Grenner, Nicolas von Solms, Leonidas Constantinou[2], Ioannis Economou[3], Michael L. Michelsen and Erling H. Stenby

IVC-SEP Engineering Research Center
Department of Chemical and Biochemical Engineering
Technical University of Denmark
Building 229, DK-2800 Lyngby
Denmark

1 Shell Global Solutions, Amsterdam, The Netherlands
2 Shell Global Solutions, The Hague, The Netherlands
3 Research Center "Demokritos", Athens, Greece

Association theories e.g. those belonging to the SAFT family and lattice theories have been extensively applied to a variety of mixtures and types of phase equilibria over the last 10-15 years. Examples of applications include mixtures containing hydrogen bonding compounds, polymers and pharmaceuticals.

In this presentation we will focus on three such theories, all equations of state, two belonging to the SAFT family (CPA and PC-SAFT) and one belonging to the lattice-fluid type models (NRHB). The models will be discussed from the application point of view emphasizing developments over the last two years.

Capabilities and limitations will be presented as well as comparison of the various approaches.
In particular, the following topics will be highlighted:
* the role of polarity and hydrogen bonding, with special emphasis on solvating phenomena (see figure 1)
* group contribution and other methods for parameter estimation
* the role of monomer fraction data
* applications to pharmaceuticals (see figure 2)

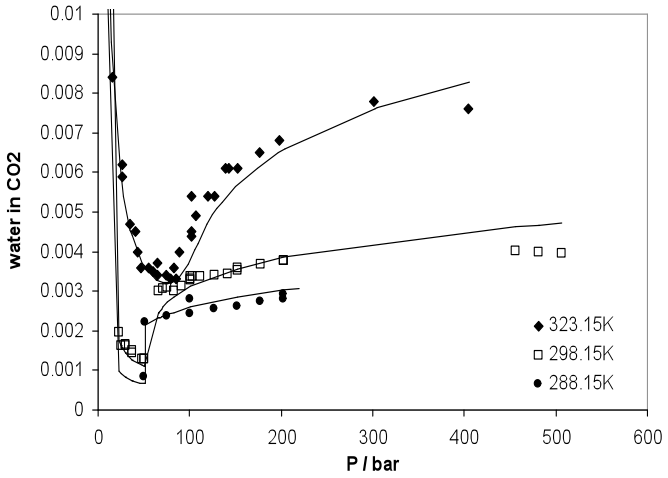

Figure 1. Correlation with CPA of the water (4C) mole fraction in CO_2 at three different temperatures. The binary interaction parameters are k_{12}=0.06 and $\beta^{A_iB_j}$ =0.075. The minimum in the water solubility is reproduced only when solvation is explicitly accounted for. Experimental data from Gillespie and Wilson, GPA research report RR-48, 1982.

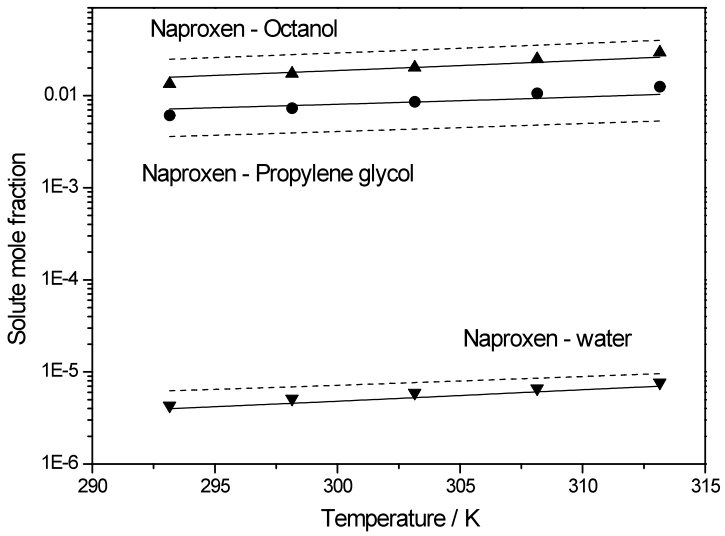

Figure 2. Solubility of naproxen in various solvents. Experimental data (points), NRHB predictions (dashed lines) and NRHB correlations (solid lines).

Coupling Thermal and Configurational Entropy in Teaching Undergraduate Physical Chemistry

Evguenii I. Kozliak

Chemistry Department, Univ. of North Dakota, Grand Forks, ND 58202, USA

ekozliak@chem.und.edu

Introduction. Thermodynamic entropy can be treated as a measure of spontaneous spreading of the available energy (e.g., temporally, among the accessible microstates, in a different one each instant, resulting in an averaged distribution) *(1,2).* Clausius' fundamental equation entails the essence of this interpretation:

$$dS = đq_{rev}/T \quad (1),$$

in combination with the Boltzmann-Planck equation:

$$S(E) = k\ln W \quad (2),$$

in which W is the number of *equiprobable* microstates (energy distribution modes) accessible by the system via random motion consequent to energy exchange events.

The problem is that, while using eq 2, entropy change may be perceived to be due solely to an explicit increase in accessible particles' positions in space, a way that W may be interpreted in eq 2 at the classical limit. This challenge is significant in teaching physical *chemistry*, given its 'molecular flavor.' The implication that there are two distinct varieties of entropy ["configurational" (i.e., spatial but temperature-independent) and "thermal" (i.e., space-independent)] is detrimental for instruction.

To teach undergraduate students that there is only ONE entropy inherently coupling "thermal" and "configurational" aspects, my approach (non-Calculus-based, which is important for teaching chemists) connects classical and quantum mechanics via the use of the "spinless" Boltzmann distribution:

$$\frac{N_i}{N} = \frac{N_i}{\sum N_i} = \frac{g_i e^{-\varepsilon_1/kT}}{\sum g_i e^{-\varepsilon_1/kT}} = \frac{g_i e^{-\varepsilon_1/kT}}{q} \quad (3a)$$

$$N_j/N_i = (g_j/g_i)e^{-\Delta\varepsilon/kT} \quad (3b)$$

where N_i, ε_i, and g_i are the population, energy, and degeneracy of a certain *i*-th energy level, respectively, *j* refers to a different energy level than *i*-th, separated from it by the energy gap, $\Delta\varepsilon$), $N = \Sigma N_i$ is the total number of particles in the system, and $q = g_i e^{-\varepsilon_1/kT}$ is the molecular partition function.

Approach. The most probable, i.e., spontaneously achieved, Boltzmann distribution assumes the maximum number of microstates for a closed system (N=const and sufficiently large) under the constraint of constant energy (i.e., the micro-canonical ensemble); normalizing the energies by temperature (thus, assuming thermal equilibrium) links it to the statistical canonical ensemble. It limits the number of possible microstates to those accessible at a given temperature for a given energy gap. The exponential factors in the Boltzmann distribution account for the

unequal probability of the lower-energy and higher-energy states, thus serving as "statistical weights"; the other statistical weight is the degeneracy factor for a particular state, g_i. Without the use of temperature-dependent Boltzmann exponential factors, some values of "entropy" may be calculated using eq 2; however, they would not necessarily be thermodynamically relevant because some of the microstates would not be attainable (*3,4*).

The microstates become equally accessible and, thus, equiprobable if the measure of an increment of energy, kT, overcomes the energy gaps between any two of given energy levels (*3,4*); or "dimensionless" energy gaps ($\Delta\varepsilon/kT$) are infinitesimal for all accessible *m* energy levels:

$$\Delta\varepsilon/kT=(\varepsilon_m-\varepsilon_1)/kT\approx 0 \quad (4)$$

The physical interpretation of this equation is that overcoming of $\Delta\varepsilon$ by the heat bath, kT, results in the equipopulation of energy levels (i.e., equiprobability of all microstates), which can be illustrated as follows. For N particles distributed among *m'* states at a given temperature (*m'*, unlike *m*, includes degeneracy), the number of available microstates in the system can be calculated:

$$W(T)=N!/N_1!N_2!\ldots N_{m'}! \quad (5)$$

For *any* $N_i=N/m'$ (i.e., equipopulation at "infinitely high" T), eqs 2 and 5 may be combined. Upon the application of Stirling's approximation, the entropy change reflecting the system's transfer from T=0 to this "infinitely high" temperature can be found:

$$\Delta S=k\ln[W(\text{"infinitely high" T})/W_0]=k\ln\{(N!/[(N/m')!]^{m'}/1\}=kN\ln m' \quad (6),$$

where $W_0=1$ is the single microstate when all of the particles are on the ground energy level.

On the other hand, by a rearrangement of $kN\ln m'$, the following equation can be obtained:

$$\Delta S(\text{"infinitely high"T})=kN\ln m'=k\ln[(m')^N] \quad (7)$$

This equation shows the inherent coupling of the "thermal" approach to configurational permutations (of finite sets of objects) because $(m')^N$ in eq 7 can be visualized as the number of possible combinations while tossing a hypothetical die – with *m'* equal sides – N times. Figuratively speaking, each molecule 'rolls a die' to 'decide' which state it will go to upon an energy exchange (*3c*).

Eq 4, with its assumption of infinitely high temperature, sets up a rather rigorous requirement which seems to be unattainable. However, this problem may be addressed by considering the molecular partition function, the denominator in the Boltzmann distribution formula, which reflects the *effective* number of equipartitioned states/energy levels. Considering the system as N identical *average* particles provides a "bridge" between the micro-canonical and canonical ensembles by calculating the entire system's partition function, which reflects the *statistical* number of equiprobable microstates in the system at a given temperature (*3c*):

$$Q(T)=W(T)=[q(T)]^N \quad (8)$$

Thus, *q*(T) (calculated as a product of partition functions for the available modes of motion) can be viewed as the *effective* number of attainable configurations at a given temperature (as *m'* in eqs 6-7). The suggested approach, connecting "thermal" and "configurational" entropy, can be applied to 1) molar entropy values, 2) residual entropy, 3) mixing, 4) the gas phase, and 5) the Gibbs paradox.

Applications.

Molar entropy values. In a naïve molecular application of configurational entropy to distinguishable particles, assuming that each particle is unique and distinguishable by its interactions with other unique surrounding particles, i.e., configurations, the number of equiprobable microstates may be calculated as

$$W=N! \quad (9)$$

At first glance, this formula, applicable also to a deck of N cards each of them having a different face value, allows for the estimate of molar *configurational* entropy of condensed phases for point-size particles which are *all* distinguishable (N_A is the Avogadro's number):

$$\Delta S(\text{configurational})=k\ln(N_A!)\approx kN_A[\ln(N_A)-1]=R\ln(N_A/e)\approx 447 \text{ J/molK} \quad (10)$$

However, eq 10 is not applicable to real systems: Standard molar entropies of common inorganic solids or liquids are much smaller, whereas the S^0 values for hydrocarbons $>C_{12}$ exceed this perceived "limit" (*3c*) Thus, configurational entropy cannot be decoupled from q(T), the number of attainable configurations per molecule at a given temperature. This consideration sets the rigorous limit to the use of a 52-card deck to illustrate entropy change. Being temperature-independent, this inadequate model does not obey the Third Law and definition of the micro-canonical ensemble. The root of the problem is that the "particles" within a card deck (having $\Delta\varepsilon=0$) are unlike the molecular systems [where $\Delta\varepsilon\approx 0$ is a useful approximation only above the characteristic temperature, $\Theta=\Delta\varepsilon/k$ (i.e., $\Delta\varepsilon<<kT$)]. Thus, in reversible thermodynamic applications, not *every* lnW may be allowed to be multiplied by k in eq 2 to yield a valid thermodynamic value; W must be temperature-dependent and be consistent with eq 8.

Residual entropy. Residual entropy can also be explained while connecting the "thermal" and "configurational" considerations (*3b*,*4*). As an example, HCl dipoles are known to be present in virtually 100% "head-to-tail" configuration near its freezing point (of a lower energy than the opposite "head-to-head" configuration due to the favorable dipole-dipole interactions), so it freezes as a "perfect" crystal. This means that, at this temperature, q(T) ≈1 for intermolecular vibrations, i.e., the system is below the characteristic temperature ($\Delta\varepsilon>>kT$) for this type of motion. If either temperature increases or the energy gap ($\Delta\varepsilon$) between the "head-to-tail" and "head-to-head" configurations decreases (e.g., as is true of CO, in contrast to HCl, near *its* freezing point), the choice of configuration is nearly random, so q(T)≈2 [in a general case, q(T)≈*m'* where *m'* reflects the number of possible intermolecular configurations, at least two of them being different in energy of intermolecular interactions]. Upon freezing followed by *reversible* cooling, the CO dipoles would realign to form a fully ordered crystal at T below the characteristic temperature. However, such realignment does not occur due to insurmountable kinetic barriers (molecules cannot rotate within crystals). This yields residual entropy at T=0 equal to

$$\Delta S_{\text{residual}}=R\ln m' \quad (11)$$

Even though systems with residual entropy are not at equilibrium, the existence of a hypothetical reversible path allows for the application of reversible thermodynamics, i.e., eq 7 (*4*).

Entropy of mixing. Configurational entropy of mixing of two liquids' equimolar amounts yields

$$\Delta S_{\text{mixing}}=-2R\times\tfrac{1}{2}\ln\tfrac{1}{2}=R\ln 2 \quad (12)$$

However, since neither energy nor temperature are involved in this derivation, it is not obvious that "thermal" entropy is applicable to the process of mixing; particularly, for ideal solutions, when $\Delta H_{\text{mixing}}\approx 0$. However, the assumption of ideal solution is tantamount to satisfying eq 4. When $m=2=q_{\text{mixing}}$, meaning that the

liquids are fully miscible, the locations within the former two liquids (i.e., before mixing, with one liquid on top of the other) become totally equiprobable for each particle regardless of its origin. Figuratively speaking, the multifaceted die to be rolled (eq 7) becomes a two-sided coin which each molecule 'tosses' to 'decide' whether it will stay in the original region or move to the other one. The fundamental problem, so far as thermodynamic entropy is concerned, is that viewing $W=(m')^N$ (eqs 7-8) as a purely statistical statement means that *all* of these substates can be degenerate with no energy difference ($\Delta\varepsilon=0$, as in macro objects like a perfect die or coin). As has been shown here, this condition may be valid in mathematics, but it does not rationalize an observable physical change in macro thermodynamics as does the micro-thermodynamic view of mobile molecules constantly moving between different energy arrangements and randomly exploring available space as well. Freezing a mixture as the ideal solution (i.e., above the characteristic temperature) yields residual entropy (*4*).

Gases ('indistinguishable' particles). The suggested treatment is also applicable to gases (i.e., indistinguishable particles), as long as attaining a non-fluctuating constant temperature (i.e., thermal equilibrium) is considered as evidence of particles' interaction. Then, the Maxwell-Boltzmann distribution is fully applicable and expansion may be viewed as degeneracy. Spreading of energy in the gas phase is tantamount to the spreading of matter because particles are the ultimate energy carriers and because the translational energy gaps are inherently small, thus assuring the applicability of eqs 4-8.

The Gibbs' paradox. The suggested treatment helps explain the Gibbs' paradox, which is based on the assumption that, from a configurational viewpoint, mixing two identical volumes of *the same* liquid would generate $\Delta S=k\mathrm{N}\ln 2$. However, there is no paradox from the "thermal" view because, since $\Delta\varepsilon=0$ between the two totally identical subsets, *m* pertaining to mixing remains equal to 1; thus, $W_2=W_1$ and $\Delta S=0$. Once there is a difference between the subsets, however small it is (e.g., two different isotopes above their characteristic temperature of mixing), $\Delta S=k\mathrm{N}\ln 2$ is exhibited (*3c*). Entropy is not a function of $\Delta\varepsilon$ (energy) but only $\Delta\varepsilon>0$ (uneven energy distribution) enables its change as a measure of energy spreading.

References.

1. Leff, H.S. *Am. J. Phys.*, **1996**, *64*, 1261-1271; *Found. Phys.* **2007**, *37*, 1744-1766.
2. Lambert, F.L. *J. Chem. Educ.*, **2002**, *79*, 187-192, 1241-1246, and **2007**, *84*, 1548-1550.
3. Kozliak, E.I. *J. Chem. Educ.*, **2004**, *81*, 1595-1598, **2007**, *84*, 493-498, and **2009**, accepted for publication.
4. Kozliak, E.; Lambert, F.L. *Entropy*, **2008**, *10*, 274-284.

Silver Plate, A mnemonic for Max Born's Mnemonic Square

J. Lewins
Magdalene College, U Cambridge
jl22@cam.ac.uk

Max Born provided a mnemonic square to assist in the application of Maxwell's relations in thermodynamic analysis. But if, for examination purposes, the instructor does no provide the Born square, how might the student remember?

Sil**V**er
-Pla**T**e

S	V
P	T

I offer the mnemonic 'SilVer-Plate' to arrive at the basic diagram

The relevant partial differentials are rtead left and right and together with the hyphen to remind the user to insert a minus sign, we arrive at the Maxwell relation derived from the Gibbs function $G(\{,T)$ in the form

$$\frac{\partial S}{\partial P}\Big)_{T} = -\frac{\partial V}{\partial T}\Big)_{P}$$

Note that the diagonals of the square have the dimensions of energy, an aid to memory. To obtain the remaining three relations there are two equivalent procedures. First, rotate the square in either direction 90^{0} at a time, changing the sign $\pm$ each time. Secondly, exchange the diagonal terms, with the same procedure for sign change.

Is Endo-reversible Theory Good or Bad Science?

J. Lewins
Magdalene College, U Cambridge
jl22@cam.ac.uk

Endo-reversible theory in which thermal engines are described as an internally reversible engine sandwiched between real irreversible heat transfer units, connecting to hot and cold reservoirs, has been with us for some fifty yeas. It is a theory that offers easy manipulation in analysis, but it has received considerable criticism from thermodynamicists, at MIT for example. How can such a simple, naïve theory be acceptable science?

I think the theory must be assessed in terms of what it claims. Typically it is used to maximise the useful power production from a thermal power plant leading to a specification of the internal temperature ratio driving the reversible engine in terms of the external ratio of the thermal reservoirs. The resulting thermal efficiency, at maximum power, is then lower than the overall Carnot efficiency. Bejan shows some ten power plants correlated by this theory and I have added data from four binary cycle plants over an 80-year period. The correlation by endo-reversible theory seems good, as good as any 'back of the envelope' might be.

So is the theory good science? If used to *design* an optimised plant, it gives little benefit. But if used to predict the result of optimising such a plant it must be considered good science and the simplicity, according to Occam's razor, makes it even better. Misused, any theory is surely bad science.

Bejan A, *Advanced Engineering Thermodynamics*, Wiley, New York, 1988 (third ed 2006).

Curzon F L and Ahlborn B, Efficiency of a Carnot engine at maximum power *Am J Phys* **43** 22-24, 1975.

Absolute Thermoelectricity for Engineers: The 'Health and Safety Warnings'

J Lewins
Magdalene College, U Cambridge
jl22@cam.ac.uk

Modern thermoelectricity is best approached through the formalism of irreversible thermodynamics, leading to Kelvin's relations and much more. But it would be well for the instructor to anticipate three conceptual problems the class might raise: our two 'health warnings'.

We suppose that the electric current density or flux is given at any point by $\mathbf{i} = \xi\left[-\nabla V - \Sigma\nabla T\right]$ where the electrical conductivity $\xi = 1/\rho$, the resistivity. Σ is the (absolute) Seebeck coefficient of the material giving rise to the further *emf* in steady state adding to the voltage gradient ∇V. The Peltier coefficient Π then describes the hidden heat carried by the electric current to be added to the Fourier or patent heat to form the heat flux vector $\mathbf{q} = -\kappa\nabla T + \Pi\mathbf{i}$ with entropy flux $\mathbf{j} = \mathbf{q}/T$. When the compound flux vector $\mathbf{J} = (\mathbf{i}, \mathbf{j})$ is expressed as a matrix equation in terms of a compound forces vector $\mathbf{X} = -(\nabla V, \nabla T)$ we have $\mathbf{J} = \mathbf{L}\mathbf{X}$ and a careful evaluation of the divergence of entropy involving $\nabla\cdot\Pi\mathbf{i} = \mathbf{i}\cdot\nabla\Pi$ shows that the dissipated power density is given by $\mathbf{X}\cdot\mathbf{L}\mathbf{X}$. In so doing we find the (absolute) i*ntrinsic* Thomson coefficient for material α, $\tau^{\alpha} = d\Pi^{\alpha}/dT$. Integrating along the electric flux through a discontinuity we have the conventional Peltier coefficient $\Pi^{\alpha\beta} = \Pi^{\beta} - \Pi^{\alpha}$.As a linear system the power dissipative density will be positive definite, satisfying the Second Law, if the determinant $|\mathbf{L}| = \dfrac{\kappa\rho}{T} > 0$ (surely it is) and the matrix is symmetric, or the Kelvin relation $\Pi/T = \Sigma$. So far, so good.

Now for the 'health and safety':

It is NOT to be assumed that a combined material can be predicted as a linear combination of $x\Sigma^{\alpha} + (1-x)\Sigma^{\beta}$ in proportion x. 'Impurities" have vastly non-linear effects.

We assumed a resistivity $\rho(T)$ *defined* for zero temperature gradient and conductivity $\kappa(T)$ *defined* for no electric current. We can reasonably expect these values to be perturbed by the conjugate forces (phonon-drag for example). The determinant may remain positive but we can no longer rely on Sylvester's condition of symmetry. Frankly I do not think Kelvin's relations exact at high gradients where we enter the world of non-linear phenomenological equations. Solution: give it to the enquiring student as a PhD project.

Students might reasonably interpret the Thomson coefficient as a heat capacity per coulomb and thus expect it to be negative. However, values for lithium and the group 11 metals are positive. The risk is a two-hour discussion of Fermi surfaces and reciprocal lattice zones. To avoid the issue, point out that this is a *transport* phenomenon, quoting the lattice of zinc and cadmium with coefficients that differs with the direction of transport, along or perpendicular to the hexagonal lattice. Offer a six-hour course in transport theory for anyone interested. I would like to come.

Peltier refrigeration optimisation with temperature varying conductivities and Seebeck coefficients

J. Lewins and T. Love
Engineering Dept, U Cambridge
jl22@cam.ac.uk

It is easy to optimise a Peltier refrigerator if we make the naïve assumption that the thermal conductivity κ and the electrical resistivity ρ and also the Seebeck coefficient Σ are independent of temperature. In an adiathermal sheath model of cross-section A and length ℓ with heat transfer only at the junctions, we may normalise the current flow to the heat conduction due to Fourier flow from the hot to cold junction, as $I^* = I\Sigma_1 \ell / A\kappa[T_0 - T_1]$ to find $I^* = 2$ for the lowest achievable cold junction at $T_{1\min}$ and $I^* = 2/(1+Q^*)$ where Q^* is a similarly normalised optimum refrigerative power at higher temperatures $T_1 > T_{1\min}$. The geometric optimisation is then a matter of a squat design, to maximise the Fourier heat of the electrically optimised system.

If the coefficients vary with temperature we are presented with the far more challenging problem of a second-order non-linear equation to optimise, where only one boundary value is known, the ambient T_0.

We show that in two cases the problem can be reduced to first order allowing a straightforward numerical integration:

The conductivities are temperature dependent but the Seebeck coefficient constant;

The Seebeck coefficient varies but the conductivities are constant.

Numerical studies show that our non-dimensional form is affected by only about 10% by these variations and so it seems reasonable to apply both corrections in the general case before evaluating the dimensional results.

Exact calculations of Auto-ignition Delay Times

J Lewins and J Heffer
Engineering Dept U Cambridge
jl22@cam.ac.uk

Standard application of Arrhenius rate theory to the calculation of delay times for auto-ignition in spark engines (or refrigeration technology) calls typically for the solution of a non-dimensional equation of the form $d\theta / d\tau = -\exp(-1/\theta)$ for a non-dimensional delay time τ and a non-dimensional temperature $\theta = 1$ at the activation temperature, conveniently taken as the onset of combustion and hence the end of delay. This equation and others like it are conventionally expanded to second order to provide a parabolic approximate solution.

We have summed an exact series solution to this and other such equations over two decades of delay times, showing that the conventional approximation rapidly becomes an under-estimate. This is unfortunate since a typical activation temperature might be 20 kK but a more reasonable end temperature might be 1 kK and a starting temperature 300 K, calling for nearly two decades cover. We show that expansion about a temperature below the activation temperature is flawed and thus recommend our exact series solution.

Natural Thermodynamics

Katalin Martinás[1] and Attila Grandpierre[2]

1: Eötvös Loránd University, Budapest, Department of Atomic Physics, Budapest,
2: Konkoly Observatory of the Hungarian Academy of Sciences, Budapest
email:martinas@ludens.elte.hu

1. Introduction

One of the most important laws of Nature, the Second Law, is formulated as requiring the increase of entropy in isolated systems. We attempt here to reformulate the Second Law of thermodynamics with the help of extropy, a thermodynamic state variable that measures the degree of nonequilibrium in entropic dimensions [J/K].

Nature does not distinguish adiabatic processes and therefore attributing a special role to them introduces a kind of arbitrariness into the foundations of thermodynamics. Here thermodynamics is constructed by dispensing with the adiabatic and quasistatic assumptions. Historically Clausius found that in a reversible adiabatic cycle

$$\oint dQ/T = 0 \qquad 1.$$

Clausius considered only the special solution of (1) corresponding to

$$dS = dQ/T \qquad 2.$$

Poór [1] showed that equation (2) is not the only solution of equation (1), but the general solution has the form

$$S^* = A\, dQ/T + df, \qquad 3.$$

here f is also a function of state variables. The unique entropy (corresponding to the case $df = 0$) is a consequence only of the fact that Clausius did not look for the general solution. Our choice will be $A=-1,\ df=1/T_0\, dU + p_0/T_0\, dV+\mu_0/T_0\, dN$, where T_0 is the temperature of the environment, and p_0 is the pressure of the environment, while μ_0 refers to the chemical potential of the environment (for the sake of brevity, we omitted here the summation for components.) That form of df leads to a new thermodynamic potential, called extropy [2-4], measuring the distance from the equilibrium. Extropy is zero in equilibrium, and later we will see that it is always positive, and it is decreasing during the equilibration processes.

2. Extropy

In this approach we do not use the classical one, as we eliminate a superfluous step at the very first and most decisive stages in the construction of thermodynamic theory. The general belief is that equilibrium is simple, and we can understand the world only through understanding equilibrium. In contrast to this idealized approach, we start from the basic fact that everything is changing, and in the actual world everything is in non-equilibrium. Thermodynamic processes occur in nature only when nonequilibrium is present, i.e., when the distance from equilibrium is not zero. It is the deviation of the thermodynamic intensive variables that generate the thermodynamic changes. We start from the space of real, nonequilibrium states. In any given environment Nature yields the sequence of states through which the equilibrium is approached. Nature is such that any system will always approach the equilibrium if the system is isolated or if it is in an equilibrium environment. This means that a distance from the equilibrium exists which will decrease in the fixed environment. It is the task of thermodynamics to determine mathematically this distance from the equilibrium with the help of measurable quantities. Equilibration is a natural law based on the presence of nonequilibrium, and the equilibrium is the result of equilibration.

To exploit this property in this chapter we consider only systems embedded into an equilibrium environment. Later, it can be extended to incorporate the isolated systems too. The equilibrium environment is characterized by its temperature T_0, pressure p_0, and the chemical potential of its constituents μ_{0i}, where index $_i$ refers to the i-th chemical component. In the following, for the sake of brevity we omit the index i, if it is convenient.

In the fixed environment the temperature and pressure scale can be fixed to the environmental values, and then these new values characterize the state of the system as deviations from the characteristics of the environment. We use the following natural temperature scale:

$$\tau = 1/T_0 - 1/T$$

We call it natural temperature scale, as it refers to the pre-thermodynamic notion of hot and cold. In our environment the average environmental temperature is 17 Celsius, so τ is positive for t>17 and negative for the opposite case. Similarly for the natural pressure scale,

$$p_n = p_0/T_0 - p/T.$$

As the energy change of the system is related to the temperature change the product of the internal energy change and the natural temperature must not be negative, so $(U_0-U)\ \tau \geq 0$, if there is only temperature difference. Similar statement is valid for the other terms. On the basis of these simple considerations, we can turn to a heuristic measure like the product of extensive and intensive parameters. Such a simple product is more easily tractable than the absolute value function. Their sum (D) is zero in equilibrium.

$$D= (U_0-U)\mu + (V_0-V)(p_n) + (N_0-N)(\mu_n) + ...$$

This quantity is similar to the radial distance in geometry, it measures the distance from the origo (which is the equilibrium state in our case.) Nevertheless D is not necessarily a monotonous function of time. In order to check this, let us calculate the time variation. Executing the derivation, we obtain

$$\begin{aligned} d/dt\ D \;=\; & \tau\, dU/dt + p_n\, dV/dt + \mu_n\, dN/dt + \\ & + (U\, d\,(1/T)\,/dt + V\, d/dt(p/T) + N\, d(\mu/T)/dt) + \\ & + U_0\, d\,(1/T)\,/dt + V_0\, d/dt(p/T) + N_0\, d(\tau/T)/dt \end{aligned}$$

The first line is always positive. The second one is zero. Nevertheless the third term can be of any sign, as there is no correlation between the equilibrium energy and the temperature change. The first line is just time derivative of extropy, defined as

$$\Pi = U\tau + V\, p_n + N\, \mu_n + ...$$

Extropy is zero in equilibrium, and in non-equilibrium it can only decrease (if the system does not get extropy from other systems), so it is zero or positive. It is the right measure of the distance from the equilibrium. In geometrical sense it is a direction dependent (irreversible) radial distance. The Second law can be formulated now in the following form: in a system embedded into equilibrium environment the extropy is decreasing until the equilibrium is reached. The intuitive notion of approaching the equilibrium is reflected by the decrease of extropy. For a non-equilibrium isolated system the extropy is the difference of the entropies of the system corresponding to equilibrium and that of the actual state of the isolated system. In isolated systems the extropy is the Brillouin negentropy.

3. Extropic Thermodynamics

Extropy leads to a new classification of thermodynamic systems, namely extropic and endtropic systems. Endtropic systems are defined as the systems embedded into an equilibrium environment (or the isolated systems), they exchange material and energy only with their reservoir environment, and do not exchange material and energy with other systems, therefore, they approach the equilibrium, and their extropy is decreasing.

Extropic systems exchange material and energy with other systems, and so they can get extropy, so their extropy may also increase. Such a system will be classified as an extropy exchanging system or shortly - extropic system. Isolated systems represent a subclass of the class of endtropic systems; therefore they do not form a separate class. Therefore, the two types of extropic classification of thermodynamic systems are the extropy-exchanging and the equilibrating systems. The extropic classification types differ from the older classification types. Extropy-exchanging systems are open systems; but equilibrating systems also can be open systems, if they exchange matter with their environment. Closed systems can still exchange energy with their environment, and so they also can be regarded as extropy-exchanging systems.

The fact that extropy as a driver of processes is based on differences presents an unexpected and fundamental challenge for us physicists accustomed to the preconceptions based on Newtonian physics. In modern physics, it is generally regarded that the basic drivers of physical processes are forces. The four fundamental forces of physics, gravitation and electromagnetism, and the weak and strong nuclear forces are forces that correspond to the properties of the objects themselves. In contrast, our finding is that the basic driver of thermodynamic processes is not a physical factor corresponding to the properties of the objects themselves, but to the relations between the objects and their environments. Modern physics credits such concepts as corresponding to the Aristotelian view in which the factor driving natural processes depends on the relation between the objects and their environment. The force beyond thermodynamic changes is not of a Newtonian type, because it is based on differences and not on the material properties of the objects themselves. This thermodynamic force is originated from the fact that the system is not in thermodynamic equilibrium.

It seems that we have to change our basic preconceptions regarding the nature of the physical world and learn to be accustomed to a new scientific world picture based on the extropic aspects of thermodynamics.

Acknowledgments

We are glad to express our thanks to Professors Robert Niven, Robert V. Ayres, George Rosenblatt, Tibor Gilányi, Zoltáan Homonnay, Sisir Roy, and to Jean Drew for lecturing the English.
The work was sponsored by the Hungarian Research Fund, OTKA K 61586.

References:

1: Veronika Poór, A Concise Introduction of the Extropy, Interdisciplinary Description of Complex Systems (INDECS), 3,72-76 ,2005,

2:Katalin Martinás Thermodynamics and sustainability a new approach by extropy, Periodica polytechnica, 42, 69-83. 1998.

3. Bernard Gaveau and Katalin Martinás and Michel Moreau and János Tóth, Entropy, extropy and information potential in stochastic systems far from equilibrium , PHYSICA A, 305,445-466, 2002.

4. Katalin Martinás and Attila Grandpierre: Thermodynamic Measure for Nonequilibrium Processes, Interdisciplinary Description of Complex Systems (INDECS), 2007, vol. 5, issue 1, pages 1-13

Unconventional thermodynamical model of vortex array in type-II superconductors

Bogdan T. Maruszewski

Poznan University of Technology
Institute of Applied Mechanics
ul. Piotrowo 3, 60-965 Poznan, Poland
bogdan.maruszewski@put.poznan.pl

The paper develops thermomechanics of a vortex array as a certain field of a special geometry in a type-II superconductor. For applied field strength less than the lower critical field H_{c1} the superconductor expels magnetic flux from the material (Meissner effect). For applied fields greater than the upper critical field strength H_{c2} the superconductivity is destroyed altogether. But between the lower H_{c1} and upper H_{c2} magnetic field strengths the superconductor is in the mixed or vortex state.
Magnetic flux can penetrate a type-II superconductor in the form of Abrikosov vortices (also called flux lines, flux tubes or fluxons) each carrying a quantum of magnetic flux. These tiny vortices of supercurrent tend to arrange themselves in a triangular or quadratic flux-line lattice.

That array forms a honeycomb-like pattern in a cross-section perpendicular to the vortex parallel cores. The vortex lines interact with each other and with the supercurrent (the Lorentz force). If the superconductor is heterogeneous and/or defective one observes pinning of the vortices on imperfections. So, the vortex lattice can have elastic properties. However, if the density of the supercurrent is above its critical value and/or the temperature is sufficiently high, there occurs a flow of vortices in the superconducting body. In such a situation vortices behave rather as a fluid than as an elastic lattice. The paper deals with a magnetothermomechanical model of such defined votex field in the superconductor if a “lattice” and “liquid” states coexist within the superconducting phase (it is not exactly known if changing temperature and/or magnetic field a transition from “lattice” to “fluid” state is singular or continuous one).

An unconventional thermodynamical model of those interactions has been presented for soft vortices (weak pinning). The model consists of a vector of state (set of independent variables), balances of mass, momentum, internal energy, evolution equations for fluxes and internal variables, electromagnetic field equations, entropy inequality, constitutive vector (set of dependent variables) and constitutive theory. A special form of the elastic stress tensor concerning both states of the vortex array has been proposed. An anomalous property of that field is observed: if temperature increases the stress always increases contrary to majority of materials in the normal state where both possibilities occur.

Basing on the above presented unconventional model the magnetoelastic field equations describing dynamics of magnetomechanical interactions have been derived. To illustrate consequences resulting from that model the following applications have been investigated: magnetoelastic waves in a superconducting heterostructure consisted of a layer put on a halfspace and compressional and flexural magnetoelastic waves in a superconducting layer placed into an external magnetic field. It occurred that dynamics of the vortex field presents some anomalous properties.

What Carnot's father taught his son about Entropy

Erich A. Müller
Imperial College London, U.K.
e.muller@imperial.ac.uk

Many traits and prejudices are brought down from generation to generation. The story of the development of the second law as we study it today arguably started with a publication by a young man, of a treaty where the behaviour of the recently appearing power-producing machines of his time was analyzed in a rational way. Thermodynamics, understood in its initial denotation as the study of machines that produce mechanical power from heat, was spawning and, as such, a theory would have to be built from scratch. It is thus not surprising that Sadi Carnot, a military engineer, son of Lazare Carnot, himself also an brilliant engineer with experience in the construction of waterwheels, was the forefather of current thermodynamics. However, Sadi Carnot did not start from a clean slate. Waterwheels were the engines of the time in the start of the 18th century, a reliable source of mechanical energy. Even today we have working examples of these machines, some modern versions powering the large hydroelectric plants in the world. The concept behind a waterwheel is fairly simple and was understood at the time by Lazare Carnot (Sadi's father): a) the higher the source of the waterfall, the more work that could be obtained b) the smoother the operation (less impact of the water, less turbulence, water exiting with zero velocity, etc.) the higher the output c) the larger the flow, the larger the amount of work. Essentially, in today's language, Lazare Carnot was convinced that in the *ideal* waterwheel none of the energy would be lost (or dissipated), and the system could be made reversible if one were to actuate the waterwheel (inputting work) to raise water. It is thus not surprising that the son took on his father's ideas and independently extrapolated them to the machines that made power from a different source of flow: heat flow. It is a remarkable stroke of luck that the simple concepts behind a water wheel could be applied to a heat engine almost directly. Few students recognize that the second law, as derived from Sadi Carnot's comments was actually stated with the assumption that heat could be treated as water flowing from a height. An excerpt from Carnot's only paper reads remarkably similar to what his father taught him:

"According to established principles at the present time, we can compare with sufficient accuracy the motive power of heat to that of a waterfall. Each has a maximum that we cannot exceed… The motive power of a waterfall depends on its height and on the quantity of the liquid; the motive power of heat depends also on the quantity of [caloric] used, and on … the difference of temperatures of the bodies between which the exchange of [caloric] is made." [1]

This paper builds on the analogy proposed almost two centuries ago by Sadi Carnot, and places it in modern terminology. Consider the case of a waterfall[2]:

Let us take as our control volume the waterfall plus the upstream and downstream sections of the river (leaving the fisherman out of the problem for the time being). Since this is a steady state system, with no accumulation of either mass or energy, from the application of the first law one can derive[3]

$$\dot{Q} + \dot{W} + \dot{m}(h + \frac{1}{2}vel^2 + gz)_{\text{upstream}} - \dot{m}(h + \frac{1}{2}vel^2 + gz)_{\text{downstream}} = 0$$

If the river has a similar width and depth before and after the fall, the average velocity of the water will be similar, thus the change in kinetic energy between the upstream and downstream of the river will not be measurable[4]. Also, the water is a compressed fluid at these conditions; therefore its enthalpy will only be a function of the temperature, which will also be constant. If there is no work output, then the first law expression simplifies to

$$\dot{Q} = -\dot{m}g(z_{upstream} - z_{downstream}) = -\dot{m}g\Delta z \tag{1}$$

In other words, the change in potential energy is dissipated in the form of heat to the environment. It is interesting to note that nothing in these equations stops us from considering the inverse process, i.e. a jump in water by extracting heat from the surroundings. We see how it is our intuition that will suggest that water is displaced from top to bottom but it will not spontaneously travel upstream, surmounting the fall. The immediacy of the irreversible nature of the waterfall is apparent. However, when placing a waterwheel at the mouth of the waterfall, we manage to extract work from the process. Making the same simplifications and assumptions as in the case of the free fall, and dismissing the heat losses to the ambient, application of the first law reveals that

$$\dot{W} = -\dot{m}g(z_{upstream} - z_{downstream}) = -\dot{m}g\Delta z \tag{2}$$

Note that, of course this is same amount of energy that the wheel-less fall dissipated, which is now converted to work. The process is intuitively reversible, suggesting that the energy is being converted efficiently.

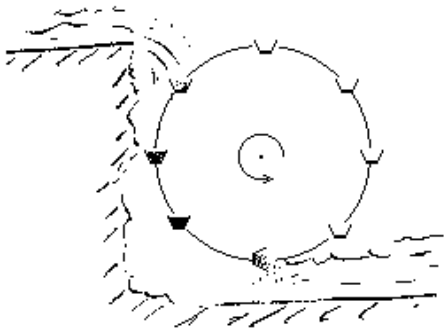

An entropy balance on the river provides significant information

$$\frac{\dot{Q}}{T} + (\dot{m}s)_{upstream} - (\dot{m}s)_{downstream} + \dot{\sigma}_{generated} = 0 \tag{3}$$

where the RHS is zero since a steady state is considered. The term $\dot{\sigma}_{generated}$ is the rate of entropy generation in the system. Using an incompressible fluid model (i.e. a constant heat capacity, *C*) the change in entropy between the upstream and downstream is seen to be null

$$(s_{upstream} - s_{downstream}) = C\ln\left(\frac{T_{downstream}}{T_{upstream}}\right) = 0 \tag{4}$$

since there is no change in the temperature of the water. Thus, the entropy generated by the process for the system without a waterwheel is,

$$\dot{\sigma}_{generated} = -\frac{\dot{Q}}{T} = \frac{mg(z_{upstream} - z_{downstream})}{T} = a\,\Delta z$$

where *a* is a positive quantity. Note that the natural behaviour (water falling down) implies a positive generation of entropy. In the awkward case where we consider the water to flow in “countercurrent”, or

upstream, the entropy change will be negative and the process impossible both from the second law expression and from common sense. If we place a waterwheel, the heat is zero, (since now the change in potential energy is converted into work and no heat is dissipated to the surroundings; c.f. eq. 2) thus, the result from eqs. 3 and 4 is that the generation of entropy of the universe is null. The result tells us that the use of a water wheel makes the energy conversion process efficient (we obtain work!) and that the process is reversible. In particular it is the best scenario, the maximum work attainable.

The analogy between this system and thermal systems, for which the students have less everyday experience is very useful. One can extract the following self-evident conclusions:

1. It is impossible to build a waterwheel that without consuming work raises water from a low height to a greater height.
2. It is impossible to build a waterwheel that converts all of the potential energy of the river water to work. (There will always be water at a lower level that would have energy equal to mgz_B).
3. The maximum work is obtained by a reversible waterwheel (where no energy is lost by dissipation).
4. Regardless of the way we design the waterwheel, the maximum amount of work extractable depends exclusively on the difference in the height of the water streams.

The clever lecturer will immediately recognize in these simple statements the analogue of the Clausius, Kelvin-Planck statements of the second law and the two principles of Carnot, respectively. This has an enormous advantage over the conventional introduction of these concepts in textbooks, where these principles are stated as applied to heat engines, of which students have no relation to and do not form part of the intuitive background common knowledge.

It is important to note that the analysis of these concepts does not parallel the historical developments, but rather stems from the modern analysis of those concepts. Carnot was not aware of the nature of energy and the fact that heat and work are mere manifestations of energy transfer and conversion. However, he did recognize the analogy and expressed it in the terms of the folklore of those days. Only after the acceptance of the concept of energy, mainly by the widespread disclosure of the works of Mayer and Joule, can one start to relate the concepts of energy and temperature in a consistent way. This synthesis of modern classical thermodynamics, and the coinage of the word entropy, was later to be performed by Clausius, almost 40 years after Carnot's book.

Nowadays, no science student has any problem grasping the concept of energy. Curiously, it would be quite a difficult concept to explain, had it not been introduced by colloquial usage from an early stage. No student thinks of energy as something "with matter" and the risk of improperly employing the waterwheel analogy is minimal. In spite of this, it is important to make it clear that the analogy proposed is actually a "crutch" that allows the understanding of the concepts of efficiency and entropy generation, and it should not be taken at face value. All simplifications and generalizations inevitably can be abused. Even the commonplace rendition of entropy as the disorder of a system can be terribly misleading[5].

Notes

[1] In modern terms, the word "caloric" should be substituted for "energy" (or heat). Taken from S. Carnot "Reflections on the motive power of fire", 1824, as edited by E. Mendoza, Dover, (1988).
[2] This and other parts of this paper are adapted and translated from the textbook "Termodinámica Básica" by E.A. Müller, Kemiteknik (2002). The notation is described therein and in the full paper.
[3] The energy and entropy equations are written here in terms of rate equations, as is preferred for open systems. A full discussion is given in the paper. The reader is referred to standard textbooks for a comprehensive treatment, i.e. J.R. Elliott and C.T. Lira, "Introductory Chemical Engineering Thermodynamics" Prentice Hall (1999)
[4] In the case of the free fall (no waterwheel) the decrease in the potential energy of the water can have two immediate effects, either to increase the enthalpy (and thus temperature) of the downstream water, or if one considers isothermal conditions, it will be dissipated as heat to the environment. The latter is possibly the sensible assumption, thus the enthalpy of the water remains constant.
[5] F.L. Lambert "Disorder - a cracked crutch for supporting entropy discussions", J. Chem. Ed. *79*, (2) 187-192 (2002)

Some Concepts of Non-Equilibrium Thermodynamics

W. Muschik
Institut für Theoretische Physik
Technische Universität Berlin
muschik@physik.tu-berlin.de

1. Introduction
A lot of different disciplines are using thermodynamical concepts: Physics and Physical Chemistry, Mechanical and Chemical Engineering, Material Sciences, Bio-Sciences, Energy Conversion Techniques, Air Conditioning, Refrigeration, Heat and Steam Turbine Engineering and much more. Hence, the slogan "Thermodynamics is everywhere" has a great evidence. Of course, the applied thermodynamical concepts are adapted to the special disciplines, but there is a common core for all because today's thermodynamics is understood as a general description of non-equilibrium systems embracing also mechanics, electromagnetics and the quantum-mechanical back-ground including the reversible process limit. Consequently, thermodynamical concepts are in vivid development because of their wide range of applications. Some of these fundamental concepts are discussed here [1].

2. A Classification
On principle, thermodynamics can be presented into two forms, as a non-equilibrium theory of discrete systems [2] including also thermostatics, the case of equilibrium [3], or in a field formulation extending the balances of continuum mechanics [4].

There are basic concepts allowing for a classification of them [5]. Such a classification can be done by answering the following questions [6]:

- Is the considered system described as a discrete one or in field formulation ?
- Are temperature and entropy primitive concepts or derived quantities ?
- Is the chosen state space small or large ?
- Are all constitutive equations properly defined on the chosen state space ?
- Is the dissipation inequality global or local in time ?
- Is the relation between heat flux density and entropy flux density universal or material-dependent ?
- What is the procedure for exploiting the dissipation inequality [7] ?
- Are complex materials described by a mesoscopic theory or by introducing additional fields and their balances [8, 9] ?

- Are the non-equilibrium processes restricted to endoreversible thermodynamics or are they described without reversible parts ?
- Has the phenomenological description of a non-equilibrium system a correct quantum mechanical background ?

3. Discrete Systems

3.1 Thermostatics

Well-known thermostatics describes discrete systems in equilibrium. The state space of these systems is spanned by the internal energy, the work variables and the mole numbers.

3.2 Non-equilibrium

Here, the state space is of higher dimension than that in equilibrium. Additional variables are the non-equilibrium contact temperature and internal variables [10].

4. Field Formulation

Systems and their properties are described by fields.

4.1 Basic fields

As for discrete systems, the basic variables have to be chosen. That are the fields of mass density or deformation gradient, velocity, internal energy and, if necessary, the spin.

4.2 Balance equations

The "equations of motion" are the balances of mass, momentum, angular momentum, total energy, internal energy, entropy and, if necessary spin.

4.3 Constitutive equations

The balances contain constitutive fields, such as the stress tensor, the heat and entropy flux densities, the entropy, its production and supply and more. Constitutive equations are defined on the state space which is different from the basic variables in general. The state space may be depend on the process history (small state space) or may be local in time (large state space). Constituive equations are restricted by material axioms [11].

5. Fluxes of Heat and Entropy

Entropy flux density may be universally defined as heat flux density over temperature, or it is a constitutive equation independent of the heat flux density.

6. Dissipation Inequality

6.1 Global or local

The dissipation inequality, representing the 2nd law, may be global in time as e.g. the Clausius inequality is, or it is local in time and position as the entropy production density is [12].

6.2 Exploitation

There are different concepts to exploit the dissipation inequality in classical irreversible thermodynamics or in rational extended thermodynamics by Coleman-Noll or Liu procedure [13].

7. Extended Thermodynamics

The basic variables of extended thermodynamics are those of 4.1 extended by the dissipative part of the stress tensor and by the heat flux density. In extended thermodynamics, the set of the basic variables is identical to the state space on which the constitutive equations are defined [14].

8. General Non-Equilibrium Thermodynamics
The choice of the basic variables and of the state space is not restricted by any rules. For exploiting the dissipation inequality, Liu's procedure is used.

9. Endoreversible Thermodynamics
Endoreversible thermodynamics models systems consisting of reversible sub-systems which interact irreversibly with each other. If the time is introduced (e.g. the cycle time), this discipline is called "Finit Time Thermodynamics" [15].

10. Mesoscopic Theory
In mesoscopic theory, the basic variables of 8. are not introduced as independent fields, but as additional variables extending space-time. Consequently, balances are not defined on 4-dimensional space-time, but on the higher-dimensional mesoscopic space which is spanned by time, position and the mesoscopic variables. The distribution function of the values of the mesoscopic variables allows for introducing macroscopic fields of order parameters which are beyond the conventional theories. The balance of the mesoscopic distribution function is of Fokker-Planck type [16].

11. GENERIC
The idea is to modify the reversible canonical equations by an additional part which introduces irreversibility. General Equation for the Non-Equilibrium Reversible-Irreversible Coupling postulates a rate for its basic variables which consists of the sum of a reversible and of an irreversible part according to the basic idea [17].

12. Evolution Criteria
Beyond the positive definitenes of the entropy production density, its Ljapunov property is postulated, that means, the rate of the entropy production is not positive. Besides this local criterion, global criteria can be derived by using the global entropy balance equation [18, 19].

13. Quantum Thermodynamics
13.1 Irreversible quantum mechanics
Irreversible quantum mechanics is based on a modified von Neumann equation allowing non-vanishing entropy rates. The Schrödinger equation is untouched.
13,2 Limited information
By introducing a relevant set of quantum mechanical observables (beobachtungsebene), the used information is restricted to the chosen set. The statistical operators are of generalized canonical form. Their dynamics is different from the von Neumann one. One of them is the Robertson dynamics [20].

References

[1] W. Muschik, Survey of some branches of thermodynamics, J. Non-Equilib. Thermodyn. 33 (2008) 165-198

[2] W. Muschik, A. Berezovski, Thermodynamic interaction between two discrete systems in non-equilibrium, J. Non-Equilib. Thermodyn. 29 (2004) 237-255

[3] J. Kestin, A Course in Thermodynamics, Vol. I, Hemisphere, Washington 1979, ISBN 0-07-034281-4

[4] W. Muschik, C. Papenfuss, H. Ehrentraut, A sketch of continuum thermodynamics, J. Non-Newtonian Fluid Mech. 96 (2001) 255-290

[5] W. Muschik, C. Papenfuss, H. Ehrentraut, Concepts of Continuum Thermodynamics, Kielce University of Technology, Technische Universität Berlin, 1996, ISBN 83-905132-7-7

[6] W. Muschik, Thermodynamical theories, survey and comparison, ZAMM 61 (1981) T213-T219

[7] W. Muschik, Formulations of the second law – Recent developments, J. Phys. Chem. Solids 49 (1988) 709-720

[8] W. Muschik, H. Ehrentraut, C. Papenfuss, Concepts of mesoscopic continuum physics, J. Non-Equilib. Thermodyn. 25 (2000) 179-197

[9] W. Muschik, C. Papenfuss, H. Ehrentraut, Mesoscopic theory of liquid crystals, J. Non-Equilib. Thermodyn. 29 (2004) 75-106

[10] W. Muschik, Empirical foundation and axiomatic treatment of non-equilibrium temperature, Arch. Rat. Mech. Anal. 66 (1977) 379-401

[11] C. Truesdell, W. Noll, Non-Linear Field Theories of Mechanics, in: S. Flügge (Ed), Encyclopedia of Physics, III/3, Sect.19, Springer, Berlin 1965

[12] W.A. Day, The Thermodynamics of Simple Materials with Fading Memory, Springer Tracts in Natural Philosophy, Vol. 22, Berlin 1972, ISBN 3-540-05704-8

[13] W. Muschik, H. Ehrentraut, An amendment to the second law, J. Non-Equilib. Thermodyn. 21 (1996) 175-192

[14] G. Lebon, An approach to extended irreversible thermodynamics, in: J. Casas-Vázquez, D. Jou, G. Lebon (Eds), Recent Developments in Nonequilibrium Thermodynamics, Lecture Notes in Physics 199, Springer, Berlin 1984, ISBN 3-540-12927-8, pp.72-104

[15] K.H. Hoffmann, J.M. Burzler, S. Schubert, Endoreversible thermodynamics, J. Non-Equilib. Thermodyn., 22 (1997) 311-355

[16] W. Muschik, H. Ehrentraut, C. Papenfuss, Concept of mesoscopic continuum physics with application to biaxial liquid crystals, J. Non-Equilib. Thermodyn., 25 (2000) 179-197

[17] H.C. Öttinger, Beyond Equilibrium Thermodynamics, Wiley, Hoboken 2005, ISBN 0-471-66658-0

[18] P. Glansdorff, I. Prigogine, Thermodynamic Theory of Structure, Stability and Fluctuations, Wiley, London 1971, ISBN 0-471-30280-5, ch. IX, sec.8

[19] W. Muschik, C. Papenfuss, An evolution criterion of nonequilibrium thermodynamics and its application to liquid crystals, Physica A 201 (1993) 515-526

[20] A. Kato, M. Kaufmann, W. Muschik, D. Schirrmeister, Different dynamics and entropy rates in quantum-thermodynamics, J. Non-Equilib. Thermodyn. 25 (2000) 63-86

Teaching the Definition of Thermodynamic Entropy in Irreversible Quantum Mechanics

W. Muschik
Institut für Theoretische Physik
Technische Universität Berlin
muschik@physik.tu-berlin.de

1. Introduction
Usually, statistical thermodynamics starts out with the basic axiom of equal probable states in the accessible part of the Γ-space. Consequently, all following results stick to equilibrium, including entropy and temperature. Therefore two steps are necessary to proceed to non-equilibrium: firstly the introduction of a non-equilibrium entropy [1] (and also of a non-equilibrium temperature [2] which is out of scope here) and secondly the adaptation of the reversible quantum mechanics to dissipation and heat exchange with an environment. Here a procedure is shortly discussed, how to achieve this irreversible quantum mechanics clearly without modifying Schrödinger dynamics and without introducing a restricted set of observables [3, 4].

2. Equilibrium
Starting out with the equilibrium entropy belonging to a grand canonical ensemble

$$S^{eq} \;=\; k_B \ln Z^{gcan} + \frac{1}{T}U - \frac{\boldsymbol{\mu}}{T}\cdot\boldsymbol{n}, \tag{1}$$

we can prove the following

Proposition: If the grand canonical distribution function p_j^{gcan} and the grand canonical density operator ϱ^{gcan} are introduced, the equilibrium entropy is of Shannon shape

$$S^{eq} \;=\; -k_B \sum_j p_j^{gcan} \ln p_j^{gcan}, \quad S^{eq} \;=\; -k_B \mathrm{Tr}(\varrho^{gcan} \ln \varrho^{gcan}). \tag{2}$$

3. Non-Equilibrium Entropy
According to (2), we postulate the

Axiom I: The non-equilibrium entropy is as the equilibrium one of Shannon shape

$$S \;=\; -k_B \mathrm{Tr}(\varrho \ln \varrho) \tag{3}$$

with the non-equilibrium density operator

$$\varrho \;=\; \sum_j p_j |\Phi^j><\Phi^j|, \qquad 0 \le p_j \le 1, \qquad \sum_j p_j = 1, \tag{4}$$

$$< \Phi^j|\Phi^j >= 1, \qquad k \neq m : < \Phi^k|\Phi^m >\neq 0, \qquad \sum_j |\Phi^j >< \Phi^j| \neq \underline{1}, \tag{5}$$

$$i\hbar\partial_t|\Phi^j > \;\; = \;\; \mathcal{H}|\Phi^j > . \tag{6}$$

4. Modified von Neumann Equation
From (4) and (6) follows the modified von Neumann equation

Proposition:

$$\partial_t \varrho \;\; = \;\; -\frac{i}{\hbar}[\mathcal{H}, \varrho] + \sum_j \dot{p}_j|\Phi^j >< \Phi^j|. \tag{7}$$

5. Non-Equilibrium Entropy Rate
Inserting the modified von Neumann equation (7) into the Shannon non-equilibrium entropy (3), we obtain the

Proposition:

$$\dot{S} \;\; = \;\; -k_B \sum_j \dot{q}_j \ln q_j, \qquad q_j := \sum_m p_m| < \Phi^m|\varphi_j > |^2 \geq 0, \qquad \sum_j q_j = 1, \tag{8}$$

$$i\hbar\partial_t|\varphi_j > = \;\mathcal{H}|\varphi_j > . \qquad < \varphi_j|\varphi_k >= \delta_{jk}, \qquad \sum_| \varphi_j >< \varphi^j| = \underline{1}, \tag{9}$$

Using (6) and $(9)_1$, from $(8)_2$ follows the

Proposition:

$$\dot{q}_j \;\; = \;\; \sum_m \dot{p}_m| < \Phi^m|\varphi_j > |^2, \qquad \sum_j \dot{q}_j \;\; = \;\; 0. \tag{10}$$

According to $(8)_1$ and $(10)_1$, we obtain the

Corollary: If the weights p_j of the statistical operator $(4)_1$ are time independent, the system undergoes an isentropic process, and if it is isolated, this process is reversible, as we will see below.

6. Environment induced Equilibrium Distribution
Up to now, the environment of the system is not taken into account. Here, the influence of the environment should not be introduced by a special Hamiltonian of interaction [2], but by an equilibrium distribution q_j^0 which is determined by the special controlling of the system by the environment. So we have the microcanonical distribution, $p_j = p^{mcan}$, $\wedge j$, if the system is isolated, the canonical distribution, if the closed system is in contact with a heat reservoir and the grand canonical distribution, if the open system contacts a heat and mass reservoir. In general, the q_j^0 are not independent of time, because the controlling of the system can change in time during the process.

7. Entropy Rate Identity
The entropy rate $(8)_1$ becomes by adding a zero

$$\frac{1}{k_B}\dot{S} = -\sum_j (\dot{q}_j - \dot{q}_j^0)[\ln q_j - \ln q_j^0] - \sum_j \dot{q}_j \ln q_j^0 - \sum_j \dot{q}_j^0 [\ln q_j - \ln q_j^0]. \tag{11}$$

The right-hand side of (11) has now to be split into the positive definite entropy production Σ and the entropy exchange Φ between the system and its environment according to

$$\dot{S} \;=\; \Sigma + \Phi., \qquad \Sigma \;\geq\; 0, \tag{12}$$

$$\Phi \;=\; 0, \text{ for isolated sytems.} \tag{13}$$

8. Relaxation Ansatz

Now we need how the non-equilibrium system relaxes to equilibrium. This relaxation equation is necessary for determining the time rate (7) of the statistical operator. The rate $\dot{q}_j$ depends on the "distance from equilibrium". Therefore, we introduce an relaxation ansatz as an

Axiom II:

$$\dot{q}_j - \dot{q}_j^0 \;=\; -M_j(q_j - q_j^0), \quad \rightarrow \quad \sum_j M_j \;=\; 0, \tag{14}$$

$M_j(x)$ strictly positive monotonous : $(dM_j/dx) > 0,\ M_j(0) = 0.$

Axiom II is now inserted into (11).

9. Entropy Production and Heat Exchange

According to (14), M_j, the first term on the right-hand side of (11) results in

$$k_B \sum_j M_j[\ln q_j - \ln q_j^0] \;=:\; \Sigma \;\geq\; 0. \tag{15}$$

Because according to (14), M_j has the same sign as the square bracket in (15), we obtain the inequality in (15) which represent the 2nd law. Consequently, the left-hand side of (15) is the definition of the entropy production Σ.

According to $(12)_1$, the remaining two terms on the right-hand side of (11) represent the entropy exchange

$$\Phi \;:=\; -k_B \sum_j \dot{q}_j \ln q_j^0 - k_B \sum_j \dot{q}_j^0[\ln q_j - \ln q_j^0]. \tag{16}$$

Using (14), we obtain

$$\Phi \;=\; k_B \sum_j M_j \ln q_j^0 - k_B \sum_j \dot{q}_j^0 \ln q_j. \tag{17}$$

Here are some arguments for verifying that (17) represents the entropy exchange:
a) Φ and Σ are independent of each other, because the entropy exchange is influenced by the environment due to $\dot{q}_j^0$ which does not appear in the entropy production (15),
b) if the system is isolated ($q_j^0 = q^{mcan},\ \dot{q}_j^0 = 0,\ \wedge j$), Φ vanishes according to $(14)_2$,
c) if the system is in equilibrium ($q_j(t) = q_j^0(t) = const_j$), the entropy production and the entropy exchange vanish according to (15) and (16),
d) if a process is reversible ($q_j(t) = q_j^0(t), \dot{q}_j^0 \neq 0$), the entropy production vanishes according to (15) and (14), whereas according to (17) the "reversible entropy exchange" is

$$\Phi^{rev} \;=\; -k_B \sum_j \dot{q}_j^0 \ln q_j \;=\; \dot{S}^0, \tag{18}$$

e) an isentropic process ($\dot{S} = 0$) is not necessarily reversible ($\Sigma = 0$) according to (12).

10. Final Remarks

If the statistical weights of a density operator are time dependent, the Schrödinger dynamics generates a modified von Neumann equation so that the Shannon entropy rate is different from zero. Therewith, the possibility is opened for describing dissipative quantum systems whose pure ensenbles obey Schrödinger dynamics. If for the rate equations of the statistical weights relaxation ansatzes are chosen, a positive definite entropy production and the entropy exchange can be defined. The interaction of the considered system with its environment is described by using the equilibrium distribution function which belongs to the special controlling of the system by the environment.

References

[1] W. Muschik, Survey of some branches of thermodynamics, J. Non-Equilib. Thermodyn. 33 (2008) 165-198

[2] W. Muschik, Empirical foundation and axiomatic treatment of non-equilibrium temperature, Arch. Rat. Mech. Anal. 66 (1977) 379-40

[3] W. Muschik, M. Kaufmann, Quantum-thermodynamical description of discrete non-equilibrium systems, J. Non-Equilib. Thermodyn. 19 (2008) 76-94

[4] A. Kato, M. Kaufmann, W. Muschik, D. Schirrmeister, Different dynamics and entropy rates in quantum-thermodynamics, J. Non-Equilib. Thermodyn. 25 (2000) 63-86

[5] W. Muschik, Contact quantities and non-equilibrium entropy of discrete systems, J. Non-Equilib. Thermodyn. 34 (2009) 1. issue

Nonextensivity of the configurational probability distribution in the classical microcanonical ensemble

Jan Naudts and Maarten Baeten
Universiteit Antwerpen, Belgium
Email: Jan.Naudts@ua.ac.be

INTRODUCTION

Many-particle systems are usually studied in the canonical or the grandcanonical ensemble. But for small systems the equivalence of ensembles breaks down and it becomes interesting to study the microcanonical ensemble. In this context several interesting questions arise, many of which are waiting for a satisfactory answer. Some of these questions have controversial answers. It is therefore important to start from generally accepted concepts. One such concept is the definition of the classical microcanonical ensemble. The problems around the ergodicity of systems of classical mechanics have been understood long ago — see for instance [1]. There appears to be an agreement in the scientific community that the microcanonical equilibrium distribution is described in phase space by a Dirac delta function giving equal probability to all states accessible for the system. The latter are parametrised by the total energy U and eventually some additional internal or external parameters. For convenience only the energy is considered here. Less clear is the answer to the question how the thermodynamic entropy $S(U)$ relates to this equilibrium distribution. This point is reviewed below. A related question is whether one can define a microcanonical temperature T or whether temperature is a property of systems in contact with a thermal bath. This point is discussed below as well. Even more controversial is the notion of microcanonical phase transitions and phase separation [2]. In our view we cannot make meaningful statements about such concepts before answering the more basic questions.

Starting point of the present work is the observation that the configurational probability distribution of classical monoatomic gases in the microcanonical ensemble is always nonextensive in the sense of Tsallis [3]. Most efforts in the Tsallis literature are based on Jaynes' maximum entropy principle [4] and are therefore not very well suited for discussing the microcanonical ensemble. But the probability distributions discussed in nonextensive thermostatistics belong to the q-exponential family, which is a special case of the generalised exponential family [5-12]. It is shown below that the configurational probability distributions of a classical real gas in the microcanonical ensemble always belong to the q-exponential family. A first observation in this direction was made in [12].

The observation that the configurational probability distribution always belongs to the q-exponential family provides a handle to discuss the above mentioned difficult questions because the subsystem of configurational degrees of freedom can be considered as a thermodynamic system, in interaction with the subsystem of the kinetic degrees of freedom. In particular, one can study the question whether the temperature derived via the equipartition law from the kinetic energy should coincide with that of the configurational subsystem. Such questions have been discussed recently in the literature [13,14].

THE MICROCANONICAL ENTROPY

A classical model of N particles with positions $\mathbf{q}_j$ and conjugated momenta $\mathbf{p}_j$ is determined by the Hamiltonian

$$H(\mathbf{q},\mathbf{p}) = \frac{1}{2m}\sum_{j=1}^{N}|\mathbf{p}_j|^2 + \mathcal{V}(\mathbf{q}), \tag{1}$$

where $\mathcal{V}(\mathbf{q})$ is the potential energy due to interaction between the particles themselves and between the particles and the walls of the system. The density of states is given by

$$\omega(U) = \frac{1}{h^{3N}}\int_{\mathbb{R}^{3N}} \mathrm{d}\mathbf{p}_1\cdots\mathrm{d}\mathbf{p}_N \int_{\mathbb{R}^{3N}} \mathrm{d}\mathbf{q}_1\cdots\mathrm{d}\mathbf{q}_N\, \delta(U - H(\mathbf{q},\mathbf{p})). \tag{2}$$

The constant h is introduced for dimensional reasons. Note that the usual factor $1/N!$ is omitted. The microcanonical ensemble is described by the singular probability density function

$$f_U(\mathbf{q},\mathbf{p}) = \frac{1}{\omega(U)}\delta(U - H(\mathbf{q},\mathbf{p})). \tag{3}$$

For simplicity, we take only one system parameter into account, namely the total energy. Its value is fixed to U.

The entropy $S(U)$, which is most often used in the classical microcanonical ensemble, is that of Boltzmann

$$S(U) = k_B \ln \omega(U). \tag{4}$$

The shortcomings of Boltzmann's entropy have been noticed long ago. A slightly different definition of entropy is [15,16] (see also [13])

$$S(U) = k_B \ln \Omega(U), \tag{5}$$

where $\Omega(U)$ is the integral of $\omega(U)$. An immediate advantage of (5) is that the resulting expression for the temperature T, defined by the thermodynamical formula

$$\frac{1}{T} = \frac{\mathrm{d}S}{\mathrm{d}U}, \tag{6}$$

coincides with the notion of temperature as used by experimentalists, assigning a kinetic energy of $\frac{1}{2}k_BT$ to each degree of freedom. But also the latter is subject to criticism. In small systems finite size corrections appear [13,14] for a number of reasons. As argued in [14], the problem is not the equipartition of the kinetic energy over the various degrees of freedom, but the relation between temperature and kinetic energy.

THE CONFIGURATIONAL SUBSYSTEM

One can integrate out the momenta from the distribution (3). This leads to the configurational probability distribution, which is given by

$$f_U^{\mathrm{conf}}(\mathbf{q}) \;=\; \frac{1}{h^{3N}}\int_{\mathbb{R}^{3N}} \mathrm{d}\mathbf{p}_1\cdots\mathrm{d}\mathbf{p}_N\, f_U(\mathbf{q},\mathbf{p}). \tag{7}$$

A short calculation gives

$$f_U^{\mathrm{conf}}(\mathbf{q}) = c_N \exp_q\left(-\alpha(\theta) - \theta\mathcal{V}(\mathbf{q})\right), \tag{8}$$

with

$$c_N = \left(\frac{2\pi m}{h^2}\right)^{3N/2}, \tag{9}$$

$$\theta = \frac{1}{(1-q)\left[\Gamma(3N/2)\omega(U)\right]^{1-q}}, \tag{10}$$

$$\alpha(\theta) = \frac{3}{2}N - 1 - \theta U, \tag{11}$$

$$q = 1 - \frac{2}{3N-2}. \tag{12}$$

The q-exponential function is defined by

$$\exp_q(u) = [1 + (1-q)u]_+^{1/(1-q)}. \tag{13}$$

The notation $[u]_+ = \max\{0, u\}$ is used. The configurational probability distribution is said to belong to the q-exponential family because it can be written into the form (8).

An immediate consequence of belonging to the q-exponential family is that the entropy function is known which is maximised by (8) under the condition that the potential energy has a given value. It is a variant of the Tsallis entropy [3] and can be written as [12] (assume $k_B = 1$ for convenience)

$$I(f) = -c_N \int_{\mathbb{R}^{3N}} \mathrm{d}\mathbf{q}_1 \cdots \mathrm{d}\mathbf{q}_N \, F\left(\frac{1}{c_N} f(\mathbf{q})\right) \tag{14}$$

with

$$F(u) = \int_0^u \mathrm{d}v \, \ln_q(v) = \frac{u}{1-q}\left(\frac{1}{2-q}u^{1-q} - 1\right). \tag{15}$$

Here, $\ln_q(x)$ is the q-deformed logarithmic function. In addition, the following identity holds

$$\frac{\mathrm{d}I(f_U^{\mathrm{conf}})}{\mathrm{d}U^{\mathrm{conf}}} = \theta. \tag{16}$$

Working out this identity yields

$$U^{\mathrm{kin}} = U - U^{\mathrm{conf}} = \frac{3N}{2}\frac{\Omega(U)}{\omega(U)}. \tag{17}$$

This well-known expression (see for instance [16]) relates the average kinetic energy with the total energy U via the density of states $\omega(U)$ and its integral $\Omega(U)$.

THERMODYNAMIC LIMIT

In the thermodynamic limit the deformation parameter q tends to 1 and (8) becomes a Boltzmann-Gibbs distribution. The entropy

$$I(f_U^{\mathrm{conf}}) = \frac{1}{2-q}\left(1 + \alpha(\theta) + \theta U^{\mathrm{conf}}\right) \tag{18}$$

converges to the Boltzmann-Gibbs value provided that

$$\left[\Gamma(3N/2)\omega(U)\right]^{1-q} \tag{19}$$

diverges in such a way that θ, as given by (10) converges to some function of the total energy U. This then links θ to the canonical inverse temperature β.

SUMMARY

The main purpose of the present work is to point out that the configurational probability distribution of a classical gas always belongs to the q-exponential family. The non-extensivity parameter q is given by (12). The latter expression has appeared quite often in the literature, see for instance [17-19].

In the limit of a large system ($N \to \infty$) the nonextensivity parameter goes to 1 and the configurational probability distribution approximates a Boltzmann-Gibbs distribution. In this limit the inverse temperature θ, defined by (10), is linked to the inverse temperature β of the canonical ensemble.

REFERENCES

[1] A.I. Khinchin, *Mathematical Foundations of Statistical Mechanics* (Dover Publications, 1949)
[2] D.H.E. Gross, *Microcanonical Thermodynamics* (World Scientific, 2001)
[3] C. Tsallis, J. Stat. Phys. **52**, 479–487 (1988).
[4] E.T. Jaynes, *Papers on probability, statistics and statistical physics*, ed. R.D. Rosenkrantz (Kluwer, 1989).
[5] J. Naudts, J. Ineq. Pure Appl. Math. **5**, 102 (2004).
[6] P.D. Grünwald and A.P. Dawid, Ann. Stat. **32**, 1367 (2004).
[7] J. Naudts, Open Systems and Information Dynamics **12**, 13–22 (2005).
[8] S. Eguchi, Sugaku Expositions **19**, 197–216 (2006), (originally Sūgaku **56**, 380 – 399 (2004) in Japanese).
[9] J. Naudts, Physica A 365, 42–49 (2006).
[10] J. Naudts, Entropy **10**, 131–149 (2008).
[11] A. Ohara and T. Wada, arXiv:0810.0624.
[12] J. Naudts, to appear in Cent. Eur. J. Phys., `http://dx.doi.org/10.2478/s11534-008-0150-x`, arXiv:0809.4764.
[13] R. B. Shirts, S. R. Burt, and A. M. Johnson, J. Chem. Phys. **125**, 164102 (2006).
[14] M.J. Uline, D.W. Siderius, and D.S. Cortib, J. Chem Phys. **128**, 124301 (2008).
[15] A. Schlüter, Z. Naturforschg. **3a**, 350–360 (1948).
[16] E.M. Pearson, T. Halicioglu, and W.A. Tiller, Phys. Rev. A, **32** 3030–3039 (1985).
[17] A. R. Plastino and A. Plastino, Phys. Lett. A **193**, 140–143 (1994).
[18] S. Abe, S. Martinez, F. Pennini, A. Plastino, Phys. Lett. A **278**, 249–254 (2001).
[19] A.B. Adiba, A.A. Moreirab, J.S. Andrade Jr., and M.P. Almeida, Physica A**322**, 276–284 (2003).

Molecular simulation of fuels. Thermodynamic and transport properties.

Carlos Nieto-Draghi[a,*], Michelle Aquing[a], Benoit Creton[a], Cyril Dartiguelongue[b], J. P. Martin Trusler[c], Fausto Ciotta[c] and Annabelle Pina[a]

[a] Thermodynamic and Molecular Simulation Department, IFP. 1 et 4 avenue de Bois-Préau, 92852 Rueil-Malmaison Cedex - France
[b] Physics and Analysis Division, Products Characterization Department, IFP. Rond-Point de l'échangeur de Solaize, BP3, 69360 Solaize - France
[c] Department of Chemical Engineering, Imperial College London, South Kensington Campus, London SW7 2AZ, U.K.
*carlos.nieto@ifp.fr

The automobile industry recently faces the challenge of developing a new generation of motor engines that both fulfils increasingly stringent regulations, reduction of operational costs as well as engine's specific consumption. While clean alternative power sources are still under development (hydrogen on fuel cells, 100% electric, etc), the optimisation of hybrid (electrical-combustion) or flexi-fuels (working with different fuel-biofuel blends) engines represent interesting short-term alternatives. An important point on the success of these technologies is the development of efficient integrated on-line optimisation devices. This fact requires the knowledge of thermo physical properties, such as liquid density and viscosity, of complex fuel mixtures under different thermodynamic conditions. Experimental data acquisition at extreme fuel injection conditions can be expensive or dangerous. At this respect, molecular simulation techniques can be used as a reliable complement to experiments for fluid property predictions. The key point of this approach is, on one hand, to have reliable intermolecular potentials able to describe the physical properties of a wide range of chemical compounds. On the other hand, to have a consistent methodology which leads to : 1) the determination of the fuel composition (by two-dimensional gas chromatography -GC×GC- or Carburane® analysis), 2) the representation of fuels by simplified pseudo-components (using an adapted lumping method designed to mimic the bulk physical properties of the initial mixture). The present approach was validated by comparing experimental measurements with simulation results for thermodynamic and transport properties over selected fuels (gasoline and diesel).

The Maximum Entropy Production Principle in Dissipative Flow Systems

Robert K. Niven
School of Aerospace, Civil and Mechanical Engineering, The University of New South Wales at ADFA, Canberra, ACT, 2600, Australia.
r.niven@adfa.edu.au

In many physical systems subject to one or more flows, the corresponding driving gradients (thermodynamic forces) at steady state are not *a priori* known, but are produced by the system in response to the flow (or vice versa). Examples include Rayleigh-Bénard convection, in which convective heat flow is established in response to a temperature gradient [1, 2]; the global atmospheric and oceanic circulation system of the Earth, in which an equator-pole temperature gradient is established in response to differential heat fluxes [3, 4, 5, 6, 7, 8, 9, 10, 11, 12]; biological ecosystems, in which a set of resource-waste chemical potential gradients are established in response to flows of nutrients [11, 13, 14]; and engineered fluid flow systems, in which shear stresses (momentum fluxes) arise in response to velocity gradients [15, 16]. Applying the non-equilibrium thermodynamic relation to such systems [17, 18]:

$$j_k = \sum_{\ell} L_{k\ell} F_{\ell} \tag{1}$$

where j_k is the kth flow and F_j is the ℓth thermodynamic force, we see that the global phenomenological coefficients $L_{k\ell}$ are themselves functions of the flows $L_{k\ell}(\{j_k\})$ and/or the forces $L_{k\ell}(\{F_\ell\})$. Such systems all involve the formation of self-organised, complex, ordered, *dissipative structures* [17, 18], for example turbulent fluid vortices, heat convection cells, water and chemical circulation cycles and/or life. Such highly non-linear responses pose tremendous difficulties for predictive modelling. Historically, three approaches have been adopted to redress this problem:

(i) whole-system dimensional models, in which dimensionless group arguments (Buckingham's Π theorem [19]) are used to correlate experimental data;

(ii) control volume analysis using empirical rules and order-of-magnitude simplifications, such as the turbulent flow models used in computational fluid dynamics; and

(iii) highly detailed control volume analysis using local linear relations (1), in which the coefficients $L_{k\ell}$ are assumed independent of fluxes and forces (the Onsager regime [20, 21]). This necessitates analysis with very small grid elements and short time scales, for example the "direct Navier-Stokes" modelling of incompressible fluid flow.

All such approaches suffer from serious limitations, including questions over the reliability of approaches (i) and (ii), and the high computational requirements of (iii). All break down if the physical solution is non-unique. Furthermore, the above approaches cannot easily be extended to the analysis of coupled transport phenomena, especially if experimental data and/or empirical constitutive relations are unavailable.

It is therefore of interest to report an additional principle which can be applied to dissipative, flow systems: the *maximum entropy production* (MEP) principle. This principle states that a many-degree-of-freedom system subject to flows and/or gradients will tend towards a steady state position at which the rate of production of thermodynamic entropy $\dot{\sigma}$ is at a maximum. The MEP principle was hypothesised in the 1970s [3, 4, 5] for the analysis of the Earth's climate

system; using a simple 10-box model, surprisingly accurate predictions are obtained of the geographic distributions of cloud cover, mean latitudinal air temperature, horizontal oceanic and atmospheric energy fluxes and net radiant energy inputs [3, 4, 5]. Since then it has been applied successfully to the analysis of a wide range of phenomena, including circulation on other planetary bodies [22], mantle convection [23, 24], biochemical systems [11, 13, 14], turbulent shear flow [2], frictional incompressible and compressible flow [25], electrical currents [26, 27, 28, 29], plasma formation and structure [30, 31], solid growth and diffusion [32, 33], chemical cycle kinetics [34], photosynthesis mechanism [35], biomolecular motors [36] and economic activity [37]. A number of detailed reviews are available [11, 38, 39, 40].

Notwithstanding the empirical successes of the MEP principle, studies of its theoretical underpinnings have been beset with difficulties. In recent years, Dewar [41, 42] analysed an unsteady flow system in terms of its probabilistic flow paths, giving a derivation of the MEP principle using an entropy defined on the set of paths. Several authors have criticised the analysis [43, 44], to suggest that it might apply only in the near-equilibrium linear (Onsager) regime. An alternative analysis was given by Attard [45, 46], also using a path entropy function, but expressed in terms of traditional statistical mechanics. Heuristic derivations of the principle have been given by Županović and co-workers [47] (also criticised [43]) and Martyushev [48]. There are also many historical antecedents to the MEP principle [38], most notably in the work of Ziegler [49].

The aim of this work is to report a conditional derivation of the MEP principle recently reported by the author [50], based on an entropy defined on the set of local fluxes. Consider a fluid flow control volume divided into infinitesimal elements, each assumed to satisfy local thermodynamic equilibrium. For an element which experiences a mean heat flux $\boldsymbol{j}_Q$, mean diffusive mass fluxes $\boldsymbol{j}_c$ of each species c (relative to the mass-average velocity $\boldsymbol{v}$ through the element), mean viscous stress tensor $\boldsymbol{\tau}$ and mean molar rate per unit volume $\hat{\dot{\xi}}_d$ of each chemical reaction $d = 1, ..., D$, the steady state thermodynamic entropy production per unit volume in each element $\hat{\dot{\sigma}}$ and overall entropy production $\dot{\sigma}$ are given by [16, 17, 51, 52]:

$$\hat{\dot{\sigma}} = \boldsymbol{j}_Q \cdot \boldsymbol{\nabla}\left(\frac{1}{T}\right) - \sum_{c=1}^{C} \boldsymbol{j}_c \cdot \left[\boldsymbol{\nabla}\left(\frac{\mu_c}{M_c T}\right) - \frac{\boldsymbol{g}_c}{T}\right] - \boldsymbol{\tau} : \boldsymbol{\nabla}\left(\frac{\boldsymbol{v}}{T}\right)^{\top} - \sum_{d=1}^{D} \hat{\dot{\xi}}_d \frac{A_d}{T} \quad \geq 0 \tag{2}$$

$$\dot{\sigma} = \iiint_{CV} \hat{\dot{\sigma}} \, dV \geq 0 \tag{3}$$

where T is absolute temperature, μ_c is chemical potential of species c, M_c is the molecular mass of species c, $\boldsymbol{g}_c$ is the specific body force on each species c and $A_d = \sum_{c=1}^{C} \nu_{cd} \, \mu_c$ is the molar chemical affinity of reaction d, in which ν_{cd} is the stoichiometric coefficient of species c in the dth reaction ($\nu_{cd} > 0$ for production) and $A_d < 0$ indicates a spontaneous forwards reaction. The stress notation of Bird *et al.* [16] is used in (2), in which $P > 0$ and $\tau_{ij} > 0$ denote compression. In a dissipative system, (2)-(3) are indeterminate, since one or more of the global fluxes and/or forces are unknown, being functions of the global conjugate forces and/or fluxes. However, by applying Jaynes' maximum entropy analysis [53, 54, 55], using a dimensionless flux entropy $\mathfrak{H}^*_{st}$ defined on the set of available instantaneous fluxes, it is possible to obtain the dimensionless potential function [50]:

$$\phi^*_{st} = -\mathfrak{H}^*_{st} - \frac{\theta \mathcal{V}}{k} \hat{\dot{\sigma}} \tag{4}$$

where θ and $\mathcal{V}$ respectively are characteristic time and volume scales of the system. Eq. (4) is analogous to the free energy function for equilibrium systems (more correctly, the negative

Massieu function [56] or Planck potential [57]), accounting for the losses of generalised potential (or increases in generalised entropy) within and outside the system. An unsteady dissipative flow system will therefore proceed to positions of lower ϕ^*_{st}, ultimately attaining a steady state of minimum ϕ^*_{st}. If the incremental dissipative losses $d\mathfrak{H}^*_{st} \geq 0$ and $\delta\hat{\sigma} \geq 0$ are unrecoverable, this will correspond to the position of maximum entropy production $\hat{\sigma} = \hat{\sigma}_{\max}$. The analysis therefore provides a conditional derivation of the MEP principle, quite different to those previously proposed in the literature.

The MEP principle and the above derivation will be presented and discussed in detail.

Acknowledgments

The author warmly thanks Bjarne Andresen, Marian Grendar, Bernd Noack and the participants of the MEP workshops hosted by the Max-Planck-Institut für Biogeochemie, Jena, Germany, in 2007 and 2008, especially Axel Kleidon, Roderick Dewar, Filip Meysman, Graham Farquhar, Michel Crucifix, Peter Cox, Tim Jupp, Adrian Bejan and Ralph Lorenz, for valuable discussions; the European Commission for financial support as a Marie Curie Incoming International Fellow (contract 039729- RKNIVEN-MC-IIF-06) under Framework Programme 6; and Bernd Noack and the Berlin Institute of Technology for financial support.

References

[1] H. Bénard, Ann. Chim. Phys. 23 (1901) 62.
[2] H. Ozawa, S. Shikokawa, H. Sakuma, Phys. Rev. E 64 (2001) article 026303.
[3] G.W. Paltridge, Quart. J. Royal Meteorol. Soc. 101 (1975) 475.
[4] G.W. Paltridge, Quart. J. Royal Meteorol. Soc. 104 (1978) 927.
[5] G.W. Paltridge, Quart. J. Royal Meteorol. Soc. 107 (1981) 531.
[6] H. Ozawa, A. Ohmura, J. Clim. 10 (1997) 441.
[7] G.W. Paltridge, Quart. J. Royal Meteorol. Soc. 127 (2001) 305.
[8] S. Shimokawa, H. Ozawa, Tellus 53A (2001) 266.
[9] S. Shimokawa, H. Ozawa, Quart. J. Royal Meteorol. Soc. 128 (2002) 2115.
[10] A. Kleidon, K. Fraedrich, T. Kunz, F. Lunkeit, Geophys. Res. Lett. 30(23) (2003) article 2223.
[11] A. Kleidon, R.D. Lorenz (eds.) Non-equilibrium Thermodynamics and the Production of Entropy: Life, Earth and Beyond, Springer Verlag, Heidelberg, 2005.
[12] G.W. Paltridge, G.D. Farquhar, M. Cuntz, Geophys. Res. Lett. 34 (2007) L14708.
[13] A. Kleidon, Climatic Change 66 (2004) 271.
[14] F.J.R. Meysman, S. Bruers, J. Theor. Biol. 249 (2007) 124.
[15] F.M. White, Viscous Fluid Flow, 3rd ed., McGraw-Hill, NY.
[16] R.B. Bird, W.E. Stewart, E.N. Lightfoot, Transport Phenomena, 2nd ed., John Wiley & Sons, NY, 2002.
[17] I. Prigogine, Introduction to Thermodynamics of Irreversible Processes, 3rd ed., Interscience Publ., NY.
[18] D. Kondepudi, I. Prigogine, Modern Thermodynamics: from Heat Engines to Dissipative Structures, John Wiley & Sons, Chichester, UK, 1998.
[19] E. Buckingham (1915) Model experiments and the forms of empirical equations, Trans. ASME, 37: 263-296
[20] L. Onsager, Phys. Rev. 37 (1931) 405.
[21] L. Onsager, Phys. Rev. 38 (1931) 2265.

[22] R.D. Lorenz, J.I. Lunine, P.G. Withers and C.P. McKay, Geophys. Res. Lett. 28 (2001) 415-418.
[23] J.P. Vanjo, G.W. Paltridge, Geophys. J. R. Astron. Soc. 66 (1981) 677.
[24] R.D. Lorenz, Proc. Lunar Planet Sci. Conf., 32 (2001) abstract 1160.
[25] D.M. Paulus, R.A. Gaggioli, Energy 29 (2004) 2487.
[26] P. Županović, D. Juretić, S. Botrić, Phys. Rev. E 70 (2004) article 056108.
[27] S. Botrić, P. Županović, D. Juretić, Croatica Chemica Acta 78(2) (2005) 181.
[28] T. Christen, J. Phys. D: Appl. Phys. 39 (2006) 4497.
[29] S. Bruers, C. Maes, K. Netočný, J. Stat. Phys. 129 (2007) 725.
[30] T. Christen, J. Phys. D: Appl. Phys. 40 (2007) 5719.
[31] Z. Yoshida, S.M. Mahajan, Physics of Plasmas 15 (2008) article 032307.
[32] L.M. Martyushev, E.G. Axelrod, JETP Letters 78(8) (2003) 476.
[33] T. Christen, J. Phys. D: Appl. Phys. 40 (2007) 5723.
[34] P. Županović, D. Juretić, Croatica Chemica Acta 77(4) (2004) 561.
[35] D. Juretić, P. Županović, Computational Biology and Chemistry 27 (2003) 541.
[36] R.C. Dewar, D. Juretić, P. Županović, Chemical Physics Letters 430 (2006) 177.
[37] A.D. Jenkins, arXiv:cond-mat/0503308v1, 2005.
[38] L.M. Martyushev, V.D. Seleznev, Physics Reports 426 (2006) 1.
[39] S. Bruers, arXiv:cond-mat/0604482v3, 2007.
[40] H. Ozawa, A. Ohmura, R.D. Lorenz, T. Pujol, Rev. Geophys. 41 (2003) article 4.
[41] R.C. Dewar, J. Phys. A: Math. Gen. 36 (2003) 631.
[42] R.C. Dewar, J. Phys. A: Math. Gen. 38 (2005) L371.
[43] S. Bruers, arXiv:0705.3226v1, 2007.
[44] G. Grinstein, R. Linsker, J. Phys. A: Math. Theor. 40 (2007) 9717.
[45] P. Attard, J. Chem. Phys. 125 (2006) article 214502.
[46] P. Attard, Phys. Chem. Chem. Phys. 8 (2006) 3585.
[47] P. Županović, S. Botrić, D. Juretić, Croatica Chemica Acta 79(3) (2006) 335.
[48] L.M. Martyushev, arXiv:0709.0152v1, 2007.
[49] H. Ziegler, An Introduction to Thermomechanics, North-Holland, Amsterdam, 1977.
[50] R.K. Niven, Derivation of the maximum entropy production principle for flow-controlled systems at steady state, http://arxiv.org/abs/0902.1568.
[51] S.R. de Groot, P. Mazur, Non-Equilibrium Thermodynamics, Dover Publications, NY, 1984.
[52] H.J. Kreuzer, Nonequilibrium Thermodynamics and its Statistical Foundations, Clarendon Press, Oxford, 1981.
[53] E.T. Jaynes, Phys. Rev., 106 (1957) 620.
[54] E.T. Jaynes, in Ford, K.W. (ed), Brandeis University Summer Institute, Lectures in Theoretical Physics, Vol. 3, Benjamin-Cummings Publ. Co., 1963, 181.
[55] E.T. Jaynes (G.L. Bretthorst, ed.) Probability Theory: The Logic of Science, Cambridge U.P., Cambridge, 2003.
[56] M. Massieu, Comptes Rendus 69 (1869) 858, 1057.
[57] M. Planck, Treatise on Thermodynamics, Engl. transl., 3rd ed., Dover Publications, NY, 1945.

Quantum size effects on self-thermal diffusion of gases

Ozturk ZF[1,2] and Sisman A[1]

[1]Energy Institute, Istanbul Technical University, 34469 Maslak, Istanbul, Turkey
[2]Department of Photonics Engineering, Technical University of Denmark,
DTU Fotonik, DK-2800 Kongens Lyngby, Denmark
ozturkzeh@itu.edu.tr

Abstract

The effects of the wave nature of particles on self-thermal diffusion coefficient is analytically derived for ideal Maxwell, Fermi and Bose gases in a rectangular transport domain. It is shown that the wave nature of particles makes the transport coefficient shape and size dependent. Therefore size and shape become additional control parameters on thermal diffusion process. Also, the variation of quantum size effects on thermal diffusion in Fermi and Bose gases with quantum degeneracy are examined. Different behaviors for Fermi and Bose gases have been observed with increasing degeneracy.

1. Introduction

If the size of a system approaches to nano scale, quantum effects appear on time and length scales of transport properties and cause deviations from the macroscopic picture. Nanotechnology enables to produce nanostructures where the particles are significantly influenced by quantum effects [1-7]. These quantum effects become important when the thermal de Broglie wavelength of particles, λ_{th}, is not negligible in comparison with the size of the confinement domain. Therefore, these effects are called quantum size effects (QSE) in general. QSE on transport coefficients have been studied for semiconductors, metals and thin films having the sizes smaller than λ_{th} in one or more directions (like quantum wells, quantum wires and quantum dots) in literature [8-12]. QSE on thermodynamic and transport properties of gases confined in nano structures, having the sizes close to but greater than λ_{th}, where the semi-classical theories can still be used, are the relatively new research topics [13-20]. In the semi-classical approach, the potential acting on the wave-like particles is different than the classical particles. The true potential acting on the wave-like particle can be represented by adding an effective quantum potential to the classical one. Therefore quantum probability density is replaced by a classical probability density as long as the modified potential is used in distribution functions. Consequently, the quantum effects on local density are represented by the effective quantum potential.

For the irreversible processes, there is a linear relation between fluxes and driving forces. The proportionality constants between fluxes and driving forces are called kinetic coefficients [21]. In the irreversible thermodynamics, each flux is a function of the all driving forces. Therefore, the flux of a quantity can be driven by more than one driving force simultaneously. For example, particle flux can be driven not only by density gradient but also by temperature gradient. In this case, temperature gradient is the secondary driving force and the particle flux due to temperature gradient is called thermal diffusion as a cross effect. Cross effects become important when the mean free

path is not negligible in comparison with the domain sizes. Therefore cross effects become significant especially in nano scale where also QSE are noticeable.

The wave character of particles causes a number of modifications on some fundamental quantities. Therefore, transport processes of gases in nano scale are different than those in macro scale. These modifications are the changes in local density, momentum spectrum of particles and the smallest values of the momentum components. These are briefly explained respectively as follows:

i) In macroscopic approach based on the particle nature of matter, probability density is constant in thermodynamic equilibrium and it is given by $1/V$ for gas particles confined in volume *V*. Therefore, density of a gas is homogenous at thermodynamic equilibrium in macro scale. In microscopic approach based on the wave nature of matter, however, probability density is represented by the quantum probability density $|\psi_w|^2$, where ψ_w is the wave function of the particle in quantum state w. Ensemble average of quantum probability density $\left\langle |\psi_w|^2 \right\rangle$, represents a quantity that can be compared with the classical one. Since $\left\langle |\psi_w|^2 \right\rangle$ depend on position, local density is not homogenous even in thermodynamic equilibrium when the wave character of particles is considered. On the other hand, the size of non-homogenous region is in the order of λ_{th}. The value of λ_{th} is usually in the order of nanometer. Therefore the effect of particle's wave character on local density becomes important in nano scale.

ii) Although the momentum values of the particles are discreet, they are assumed to be continuous in macroscopic scale. However, if the domain size, in one or more directions, approaches to the thermal de Broglie wavelength of particles, this assumption breaks down and the discreet nature of the momentum values becomes important.

iii) The lowest value of the momentum components cannot be zero due to the wave nature of particles. In other words, particles never move parallel to the boundaries of the domain. Hence, the false contribution from the surface modes to the thermodynamic and transport properties in theoretical macroscopic models should be excluded. This false contribution can be ignored in macro systems since the contribution from the surface modes is negligible in comparison with that of the bulk modes. On the other hand, it becomes noticeable in nano scale and the exclusion of the false contribution from the surface modes constitutes the origin of quantum size effects on thermodynamic and transport properties considered here.

In this study, particle flux due to temperature gradient is analytically derived by considering QSE for ideal Maxwell, Fermi and Bose gases confined in a rectangular channel. Size of the nano channel in transport direction is assumed to be much longer than both λ_{th} and the mean free path of the particles l while the sizes in other directions are much smaller than l but still bigger than λ_{th}. Therefore, it is still possible to follow the classical methodology to define and calculate the transport coefficient while the calculations should be done in a more precise way by considering the modifications mentioned above. For this size configuration, particle-boundary collisions are dominant. It is shown that, in nano scale, size and shape become additional control parameters on thermal diffusion process.

2. Self-thermal diffusion coefficient under quantum size effects

Thermal diffusion is the diffusion process driven by temperature gradient and thermal diffusion coefficient is defined as

$$D_T = -\vec{J}_N \Big/ \vec{\nabla} T \,. \tag{1}$$

If the gas consists of single specie, then thermal diffusion is called self-thermal diffusion. To examine QSE on self-thermal diffusion coefficient, a rectangular channel occupied by an ideal gas is considered. The channel is subjected to a temperature gradient in one direction, x_1, where the size is longer than both λ_{th} and l. In transverse directions, sizes of the channel are smaller than l and bigger than λ_{th}. Therefore particle-boundary collisions are dominant. To obtain the non-equilibrium distribution function f, relaxation time approximation is used while the summations over the particle velocities (v_1, v_2, v_3) are calculated by using the Poisson summation formula to make the calculations precisely and exclude the false contribution from the surface modes. Particle flux due to temperature gradient is obtained for ideal monatomic Maxwell, Fermi and Bose gases as,

$$J_1^N = \sum_{v_1,v_2,v_3} v_1 f = -\frac{l_g}{TV}\left(\frac{2k_bT}{m}\right)^{1/2}(g_2 - \Lambda g_0)\frac{\partial T}{\partial x_1} \tag{2}$$

where $\Lambda = \mu / k_bT$, μ is the chemical potential, k_b is the Boltzmann's constant, T is the temperature, l_g is the mean free path for particles-boundary collisions (geometric mean free path, nearly half of the volume over surface area of the transport domain), m is the particle mass and V is the transport volume. For a rectangular transport domain of dimensions L_1, L_2 and L_3, g_b is obtained for Fermi and Bose gases as

$$g_b = \mp \frac{2\pi\Gamma\left(\frac{4+b}{2}\right)}{3\alpha_1\alpha_2\alpha_3} Li_{\frac{2+b}{2}}\left[1 - \frac{3(\alpha_2+\alpha_3)}{4}\frac{\Gamma\left(\frac{3+b}{2}\right)}{\Gamma\left(\frac{4+b}{2}\right)}\frac{Li_{\frac{1+b}{2}}}{Li_{\frac{2+b}{2}}}\right] \tag{3}$$

where Γ is the gamma function, α_i is defined as $\alpha_i = L_c / L_i$, L_i is the dimension of the domain in direction x_i and L_c is the half of the most probable de Broglie wavelength, $L_c = h/\sqrt{8mk_bT}$, Li is used for the abbreviation of Polylogarithm function with an exponential argument of $\mp\exp(\Lambda)$. Plus (minus) sign is used for Bose (Fermi) gas. To represent the pure QSE on self-thermal diffusion coefficient, dimensionless form is defined as $\hat{D}_T = D_T / D_T^0$; where D_T^0 is transport coefficient calculated without QSE, $(\alpha_2, \alpha_3) \to 0$. Therefore, self-thermal diffusion coefficient is determined by using Eqs.(1)-(3) in dimensionless form as

$$\hat{D}_T = \frac{2Li_2\left(1 - \frac{9\sqrt{\pi}}{32}(\alpha_2+\alpha_3)\frac{Li_{3/2}}{Li_2}\right) - \Lambda Li_1\left(1 - \frac{3\sqrt{\pi}}{8}(\alpha_2+\alpha_3)\frac{Li_{1/2}}{Li_1}\right)}{2Li_2 - \Lambda Li_1} \tag{4}$$

For high temperature and/or low density conditions, quantum degeneracy becomes negligible and Eq.(4) can be simplified by using the asymptotic forms of the Polylogarithm functions as follows for a Maxwellian gas

$$\hat{D}_T = \frac{2\left(1 - \frac{9\sqrt{\pi}}{32}(\alpha_2+\alpha_3)\right) - \Lambda\left(1 - \frac{3\sqrt{\pi}}{8}(\alpha_2+\alpha_3)\right)}{2 - \Lambda} \tag{5}$$

The terms in the brackets of Eqs.(4) and (5) represent the QSE and make the thermal diffusion coefficient size and shape dependent since α_2 and α_3 depend on L_2 and L_3.

3. Results and Discussion

The effect of quantum degeneracy on $\hat{D}_T$ is shown in Fig.1. It is seen that QSE decrease with increasing degeneracy for Fermi gas. Mean de Broglie wave length of particles decreases with increasing degeneracy and the wave character becomes negligible. Therefore QSE are weaker for high degeneracy conditions. On the contrary, mean de Broglie wave length of particles increases with increasing degeneracy in a Bose gas. Thus, QSE become stronger near to Bose-Einstein condensation point. For Maxwellian limit, ($\Lambda << -1$), both curves converge to the same value.

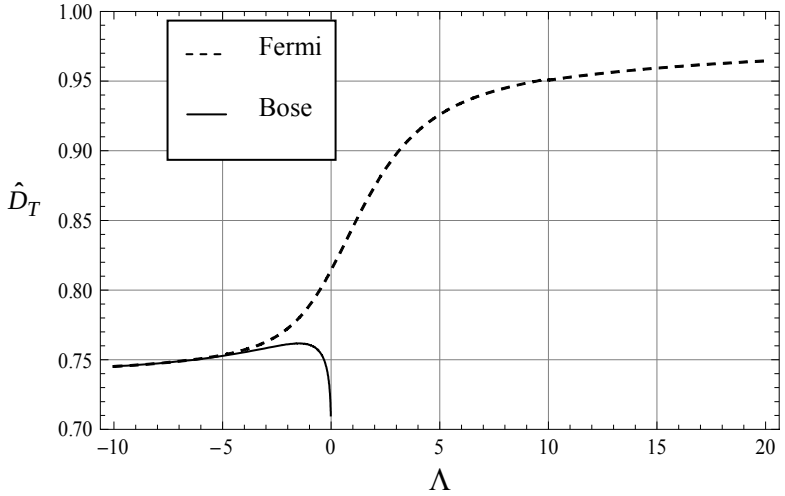

Figure 1. Variation of QSE on $\hat{D}_T$ with increasing degeneracy for Fermi and Bose Gases, $\alpha_2 = \alpha_3 = 0.2$.

Acknowledgements

This work is supported by Scientific and Technological Research Council of Turkey, TUBİTAK, under the contract number of 105T086 and Istanbul Technical University Scientific Research Program.

References

[1] Goddard, W.A., Brenner, D.W., Lyshevski, S.E. and Iafrate, G.J., (Editors) 2003, *Handbook of Nanoscience, Engineering, and Technology*, Boca Raton: CRC Press.
[2] Wolf, E.L., 2004, *Nanophysics and Nanotechnology*, Weinheim: WILEY-VCH.
[3] Kang, J.W. and Hwang, H.J., 2004, *Nanotechnology*, 15, 1633-38.
[4] Li, Z. and Ling, H., 2007, *The Journal of Chemical Physics*, 127, 0747706/1-5.
[5] Schöll, E.,1998, *Theory of Transport Properties of Semiconductor Nanostructures*, Chapman & Hall.
[6] Roldughin, V.I. and Zhdanov, M.V., 2003, *Colloid Journal*, 65, 598-601.
[7] Skoulidas, A.I., Ackerman, D.M., Johnson, J.K. and Sholl, D.S., 2002, *Physical Review Letters*, 89, 185901/1-4.
[8] Freeman, W.L. and Gettys, E.W., 1978, *Phys. Rev. B,* 17, 529-34.
[9] Arora, V.K., and Awad, F.G., 1981, *Phys. Rev.* B, 23, 5570-5575.
[10] Trivedi, N. and Ashcroft, N.W., 1988 *Phys. Rev. B,* 38, 12298-309.
[11] Rogacheva, E.I., Grigorov, S.N., Nashchekina, O.N., Lyubchenko, S. and Dresselhaus M.S., 2003, *Applied Physics Letters*, 82, 2628-30.
[12] Liu, X., Zhang, S.B., Ma, X.C., Jia, J.F., Xue, O.K., Bao, X.H. and Li, W.X., 2008, *Applied Physics Letters*, 93, 093105.
[13] Sisman, A., Ozturk, Z.F. and Firat, C., 2007, *Phys. Lett.* A, 362, 16-20.
[14] Dai, W.S. and Xie, M., 2007, *J. Math. Phys.*, 48, 123302.
[15] Pang, H., Dai, W.S. and Xie, M., 2006, *J. Phys.* A*: Math. Gen.*, 39, 2563-71.
[16] Sisman, A., 2004, *J.Phys.* A: *Math. Gen.*, 37, 11353-61.
[17] Sisman, A. and Müller, I., 2004, *Phys. Lett.* A, 320, 360-6.
[18] Dai, W.S. and Xie, M., 2004, *Phys. Rev.* E, 70, 016103-1.
[19] Pathria, R.K., 1998, *Am. J. Phys*., 66, 1080-85.
[20] Molina, M.I., 1996, *Am. J. Phys*., 64, 503-5.
[21] de Groot, S.R., Mazur, P., *Non-Equilibrium Thermodynamics*, 1984, Dover Publication, New York.

Comparison of macroscopic internal variable theory and mesoscopic theory based on the Second Law of Thermodynamics

Christina Papenfuss
Technical University of Berlin
Strasse des 17. Juni 135
Germany
c.papenfuss@gmx.de

Abstract

Polymers, micro-crystalline solids, ferrofluids, liquid crystals and solids with micro-cracks are typical examples for materials with an internal structure. They show complex macroscopic material behavior, because the internal structure can change under the action of external fields. There is some influence of the structure on the microscopic level to the material behavior on the macroscopic level. There are two principally different possibilities to deal with complex materials within continuum thermodynamics: The first way is to introduce additional fields depending on position and time, i.e. on the macroscopic level. These fields can be internal variables, order or damage parameter, Cosserat triads, directors, alignment and conformation tensors. The other way is a so called mesoscopic theory. The idea is to enlarge the domain of the field quantities. The new mesoscopic fields are defined on the space $\mathbb{R}^3_x \times \mathbb{R}_t \times M$. The manifold M is given by the set of values the internal degree of freedom can take. Therefore the choice of M depends on the complex material under consideration. We call this way of dealing with the internal structure of complex materials a mesoscopic concept, because it includes more information than a macroscopic theory on $\mathbb{R}^3_x \times \mathbb{R}_t$, but the molecular level is not considered like in a microscopic approach. The mesoscopic level is between the microscopic and the macroscopic level. The domain of the mesoscopic field quantities $\mathbb{R}^3_x \times \mathbb{R}_t \times M$ is called mesoscopic space. The aim of the present paper is to show the connection between the macroscopic internal variable theory on one hand and the mesoscopic theory on the other hand.

Especially, we will investigate the relation between an internal variable theory and the mesoscopic theory on the example of liquid crystals. For special substances the liquid crystalline phase exists in a certain temperature range between the ordinary isotropic phase and the solid crystalline phase. It is a fluid-like phase, but showing anisotropic material properties. As macroscopic internal variable, the second order alignment tensor, or the scalar order parameter in the uniaxial case, are introduced, respectively. An equation of motion for the internal variable can be derived from macroscopic thermodynamics. This results in a differential equation of the form applied in dynamical Landau-theory of phase transitions.

On the mesoscopic level, the orientation of the non-spherical particles, the microscopic director, is introduced as the additional variable [2, 4]. The distribution function is an orientation distribution. The alignment tensor can be defined in terms of the mesoscopic distribution function, as a moment of the distribution. Its

equation of motion can be derived, starting from the mesoscopic theory. Under some simplifying assumption, we will find the same type of equation of motion [1] for the second order alignment tensor as from macroscopic thermodynamics.

The comparison between mesoscopic and macroscopic theory gives some information on the mesoscopic distribution function, too. It is not possible to reconstruct completely the distribution function on the mesoscopic level, knowing only the value of one macroscopic internal variable. This would be possible only in case of an infinite set of macroscopic variables, i.e. all moments of the distribution function. Therefore, the reconstruction of the distribution function is possible only within a certain restricted class of functions, namely the distribution functions maximizing the entropy under the constraint of a prescribed value of certain moments [3]. This leads to a certain exponential form of distribution function with one yet unknown parameter. The parameter in the distribution function is identified by exploiting the entropy production. We end up with an orientation distribution function, given in terms of the mesoscopic variable, the microscopic director, and a derivative of the macroscopic entropy density.

References

[1] W. Muschik, C. Papenfuss, and H. Ehrentraut. Alignment tensor dynamics induced by the mesoscopic balance of the orientation distribution function. *Proc. Estonian Acad. Sci. Phys. Math.*, 46:94–101, 1997.

[2] C. Papenfuss. Theory of liquid crystals as an example of mesoscopic continuum mechanics. *Computational Materials Science*, 19:45 – 52, 2000.

[3] C. Papenfuss. A closure relation for the higher order alignment tensors in liquid crystal theory and the alignment-fabric tensors in damage mechanics from a statistical background. *Physica A*, 331: 23–41, 2003.

[4] W. Muschik, C. Papenfuss, and H. Ehrentraut Mesoscopic theory of liquid crystals. *J. Non-Equilib. Thermodyn.*, 29: 75–106, 2004.

ENTROPY AND NEWTONIAN MECHANICS

A. Pérez-Madrid[a]
Departament de Física Fonamental, Facultat de Física,
Universitat de Barcelona,
Diagonal 647, 08028 Barcelona, Spain
[a] Electronic mail: agustiperezmadrid@ub.edu

Based on Newton's laws reformulated in the Hamiltonian dynamics, we show that a suitably defined nonequilibrium entropy of an N-body isolated system is not a constant of the motion, in general. This entropy varies between well defined bounds determined by the thermodynamic entropy, i.e., the equilibrium entropy. We define this nonequilibrium entropy as a convex functional of the set of n-particle reduced distribution functions ($n \leq N$) generalizing the Gibbs fine-grained entropy formula. Additionally, as a consequence of our microscopic analysis we find that this nonequilibrium entropy behaves as a free entropic oscillator. Therefore, a new conception of time and the time arrow arises. In the approach to the equilibrium regime, we find relaxation equations of the Fokker-Planck type, particularly for the one-particle distribution function.

Prediction of thermodynamic properties of pure components and mixtures: cubic equations of state versus molecular theory-derived equations of state: a short comparison

Romain Privat[(a),(b),*], Rafiqul Gani[(a)] and Jean-Noël Jaubert[(b)]

(a) CAPEC, Department of Chemical & Biochemical Engineering, Soltofts Plads, Building 229, Technical University of Denmark, DK-2800 Lyngby, Denmark.
(b) Institut National Polytechnique de Lorraine, Ecole Nationale Supérieure des Industries Chimiques, Laboratoire de Thermodynamique des Milieux Polyphasés, 1, rue Grandville, BP 20451, Nancy Cedex 9, France.

* *e-mail:* rop@kt.dtu.dk

Since many years, equations of state (EOS) are acknowledged through industrial and academic worlds as powerful thermodynamics models to represent the phase behaviours of pure substances and multicomponent systems. Initially developed by Van der Waals, the first EOS capable of handling both liquid and gas phases, has shown the way to several generations of thermodynamicists. Numerous models are then born and among these: the cubic EOS that industrialists nearly exclusively used until the end of the twentieth century. However, since the beginning of the 90's, a new generation of EOS is emerging and drawing more and more the attention: the molecular theory-derived EOS and among these, the SAFT (Statistical Associating Fluid Theory) equations.

These models are much more complicated than the cubic ones but are also very promising. As an example, SAFT EOS appear able to represent complex molecules like associating fluids (ammonia, water, alcohols, etc.) or polymers which are often considered as borderline cases for cubic EOS.

In this work, we propose to make a comparison between two predictive models [1,2] based on EOS reputed for their efficiency and issued from different backgrounds: the one stemming from the cubic Peng-Robinson EOS [3] and the second one, from the PC-SAFT EOS [4]. The two considered predictive models use the group contribution concept. It means that the thermodynamic properties can be deduced from the chemical structure of the compounds making up the studied mixture.

In this way, the ability of the two models to predict the phase behaviour is tested out on some pure components and binary systems, ordered according to their chemical family. The reliability and the efficiency of these equations for industrial purposes will be discussed.

References.

[1] R. Gani, P. M. Harper, M. Hostrup, Industrial & Engineering Chemistry Research, (2005), 44(18), 7262-7269.
[2] J.N. Jaubert, F. Mutelet, Fluid Phase Equilibria, (2004), 224(2), 285-304.
[3] D.B. Robinson, D.Y. Peng, Gas Processors Association, Research Report RR-28, 1978.
[4] J. Gross, G. Sadowski, Industrial & Engineering Chemistry Research, (2001), 40, 1244-1260.

Numeric Experiments in Relativistic Thermodynamics

Constantin Rasinariu *

Department of Science and Mathematics

Columbia College Chicago, Chicago, USA

February 9, 2009

Abstract

In this paper we simulate a two dimensional relativistic ideal gas by implementing a relativistic elastic binary collision algorithm. We show that the relativistic gas faithfully obeys Jüttner's speed distribution. Furthermore, using this numeric simulation in conjunction with the relativistic equipartition theorem for a relativistic gas, we find compelling numerical evidence that moving objects should appear cooler.

1 Introduction

Let us denote by T the temperature of a thermodynamic system as measured in its rest frame K, and by T' the temperature of the same system measured by an inertial frame K' in motion with speed u relative to K.

In 1907 Mosengeil, Planck, and Einstein [1, 2, 3], independently showed that

$$T' = T/\gamma \ , \tag{1}$$

where $\gamma = (1 - u^2/c^2)^{-1/2}$ is the relativistic factor. In other words, a moving system appears cooler.[1] In 1963 Ott [8] arrived to a completely different result

$$T' = T\gamma \ . \tag{2}$$

According to Ott, a moving system is hotter. Although hints of Eq. (2) appeared in literature [6] before Ott, it is Ott's paper that have ignited the controversy on rendering the thermodynamic quantities in their special relativistic form. Despite the large number of papers published on this subject, today there is no

*E-mail: crasinariu@colum.edu

[1] From now on, we will refer to Eq. (1) as "Plank's formula" for the relativistic transformation of the temperature.

general consensus regarding the special relativistic thermodynamics. Because an exhaustive discussion on the history of this issue is beyond the scope of our paper, the interested reader should consult [11, 12, 13, 15] and the references therein. To illustrate the relativistic thermodynamics imbroglio, we will limit to just a few examples. In 1966 Landsberg proposed the invariance of temperature [9]

$$T' = T \ , \tag{3}$$

while Balescu [10] explored the possibility that all relativistic transformations are in fact equivalent to each other, via some sort of "gauge" transformations. It is interesting to note that in 1952, in an unpublished letter to von Laue [13], Einstein argued in favor of temperature transformation (2), thus contradicting his previous results [3]. However, one year later, in another letter to von Laue [13], Einstein pondered whether the temperature should be actually considered a relativistic invariant. Landsberg [15], will revisit several times this question, before concluding that special relativistic thermodynamic transformations are impossible. Probably, the lack of a general agreement on how to transform relativistically the thermodynamic quantities is the main reason that special relativistic thermodynamics is absent from most modern physics textbooks.

A direct experiment on relativistic thermodynamics is hampered by the high temperatures and the relativistic speeds involved. In this paper, we are trying to partially overcome this difficulty, by using computer simulations of a two-dimensional relativistic ideal gas. We simulate a two dimensional gas enclosed inside a rectangular container, whose point-like particles move relativistically, and experience only elastic collisions. How hot is this gas? If the gas simulated in this paper would be a classical (i.e. non-quantum) proton gas, then we simulate a container whose temperature reaches $5.44 \times 10^{12}\, K$, and which is boosted to speeds up to 80% of the speed of light. These are conditions that cannot be easily realized in laboratory. In this simple model, we find that our relativistic gas faithfully obeys Jüttner's speed distribution [4]. In addition, by using the relativistic equipartition theorem [12], we find that our numeric simulations, strongly favor Planck's transformation formula (1). Thus, we uncover compelling numeric evidence that moving objects should appear cooler.

2 Computer Simulations

We consider a two-dimensional ideal relativistic gas whose point-like particles experience only elastic collisions. The gas is enclosed inside a rectangular container, with perfectly reflecting walls, which conserve the energy-momentum of the colliding particles. Throughout the rest of this paper we will use a system of units where the speed of light, the mass of the particles, and Boltzmann's constant are all taken equal to one: $c = 1, m = 1, k_B = 1$.

The thermodynamic system is at rest in the lab when the container is at rest, and the average velocity of its particles is zero $\langle \vec{v} \rangle = 0$. If the gas is in thermal equilibrium at temperature $T = 1/\beta$, its speed distribution is given by Jüttner's formula [4, 7]

$$f(v) = v\gamma_v^4 \exp\left(-\beta\,\gamma_v\right)/Z \ , \tag{4}$$

where $\gamma_v = (1-v^2)^{-1/2}$ is the Lorentz factor, and $Z = e^{-\beta}(1+\beta)/\beta^2$ is a normalization constant, chosen such that $\int_0^1 f(v)\,dv = 1$. Then, the average energy is given by $\langle E\rangle \equiv \int_0^1 Ef(v)dv = (\beta^2+2\beta+2)/(\beta^2+\beta)$. We will use this information to find the reciprocal of the temperature of the system at rest, from measuring its average energy. We get

$$\beta = \left(2 - \langle E\rangle + \sqrt{\langle E\rangle^2 + 4\,\langle E\rangle - 4}\right) / \left(2\langle E\rangle - 2\right) \ . \tag{5}$$

2.1 Numeric results

For the experimental setup we took $100,000$ identical particles, which initially, were randomly distributed inside a rectangular box, and given the same initial speed in arbitrary directions. We chose the following initial speeds: $v_{init} = 0.2,\ 0.5$, and 0.8. After thermalization, these initial conditions lead to the following reciprocal temperatures $\beta = 49.45,,\ 7.25$, and 2.00 respectively.

During one time step the computer algorithm checks for possible collisions with *a)* the wall of the container (the box has the edges parallel with x and y axes), and *b)* with another particle. If none occurs, the particle advances one time step with the same velocity.

a) *Collisions particle–wall:* If the particle hits the left or right wall, it reflects around the x-axis. If it hits the top or the bottom wall, the particle reflects around the y-axis.

b) *Collisions particle–particle:* Point-like particles have practically no chance to collide if only contact, zero-range interactions are present. To bypass this difficulty, we defined an "interaction area" around each particle as follows. If (x_i, y_i) are the coordinates of particle i as measured by an observer at rest with respect to the container, and if particle j arrives at (x_j, y_j) such that $(x_i - x_j)^2 + (y_i - y_j)^2 \leq R^2$, then the two particles "collide". The distance R is chosen to be much smaller than the linear dimensions of the container. The algorithm "locks" the two particles when colliding, thus ignoring the possibility of a third particle to participate in collision. This simplifies the simulation and does not introduce errors greater than a one percent. Knowing the "in" states of the particles entering the collision we determine the "out" states by using only the conservation of the energy-momentum. However, in this last step, which is solved in the center of mass of the two particles, one has to choose an "interaction angle" θ for the outgoing particles, as

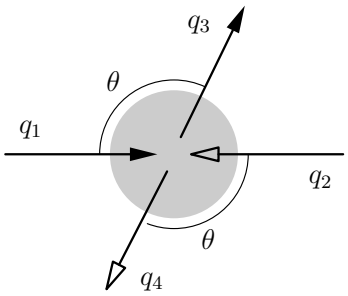

Figure 1: The interaction as seen in the center of mass of the two particles. Here q_1 and q_3 are the momenta of the incoming and respectively outgoing particle 1. Similarly, q_2 and q_4 are the momenta of the incoming and respectively outgoing particle 2. The angle θ between incoming and outgoing particles is chosen randomly.

illustrated in figure (1). Since particles are modeled as zero-size points experiencing only elastic collisions, θ is not meaningfully defined. Therefore, we used a pseudo-random number generator to assign a random value to the "interaction" angle θ, for each collision.

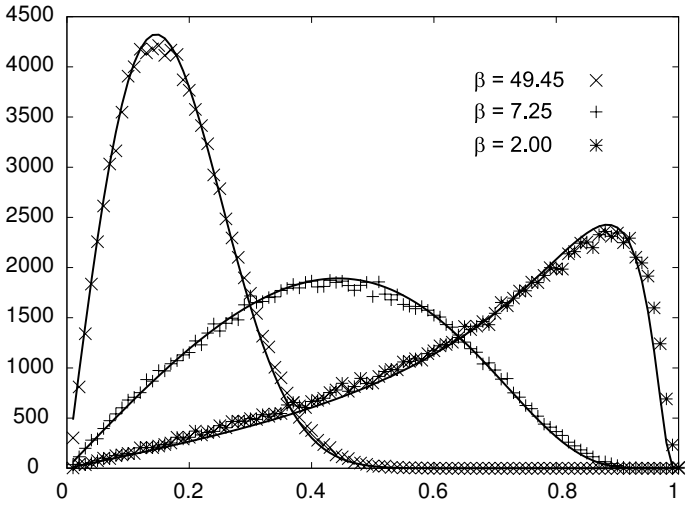

Figure 2: Jüttner's speed distribution curves (plain lines) vs. the experimental speed distribution (dotted lines) for a relativistic 2-d gas at reciprocal temperatures $\beta = 49.45$, $\beta = 7.25$, and $\beta = 2.00$ respectively. The area under each distribution curve is equal to the total number of particles, $N = 100,000$.

We monitored the average energy per particle, and considered that the system reached thermal equilibrium when the average energy per particle fluctuated by less than 0.001%. From the onset of the experiment, the equilibrium was usually achieved after $40,000$ time steps. After the system reached thermal equilibrium, we determined its temperature by means of Eq. (5). By plugging the measured value back into Eq. (4), we

were able to compare the theoretical curves with the histograms of the speed distribution obtained from our computer modeling. In figure (2) we illustrate the experimental results versus the theoretical predictions for the 2-d relativistic gas. The figure collects data from three different experiments: low temperature (with the corresponding reciprocal temperature $\beta \equiv mc^2/k_BT = 49.45$), intermediate temperature ($\beta = 7.25$), and respectively high temperature ($\beta = 2.00$). The agreement with Jüttner's distribution is remarkable in all cases.

3 Statistic temperature and the relativistic equipartition

In classic (non-relativistic) statistical thermodynamics, we used the energy equipartition theorem to establish a connection between the average kinetic energy and the temperature. Specifically, the average kinetic energy per each degree of freedom i (in $k_B = 1$ units) is equal to

$$\langle KE_i \rangle = \frac{1}{2}\, T_{classic} \equiv \frac{1}{2\beta_{classic}} \quad , \quad i = x, y, z \ . \tag{6}$$

Eq. (6) is a very general result, which we want to extend to the relativistic gas.

3.1 Relativistic equipartition

It is well-known [7] that for a relativistic gas, neither the relativistic kinetic energy, nor the total relativistic energy is equipartitioned. Therefore, we want to find a dynamical variable whose average per degree of freedom is related to β, and which can be consistently generalized to systems in motion.

Let us define [5, 14]

$$L_i = \frac{p_i^2}{2\sqrt{p^2 + m^2}} \ , \quad i = x, y, z \ . \tag{7}$$

Then, using Jüttner distribution (4), one can immediately show that for our two dimensional gas one obtains

$$\langle L_x \rangle = \langle L_y \rangle = \frac{1}{2\beta} \ . \tag{8}$$

This equation is the relativistic equivalent of Eq. (6). It can be used to define the temperature of the relativistic gas, and it should give the same numerical values as Eq. (5).

We have experimentally checked the validity of formula (8) for several reciprocal temperatures. The results are summarized in Table 1, where we have denoted $\beta_x = [2\langle L_x \rangle]^{-1}$ and $\beta_y = [2\langle L_y \rangle]^{-1}$. The control parameter is the reciprocal temperature β obtained via Eq. (5), and is recorded in the first column. Ideally, we would expect that $\beta = \beta_x = \beta_y$. Note that the numeric simulations show a good agreement with the theory.

β	β_x	β_y
199.49	198.94	200.11
49.45	49.63	49.33
21.63	21.87	21.42
7.25	7.34	7.18
2.00	1.99	2.03

Table 1: Relativistic equipartition for the ideal gas.

3.2 The relativistic transformation of temperature

The main idea is to use the equipartition theorem to gain intuition into the relativistic transformation of the temperature. To this end, we should find first an extension of Eq. (8) to moving systems. Then, based on the success with the systems at rest, we *define* the temperature of the moving system using the analog of Eq. (8). Finally, we will check numerically whether this newly defined temperature transforms according to Planck's formula, Ott formula, or obeys another transformation law.

Following reference [12], we rewrite L_i as $L_i = p_i\, v_i/2$, $i = x, y$. Then, the equipartition theorem (8) becomes

$$T \equiv 1/\beta = \langle p_x\, v_x \rangle = \langle p_y\, v_y \rangle \ . \tag{9}$$

In this form, we can readily construct a generalization of the equipartition theorem for moving systems. We say that an ideal gas system is in translation with the speed $\vec{u}$ with respect to the lab, if the average velocity of all its particles measured by a stationary observer in the lab is $\langle \vec{v} \rangle = \vec{u}$. Without loss of generality, we will consider the system moving along the x-axis. Then, for the moving system K', we can check that the quantities $L'_x = p'_x\,(v'_x - u)\,/\,2$ and $L'_y = p'_y v'_y\,/\,2$ are equipartitioned. For a detailed proof of this result, the reader should consult the reference [12].

Consequently, we *define* the temperature of the moving system K' via

$$1/\beta' \equiv T' = \langle p'_x\,(v'_x - u) \rangle = \langle p'_y\, v'_y \rangle \ . \tag{10}$$

Equation (10) is a good tool to identify which of the various relativistic transformation temperature formulas proposed in literature is consistent with this experiment. Planck's formalism gives $\beta'_{Planck} = \beta\,\gamma_u$, while Ott's formalism gives $\beta'_{Ott} = \beta/\gamma_u$, where $\gamma_u = (1 - u^2)^{-1/2}$ is the usual Lorentz factor.

Choosing the same rest reciprocal temperatures as before ($\beta = 49.46,\ 7.25$ and 2.00), we tested Eq. (10) for the boost speeds $u = 0.2,\ 0.4,\ 0.6$, and respectively 0.8. The results are presented in Figure 3. The

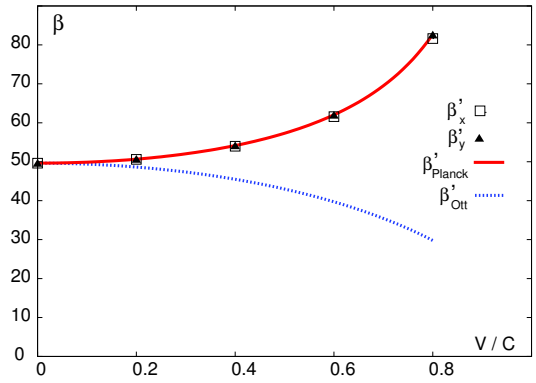

(a) The relativistic transformation of temperature for a relative low rest reciprocal temperature $\beta = 49.45$.

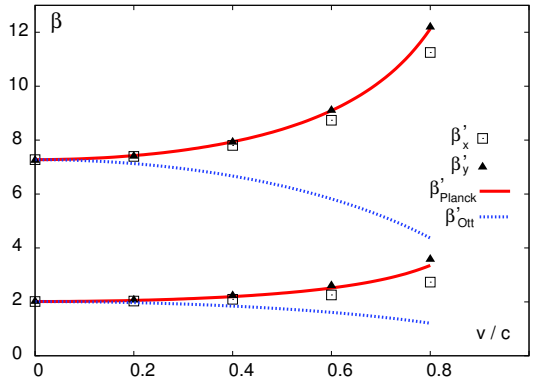

(b) The relativistic transformation of the temperature for relative medium ($\beta = 7.25$) and high ($\beta = 2.00$) rest reciprocal temperatures.

Figure 3: Note that for the boost speeds $u = 0.2,\ 0.4,\ 0.6$, and 0.8 the agreement between β'_x, β'_y and β'_{Planck} is remarkable. We observe that with the increase of the temperature, β'_x shifts slightly below the values of β'_y. In contrast, β'_{Ott} is clearly diverging from the experimental trend.

robustness of the numeric algorithm was checked by repeating the experiments with different form factors for the rectangular box.

4 Conclusions

In this paper we solved the non-trivial problem of relativistic two-dimensional molecular dynamics and showed that a relativistic ideal gas faithfully satisfies Jüttner's speed distribution function. Using as guidance the relativistic equipartition theorem, we have experimentally checked that the numeric simulations strongly favor the Mosengeil, Planck, and Einstein relativistic transformation formula. Thus, according to our simulations, moving objects should appear cooler.

Acknowledgements

I would like to thank Asim Gangopadhyaya, Ovidiu Lipan and Mircea Pigli for valuable comments and discussions.

References

[1] K. von Mosengeil, Ann. Physik, **327** 867 (1907).

[2] M. Planck, Sitzber. Preuss. Akad. Wiss. Berlin 542 (1907).

[3] A. Einstein, Jahrb. Rad. E. **4** 411 (1907).

[4] F. Jüttner, Ann. der Physik, **339** 856 (1911).

[5] R.C. Tolman, Phys. Rev. **11** 261 (1918).

[6] D. Blanuša, Glasnik Mat.DFiz. i Astr., Ser. II 2, 249 (1947).

[7] J. L. Synge, *The Relativistic Gas*, Interscience Publishers, Inc., New York, (1957).

[8] H. Ott, Zeit. für Physik **175** 70 (1963).

[9] P.T. Landsberg, Proc. Phys. Soc.**89** 1007 (1966).

[10] R. Balescu, Physica **40** 309 (1968).

[11] H. Arzelies, *Thermodynmique Relativiste et Quantique*, Gauthier-Villars Eds., Paris (1969).

[12] A. Guessous, *Thermodynamique Relativiste*, Gauthier-Villars Eds., Paris (1970).

[13] C. Liu, Einstein and Relativistic Thermodynamics, Brit. J. Hist. Sci. **25** 185 (1992).

[14] A. Komar, Gen. Rel. Grav. **28** 379 (1996).

[15] P.T. Landsberg and G.E.A. Matsas, Physica **A 340** 92 (2004).

On a thermodynamic theory for magnetic relaxation phenomena due to n microscopic phenomena described by n internal variables

Liliana Restuccia
Department of Mathematics
University of Messina, Contrada Papardo,
Salita Sperone 31, 98166 Messina, Italy
lrest@dipmat.unime.it

Abstract

This review article deals with a synthetic presentation of results derived in [1], where an approach for describing magnetic after-effects phenomena in continuous media was presented, in the framework of non-equilibrium thermodynamics [2]-[7].

In particular, a thermodynamic theory for magnetic relaxation phenomena was developed by the author and G.A.Kluitenberg in the joint work [1], assuming that an arbitrary number of microscopic phenomena occur which give rise to magnetic relaxation and that it is possible to describe the contributions of these microscopic phenomena to the macroscopic magnetization using n macroscopic vectorial internal variables of axial character $\mathbf{m}^{(i)}$ $(i = 1, ..., n)$ so that the total specific magnetization $\mathbf{m}$ can be split in n+1 parts

$$\mathbf{m} = \mathbf{m}^{(0)} + \mathbf{m}^{(1)} + ... + \mathbf{m}^{(n)}. \tag{1}$$

Introducing in the expression of the entropy these partial specific magnetizations, the phenomenomenological equations are derived in the anisotropic and isotropic cases.

Furthermore, using a suitable form for the specific free energy f to linearize the equations of state, provided the phenomenological coefficients may be regarded as constants, generalizations of Snoek equation for magnetic relaxation phenomena in the anisotropic and isotropic cases are obtained, if the internal variables are eliminated from the formalism, and these relations are used nowadays by theoretical mechanicians, applied physicists and electronic engineers to study magnetic after-effects in magnetizable complex media in many physical situations.

In the isotropic case this relaxation equation has the form of a linear relation among the magnetic field $\mathbf{B}$, the first n derivatives with respect to time of this field, the total magnetization vector $\mathbf{M}$ (being $\mathbf{M} = \rho\mathbf{m}$ with ρ the mass density) and the first n + 1 derivatives with respect to time of $\mathbf{M}$

$$\chi_{BM}^{(0)}\mathbf{B}+\chi_{BM}^{(1)}\frac{d\mathbf{B}}{dt}+...+\chi_{BM}^{(n-1)}\frac{d^{n-1}\mathbf{B}}{dt^{n-1}}+\frac{d^{n}\mathbf{B}}{dt^{n}}=$$

$$\chi_{MB}^{(0)}\mathbf{M}+\chi_{MB}^{(1)}\frac{d\mathbf{M}}{dt}+...+\chi_{MB}^{(n)}\frac{d^{n}\mathbf{M}}{dt^{n}}+\chi_{MB}^{(n+1)}\frac{d^{n+1}\mathbf{M}}{dt^{n+1}}, \tag{2}$$

where $\chi_{BM}^{(k)}$ $(k=0,1,...,n-1)$ and $\chi_{MB}^{(k)}$ $(k=0,1,...,n+1)$ are constant quantities, which are algebraic functions of the coefficients occurring in the phenomenological equations and in the equations of state, and n is the number of phenomena that give rise to the magnetization vector.

These results generalize some results derived by G.A.Kluitenberg in [8]-[10]. In particular, in [8] G.A. Kluitenberg developed a thermodynamic theory for some types of dielectric and magnetic relaxation phenomena, by assuming that a polar and an axial vector field occur as internal thermodynamic degrees of freedom and that these fields influence the polarization and magnetization, respectively. Snoek equation for magnetic after-effects and Debye theory for dielectric relaxation phenomena in polar fluids are obtained as special cases of this theory.

In [9], it was shown that if there is a "hidden" vectorial internal variable $\mathbf{Z}$, which influences the magnetization $\mathbf{M}$, this leads to the possibility to write the total magnetization in the form

$$\mathbf{M}\ =\mathbf{M}^{(0)}+\mathbf{M}^{(1)}, \tag{3}$$

where $\mathbf{M}^{(0)}$ is proportional to the magnetic field $\mathbf{B}$ and is called reversible part of $\mathbf{M}$, because there corresponds a sudden change in $\mathbf{M}^{(0)}$ to an instantaneous change in the magnetic field $\mathbf{B}$. $\mathbf{M}^{(1)}$ is a function of $\mathbf{Z}$ only and may replace $\mathbf{Z}$ as internal variable. It is connected with magnetic after-effects (i.e. $\mathbf{M}^{(1)}$ is the irreversible part of $\mathbf{M}$). $\mathbf{M}^{(1)}$ is a measurable quantity in contradistinction to an arbitrary "hidden" vectorial internal degree of freedom which is not measurable in general. Furthermore, it was shown that this theory (with $\mathbf{M}^{(1)}$ as internal variable) becomes formally completely analogous to the Snoek theory if the equations of state are linearized, and that in the isotropic case the following relation may be derived

$$\chi_{BM}^{(0)}\mathbf{B}+\frac{d\mathbf{B}}{dt}=\chi_{MB}^{(0)}\mathbf{M}+\chi_{MB}^{(1)}\frac{d\mathbf{M}}{dt}, \tag{4}$$

where $\chi_{BM}^{(0)}$, $\chi_{MB}^{(0)}$ and $\chi_{MB}^{(1)}$ are constants.

In [10] the theory developed in [8] and [9] is generalized and a different formulation is given by assuming that in principle all changes in the magnetization are irreversible phenomena so that both changes in $\mathbf{M}^{(0)}$ and $\mathbf{M}^{(1)}$ are irreversible processes (a change of the magnetization cannot be infinitely fast because it is connected with the motion of any kind of microscope particles) and in the linear approximation, eliminating the internal degree of freedom from the formalism, for isotropic media the following relaxation equation is obtained

$$\chi_{BM}^{(0)}\mathbf{B}+\frac{d\mathbf{B}}{dt}=\chi_{MB}^{(0)}\mathbf{M}+\chi_{MB}^{(1)}\frac{d\mathbf{M}}{dt}+...+\chi_{MB}^{(2)}\frac{d^{2}\mathbf{M}}{dt^{2}}, \tag{5}$$

where $\chi^{(0)}_{BM}$ and $\chi^{(k)}_{MB}$ $(k = 0, 1, 2)$ are constant quantities.

Equation (2) is a generalization of Snoek equation for magnetic relaxation phenomena.

Furthermore, we notice that this magnetic relaxation equation has the same mathematical structure of a stress-strain relation for mechanical distorsional phenomena in isotropic media (a generalization of Burgers equation), derived in 1968 by G. A. Kluitenberg in [11], where a thermodynamic theory for mechanical phenomena in continuous media was developed using analogous procedures, in the frame of non-equilibrium thermodynamics [2]-[7]. Assuming that n microscopic phenomena give rise to inelastic strains (for instance, slip, dislocations, etc.) and that the total inelastic deformation is additively composed of contributions of these inelastic strains, introducing these inelastic strains as internal variables in the Gibbs relation, the following relation is obtained

$$R^{(\tau)}_{(d)0}\tilde{\tau}_{\alpha\beta} + R^{(\tau)}_{(d)1}\frac{d\tilde{\tau}_{\alpha\beta}}{dt} + ... + R^{(\tau)}_{(d)n-1}\frac{d^{n-1}\tilde{\tau}_{\alpha\beta}}{dt^{n-1}} + \frac{d^{n}\tilde{\tau}_{\alpha\beta}}{dt^{n}} =$$

$$R^{(\epsilon)}_{(d)0}\tilde{\epsilon}_{\alpha\beta} + R^{(\epsilon)}_{(d)1}\frac{d\tilde{\epsilon}_{\alpha\beta}}{dt} + ... + R^{(\epsilon)}_{(d)n}\frac{d^{n}\tilde{\epsilon}_{\alpha\beta}}{dt^{n}} + R^{(\epsilon)}_{(d)n+1}\frac{d^{n+1}\tilde{\epsilon}_{\alpha\beta}}{dt^{n+1}}, \qquad (6)$$

where $R^{(\tau)}_{(d)m}$ $(m = 0, 1, ..., n-1)$ and $R^{(\epsilon)}_{(d)m}$ $(m = 0, 1, ..., n+1)$ are constant quantities, which are algebraic functions of the coefficients occurring in the phenomenological equations and in the equations of state, and n is the number of phenomena that give rise to inelastic strains, $\tilde{\tau}_{\alpha\beta}$ is the deviator of the mechanical stress tensor and $\tilde{\epsilon}_{\alpha\beta}$ is the deviator of the tensor of total strain.

The stress -strain relations for ordinary viscous fluids, for thermoelastic media, and for Burgers, Maxwell, Kelvin, Jeffreys and Poynting- Thomson media are special cases of the more general relation mentioned above

Also, we notice that equation (2) has the same mathematical structure of a dielectric relaxation equation, obtained by the author and G. A. Kluitenberg in 1988 in [12], where a thermodynamic theory for dielectric relaxation phenomena was developed, assuming that n arbitrary microscopic phenomena give rise to the total polarization vector and that it is possible to describe the contributions of these microscopic phenomena introducing n partial polarization vectors as n macroscopic vectorial internal variables in the expression of the entropy.

This dielectric relaxation equation is a generalization of Debye equation and it has the following form in the isotropic case

$$\chi^{(0)}_{EP}\mathbf{E} + \chi^{(1)}_{EP}\frac{d\mathbf{E}}{dt} + ... + \chi^{(n-1)}_{EP}\frac{d^{n-1}\mathbf{E}}{dt^{n-1}} + \frac{d^{n}\mathbf{E}}{dt^{n}} =$$

$$\chi^{(0)}_{PE}\mathbf{P} + \chi^{(1)}_{PE}\frac{d\mathbf{P}}{dt} + ... + \chi^{(n)}_{PE}\frac{d^{n}\mathbf{P}}{dt^{n}} + \chi^{(n+1)}_{PE}\frac{d^{n+1}\mathbf{P}}{dt^{n+1}}, \qquad (7)$$

where $\mathbf{E}$ and $\mathbf{P}$ are the electric strength field and the polarization vector, respectively, $\chi^{(k)}_{EP}(k = 0, 1, ..., n-1)$ and $\chi^{(k)}_{PE}(k = 0, 1, ..., n+1)$ are constant quantities, algebraic functions of the coefficients occurring in the phenomenological equations and in the equations of state, and n is the number of phenomena that give rise to the total polarization vector.

We hope that such a synthetic approach to the magnetic relaxation phenomena in continuous media contributes to a better understanding of the links, correlations and differences that exist beteween the various theories at our disposal in a subject matter in full development.

References

[1] L. Restuccia, G.A. Kluitenberg, On generalizations of the Snoek equation for magnetic relaxation phenomena, Atti Accademia Peloritana dei Pericolanti , LXVII (1989), 141-194.

[2] I. Prigogine, Etude Thermodynamique des Phénomènes Irréversibles (Dunod, Paris et Editions Desoer, Liège, 1947).

[3] S.R. De Groot, Thermodynamics of Irreversible Processes (North-Holland Publishing Company, Amsterdam and Interscience Publishers Inc., New York, 1951).

[4] J. Meixner and H. G. Reik, Thermodynamik der Irreversiblen Prozesse, Handbuch der Physik, Band III/2 (Springer, Berlin 1959)

[5] I. Prigogine, Introduction to Thermodynamics of Irreversible Processes (Interscience Publishers-John Wiley & Sons, New York-London, 1961).

[6] S.R. De Groot, P.Mazur, Non-equilibrium Thermodynamics (North-Holland Publishing Company, Amsterdam, 1962).

[7] G.A. Kluitenberg, Plasticity and Non-equilibrium Thermodynamics, CISM Lecture Notes (Springer, Wien, New York, 1984)

[8] G.A. Kluitenberg, On dielectric and magnetic relaxation phenomena and non-equilibrium thermodynamics, Physica, 68 (1973), 75-92.

[9] G.A. Kluitenberg, On dielectric and magnetic relaxation phenomena and vectorial internal degrees of freedom in thermodynamics, Physica A 87 (1977), 302-330.

[10] G.A. Kluitenberg, On vectorial internal variables and dielectric and magnetic relaxation phenomena, Physica A 109 (1981), 91-122.

[11] G.A. Kluitenberg, A thermodynamic derivation of the stress-strain relations for Burgers media and related substances, Physica 38 (1968), 513-548.

[12] L.Restuccia and G.A.Kluitenberg, On generalizations of the Debye equation for dielectric relaxation, Physica A 154 (1988), 157-182.

BRINGING THERMODYNAMICS TO NON-EQUILIBRIUM MICROSCOPIC PROCESSES

J. M. Rubi
Departament de Fisica Fonamental,
Facultat de Física, Universitat de Barcelona
Diagonal 647, 08028 Barcelona, Spain
E-mail: mrubi@ub.edu

Concepts of everyday use like energy, heat, and temperature have acquired a precise meaning after the development of thermodynamics. Thermodynamics provides the basis for understanding how heat and work are related and with the general rules that the macroscopic properties of systems at equilibrium follow. Outside equilibrium and away from macroscopic regimes most of those rules cannot be applied directly. We present recent developments that extend the applicability of thermodynamic concepts deep into small-scale and irreversible regimes. We show how the probabilistic interpretation of thermodynamics together with probability conservation laws can be used to obtain kinetic equations for the relevant degrees of freedom. This approach provides a systematic method to obtain the stochastic dynamics of a system directly from its equilibrium properties. A wide variety of situations can be studied in this way, including many that were thought to be out of reach of thermodynamic theories, such as non-linear transport in the presence of potential barriers, activated processes, slow relaxation phenomena, and basic processes in biomolecules, like translocation and stretching.

REFERENCES

1. Vilar, J.M.G.; Rubi, J.M. Proc. Nat. Acad. Sci. **2001**, 98, 11081.
2. Reguera, D.; Rubi, J.M.; Vilar J.M.G. J. Phys. Chem. B **2005**, 109, 21502; (feature article).
3. Rubi, J.M.; Scientific American, November, **2008**, 40-45.

Identification of an average temperature and a dynamical pressure in a multi-temperature mixture of fluids

Tommaso Ruggeri
Department of Mathematics and
Research Center of Applied Mathematics - (C.I.R.A.M.) -
University of Bologna, Via Saragozza 8, 40123 Bologna, Italy.
e-mail: ruggeri@ciram.unibo.it

We first present the different models of a mixture of compressible fluids and we discuss in the case of Euler fluids the local and global well-posedness of the relative Cauchy problem for smooth solutions. Then we present a classical approach of mixture of compressible fluids when each constituent has its own temperature. The introduction of an *average temperature* together with the entropy principle dictates the classical Fick law for diffusion and also new constitutive equations associated with the difference of temperatures between the components. The constitutive equations fit with results obtained through the *Maxwellian iteration* procedure in extended thermodynamics theory of multi-temperature mixtures. The differences of temperatures between the constituents imply the existence of a new *dynamical pressure* even if the fluids have a zero bulk viscosity. The non-equilibrium dynamical pressure can be measured and may be convenient in several physical situations as for example in cosmological circumstances where - as many authors assert - a dynamical pressure played a major role in the evolution of the early universe.

References

[1] T. Ruggeri, S. Simić, *On the Hyperbolic System of a Mixture of Eulerian Fluids: A comparison between single and multi - temperature models*. Math. Meth. Appl. Sci., **30**, 827, (2007).

[2] H. Gouin, T. Ruggeri, *Identification of an average temperature and a dynamical pressure in a multi-temperature mixture of fluids*. Phys. Rev. E **78**, 016303, (2008).

[3] I. Müller, T. Ruggeri, *Rational Extended Thermodynamics*, Springer Tracts in Natual Philosophy **37**, 2nd Ed., Springer Verlag (1998)

A mesoscopic entropy production analysis of the transition to the irreversibility in sheared suspensions

I. Santamaría-Holek[1], G. Barrios[1], J. M. Rubi[2]
[1] Facultad de Ciencias, Universidad Nacional Autónoma de México. Circuito exterior de Ciudad Universitaria. 04510, D. F., México.
[2] Facultat de Física, Universitat de Barcelona, Av. Diagonal 647, 08028, Barcelona, Spain

e-mail: isholek.fc@gmail.com

Abstract

We study the shear-induced diffusion effect and the transition to irreversibility in suspensions under oscillatory shear flow by performing an analysis of the mesoscopic entropy production associated with the motion of the particles. We show that the Onsager coupling between different contributions to the entropy production is responsible for the scaling of the mean square displacement on particle diameter and applied strain. We also show that the shear-induced effective diffusion coefficient depends on the volume fraction, and use lattice-Boltzmann simulations to characterize the effect through the power spectrum of particle positions for different Reynolds numbers and volume fractions. Our study gives a thermodynamic explanation of the transition to irreversibility through a pertinent analysis of the second law of thermodynamics.

1. Introduction

To understand how the behavior of many-particle systems may become irreversible upon the action of an external driving force is one of the fundamental problems of thermodynamics and statistical physics since their foundation [1]. An analysis based on the second law of thermodynamics reveals that this transition can be explained within the framework of non-equilibrium thermodynamics [2].

The transition from a reversible (oscillatory) to an irreversible (chaotic) behavior of massive (non-Brownian) particles subjected to an oscillatory shear in a Taylor-Couette cell [3, 4] is described from the mesoscopic entropy production rate of the particles, derived from the second law, and the Onsager relations connecting the diffusion current to the driving force, the shear flow [2, 5]. This mesoscopic entropy analysis leads to the formulation of a Fokker-Planck equation for the N-particle distribution function describing the dynamics of the suspended phase, and from which the dynamical description of the system is performed [2].

The observed chaotic behavior of the trajectories of the particles, whose origin is the presence of hydrodynamic interactions, can be interpreted macroscopically as a shear-induced diffusion effect in which the diffusion coefficient D_{eff} scales according to the relation [2, 3, 6]

$$D_{eff} \simeq d^2\dot{\gamma}, \tag{1}$$

where d is the diameter of the suspended particle and $\dot{\gamma}$ is the shear rate.

We have analyzed this diffusion process by means of the mentioned Fokker-Planck and computed the corresponding effective diffusion coefficient after performing a contraction of the description [2, 5, 7, 8]. Our analysis explains the behavior of the mean square displacement $\langle r^2\rangle_{exp}(t)$ observed in the experiments when the applied shear is small [3]

$$\langle x^2\rangle_{exp}(t) \sim D_{eff}t. \tag{2}$$

Our theoretical analysis, complemented with Lattice Boltzmann simulations [9], shows that the irreversibility inherent to the chaotic behavior of the macroscopic motions of particles is perfectly compatible with the second law of thermodynamics.

2. The mesoscopic entropy production and the shear induced diffusion

We consider a suspension of N non-interacting spherical particles of radius a and mass m in a fluid which moves with velocity $\vec{v}^{\,0}(\vec{r},t)$. Since the system is in contact with a heat bath that evolves in time, we will determine the

physical nature of the coupling forces by taking into account two factors. The first one is that the evolution of the system can be described at mesoscopic level by means of the normalized N-particle probability distribution function $P^{(N)}(\Gamma^N, t)$, that depends on the instantaneous positions $\{\vec{r}\}^N \equiv (\vec{r}_1, ..., \vec{r}_N)$ of the particles and their velocities $\{\vec{u}\}^N \equiv (\vec{u}_1, ..., \vec{u}_N)$ through the phase space vector $\Gamma^N = (\{\vec{r}\}^N, \{\vec{u}\}^N)$. The second factor is that the interactions between the system and the heat bath, involving dissipation, suggest the use of the nonequilibrium entropy $s(t)$ as a thermodynamic potential from which the entropy production $\sigma(t)$ can be calculated, and used to obtain the explicit expressions for the mentioned coupling forces [10].

Using probability conservation and the generalized Gibbs entropy postulate,

$$\delta s(t) = -k_B \int \sum_{i=1}^{N} P^{(N)} \ln \frac{P^{(N)}}{P^{(N)}_{l.eq.}} \delta(\vec{r}_i - \vec{r}) d\Gamma^N, \tag{3}$$

where δs is the entropy change with respect to a local equilibrium reference state characterized by the local equilibrium distribution function

$$P^{(N)}_{l.eq.} = e^{\frac{m}{k_B T}\left[\mu_B - \sum_{i=1}^{N} \frac{1}{2}(\vec{u}_i - \vec{v}_i^{\,0})^2\right]}. \tag{4}$$

and where μ_B is the local equilibrium chemical potential per mass unit and $\vec{v}_i^{\,0} = \vec{v}^{\,0}(\vec{r}_i, t)$, after calculating the entropy production, identifying the different contributions and coupling currents and forces using linear relationships, one obtains the multivariate Fokker-Planck equation describing the evolution of the N-particle distribution function

$$\frac{\partial P^{(N)}}{\partial t} + \sum_{i=1}^{N} \nabla_{\vec{r}_i} \cdot (\vec{u}_i P^{(N)}) = \sum_{i,j=1}^{N} \frac{\partial}{\partial \vec{u}_i} \cdot \left\{ \left[(\vec{u}_j - \vec{v}_j^{\,0}) \cdot \vec{\vec{\beta}}_{ij} - \vec{\vec{\zeta}}_{ij} \cdot \vec{F}_j \right] P^{(N)} + \frac{k_B T}{m} \vec{\vec{\alpha}}_{ij} \cdot \frac{\partial P^{(N)}}{\partial \vec{u}_j} \right\}, \tag{5}$$

where $\vec{\vec{\alpha}}_{ij} = \vec{\vec{\beta}}_{ij} - \vec{\vec{\epsilon}}_{ij} \cdot \nabla_{\vec{r}_j} \vec{v}_j^{\,0}$ and the tensors $\vec{\vec{\zeta}}$, $\vec{\vec{\epsilon}}$ and $\vec{\vec{\beta}}$ are related to the Onsager coefficients. This full N-particle description can be reduced to the single-particle description by contracting it over N-1 particles and by assuming an effective medium theory [11]. This contraction leads to the effective Smoluchowski equation

$$\frac{\partial \rho}{\partial t} = -\nabla \cdot \left[\rho \vec{v}_0 - \rho \beta_0^{-1} \left(\vec{\vec{1}} + \vec{\vec{\mu}} \right) \cdot \vec{f} - \rho \zeta \beta_0^{-1} \left(\vec{\vec{1}} + \vec{\vec{\mu}} \right) \cdot \vec{F} \right] + \nabla \cdot \left(\vec{\vec{D}} \cdot \nabla \rho \right), \tag{6}$$

where we have found the effective diffusion tensor

$$\vec{\vec{D}}(\vec{r}, t) = k_B T/m \vec{\vec{\mu}} + \frac{a^2}{6} (1 + 2a\,\alpha) \left[\left(\vec{\vec{1}} + \vec{\vec{\mu}} \right) \cdot (\vec{\vec{E}} - \vec{\vec{1}}) \cdot \nabla \vec{v}^0 \right]^s. \tag{7}$$

In Eqs. (6) and (7), the force $\vec{f}$ is due to hydrodynamic interactions as $\vec{f} = -(k_B T/m) \nabla \cdot \vec{\vec{A}}$ and the mobility tensor $\vec{\vec{\mu}} = \vec{\vec{B}}^{-1} - \beta_0^{-1} \vec{\vec{1}}$ is defined through the average of the hydrodynamic interactions over the structure of the system

$$\vec{\vec{B}}(\vec{r}, t; \phi) = \beta_0^{-1} \int \vec{\vec{\beta}}(\vec{r}') \cdot \vec{\vec{\beta}}(\vec{r}') g(\vec{r} - \vec{r}', t; \phi, T) d\vec{r}. \tag{8}$$

The tensor $E(\phi)$ is also defined in terms of an average over the structure of the system. The dependence of these tensors on the volume fraction ϕ is due to the fact that the two-particle correlation function g may in general depend on the volume fraction and the temperature, [12].

From the Smoluchowski equation one may compute $\langle r^2 \rangle_{exp}(t)$ which, for low oscillation frequencies and low shear amplitudes in the limit of non-Brownian particles, that is when $k_T/m \to 0$, gives

$$\langle r^2 \rangle \sim \frac{1}{6} \tilde{\mu}_{xy}(\phi) [E(\phi) - 1] d^2 \dot{\gamma} t. \tag{9}$$

Thus, the theoretical effective diffusion equation $D_{eff} = \frac{1}{6} \tilde{\mu}_{xy}(\phi) [E(\phi) - 1] d^2 \dot{\gamma}$ has the same scaling as the experimental one and implies that it is dependent on the volume fraction due to the hydrodynamic interactions between particles.

The analysis of the behavior of the system can be complemented by performing Lattice Boltzmann simulations [2, 9]. These simulations confirm the linear dependence of the shear induced diffusion coefficient on the Reynolds number of the particles and allows to characterize in more detail the transition between deterministic oscillating dynamics of the particles in terms of the power spectrum of particle trajectories, as it is shown in Figures 1 and 2.

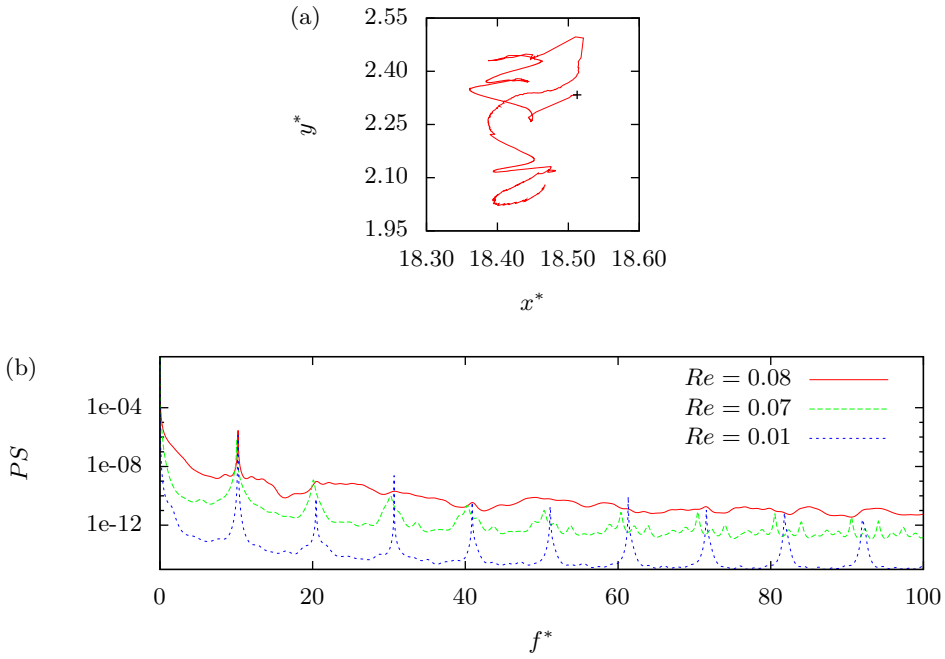

FIG. 1: (a) Trajectory and (b) power spectrum of the $x-$displacements of one particle for different Reynolds numbers when $\phi = 0.14$ and the oscillating frequency is $f^* = 10.0$. The power spectrum of the $y-$displacements displays a similar behaviour.

3. Conclusions

The transition from a reversible (oscillating) to and irreversible (chaotic) dynamics observed in the macroscopic motions of a suspension of non-Brownian particles under oscillating shear flows is fully compatible with the second law of thermodynamics. The analysis of the mesoscopic entropy production shows that it is due to an Onsager coupling mediated by hydrodynamic interactions, and that it depends on the volume fraction, in accordance with experiments and simulations.

3. Acknowledgments

We acknowledge financial support by DGAPA-UNAM under the grant No. IN102609.

[1] I. Prigogine, *Les lois du chaos* (Flammarion, Paris, 1993).
[2] I. Santamaría-Holek, G. Barrios and J. M. Rubi, Phys. Rev. E **79**, 031201 (2009).
[3] D. J. Pine, J. P. Gollub, J. F. Brady, A. M. Leshansky, Nature **438**, 997 (2005).
[4] D. Drazer, J. Koplik, B. Khusid, A. Acrivos, J. Fluid Mech. **460**, 307 (2002).
[5] D. Reguera, J. M. G. Vilar, J. M. Rubi, J. Phys. Chem. B **109**, 21502 (2005).
[6] A. Seriou, J. F. Brady, J. Fluid Mech. **506** 285 (2004).
[7] I. Santamaría-Holek, D. Reguera and J. M. Rubi, Phys. Rev. E **63**, 051106 (2001).
[8] I. Santamaría-Holek, J. M. Rubi, A. Pérez-Madrid, New J. Phys **7**, 35 (2005).
[9] A. J. C. Ladd, J. Fluid Mech. **271**, 285 (1994); A. J. C. Ladd, J. Fluid Mech. **271**, 311 (1994).
[10] S. R. de Groot, P. Mazur, *Non-equilibrium Thermodynamics* , (Dover, New York, 1984).
[11] K. F. Freed and M. Muthukumar, J. Chem. Phys. **69**, 2657 (1978).
[12] T. L. Hill, *An introduction to Statistical Thermodynamics* (Dover, New York, 1986).

Finite time thermodynamics and the liquid-gas transition

M. Santoro, J. C. Schön, M. Jansen
Max-Planck-Institute for Solid State Research, D-70569 Stuttgart, Germany
e-mail: C.Schoen@fkf.mpg.de

Finite time thermodynamics concepts are usually applied to the optimization of processes in systems, where the underlying working medium changes only continuously. In particular, the most powerful applications are of the horse-carrot type, where the optimal control of the process is achieved by establishing a small and essentially constant thermodynamic distance between the control and the system.

If the process involves a first-order phase transition, however, the thermodynamic metric exhibits a singularity, and it becomes necessary to set up and solve the full optimal control problem which is dominated by the dissipative effects due to the transition. As an example, we investigate the transition from the gaseous to the liquid state by modeling the liquification of the gas in a finite time.[1] We introduce and solve the optimal control problem in which we aim to achieve the gas-liquid first-order phase transition through supersaturation within a fixed time in an optimal fashion, in the sense that the work required to supersaturate the gas, called excess work, is minimized by controlling the appropriate thermodynamic parameters. The resulting set of coupled non-linear differential equations is solved for three systems, nitrogen, oxygen and water.

Literature:

1. M. Santoro, J. C. Schön, M. Jansen: Physical Review E, **76**, (2007), 061120-1-14

Phase Layering in Binary Liquid Mixtures in Temperature Gradients

Semen N. Semenov[1] and Martin E. Schimpf[2]
[1]*Institute of Biochemical Physics RAS, 117977 Moscow, Kosygin Street 4, Russia, sem@triniti.ru*
[2]*Department of Chemistry, Boise State University, Boise ID 83725, USA*

Abstract
The two-phase and critical behavior in non-isothermal binary liquid mixtures is examined. The approach developed earlier is used to calculate the necessary dynamic parameters. The stationary concentration distribution in the temperature gradient is calculated. At certain critical temperature and below, the resulting expression predicts a critical behavior and the layering of liquid phases in the mixture. At the critical temperature, the inflection point appears at the concentration distribution at the respective coordinate point. With decrease of temperature, this inflection is transformed into a jump in the concentration, which corresponds to the thermodynamically equilibrium concentrations of the components at the temperature established at this point. If the temperature gradient exceeds a certain critical value, the stepwise concentration distribution is predicted. It allows binodal-like and spinodal-like behavior in non-isothermal systems to be considered.

Introduction

The aim of this article is the analysis of critical and two-phase behavior in binary liquid systems placed in a temperature gradient using the mass transport equations obtained previously. When a liquid mixture is placed in a temperature gradient, there is movement of the components, generating a concentration gradient, what is known as thermodiffusion or the Ludwig-Soret effect. Experimental and theoretical results on thermodiffusion can be found in Ref. [1].

As the thermodiffusion experiments are based on the data on the temperature-induced concentration distribution, equations describing the mass transport are necessary. In our previous paper (Ref. [2]) the equations of the mass transport in thermodiffusion were obtained. This approach uses the standard form of the mass conservation equations for the components

$$\partial \phi_i / \partial t = -\nabla \vec{J}_i \tag{1}$$

where ϕ_i is the volume fraction of the ith component, $\vec{J}_i$ is its mass flux, and t is time. The dynamic parameters (mass diffusion, cross-diffusion and thermodiffusion coefficients) are calculated by the hydrodynamic approach suggested in Ref. [3]. About the same results can be obtained by the thermodynamic approach.

This hydrodynamic approach considers the flow of liquid around the particle caused by a local pressure gradient, as defined by the Navier-Stokes equation

$$\eta \Delta \vec{u} = -\nabla \Pi_{loc} + \vec{f}_{loc} \tag{2}$$

where $\vec{u}$ is the velocity of the liquid, Π_{loc} is the local pressure distribution around the particle, η is the dynamic viscosity of the liquid, and $\vec{f}_{loc}$ is the local volume force in the surrounding liquid.

Modifying the approach used in the theory of particle diffusiophoresis [4], we showed [3] that the local pressure distribution can be obtained from the condition of hydrostatic equilibrium in the uniform liquid taken together with condition of the local equilibrium in temperature gradients. These conditions give the local pressure gradient in a liquid around the molecule of ith kind

$$\nabla \Pi^i_{loc} = \frac{\Phi_{ij}}{\nu_j} \sum_{j=1}^{N} \alpha_j \phi_j \nabla T - \nabla \phi_j \tag{3}$$

where α_j is the cubic thermal expansion coefficient of the liquid of molecules of type *j*, ϕ_j is the volume fraction of these molecules, v_j is the specific molecular volume for the molecule of the j^{th} kind, and Φ_{ij} is the interaction potential between molecules of the i^{th} and j^{th} kind.

For liquids with low electrical conductivity

$$\Phi_{ij}(r) = -16\sqrt{A_i A_j}\left(r_i r_j\right)^3 \Big/ 9r^6 \tag{4}$$

where A_i and A_j are the respective Hamaker constants, r is the radial coordinate for a spherical molecule, and r_i and r_j are the molecular radii. In the hydrodynamic approach, we have the following expressions for the partial cross-diffusion coefficient and the partial thermodiffusion coefficient defined as the velocity of a selected particle of the i^{th} kind per unit concentration gradient of the j^{th} component and per the unit temperature gradient, respectively:

$$b_{Dij} = 8r_{iH}^2\sqrt{A_i A_j}\Big/ 27\eta v_j \tag{5};$$

$$b_{Tij} = -\alpha_j b_{Dij} \tag{6}$$

where r_{iH} is the hydrodynamic radius of the particle.

Substituting the drift flux of the considered component into respective Eq. (1), we obtain the mass transport equations. In a system, where a temperature and/or concentration gradient exist, a macroscopic pressure gradient should be established to keep the hydrostatic equilibrium in the system. The respective barophoretic mass fluxes also are included in the mass transport equations. In general case, the macroscopic pressure gradient is derived from the mass transport equations. For the closed steady-state systems it can be described by the Gibbs-Duhem equation (Ref. [5]).

In a temperature gradient, the mass transport equation for the components can be written as

$$\frac{\partial\phi}{\partial t} = \nabla\left\{\frac{D_2}{1-\phi+\Delta\phi}\left\{\left[1-\phi+\frac{v_2}{v_1}\phi-\frac{v_2}{v_1}\sigma(\delta-1)(1-\phi)\phi\right]\nabla\phi-\sigma\left(\frac{v_2}{v_1}-\delta_H\right)(1-\phi)\phi\left[\alpha_1(1-\phi)+\delta\alpha_2\phi\right]\nabla T\right\}\right\} \tag{7}$$

where $\phi_2 = \phi$ and $\phi_1 = 1-\phi$ are the volume fractions of the respective components, D_1, D_2 are their diffusion coefficients, $\overline{v}_1$, $\overline{v}_2$ are the partial volumes of the components, which are about the same as their specific molecular volumes v_1, v_2, $v_{1,2H} = 4\pi r_{1,2H}^3/3$, $\sigma = b_{D11}/D_1 = 4v_{1H}A_1/3v_1kT$, $\delta = v_1\sqrt{A_2}/v_2\sqrt{A_1}$, $\delta_H = v_{1H}\sqrt{A_2}/v_{2H}\sqrt{A_1}$, and $\Delta = v_2 D_2/v_1 D_1$ is the parameter related to the dynamic pressure gradient established in the non-stationary system. In Eq. (7), the parameter σ characterizes the value of the intermolecular interaction in one component, and the parameter δ characterizes the ratio in the intermolecular interactions between the components.

Results and Discussion

The term

$$D_{eff} = \frac{D_2}{1-\phi+\Delta\phi}\left[1-\phi+\frac{v_2}{v_1}\phi-\frac{v_2}{v_1}\sigma(\delta-1)(1-\phi)\phi\right] \tag{8}$$

in Eq. (7) is the effective diffusion coefficient. In stable systems, $D_{eff} > 0$ (Ref. [5]). However, at $\delta > 1$, the diffusion coefficient becomes zero at the point x_c, where

$$\phi_c = \left(1+\sqrt{v_2/v_1}\right)^{-1} \tag{9};$$

$$T_c = 4v_{1H}(\delta-1)A_1/3v_1k\phi_c^2 \tag{10}$$

At $T < T_c$, there is the two-phase domain described by the equilibrium curve

$$T(x)/T_c = \phi(x)\left[1-\phi(x)\right]\Big/\left[(1-2\phi_c)\phi(x)+\phi_c^2\right] \tag{11}$$

which separates stable equilibrium concentrations $\phi \le \phi_{e1}(T), \phi \ge \phi_{e2}(T)$ from unstable region where $D_{eff} < 0$ *T*. The equilibrium concentrations are obtained from Eq. (11). Note, that in the non-isothermal system, the equilibrium concentration and temperature are the function spatial distribution of the temperature.

Near the critical point, the stationary mass transport equation [Eq. (7)] can be written as

$$\left(\phi-\phi_c\right)^2\nabla\phi=\left(1-\phi_c\right)\phi_c\left[\alpha_1\left(1-\phi_c\right)+\delta\alpha_2\phi_c\right]\varepsilon\nabla T \tag{12}$$

where $\varepsilon=\left[\delta\left(\nu_{2H}/\nu_{1H}\right)-1\right]/\left(\delta-1\right)$. The solution of Eq. (12) is

$$\phi(x)=\phi_c+\sqrt[3]{3\left(1-\phi_c\right)\phi_c\left[\alpha_1\left(1-\phi_c\right)+\delta\alpha_2\phi_c\right]\varepsilon\left[T_c-T\left(x\right)\right]} \tag{13}$$

The concentration distribution described by Eq. (13) is the continuous function and it has the inflection point at the position x_c, where $\phi=\phi_c$ and $T=T_c$. See Fig.1 (a).

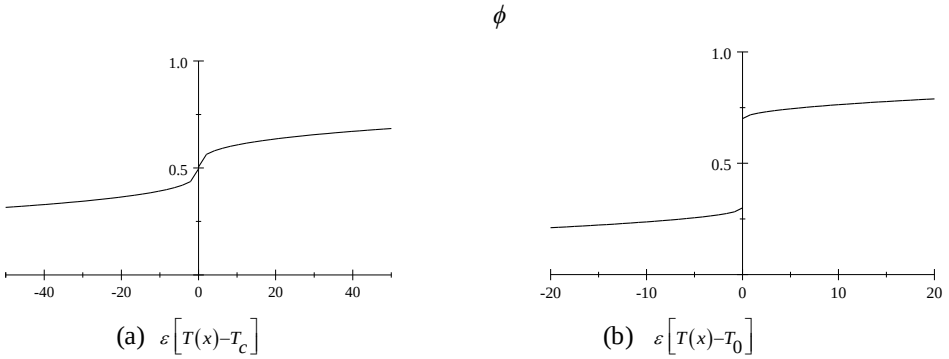

Fig. 1. *A typical concentration distribution in binary mixture* **(a)** *around the critical point and* **(b)** *in the two-phase domain*

The typical critical concentration distribution is shown in Fig. 1a. The condition of the mass conservation

$$\int_0^L\phi\left(x\right)dx=\bar{\phi}L \tag{14}$$

imposes some limitations on the concentration range, where critical concentration distribution with the inflection point can be established. Here, $\bar{\phi}$ is the mean volume fraction of the second component in the uniform mixture, and *L* is the dimension of the measurement cell. According to evaluations, the maximal deviation in the initial mean volume fraction from the critical volume fraction $\phi_c\approx1/2$ is about several percent.

This situation possesses the characteristic "critical" features. It is realized only at the unique temperature and the concentration, and within narrow range of the initial uniform concentrations.

When temperatures in the system are decreased below the critical point, the effective diffusion coefficient D_{eff} [Eq. (8)] becomes negative for two volume fractions ϕ_{e1},ϕ_{e2}, which are the equilibrium concentrations in the two-phase system at the temperature corresponding to some point x_0 [see Fig. 1(b)].

In this two-phase system, the stationary Eq. (9) can be written in two different forms:

$$\left(\phi_{e1}-\phi\right)\frac{\partial\phi}{\partial x}=\alpha_1\phi_{e1}\varepsilon\nabla T,\quad \text{at } \phi\approx\phi_{e1} \tag{15a}$$

$$\left(\phi-\phi_{e2}\right)\frac{\partial\phi}{\partial x}=\delta\alpha_2\varepsilon\nabla T,\quad \text{at } \phi\approx\phi_{e2} \tag{15b}$$

The solution of Eqs. (17a, b) is:

$$\phi_-\left(x\right)=\phi_{e1}-\sqrt{2\alpha_{T1}\phi_{e1}\varepsilon\left[T\left(x\right)-T_0\right]} \tag{16a}$$

$$\phi_+\left(x\right)=\phi_{e2}+\sqrt{2\alpha_{T2}\left(1-\phi_{e2}\right)\varepsilon\left[T_0-T\left(x\right)\right]} \tag{16b}$$

The designations $\phi_-\left(x\right)$ and $\phi_+\left(x\right)$ are used for the domains with the lower and higher concentration, respectively.The position of the point x_0 and temperature $T_0\left(x_0\right)$ can be found by the condition of the mass conservation

$$\int_0^{x_0}\phi_-\left(x\right)dx+\int_{x_0}^L\phi_-\left(x\right)dx=\bar{\phi}L \tag{17}$$

For systems, which are far from the critical point, Eq. (17) takes the form

$$\frac{x_0}{L} = \frac{1 - \phi_c^2 \nu_2 T_0(x_0)/\nu_1 T_c - \bar{\phi}}{1 - (1 + \nu_2/\nu_1)\phi_c^2 T_0(x_0)/T_c} \tag{18}$$

In the raise of the mean volume fraction $\bar{\phi}$ from ϕ_{e1} to ϕ_{e2}, the position x_0 changes gradually from L to zero, respectively, and the layers of different thickness may be obtained.

In two-phase domain, the position x_0 of the concentration jump corresponding to the phase boundary may be controlled in a wide range. It may be done by the gradual change in the mean uniform concentration $\bar{\phi}$ and by the scanning the temperature profile in the cell, while maintaining the same temperature drop between the walls.

Binodal- and spinodal-like behavior

When the temperature gradient is too high, the solutions expressed by Eqs. (13, 16) cannot hold the place along the whole system. In some point in the space, the slowly changed curve of the concentration distribution (13) or (16) should have the intersection with the curve of the spatial distribution of the equilibrium concentration [Eq. (11)] changed faster. At this point, we will have again the situation similar to the point x_0 considered above, but at a lower temperature. Near this point, the concentration distribution should have the shape similar to one of the branches described by Eqs. (16). in this way, we will have a step of the concentration. This step, in turn, will have the own intersection with the equilibrium curve (11). The number of these steps will depend on the system parameters and can be calculated. These calculations show that this stepwise concentration distribution can begin from both critical point, if it is present, and from the point of the temperature jump. The relations between the number and the height of the concentration steps and the physical parameters of the system are obtained. These features of the concentration distribution allow the behavior of the non-isothermal system to be considered in terms of the binodal (smooth) and spinodal (stepwise) layering. This analogy is discussed, as well as the thermodynamic stability of the obtained concentration distributions.

Conclusions

The critical behavior and phase layering in non-isothermal binary liquid mixtures are examined using the mass transport equations. The stationary concentration distribution in the temperature gradient is calculated. Close to critical temperature and below, the resulting expression predicts a critical behavior and the layering of liquid phases in the mixture. At the critical temperature, the inflection point appears in the concentration distribution at the corresponding coordinate point. This situation may be seen in an experiment in a very narrow range of the concentrations, about several percent, around the critical concentration. With decrease of temperature, this inflection is transformed into a jump in the concentration, which corresponds to the thermodynamically equilibrium concentrations of the components at the temperature established at this point. At temperatures significantly lower than the critical one, the phase layering with the controllably changed position of the phase boundary can be obtained. This situation can be used to manipulate the suspended particles in the predetermined manner.
When the temperature gradient exceeds some critical value, the steps in the concentration distribution are appeared. This stepwise concentration distribution can be considered as the analog of the spinodal decomposition in uniform system.

References

[1] *Thermal Nonequilibrium Phenomena in Liquid Mixtures*, edited by W. Köhler and S. Wiegand (Springer, Berlin, 2002).
[2] S. N. Semenov, M. E. Schimpf, *Phys. Rev. E*, 72, 041202 (2005).
[3] M. E. Schimpf and S. N. Semenov, *J. Phys. Chem. B* **104**, 9935 (2000).
[4] J. L. Anderson, *Ann. Rev. Fluid Mechanics* **21**, 61 (1989).
[5] S. R. De Groot, P. Mazur, *Non-equilibrium Thermodynamics* (North-Holland, Amsterdam, 1962).
[6] S. N. Semenov and M. E. Schimpf, *Phys. Rev. E* **69**, 011201 (2004).

Thermodynamics of Molecular Mass Transport in Liquids.

Semen N. Semenov[1] and Martin E. Schimpf[2]
[1]*Institute of Biochemical Physics RAS, 117977 Moscow, Kosygin Street 4, Russia, sem@triniti.ru*
[2]*Department of Chemistry, Boise State University, Boise ID 83725, USA*

Abstract
A thermodynamic approach to mass transport is applied to liquid mixtures in a temperature gradient. The consistency of the Onsager equations for the component mass flux is evaluated with the resulting conclusion that heats of transport are equal to the chemical potentials of the components to eliminate thermodiffusion in pure liquids. In an open and/or non-stationary system, consistency between the Gibbs-Duhem equation and the Onsager equations is impossible. The dynamic pressure gradient is calculated. Coefficients of mass and thermodiffusion are described adequately over the entire compositional range of a mixture. It is shown that the thermodynamic approach combined with the microscopic calculation of the chemical potential provides the same results as the previous hydrodynamic approach in the derivation of the thermodiffusion coefficient in diluted molecular system.

Introduction

Certain refinements in non-equilibrium thermodynamics are necessary for non-isothermal mixtures when the components are not diluted. In order to simplify the problem, we examine here a binary mixture. Our motivation is based on three observations:

1. Current non-equilibrium thermodynamics approaches to mass transport fail to provide an unambiguous description of concentrated systems, in that component behavior depends on which component is considered to be the solvent.
2. In thermodynamic theories of thermal diffusion, the heat of transfer is formulated into equations for the Soret coefficient. We argue that a component's heat of transfer must equal its chemical potential. Without such equality, certain consequences follow that violate the condition of hydrostatic equilibrium in the non-isothermal system.
3. Usually, the Gibbs-Duhem equation is used to derive the pressure gradient. We will show that viscous drag in an open or/and non-stationary system causes additional dynamic pressure gradient.

Consistency Conditions for Onsager Mass Fluxes

The thermodynamic approach is based on the rate of entropy production σ [1, 2]:

$$\sigma = \vec{J}_e \cdot \nabla\left(1/T\right) - \vec{J}_1 \cdot \nabla\left(\mu_1/T\right) - \vec{J}_2 \cdot \nabla\left(\mu_2/T\right) \tag{1}$$

Here, $\vec{J}_e$ is the energy flux, $\vec{J}_1$ and $\vec{J}_2$ are the mass fluxes of the two components, μ_1 and μ_2 are their chemical potentials, and T is temperature. The energy flux and temperature profile are defined by the difference in temperature at the system boundaries ([2], Ch. 16), while the mass flux is defined by the following continuity equation:

$$\partial n_i/\partial t = -\nabla \vec{J}_i \tag{2}$$

Here n_i is the numeric volume concentration of the i^{th} component and t is time. The mass flux is further defined by non-equilibrium thermodynamics as [1, 2]:

$$\vec{J}_i = -n_i L_i \nabla\left(\mu_i/T\right) - n_i L_{iQ} \nabla\left(1/T\right) \tag{3}$$

where L_i and L_{iQ} are the Onsager coefficients.

In order to utilize Eq. (3) in a predictive capacity, it is transformed into a form that contains component concentrations and other physically measurable system parameters:

$$\nabla \mu_\kappa = \sum_{l=1}^{2} \frac{\partial \mu_k}{\partial n_l} \nabla n_l - \overline{v}_k \nabla P + \frac{\partial \mu_k}{\partial T} \nabla T \tag{4}$$

where P is the internal macroscopic pressure of the system and $\overline{v}_k$ is the partial molecular volume. The thermodynamic approach utilizes the Gibbs-Duhem equation for the pressure gradient [3, 4]:

$$\nabla P = \sum_{i=1}^{2} n_i \left(\sum_{k=1}^{2} \frac{\partial \mu_i}{\partial n_k} \nabla n_k + \frac{\partial \mu_i}{\partial T} \nabla T \right) \tag{5}$$

Eq. (5) defines the pressure gradient required to maintain hydrostatic equilibrium. Substitution of Eqs. (4, 5) into Eqs. (3) yields

$$\vec{J}_1 = \frac{L_1 v_1}{T v_2}\left[\phi(1-\phi)\left(2\frac{\partial \mu^*}{\partial \phi}\nabla\phi + \frac{\partial \mu^*}{\partial T}\nabla T\right) - (1-\phi)(\mu_1 - q_1)\frac{\nabla T}{T}\right] \tag{6}$$

$$\vec{J}_2 = -\frac{L_2}{T}\left[\phi(1-\phi)\left(2\frac{\partial \mu^*}{\partial \phi}\nabla\phi + \frac{\partial \mu^*}{\partial T}\nabla T\right) + \phi(\mu_2 - q_2)\frac{\nabla T}{T}\right] \tag{7}$$

where $q_i = L_{iQ}/L_i$ is the heat of transport, and $\mu^* = \mu_2 - (v_2/v_1)\mu_1$ is the combined chemical potential [1, 2].

An equation similar to Eq. (5) has been used to calculate diffusion and thermal diffusion coefficients [5]. In formulating Eqs. (6, 7) we have introduced the volume fractions $\phi_2 = n_2 v_2 = \phi$ and $\phi_1 = n_1 v_1 = 1-\phi$, and substituted specific molecular volumes v_1 and v_2 for the partial molecular volumes $\bar{v}_k$ used in Eq. (4) and (5).

Equations (6) and (7) are two non-equivalent expressions that relate mass flux to the volume fraction ϕ of a component in a non-isothermal system. Consequently, the result will depend on which equation is used. In practice Eq. (7) is used to define the transport of the dilute component in a mixture, while transport of the solvent is defined through conservation of mass. In mixtures where more than one component is concentrated, the result will differ depending on which component is selected as the solvent.

In order for Eqs. (6) and (7) to be made consistent, the following conditions must be met:

$$\mu_1 = q_1 \quad (8); \qquad \mu_2 = q_2 \quad (9); \qquad \vec{J}_1 = \vec{J}_2 = 0 \quad (10)$$

The conditions defined by Eqs. (8) and (9) eliminate the motion of pure liquid in a temperature gradient, which would be inconsistent with the Gibbs-Duhem equation.

While the condition defined by Eqs. (8) and (9) should be accepted for any system, Eq. (10) is fulfilled only in a closed system that is stationary. Consequently, Eqs. (6) and (7) are incompatible with the Gibbs-Duhem equation for any system that is open and non-stationary.

Combining either of Eqs. (6) and (7) with Eqs. (8-10), we obtain the equation:

$$\phi(1-\phi)\left(2\frac{\partial \mu^*}{\partial \phi}\nabla\phi + \frac{\partial \mu^*}{\partial T}\nabla T\right) = 0 \tag{11}$$

which can be used to obtain the stationary concentration distribution and any related parameters. Then, we obtain the following expression for the Soret coefficient in the diluted system:

$$S_T = -\frac{\nabla\phi}{\phi(1-\phi)\nabla T} \approx \frac{1}{2kT}\frac{\partial}{\partial T}\left[\mu_2^0 - \mu_1^0(v_2/v_1)\right] \tag{12}$$

where μ_1^0 and μ_2^0 are the chemical potentials of the pure component and the isolated specie of the second component in the solvent, respectively,

Dynamic Pressure Gradient and Barodiffusion

In an open or non-stationary system, the total mass flux or the component fluxes can be non-zero.

Here, the mass transport equations can be obtained, calculating the pressure gradient using Eqs. (7) and (8), and considering ∇P and ϕ as unknown functions:

$$\nabla P = \frac{-\frac{\vec{J}}{L_1} + 2[(1-\phi)\frac{\partial \mu_1}{\partial \phi} + \frac{L_2}{L_1}\phi\frac{\partial \mu_2}{\partial \phi}]\nabla\phi + [(1-\phi)\frac{\partial \mu_1}{\partial T} + \frac{L_2}{L_1}\phi\frac{\partial \mu_2}{\partial T}]\nabla T}{v_1\left[1-\phi+(D_2 v_2/D_1 v_1)\phi\right]} \tag{13}$$

$$\frac{\partial \phi}{\partial t} = \frac{L_2}{T}\nabla\left[\frac{\phi(1-\phi)\left(2\frac{\partial \mu^*}{\partial \phi}\nabla\phi + \frac{\partial \mu^*}{\partial T}\nabla T\right) - \phi\frac{\vec{J}}{L_1}}{1-\phi+(D_2 v_2/D_1 v_1)\phi}\right] \tag{14}$$

Eq. (13) described the dynamic pressure gradient established in open and non-stationary systems. It is different of the Gibbs-Duhem pressure gradient predicted by Eq. (5).

Similar equations were obtained using a kinetic approach [6, 7]. Compared to Eq. (11), the mass flux in Eq. (14) contains the term $\sim \vec{J}$ responsible for the solute drift in the open system. When the molecules entering through one boundary may leave the system through another, the component meets viscous resistance, which creates a dynamic pressure gradient and barodiffusion in the system. This situation is not considered in the Gibbs-Duhem equation.

For ideal solutions, the effective diffusion coefficient given by Eq. (14) can be expressed as

$$D_{eff} = D_2(\phi)\frac{1-\phi+(v_2/v_1)\phi}{1-\phi+(D_2v_2/D_1v_1)\phi} \tag{15}$$

where $D_i(\phi)$ is the Stokes-Einstein diffusion coefficient in the real liquid mixture. Eq. (15) accurately predicts the diffusion coefficient at any concentration. For dilute systems, the dynamic barodiffusion factor $\left[1-\phi+(D_2v_2/D_1v_1)\phi\right]^{-1}$ allows the effective diffusion coefficient described by Eq. (18) to be transformed into the Stokes-Einstein expression. Without such a factor the model of Dhont [5] and the other models fail to provide this physically reasonable behavior, even in ideal solutions.

The effect of dynamic barodiffusion on measurements of diffusion and thermodiffusion is even more significant for polymers and colloidal particles because parameter D_2v_2/D_1v_1, which reflects the role of the dynamic pressure gradient, can be quite large. For example, in a study by Duhr and Braun of DNA molecules [8], the thermodiffusion coefficient of DNA was reported to decrease with chain length. To date there is no theoretical explanation for this observation.

For dilute systems, the expression for the thermodiffusion coefficient is

$$D_T = \left\{\frac{D_2}{2kT}\frac{\partial}{\partial T}\left[\mu_2^0-\mu_1^0(v_2/v_1)\right]\right\}\Big/\left[1-\phi+(D_2v_2/D_1v_1)\phi\right] \tag{16}$$

According to Eq. (16), the thermodiffusion coefficient may decrease with increasing solute size, provided $(D_2v_2/D_1v_1)\phi \gg 1$. This condition can be fulfilled even at $\phi \ll 1$. Therefore, Eq. (16) is consistent with the behavior of diluted DNA solutions reported by Duhr and Braun [8].

Microscopic calculation of $\partial\mu^*/\partial T$

In this section, we calculate the parameter $\partial\mu^*/\partial T$ involved in the Soret coefficient [Eq. (12)] and compare the results obtained with the hydrodynamic approach [6].

In the calculation of the parameter $\frac{\partial\mu^*}{\partial T}$, it is convenient to use the microscopic approach and consider the diluted system. We can use the thermodynamic theory of the perturbation [9]. The chemical potential of the isolated suspended molecule can be written as [9]

$$\mu_2^0(\vec{r}) = \left\langle \sum_i \Phi_{12}(\vec{r}-\vec{r}_{1i}) + \frac{\vec{p}^2}{2m_2} + \delta\left[\frac{1}{2}\sum_{i,j}\Phi_{11}(\vec{r}_{1j}-\vec{r}_{1i})\right]\right\rangle \tag{17}$$

where Φ_{11} and Φ_{12} are the intermolecular interaction potentials solute-solvent and solvent-solvent, respectively, $\vec{p}^2/2m_2$ is the kinetic energy of the particle expressed through its momentum $\vec{p}$ and m_2, and the last right-hand term corresponds to the change in the solvent-solvent interaction due to the presence of the solute. The angular brackets mean the averaging in the thermodynamic sense using the Hamiltonian of the unperturbed system. For the averaged kinetic energy, we obtain $\left\langle \vec{p}^2/2m_2 \right\rangle = 3kT/2$, both for the solute and solvent molecules. For this reason this term cannot cause any thermodiffusion. The last term in the angular brackets can be expressed as a local pressure gradient $\nabla\Pi$ established around the solute. After the calculations, where the principle of the local equilibrium is systematically used, we obtain

$$\Pi(\vec{r}_1) - \Pi_0 = \Phi_{12}(\vec{r}_1)/v_1 \tag{18}$$

Here Π_0 is the macroscopic pressure which is changed very weakly at the molecular length but may be non-uniform at the macroscopic length. It is calculated from the condition that the solvent must be at the mechanical equilibrium, that is $\partial\mu_1^0(\vec{r})/\partial\vec{r} = 0$.

The intermolecular interaction potential can be written as [6, 7]

$$\Phi_{12} = -\varepsilon_{12}\left(\sigma_{12}/r_1\right)^6 \tag{19}$$

where ε_{12} is the energy of the interaction, and σ_{12} is the closest approach distance. Using Eq. (19), we obtain:

$$\frac{\partial \mu_2^0(\vec{r})}{\partial \vec{r}} = \alpha_T \varepsilon_{12} \frac{v_{12}}{v_1}\left(1 - \frac{v_{11}v_2\varepsilon_{11}}{v_{12}v_1\varepsilon_{12}}\right)\nabla T_\infty \tag{20}$$

$$S_T = -\alpha_T \frac{\pi\varepsilon_{12}}{8kT}\frac{v_{12}}{v_1}\left(1 - \frac{v_{11}v_2\varepsilon_{11}}{v_{12}v_1\varepsilon_{12}}\right) \tag{21}$$

where $v_{12} = 4\pi\sigma_{12}^3/3$, and α_T is the solvent thermal expansion coefficient. The respective parameters for the solvent are v_{11}, σ_{11}, and ε_{11}.

Eq. (21) is very close to the expression for the Soret coefficient obtained in [10] by the hydrodynamic approach, when one assumes $\varepsilon_{12} = \sqrt{\varepsilon_{11}\varepsilon_{22}}$, and introduces the respective hydrodynamic radii equal to σ_{11}, σ_{12}. The "thermodynamic" and "hydrodynamic" expressions predict the same dynamic behavior of the isolated solute molecule or homopolymer chain, and the differences are related rather to the approximations used in the calculations. For example, the direction of the thermophoretic motion always is determined by the inequalities $v_{11}v_2\varepsilon_{11}/v_{12}v_1\varepsilon_{12} > 1$, $v_{11}v_2\varepsilon_{11}/v_{12}v_1\varepsilon_{12} < 1$, and the parameter $v_{11}v_2\varepsilon_{11}/v_{12}v_1\varepsilon_{12}$ is determined mainly by the geometry and physical properties of the molecules but not by their dimensions.

Conclusions

When the thermodynamic approach is evaluated, we find that the equations for mass flux are inconsistent unless the heats of transport are equal to the respective chemical potentials. Then, the unacceptable effect of motion in pure non-isothermal liquids is eliminated.

Our analysis also demonstrates that the Gibbs-Duhem equation is inadequate for open and non-stationary systems. By defining the dynamic pressure gradient, a distinction is made between the equilibrium pressure gradient predicted by the Gibbs-Duhem equation and the dynamic pressure gradient in an open and/or non-steady state system.

Application of the model to ideal systems accurately predicts the diffusion coefficient at any concentration.

Highly structured macromolecules suspended in a solvent can create large dynamic pressure gradients. It is found that such effects may qualitatively explain the measured size dependence of thermodiffusion in DNA experiments.

The microscopic calculations of the chemical potential for the isolated solute give the expression for Soret coefficient close to the respective expressions obtained by the hydrodynamic approach.

References

1. S. R. De Groot, P. Mazur, *Non-equilibrium Thermodynamics* (North-Holland, Amsterdam, 1962).
2. D. Kondepudi, I. Prigogine, *Modern Thermodynamics* (Wiley, New York, 1999).
3. K. Ghoraeb, A. Firoozabadi, *AIChE*, 46 883 (2000).
4. S. Pan, M. Z. Sahgir, M. Kawaji, C. G. Jiang, Y. Yan, *J. Chem. Phys.* **126**, 014502 (2007).
5. J. K. G. Dhont, *J. Chem. Phys.* **120**, 1632 (2004).
6. M. E. Schimpf, S. N. Semenov, *Phys. Rev. E*, 70, 031202 (2004).
7. S. N. Semenov, M. E. Schimpf, *Phys. Rev. E*, 72, 041202 (2005).
8. S. Duhr, D. Braun, *PNAS published online*, Dec 12, 2006. doi:10.1073/pnas. 0603873103.
9. L. D. Landau, E. M. Lifshitz, Statistical Physics, Part 1, Chapter IX, "Nauka" Publishing, Moscow 1976 (In Russian)
10. Semenov, S. N., Schimpf, M. E., *Phys. Rev. E*, **69**, 011201 (2004).

AXIOMATIC EXPOSITION OF EXTENDED THERMODYNAMICS

S.I. Serdyukov

Chemistry Department, Moscow State University, 119992 Moscow, Russia
Electronic address: serdkv@tech.chem.msu.ru

A non-statistical paradigm of the thermodynamics exposition[1,2] can be extended on the uniform systems, given by usual thermodynamic variables and their time derivatives. Such systems are considered within the framework of extended thermodynamics.

A state of a system is characterized by external parameters $\beta = \{\beta_1, \ldots, \beta_{N'}\}$, amounts of constituents $n = \{n_1, \ldots, n_N\}$, time derivatives $\dot{\beta} = \{\dot{\beta}_1, \ldots, \dot{\beta}_{N'}\}$, $\dot{n} = \{\dot{n}_1, \ldots, \dot{n}_N\}$. In the equilibrium state (stable or not stable) $\dot{\beta} = 0$, $\dot{n} = 0$. Generally, at $\dot{\beta} \neq 0$, $\dot{n} \neq 0$ the state is uniform, not equilibrium.

The *First Law*[1] of thermodynamics "asserts that any two states of a system may always be the initial and final states of a weight process. Such a process involves no net effects external to the system except the change in elevation between z_1 and z_2 of a weight, that is, solely a mechanical effect[3]".

The property energy E is implication of the First Law of thermodynamics, and is function of the β, n, not $\dot{\beta}$, $\dot{n}$. A state of a system can be given by variables E, β, n, and $\dot{E}$, $\dot{\beta}$, $\dot{n}$.

The *Second Law* of thermodynamics[1] asserts that among all the states of a system with a given value of the energy E, given values of the external parameters β and the amounts of constituents n, there exists one and only one stable equilibrium state.

Let us introduce reference reservoir R_0 with a set of stable equilibrium states. Further, let us introduce reservoir R with variables E, β, n, and reservoir R$'$ with the same E, β, n and additional variables $\dot{E}$, $\dot{\beta}$, $\dot{n}$.

To define the properties of reservoirs R_0 and R, we consider arbitrary auxiliary system A, arbitrary states A_1 and A_2, and reversible weight process for the composite systems AR_0 and AR in which system A changes state from A_1 to A_2. We can obtain

[1]E.P. Gyftopoulos, G.P. Beretta, *Thermodynamics: Foundations and Applications*, 1991.
[2]G.P. Beretta, *Int. J. of Thermodynamics*, 11 (2008) 39.
[3]E.P. Gyftopoulos, *Physica A*, 307 (2002) 405. 9 (2006) 137.

change in energy $(\Delta E_{R_0})^{\mathrm{sW,rev}}_{\mathrm{A_1A_2}}$ and $(\Delta E_R)^{\mathrm{sW,rev}}_{\mathrm{A_1A_2}}$ for the R_0 and R, respectively. Reservoir R$'$ can be interconnected to reservoir R by means of reversible weight process and, consequently, we can obtain change in energy $(\Delta E_{R'})^{\mathrm{sW,rev}}_{\mathrm{A_1A_2}}$ for the reservoir R$'$.

Using $(\Delta E_{R_0})^{\mathrm{sW,rev}}_{\mathrm{A_1A_2}}$ and $(\Delta E_{R'})^{\mathrm{sW,rev}}_{\mathrm{A_1A_2}}$, the generalized temperature $\theta_{R'}$ with respect to temperature T_{R_0} of reference reservoir R_0 can be defined:

$$\theta_{R'} = \left.\frac{(\Delta E_{R'})^{\mathrm{sW,rev}}_{\mathrm{A_1A_2}}}{(\Delta E_{R_0})^{\mathrm{sW,rev}}_{\mathrm{A_1A_2}}}\right|_{\beta,n,\dot{E},\dot{\beta},\dot{n}} T_{R_0}.$$

By analogy, for a system with variable values of $\beta_1 = V$ and n and fixed $\{\beta_2, \ldots, \beta_N\}$, we can introduce generalized pressure $\pi_{R'}$

$$\pi_{R'} = -\left(\frac{\Delta E_{R'}}{\Delta V_{R'}}\right)^{\mathrm{sW,rev}}_{\mathrm{A_1A_2}}\Bigg|_{\beta',n,\dot{E},\dot{\beta},\dot{n}} + \frac{\theta_{R'}}{T_{R_0}}\left[p_{R_0} + \left(\frac{\Delta E_{R_0}}{\Delta V_{R_0}}\right)^{\mathrm{sW,rev}}_{\mathrm{A_1A_2}}\Bigg|_{\beta',n}\right]$$

and generalized total potential $\tilde{\mu}_{iR'}$

$$\tilde{\mu}_{iR'} = \left(\frac{\Delta E_{R'}}{\Delta n_{iR'}}\right)^{\mathrm{sW,rev}}_{\mathrm{A_1A_2}}\Bigg|_{\beta,n',\dot{E},\dot{\beta},\dot{n}} - \frac{\theta_{R'}}{T_{R_0}}\left[\mu_{iR_0} - \left(\frac{\Delta E_{R_0}}{\Delta n_{iR_0}}\right)^{\mathrm{sW,rev}}_{\mathrm{A_1A_2}}\Bigg|_{\beta,n'}\right].$$

Apart from, we can introduce intensive values $\Lambda_{R'}$, $\Xi_{R'}$ and $\Gamma_{iR'}$ corresponding to $\dot{E}_{R'}$, $\dot{V}_{R'}$, and $\dot{n}_{iR'}$, respectively:

$$\Lambda_{R'} = -\left(\frac{\Delta E_{R'}}{\Delta \dot{E}_{R'}}\right)^{\mathrm{sW,rev}}_{\mathrm{A_1A_2}}\Bigg|_{\beta,n,\dot{\beta},\dot{n}}, \qquad \Xi_{R'} = -\left(\frac{\Delta E_{R'}}{\Delta \dot{V}_{R'}}\right)^{\mathrm{sW,rev}}_{\mathrm{A_1A_2}}\Bigg|_{\beta,n,\dot{E},\dot{\beta}',\dot{n}},$$

and $$\Gamma_{iR'} = -\left(\frac{\Delta E_{R'}}{\Delta \dot{n}_{iR'}}\right)^{\mathrm{sW,rev}}_{\mathrm{A_1A_2}}\Bigg|_{\beta,n,\dot{E},\dot{\beta},\dot{n}'}.$$

According the theorems of the first and second laws there are exists property entropy, with the value denoted by S. For a system with variable values of $\beta_1 = V$ and n and fixed $\{\beta_2, \ldots, \beta_N\}$, the entropy diffrence can be defined as

$$S_2 - S_1 = \frac{1}{\theta'_R}[(E_2 - E_1) - (\mathcal{E}^{R'}_2 - \mathcal{E}^{R'}_1) + \pi_{R'}(V_2 - V_1) - \sum \tilde{\mu}_{iR'}(n_{i2} - n_{i1}) +$$
$$+\Lambda_{R'}(\dot{E}_2 - \dot{E}_1) + \Xi_{R'}(\dot{V}_2 - \dot{V}_1) - \sum \Gamma_{iR'}(\dot{n}_{i2} - \dot{n}_{i1})],$$

where $\mathcal{E}^{R'}$ is the generalized available energy.

The entropy of the system is given by the fundamental relation, that is a function of the form

$$S = S(E, \beta, n; \dot{E}, \dot{\beta}, \dot{n}).$$

For a system with $\beta = \{V\}$ and $E = U$ (U is the internal energy), we have

$$S = S(U, V, n; \dot{U}, \dot{V}, \dot{n})$$

and $\theta = 1/(\partial S/\partial U)_{V,n;\dot{U},\dot{V},\dot{n}}$ is the generalized temperature, $\pi = \theta(\partial S/\partial V)_{U,n;\dot{U},\dot{V},\dot{n}}$ is the generalized pressure, $\tilde{\mu}_i = -\theta(\partial S/\partial n_i)_{U,V,n';\dot{U},\dot{V},\dot{n}}$ is the generalized chemical potential of the ith constituent,

$$\Lambda = \theta\left(\frac{\partial S}{\partial \dot{U}}\right)_{U,V,n;\dot{V},\dot{n}}, \qquad \Xi = \theta\left(\frac{\partial S}{\partial \dot{V}}\right)_{U,V,n;\dot{U},\dot{n}}, \qquad \Gamma_i = -\theta\left(\frac{\partial S}{\partial \dot{n}_i}\right)_{U,V,n;\dot{U},\dot{V},\dot{n}'}$$

are a new intensive quantities. The first differential for S is

$$\theta dS = dU + \pi dV - \sum_i \tilde{\mu}_i dn_i + \Lambda d\dot{U} + \Xi d\dot{V} - \sum_i \Gamma_i d\dot{n}_i.$$

To construct a thermodynamic formalism for the nonuniform system, instead of the local equilibrium hypothesis, we propose a *local uniformity hypothesis*: the system that is nonuniform as a whole will be regarded as uniform at each point. This means that the nonuniform system should be described in terms of the same variables u, v ($= 1/\rho$), c_i ($= n_i/\sum n_i$), $\dot{u}$, $\dot{v}$, and $\dot{c}_i$. Then, instead of last relation, we obtain a similar relation in the form

$$\theta ds = du + \pi dv - \sum_i \tilde{\mu}_i dc_i + \Lambda d\dot{u} + \Xi d\dot{v} - \sum_i \Gamma_i d\dot{c}_i.$$

Only in the particular case where entropy density is function of $\dot{u} + p\dot{v}$,

$$s = s(u, v, c_1, \ldots, c_N; \dot{u} + p\dot{v}, \dot{c}_1, \ldots, \dot{c}_N),$$

the formalism of extended irreversible thermodynamics is considered[4].

[4]S.I. Serdyukov, *Phys. Lett. A*, 316 (2003) 177; 324 (2004) 262. S.I. Serdyukov, *C. R. Physique*, 8 (2007) 93.

COMPARISON OF THREE VERSIONS OF EXTENDED THERMODYNAMICS

S.I. Serdyukov

Chemistry Department, Moscow State University, 119992 Moscow, Russia

serdkv@tech.chem.msu.ru

Three different versions of extended thermodynamics are considered.

1^o. The conventional version of extended irreversible thermodynamics (EIT) [1-5], which is based on the assumption that entropy density s is function of both conventional thermodynamic variables and corresponding dissipative fluxes:

$$s = s(u, v; \mathbf{J}, \overset{\circ}{\mathbf{P}}{}^v, p^v), \tag{1}$$

where u is the internal energy density, v is the specific volume, $\mathbf{J}$ is the heat flux, $\overset{\circ}{\mathbf{P}}{}^v$ is the viscous pressure tensor, and p^v is the bulk pressure.

2^o. Internal-variable thermodynamics (IVT) [6-9], which is based on the supposition that additional variables must be selected on the basis of microscopic analysis or left unidentified.

3^o. The third version of extended thermodynamics proceeds from the postulate that additional variables are generally material time derivatives of the conventional variables [10-12]:

$$s = s(u, v; \dot{u}, \dot{v}). \tag{2}$$

Within the framework of third version the generalized constitutive equations are obtained:

$$\mathbf{J} + \tau_1 \frac{\partial \mathbf{J}}{\partial t} = -\lambda \nabla T - \varepsilon \frac{\partial \nabla T}{\partial t} + \beta_2 \lambda T^2 \nabla \cdot \overset{\circ}{\mathbf{P}}{}^v + \beta_1 \lambda T^2 \nabla p^v, \tag{3}$$

$$\overset{\circ}{\mathbf{P}}{}^v + \tau_2 \frac{\partial \overset{\circ}{\mathbf{P}}{}^v}{\partial t} = -2\eta \left(\overset{\circ}{\mathbf{V}} + \lambda_2 \frac{\partial \overset{\circ}{\mathbf{V}}}{\partial t} \right) + 2\beta_2 \eta T (\overset{\circ}{\nabla} \mathbf{J})^s, \tag{4}$$

$$p^v + \tau_0 \frac{\partial p^v}{\partial t} = -\zeta \left(\nabla \cdot \mathbf{v} + \lambda_0 \frac{\partial \nabla \cdot \mathbf{v}}{\partial t} \right) + \beta_1 \zeta T \nabla \cdot \mathbf{J}, \tag{5}$$

where T is the temperature, $\overset{\circ}{\mathbf{V}}$ is the traceless strain rate tensor ($\mathbf{V} = \frac{1}{2}[\nabla \mathbf{v} + (\nabla \mathbf{v})^+]$ is the symmetric part of the velocity gradient $\nabla \mathbf{v}$), λ is the thermal conductivity, η is

the shear viscosity, and ζ is the bulk viscosity; τ_1, τ_2, τ_0 are the relaxation times, ε/λ, λ_2, λ_0 are the retardation times; $\dot{\mathbf{J}}_q$, $(\overset{\circ}{\mathbf{P}}{}^v)^{\cdot}$, and $\dot{p}^v$ are the material time derivatives of the dissipative fluxes; $(\overset{\circ}{\nabla}\mathbf{J}_q)^s$ is the traceless symmetric gradient of the heat flux; and β_1 and β_2 are independent coefficients.

Equations (3)–(5) cover both constitutive equations of EIT[1] (at $\varepsilon = \lambda_2 = \lambda_0 = 0$),

$$\mathbf{J}_q + \tau_1 \dot{\mathbf{J}}_q = -\lambda \nabla T + \beta_2 \lambda T^2 \nabla \cdot \overset{\circ}{\mathbf{P}}{}^v + \beta_1 \lambda T^2 \nabla p^v, \tag{6}$$

$$\overset{\circ}{\mathbf{P}}{}^v + \tau_2 (\overset{\circ}{\mathbf{P}}{}^v)^{\cdot} = -2\eta \overset{\circ}{\mathbf{V}} + 2\beta_2 \eta T (\overset{\circ}{\nabla}\mathbf{J}_q)^s, \tag{7}$$

$$p^v + \tau_0 \dot{p}^v = -\zeta \nabla \cdot \mathbf{v} + \beta_1 \zeta T \nabla \cdot \mathbf{J}_q, \tag{8}$$

and dual-phase-lag constitutive equations (at $\beta_1 = \beta_2 = 0$),

$$\mathbf{J}_q + \tau_1 \frac{\partial \mathbf{J}_q}{\partial t} = -\lambda \nabla T - \varepsilon \frac{\partial \nabla T}{\partial t}, \tag{9}$$

$$\overset{\circ}{\mathbf{P}}{}^v + \tau_2 \frac{\partial \overset{\circ}{\mathbf{P}}{}^v}{\partial t} = -2\eta \left(\overset{\circ}{\mathbf{V}} + \lambda_2 \frac{\partial \overset{\circ}{\mathbf{V}}}{\partial t} \right), \tag{10}$$

$$p^v + \tau_0 \frac{\partial p^v}{\partial t} = -\zeta \left(\nabla \cdot \mathbf{v} + \lambda_0 \frac{\partial \nabla \cdot \mathbf{v}}{\partial t} \right). \tag{11}$$

The connection of the formalism of third version (generalized temperature definition, expression for the entropy flux and source, double number of phenomenological equations) with formalisms of EIT and IVT is considered.

This work was supported by the Russian Foundation for Basic Research (project no. 04-03-32821).

[1] Jou, D., Casas-Vázquez, J., Lebon, G., Extended Irreversible Thermodynamics, 2nd ed, Springer, Berlin, 1996.

[2] Jou, D., Casas-Vázquez, J., Lebon, G., Rep. Prog. Phys., 62 (1999) 1035.

[3] Müller, I., Ruggeri, T., Extended Thermodynamics, Springer, New York, 1993.

[4] Garsia-Cólin, L.S., Uribe, F.J., J. Non-Equilib. Thermodyn., 16 (1991) 89.

[1] With the difference that equations (3)–(5) include material derivatives of fluxes, $\dot{\mathbf{J}}_q$, $(\overset{\circ}{\mathbf{P}}{}^v)^{\cdot}$, and $\dot{p}^v$, whereas equations (6)–(8) involve local derivatives, $\partial_t \mathbf{J}_q$, $\partial_t \overset{\circ}{\mathbf{P}}{}^v$, and $\partial_t p^v$.

[5] Netletton, R.E., Sobolev, S.L., J. Non-Equilib. Thermodyn., 20 (1995) 205.

[6] Restuccia, L., Kluitenberg, G.A., Physica A, 154 (1988) 157.

[7] Ciancio, V., Restuccia, L., Kluitenberg, G.A., J. Non-Equilib. Thermodyn., 15 (1990) 157.

[8] Ciancio, V., Verhas, J, J. Non-Equilib. Thermodyn., 16 (1991) 57.

[9] Maugin, G.A., Muschik, W, J. Non-Equilib. Thermodyn., 19 (1994) 217.

[10] S.I. Serdyukov, Phys. Lett. A, 316 (2003) 177.

[11] S.I. Serdyukov, Phys. Lett. A, 324 (2004) 262.

[12] S.I. Serdyukov, C. R. Physique, 8 (2007) 93.

PHASE RULE IN EXTENDED THERMODYNAMICS AND NON-EQUILIBRIUM PHASE DIAGRAM OF CARBON

S.I. Serdyukov

Chemistry Department, Moscow State University, 119992 Moscow, Russia
serdkv@tech.chem.msu.ru

Recently [1], an analysis of numerous literature data has shown that the carbon phase diagram (in the vicinity of the solid-liquid-vapor triple point) depends on the carbon heating rate V ($10^3 < V < 10^8$ K/s). Under the fast heating at temperature 3800-4800 K carbon has structure of activated material. Activated carbon "consist of aromatic sheets and strips, often bent and resembling a mixture of wood shavings and crumpled paper, with variable gaps of molecular dimensions between them" [2] (fig. 1).

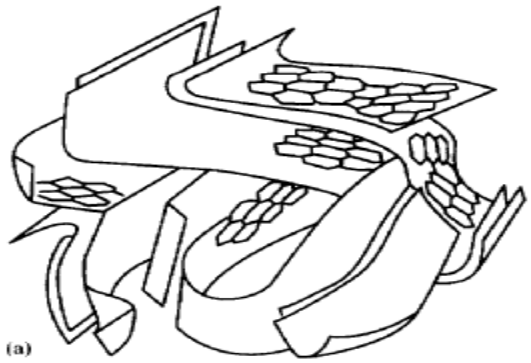

Figure 1: Schematic representation of the structure of activated carbon (adapted from Ref. [3]).

It has been proposed [1] to construct the carbon phase diagram as non-equilibrium phase diagram in the coordinates T, p, dT/dt (generally, in the coordinates T, p, dT/dt and dp/dt). In this communication, the choice of variables for the non-equilibrium phase diagram is substantiated and the phase rule in a four-dimensional phase is formulated.

Following previous works [4-6], it is postulated that the entropy density s of the single-phase system depends on conventional variables (the internal energy density u,

the specific volume v, and the mass fractions of K components $c_1, \ldots, c_K$) and on additional variables (in the general case, the material time derivatives $\dot{u}$, $\dot{v}$, $\dot{c}_1, \ldots, \dot{c}_K$):

$$s = s(u, v, c_1, \ldots, c_K; \dot{u}, \dot{v}, \dot{c}_1, \ldots, \dot{c}_K).$$

Within the framework of this version of extended irreversible thermodynamics the uniform systems can be considered, where dissipative fluxes are absent by definition.

The Gibbs free energy g depends on the same additional variables, and

$$dg = -sd\theta + vd\pi + \sum_k \mu_k dc_k - \Lambda d\dot{u} - \Xi d\dot{v} + \sum_k \Gamma_k d\dot{c}_k, \tag{1}$$

where θ is generalized temperature, π is the generalized pressure, μ_k is the non-equilibrium chemical potential, Λ, Ξ and Γ_k are the new intensive quantities.

Expression (1) shows that the non-equilibrium phase diagram should be constructed using the variables on which the Gibbs free energy depends, i.e., the variables θ, π, $\dot{u}$, and $\dot{v}$, rather than dT/dt and dp/dt. The state of the system containing ϕ phases, provided that the time derivatives of the mass fractions are zero,

$$\dot{c}_1^\alpha = 0, \quad \dot{c}_2^\alpha = 0, \quad \ldots, \quad \dot{c}_K^\alpha = 0, \qquad \alpha = 1, \ldots, \phi, \tag{2}$$

is given by $4+\phi(K-1)$ variables, i.e., T, p, $\dot{u}$, $\dot{v}$, $c_1^1, \ldots, c_{K-1}^1, \ldots, c_1^\phi, \ldots, c_{K-1}^\phi$. Taking into account $K(\phi-1)$ equations $\mu_k^1 = \mu_k^2 = \ldots = \mu_k^\phi$ $(k = 1, 2, \ldots, K)$, one can obtain the phase rule in the four-dimensional space (N_f is the number of degrees of freedom):

$$N_f = 4 + K - \phi. \tag{3}$$

In a particular case, under conditions (2) and the additional conditions $\dot{u} = 0$ and $\dot{v} = 0$, the classical phase diagram on the plane and the known phase rule, $N_f = 2 + K - \phi$, take place.

Further, the non-equilibrium phase diagram of carbon and relationship between generalized temperature θ and equilibrium temperature T in triple point are discussed.

This work was supported by the Russian Foundation for Basic Research (project no. 04-03-32821).

[1] I.I. Klimovskii and V.V. Markovets, in *Sci. Proc. Inst. High Energy Dens. of Ass. IHT RAS*, Iss. 6 - 2003/ V.E. Fortov and A.P. Likhachev, Eds., Moscow: Ass. IHT RAS, 2004, P. 73-80.

[2] F. Rodriguez-Reinozo, *Carbon*, 36 (1998) 159.

[3] H.F. Stoeckli, *Carbon*, 28 (1990) 1.

[4] S.I. Serdyukov, *Phys. Lett. A*, 316 (2003) 177.

[5] S.I. Serdyukov, *Phys. Lett. A*, 324 (2004) 262.

[6] S.I. Serdyukov, *C. R. Physique*, 8 (2007) 93.

ON THE OSCILLATING SYSTEMS IN EXTENDED THERMODYNAMICS AND CLASSICAL MECHANICS

S.I. Serdyukov, N.M. Voskresenskii

Chemistry Department, Moscow State University, 119992 Moscow, Russia
serdkv@tech.chem.msu.ru

On the front cover of work [1] dependence of total entropy S verses time t for the model isolated oscillating system is presented (fig.1, continuous curve, calculated in [2]). In this case heat conduction is described by the Maxwell-Cattaneo law

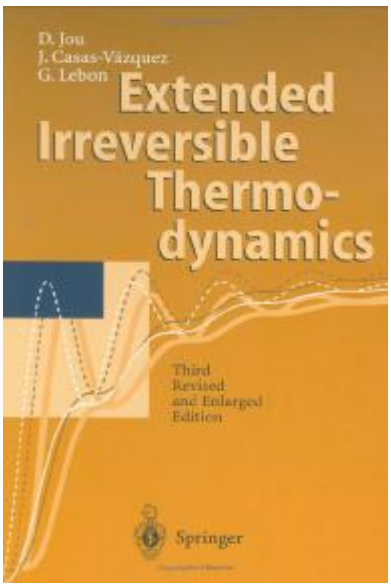

Figure 1: The evolution of the classical entropy $S_{\rm CIT}$ (- - - -) and extended entropy $S_{\rm EIT}$ (——) of an isolated system described by the Eq. (1) and (2).

$$\tau\frac{\partial \mathbf{J}}{\partial t}+\mathbf{J}=-\lambda\nabla T, \qquad (1)$$

and there is an oscillatory approach to equilibrium according to the telegraphe equation

$$\tau\frac{\partial^2 T}{\partial t^2}+\frac{\partial T}{\partial t}=\kappa\nabla^2 T, \qquad (2)$$

where T is the temperature, $\mathbf{J}$ is the heat flux, τ is the relaxation time, λ is the thermal conductivity, $\chi=\lambda/(\rho C_v)$ is the thermal diffusivity, ρ is the mass dencity, C_v is the heat capacity per unit mass, and t the time.

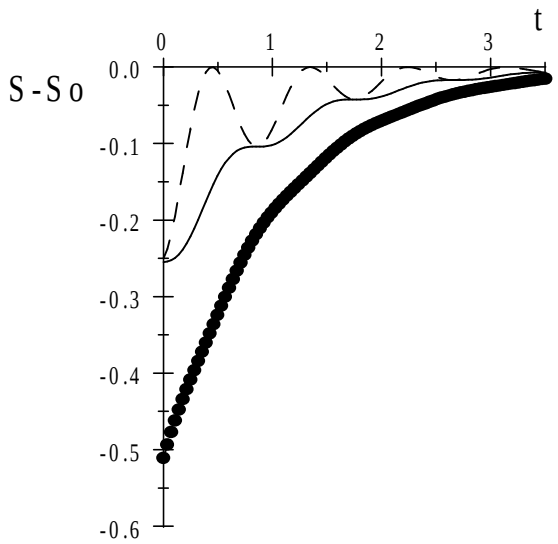

Figure 2: The change in the classical entropy $\tilde{S}_{\rm CIT}-\tilde{S}_0$ (dashed curve), the change in the incomplete extended entropy $\tilde{S}_{\rm EIT}-\tilde{S}_0$ (solid curve) and the change in the complete extended entropy $\tilde{S}_{\rm COMPL}-\tilde{S}_0$ (dotted curve) are shown.

This important result is unsatisfactory, since $S_{\rm EIT}$ is not strictly monotonic (at certain t entropy does not increase, i.e. $dS/dt=0$). This drawback indicates incompleteness of the traditional version of extended irreversible thermodynamics (EIT) [1-6]. In this work, we will construct a more complete extended thermodynamic theory and show that the total entropy of a model isolated system within this theory increases strictly monotonically (fig.2).

Extended thermodynamics. Let us consider extended thermodynamic theory [7-9] based on the postulate that the entropy density s is a function of the internal energy density u and time derivative $\dot{u}$:

$$s=s(u,\dot{u}), \qquad (3)$$

where $\dot{u}=\partial u/\partial t$. Then, the fundamental equations

are[1] $\theta ds = du + \Lambda d\dot{u}$ and

$$\frac{\partial s}{\partial t} = \theta^{-1}\frac{\partial u}{\partial t} + \theta^{-1}\Lambda\frac{\partial \dot{u}}{\partial t}, \tag{4}$$

where generalized temperature $\theta = \theta(u, \dot{u})$ and the quantity $\Lambda = \Lambda(u, \dot{u})$ depend on the additional variable $\dot{u}$.

The balance equations for u and $\dot{u}$ are

$$\rho\dot{u} = -\nabla\cdot\mathbf{J}, \qquad \rho\frac{\partial \dot{u}}{\partial t} = -\nabla\cdot\dot{\mathbf{J}}. \tag{5}$$

where $\dot{\mathbf{J}} = \partial\mathbf{J}/\partial t$. Based on the equation (4), we write the rate of change in entropy with time: $\rho\frac{\partial s}{\partial t} = -\nabla\cdot(\theta^{-1}\mathbf{J} + \theta^{-1}\Lambda\dot{\mathbf{J}}) + \mathbf{J}\cdot\nabla\theta^{-1} + \dot{\mathbf{J}}\cdot\nabla(\theta^{-1}\Lambda)$, from which the expressions for the entropy flux and the entropy source are found:

$$\mathbf{J}_s = \theta^{-1}\mathbf{J} + \theta^{-1}\Lambda\dot{\mathbf{J}}, \tag{6}$$

$$\sigma = \mathbf{J}\cdot\nabla\theta^{-1} + \dot{\mathbf{J}}\cdot\nabla(\theta^{-1}\Lambda) \geq 0. \tag{7}$$

Expression (7) shows that, to the heat flux $\mathbf{J}$, the thermodynamic force $\nabla\theta^{-1}$ corresponds, and to the time derivative $\dot{\mathbf{J}}$, the thermodynamic force $\nabla(\theta^{-1}\Lambda)$ corresponds.

To a first approximation, the thermodynamic forces are linearly related to the corresponding fluxes and flux rates. Therefore, from expression (7), we have

$$\nabla\theta^{-1} = R_{11}\mathbf{J} + R_{12}\dot{\mathbf{J}}, \tag{8}$$

$$\nabla(\theta^{-1}\Lambda) = R_{21}\mathbf{J} + R_{22}\dot{\mathbf{J}}. \tag{9}$$

Thus, for a single irreversible process, we obtained two phenomenological equations. According to the Onsager-Casimir principle, the matrix of the coefficients R_{ij} is antisymmetric, i.e.,

$$R_{12} = -R_{21}. \tag{10}$$

Using phenomenological equations (8) and (9), we replace the thermodynamic forces in expression (7) for the entropy production:

$$\sigma_{\text{COMPL}} = \overbrace{\underbrace{R_{11}\mathbf{J}\cdot\mathbf{J}}_{\sigma_{\text{EIT}}} + R_{12}\mathbf{J}\cdot\dot{\mathbf{J}}}^{\sigma_{\text{CIT}}} + R_{21}\mathbf{J}\cdot\dot{\mathbf{J}} + R_{22}\dot{\mathbf{J}}\cdot\dot{\mathbf{J}} \geq 0. \tag{11}$$

[1] Conventional version of EIT is based on the postulate that entropy density is function of dissipative fluxes, i.e., $s = s(u, \mathbf{J})$.

Since the matrix of phenomenological coefficients is antisymmetric (relation (10)), the expression for the entropy production is considerably simplified:

$$\sigma_{\text{COMPL}} = \underbrace{R_{11}\mathbf{J}\cdot\mathbf{J}}_{\sigma_{\text{EIT}}} + R_{22}\dot{\mathbf{J}}\cdot\dot{\mathbf{J}} \geq 0, \tag{12}$$

from which it follows that the diagonal coefficients are positive: $R_{11} > 0$, $R_{22} > 0$.

Let us transform phenomenological equation (8) in the form

$$\frac{R_{12}}{R_{11}}\frac{\partial\mathbf{J}}{\partial t} + \mathbf{J} = -\frac{1}{R_{11}\theta^2}\nabla\theta. \tag{13}$$

Comparing equations (13) and (1), we find the expression for generalized temperature,

$$\theta = T, \tag{14}$$

and relationship between the coefficients: $R_{11} = \frac{1}{\lambda T^2}$, $R_{12} = \frac{\tau}{\lambda T^2}$.

The expression for the phenomenological coefficient R_{22} can be found from Gibbs-Duhem equation in the form

$$u\frac{\partial\theta^{-1}}{\partial t} + \dot{u}\frac{\partial(\theta^{-1}\Lambda)}{\partial t} = 0. \tag{15}$$

By analogy with expressions for R_{11} and R_{12} and from dimension considerations, one might expect that $R_{22} = \frac{\tau_1^2}{\lambda T^2}$, where τ_1 has the dimensions of time.

Let us integrate the entropy production (12) with respect to volume and time from a certain unsteady state of isolated system to the equilibrium state (from t to ∞), which gives

$$S_{\text{COMPL}} - S_0 = \overbrace{-\int\int_t^\infty R_{11}\mathbf{J}\cdot\mathbf{J}dVdt}^{S_{\text{EIT}}-S_0} - \int\int_t^\infty R_{22}\dot{\mathbf{J}}\cdot\dot{\mathbf{J}}dVdt, \tag{16}$$

where S_0 is the entropy of the system in the equilibrium state.

Entropy change of the model isolated system. Let us consider a heat-insulated solid rod of length L in which the initial temperature distribution has the form

$$T(x, 0) = T_0 + a\cos(kx), \tag{17}$$

where T_0 is the equilibrium temperature that is reached in the isolated rod, a is the initial deviation

from T_0 at the rod boundaries and $k = m\pi/L$, $m = 1, 2, ...$

The solution to telegraphe equation (2) under initial conditions (17) and time derivative of solution have the form

$$T(x,t) = T_0 + a\cos(\omega t)e^{-t/2\tau}\cos(kx), \tag{18}$$

$$\dot{T}(x,t) = -\frac{a}{2\tau}[2\omega\tau\sin(\omega t) + \cos(\omega t)]e^{-t/2\tau}\cos(kx), \tag{19}$$

where $\omega = \frac{1}{2\tau}\sqrt{4k^2\chi\tau - 1}$ is the frequency of damped oscillations of temperature $T(x,t)$ in the vicinity of T_0 (provided that the inequality $4k^2\chi\tau > 1$ is valid).

The heat flux that is the solution to Maxwell-Cattaneo equation (1) and the rate of change in the flux are respectively written as

$$\begin{aligned} J(x,t) &= \frac{2k\lambda a}{(4\omega^2\tau^2+1)}[2\omega\tau\sin(\omega t) + \\ &\quad + \cos(\omega t)]e^{-t/2\tau}\sin(kx), \end{aligned} \tag{20}$$

$$\begin{aligned} \dot{J}(x,t) &= -\frac{2k\lambda a}{(4\omega^2\tau^2+1)}\frac{1}{\tau}\left[2\omega\tau\sin(\omega t) - \right. \\ &\quad \left. -\frac{4\omega^2\tau^2-1}{2}\cos(\omega t)\right]e^{-t/2\tau}\sin(kx). \end{aligned} \tag{21}$$

Let us consider phenomenological equations (8), (9) at constant phenomenological coefficients:

$$\begin{aligned} \frac{\partial\theta^{-1}}{\partial x} &= \frac{1}{\lambda T_0^2}J + \frac{\tau}{\lambda T_0^2}\dot{J} = \\ &= \frac{ak}{T_0^2}\cos(\omega t)e^{-t/2\tau}\sin(kx), \end{aligned} \tag{22}$$

$$\begin{aligned} \frac{\partial(\theta^{-1}\Lambda)}{\partial x} &= -\frac{\tau}{\lambda T_0^2}J + \frac{\tau_1^2}{\lambda T_0^2}\dot{J} = \\ &= \frac{2k\tau a}{T_0^2(4\omega^2\tau^2+1)}\left[\frac{2\omega\tau(\tau_1^2+\tau^2)}{\tau^2}\sin(\omega t) - \right. \\ &\quad \left. -\frac{\tau_1^2(4\omega^2\tau^2-1)-2\tau^2}{2\tau^2}\cos(\omega t)\right]e^{-t/2\tau}\sin(kx). \end{aligned} \tag{23}$$

The thermodynamic forces (22), (23) can be represented by gradients of temperature and temperature time derivative:

$$\frac{\partial\theta^{-1}}{\partial x} = -\frac{1}{T_0^2}\frac{\partial T}{\partial x}, \tag{24}$$

$$\frac{\partial(\theta^{-1}\Lambda)}{\partial x} = -\frac{\tau_1^2}{\tau T_0^2}\frac{\partial T}{\partial x} - \frac{4(\tau_1^2+\tau^2)}{T_0^2(4\omega^2\tau^2+1)}\frac{\partial\dot{T}}{\partial x}. \tag{25}$$

Integration of the equations (24), (25) gives

$$\theta^{-1} = T_0^{-1} - \frac{1}{C_v T_0^2}u, \tag{26}$$

$$\theta^{-1}\Lambda = -\frac{\tau_1^2}{\tau C_v T_0^2}u - \frac{4(\tau_1^2+\tau^2)}{C_v T_0^2(4\omega^2\tau^2+1)}\dot{u}, \tag{27}$$

where $\dot{u} = C_v\dot{T}$ and

$$u = C_v(T - T_0). \tag{28}$$

We have used phenomenological coefficients $R_{11} = 1/(\lambda T_0^2)$, $R_{12} = -R_{21} = \tau/(\lambda T_0^2)$ at $T = T_0$. The condition $T = T_0$ at any x is met at $\cos\omega t = 0$ (18), i.e., at $\omega t = \frac{\pi}{2} + n\pi$, where $n = 0, 1, 2\ldots$. Let us next find the coefficient R_{22} at $T = T_0$. Taking into account (28), (26) and (27), let us solve Gibbs-Duhem equation (15) and consider this solution at $\omega t = \frac{\pi}{2} + n\pi$. We obtain in this way simple expressions: $\tau_1^2 = 4\tau^2/(4\omega^2\tau^2 - 3)$ and

$$R_{22} = \frac{4\tau^2}{\lambda T_0^2(4\omega^2\tau^2-3)}. \tag{29}$$

Further, we will obtain an explicit expression for (16) in one-dimensional case,

$$\begin{aligned} S_{\mathrm{COMPL}} - S_0 &= -\frac{1}{\lambda T_0^2}\int_t^\infty\int_0^L J^2\,dx\,dt - \\ &\quad -\frac{4\tau^2}{\lambda T_0^2(4\omega^2\tau^2-3)}\int_t^\infty\int_0^L \dot{J}^2\,dx\,dt. \end{aligned} \tag{30}$$

Introducing dimensionless quantities $\tilde{t} = t/\tau$, $\tilde{\omega} = \omega\tau$, $\tilde{x} = x/L$,

$$\tilde{S}_{\mathrm{COMPL}} - \tilde{S}_0 = \frac{T_0^2(4\tilde{\omega}^2+1)}{4k^2L\lambda a^2\tau}(S_{\mathrm{COMPL}} - S_0),$$

and using (20), (21), we bring equality (30) to the dimensionless form and integrate with respect to $\tilde{x}$ and $\tilde{t}$. As a result, we obtain expression

$$\tilde{S}_{\mathrm{COMPL}} - \tilde{S}_0 = -\frac{2\tilde{\omega}^2 - \cos^2(\tilde{\omega}\tilde{t})}{4\tilde{\omega}^2 - 3}\,e^{-\tilde{t}}. \tag{31}$$

Figure 2 presents the graphs of $\tilde{S}_{\mathrm{COMPL}} - \tilde{S}_0$ versus $\tilde{t}$ at $\tilde{\omega} = 3.5$. At $\tilde{\omega} \to \infty$, we have $\tilde{S}_{\mathrm{COMPL}} - \tilde{S}_0 \to -e^{-\tilde{t}}/2$. It is seen that $S_{\mathrm{COMPL}} - S_0$ is more general than the corresponding expression in the conventional version of EIT (expressions (30), (16)). A more general expression for the total entropy allowed us to determine the strictly monotonic dependence that adequately describes the behavior of the entropy of the model isolated system.

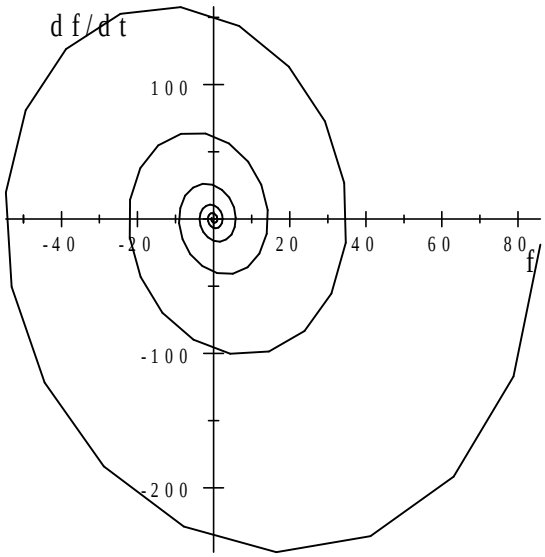

Figure 3: The time derivative of f versus f at $\omega = 3.5$ and $\tau = 1$.

Comparison with the damped oscillator. Let us enter value f which is independent of the spatial coordinate x:

$$f(t) = \frac{1}{a}\sqrt{\frac{4\tau^2}{C_v^2}\dot{u}^2 + \frac{(4\tilde{\omega}^2+1)^2}{4k^2\lambda^2}J^2} =$$

$$= [2\omega\tau\sin(\omega t) + \cos(\omega t)]e^{-t/2\tau}.$$

In Fig 3 is presented f—$\dot{f}$ relation which is similar to the damped oscillator phase-plane portrait, well known in classical mechanics. It indicates the uniformity of the description of oscillating systems in extended thermodynamics and classical mechanics.

[1] D. Jou, J. Casas-Vázquez, G. Lebon, Extended Irreversible Thermodynamics, Third Ed., Springer, Berlin, 1996.

[2] M. Criado-Sancho, J.E. Llebot, Phys. Rev. E. 47 (1993) 4104.

[3] D. Jou, J. Casas-Vázquez, G. Lebon, Rep. Prog. Phys. 62 (1999) 1035.

[4] I. Müller, T. Ruggeri, Extended Thermodynamics, Springer, New York, 1993.

[5] L.S. Garsia-Cólin, F.J. Uribe, J. Non-Equilib. Thermodyn. 16 (1991) 89.

[6] R.E. Netletton, S.L. Sobolev, J. Non-Equilib. Thermodyn. 20 (1995) 205.

[7] S.I. Serdyukov, Phys. Lett. A 316 (2003) 177.

[8] S.I. Serdyukov, Phys. Lett. A 324 (2004) 262.

[9] S.I. Serdyukov, C. R. Physique 8 (2007) 93.

A method to obtain thermodynamic fundamental equations

André Serrenho, Tânia Sousa and Tiago Domingos

Environmental and Energy Section, DEM and IN+ Center for Innovation, Technology and Policy Research, Instituto Superior Técnico, Av. Rovisco Pais, 1, 1049-001 Lisboa, Portugal

andre.cabrera.serrenho@ist.utl.pt

The Gibbs-Tisza-Callen formalism presents a deductive and axiomatic nature. This thermodynamic formalism started with Gibbs' studies, which are often known as Gibbsian thermostatics, introduced a new approach in thermodynamics. These works achieve an elegant and economic way of expressing all classical thermodynamic principles on an equation on entropy, internal energy, volume and mole numbers of all intervening chemical compounds: the so-called fundamental equation of the system [1-2].

Many authors obtain equations of state or other relations based on empirical assessments that translate the thermodynamic properties of a given system in a given range of conditions [3-5]. However, according to the Gibbs-Tisza-Callen formalism, it is of great importance to know the fundamental equation, because it summarizes all available information within a single equation that contains more than the initially available equations. With the fundamental equation we are then able to determine all equations of state, the thermodynamic coefficients and the equilibrium conditions, thus obtaining a full knowledge on the system's behavior.

However obtaining the fundamental equation of a thermodynamic system is not always an easy task, once the available data is often acquired from empirical assessments. Thus this data leads to empirical models based on equations whose variables are necessarily experimentally measurable, like temperature, pressure and volume, among others. With these equations it is not straightforward to obtain a fundamental equation because they are not functions of internal variables like entropy or internal energy.

In addition, the complexity of the procedure to obtain a fundamental equation is strongly related to the nature of the variables presented in the available equations. However the basis of the method followed to obtain the fundamental equation is the same, i.e. the resolution of a system of partial differential equations

subjected to all available information and the constraints from intensive variables and definition of thermodynamic coefficients.

Due to the diversity among the empirical information that might be available it becomes impossible to set up a clear method which necessarily results in obtaining the system's fundamental equation. However a set of recommendations in order to obtain the fundamental equation should take into account the following goals by order of relevance:

a. decrease the level of differentiation of the variables, through integration;
b. determine the unknown functions that result from the integration processes, given that we are integrating partial derivatives.

In this context we developed an iterative sequence of procedures in order to obtain the fundamental equation from equations of state, thermodynamic coefficients or other equations involving any combinations of variables and taking into account the mathematical framework of Gibbs-Tiszia-Callen formalism and the use of Maxwell relations:

---

1. Integrate, if possible, one of the available partial derivatives, considering both the entropy and the energy scheme. If it is not possible to integrate any available partial derivative, try to replace variables in order to obtain equations with partial derivatives that allow integration.

Execute step 2 only if it was impossible to perform step 1.

2. For equations without thermodynamic coefficients or first derivatives of unknown functions obtain other partial derivatives. For each partial derivative obtained:
    a. Use Maxwell relation to transform partial derivatives in other derivatives.
    b. If there are other equations that involve thermodynamic coefficients, use their definitions and, if necessary, Maxwell relations to obtain other thermodynamic coefficients from partial derivatives already obtained.

Execute step 3 only if it was impossible to perform step 2.

3. If the available equations contain thermodynamic coefficients, use the following relations in order to obtain other coefficients (note that only two of these equations are independent).

$$C_P = C_v + \frac{vT\alpha^2}{\kappa_T} \;\; ; \;\; \kappa_T = \kappa_s + \frac{vT\alpha^2}{C_P} \;\; ; \;\; \frac{C_P}{C_v} = \frac{\kappa_T}{\kappa_s}$$

Execute step 4 after each previous step (1 to 3) successfully achieved.

4. For equations with unknown functions, perform the following:
    a. For equations of one variable and one unknown function, determine directly the unknown function.

b. For equations of two variables, apply the separation of variables and perform step 4a with the equation obtained.

c. For more than one equations of the same three variables with unknown functions of only one or two of them, try to eliminate the remaining variable(s) and perform step 4 again.

If the fundamental equation is not obtained, resume step 1 considering all supplementary information.

The proposed method for obtaining fundamental equations for systems of a single component was verified for the examples presented in Table 1. These results show a wide range of applicability of the method.

Table 1: Examples in obtaining the fundamental equation for systems with a single component following the proposed method.

Initial information	Fundamental equation
$T = \frac{3As^2}{v}$ $P = \frac{As^3}{v^2}$	$u = u_0 + \frac{As^3}{v} - \frac{As_0^3}{v_0}$
$\alpha = \frac{AP}{vT^2}$ $u = BT^2$	$s = \pm\frac{\sqrt{B}}{2}\left(\sqrt{u} + \frac{v}{v_0}\sqrt{u_0}\right) \mp \frac{vs_0}{v_0} \pm \frac{v}{2A}(v + v_0)$
$Pv = RT$ $\frac{\kappa_T}{\kappa_s} = a$	$s = s_0 \frac{\ln v\left(\frac{a-1}{R}u\right)^{\frac{1}{a-1}}}{\ln v_0\left(\frac{a-1}{R}u_0\right)^{\frac{1}{a-1}}}$
perfect gas model $u = cRT$ $C_P = C_v + R$ $\lim_{T\to 0} v = 0$	$s = s_0 + cR\ln\frac{u}{u_0} + K_1\ln\frac{v}{v_0}$
virial model $P = RT\sum_{i=1}^{\infty}\frac{B_i}{v^i}$ $\lim_{v\to\infty}\left(s - s^{(GP)}\right) = 0$ $\lim_{v\to\infty}\left(u - u^{(GP)}\right) = 0$	$s = s_0 + R\ln\frac{v}{v_0} + cR\ln\frac{u}{u_0} - R\sum_{i=2}^{\infty}\frac{B_i}{v^{i-1}}$
van der Waals model $P = \frac{RT}{v-b} - \frac{a}{v^2}$ $\lim_{v\to\infty}\left(s - s^{(GP)}\right) = 0$ $\lim_{v\to\infty}\left(u - u^{(GP)}\right) = 0$	$s = s_0 + R\ln\left[\left(\frac{uv + a}{vu_0}\right)^c \frac{v-b}{v_0}\right]$

Furthermore the proposed method allowed us to obtain, as far as we know, some new results, e.g. the fundamental equation for a simplified virial equation with constant coefficients.

Our method also allowed us to determine the fundamental equation from the van der Waals equation of state already determined by Callen [2] who argued that it was an arbitrary result. However by using the proposed procedure we concluded that this is a consistent and logical result because we only used the equation of state and the assumption that the van der Waals model should reduce to the perfect gas model with an infinite volume or a null pressure.

Acknowledgements

This work was supported by the FCT grant no. SFRH/BD/46794/2008.

List of references

[1] L. Tisza, *Generalized Thermodynamics*. (The MIT Press, Massachusets, 1966).

[2] H. B. Callen, *Thermodynamics and an Introduction to Thermostatistics*, 2nd ed. (John Wiley & Sons Ltd, New York, 1985).

[3] I Made Astina and Haruki Sato, *Fluid Phase Equilibr.* **221**, 103-111 (2004).

[4] Q. Chen, R. Hong and G. Chen, *Fluid Phase Equilibr.* **269**, 113-116 (2008).

[5] H. Miyamoto, T. Koshi and M.Uematsu, *J. Chem. Thermodyn.* **40**, 558-566 (2008).

Theoretical Limits of Internal Combustion Engines Miniaturization

E. Sher[1], I. Sher[2] and D. Sher[3]

[1]The Sir Bagrit Professor, The Pearlstone Center for Aeronautical Studies, Department. of Mechanical Engineering, Ben-Gurion University of the Negev, Beer-Sheva, Israel, sher@bgu.ac.il
[2]Department of Process and Systems Engineering, Cranfield University, Cranfield, Bedfordshire MK43 0AL, United Kingdom
[3]Department. of Mechanical Engineering, Ben-Gurion University of the Negev, Beer-Sheva, Israel

Small-scale energy conversion devices are being developed for a variety of applications; these include propulsion units for MAV. In some cases, batteries supply the required power, though their low energy density significantly limits their energy capacity per weight, and the energy supply units represent a substantial fraction of the total load carried by the assigned platform.

The high specific energy of hydrocarbon and hydrogen fuels, as compared to other energy storing means, like, batteries, elastic elements, flywheels, pneumatics, and fuel cells, appears to be an important advantage, and favors the ICE as a candidate. In addition, the specific power (power per mass of unit) of the ICE seems to be much higher than that of other candidates like fuel cells, photovoltaic, and battery units.

However, micro ICE engines are not simply smaller versions of full-size engines. Physical processes such as combustion, gas exchange, and heat transfer, are performed in regimes different from those occur in full-size engines. Consequently, engine design principles are different at a fundamental level, and have to be re-considered before they are applied to micro-engines. Scaling-down results in larger heat losses to the cylinder walls (due to the high area to volume ratio of the combustion chamber), smaller effective combustion volume and higher fuel consumption (due to the high portion of the quenching volume), and, higher flow losses, slower combustion and mixing processes (due to the small dimensions, thus low Reynolds numbers).

When a Spark-Ignition (SI) cycle is considered, part of the energy that is released during combustion is used to heat-up the mixture in the quenching volume, and therefore the flame-zone temperature is lower and in some cases can theoretically fall below the self-sustained combustion temperature. The flame quenching thus seems to limit the minimum dimensions of a SI engine. This limit becomes irrelevant when a Homogeneous-Charge Compression-Ignition (HCCI) cycle is considered. In this case friction losses and charge leakage through the cylinder-piston gap become dominant, constrain the engine size, and impose minimum engine speed limits.

In the present work a phenomenological model has been developed to consider the relevant procuresses inside the cylinder of a Homogeneous-Charge Compression-Ignition (HCCI) engine. The lower possible limits of scaling-down HCCI cycle engines are proposed. The present work postulates the inter-relationships between the pertinent parameters, and constitutes the lower possible miniaturization limits of IC engines.

Energetic criteria for droplet breakup

I. Sher[1] and E. Sher[2]

[1]*Department of Process and Systems Engineering, Cranfield University, Cranfield, Bedfordshire MK43 0AL, United Kingdom*
[2]*The Sir Bagrit Professor, The Pearlstone Center for Aeronautical Studies, Department. of Mechanical Engineering, Ben-Gurion University of the Negev, Beer-Sheva, Israel*

A liquid droplet in high speed trajectory through ambient gas is a prevalent case in spray injection systems. The fate of such a droplet is of importance to the prediction of overall spray characteristics. The phenomenon of droplets breakup to smaller droplets is referred to as secondary breakup in the context of spraying systems. This phenomenon poses some fundamental problems of transformation between different energetic states.

A theoretical analysis of the problem is presented, in which an overall energy balance is examined, that includes surface, kinetic and dissipation energies. Transformation between states, i.e. between a droplet and its breakup products, is a spontaneous process, under instantaneous trajectory conditions that include drag forces. Transformation involves the reversible surface and kinetic energy transitions, and the irreversible viscous dissipation energy.

Non-isothermal conditions, as in the common case of injection into a hot ambient, poses a further effect of transient surface tension, and consequently transient surface energy. These can be determined by an additional balance of thermal energy, and a simple model of surface tension dependency on temperature, based on a modified van der Waals state equation.

Surface Tension and Excess Molar Volumes of Trimethyl benzene with Tetrahydrofuran ,Tetra-chloromethane and Dimethyl Sulfoxide

R.K.Shukla[*1], Vatsala Dwivedi[2] and Atul Kumar[3]
[1]Department of Chemistry, V.S.S.D.College, Kanpur, U.P. (India) ,
e-mail: rajeevshukla47@rediffmail.com,
[2]Department of Chemistry, Atarra P.G.College, Atarra, U.P. (India),
[3]Department of Chemistry, P.S.I.T, Kanpur, U.P. (India)

Prediction of surface tension and excess volume is of out standing importance in many scientific and technological areas. As a fundamental parameter, surface tension is the single most accessible parameter that describes the thermodynamic state and contains implicit information on the internal structure of a liquid interface. Apart from this theoretical interest, a detailed understanding of the behaviour of a vapor-liquid interface, such as enrichment of one component in a liquid surface is important for modeling a distillation process. The study of excess volume leads with the two structural aspects that is, size difference of molecules and interaction forces between molecules.

In the present work, the Prigogine [1] corresponding states principle for the bulk properties of liquids is extended[2] to their surface tension. The Prigogine-Saraga cell model theory [3] of surface tension is then used together with the statistical mechanical theory of Flory [4]. The component liquids (six binaries) which are taken in the present work are (tetrahydrofuran+ 1,2,4-trimethyl benzene, tetrahydrofuran+1,3,5-trimethyl benzene, tetrachloromethane +1,2,4- trimethyl benzene, tetrachloromethane +1,3,5- trimethyl benzene, dimethyl solfoxide+ 1,2,4- trimethyl benzene and dimethyl solfoxide+ 1,3,5- trimethyl benzene over the entire concentation range at 298.15 K. for theoretical prediction of surface tension and excess molar volume. Though the model was derived for γ-meric spherical chain molecules, but its application to polar-non polar cyclic liquid mixture have been carried out successfully which have immence sense of applicability in organic separation and synthesis as solvent. Further, we found that computed results are in good agreement with the experimental findings. The results so obtained have been explained on the basis of packing effect and dipolar-dipolar interactions. An attempt has also been made to study the excess thermodynamic functions which are the measure of extent of molecular interactions involved in the liquid mixture.

Theoretical

Prigogine and Sarage [3] have given a simple cell model of the surface tension of spherical molecule liquids based on (6,12) potential. In the following extension, a segment is moving from the bulk to the surface experiences an increase of the configurational energy equal to $-M\tilde{U}(\tilde{U})$ due to the loss of a fraction, M, of its nearest neighbour at the surface. The resulting reduced surface tension in case of vander Waals liquid is;

$$\tilde{\sigma}(\tilde{v}) = \left[M\tilde{v}^{-5/3} - \left(\frac{\tilde{v}^{1/3} - 1.0}{\tilde{v}^{2}} \right) \ln \left(\frac{\tilde{v}^{1/3} - 0.5}{\tilde{v}^{1/3} - 1.0} \right) \right] \qquad (1)$$

The statistical theory of Flory [4] yields the following equation for surface tension of liquid and liquid mixtures as;

$$\sigma = \sigma^{*}\,\tilde{\sigma}(\tilde{v}) \tag{2}$$

Flory theory is closely connected with the corresponding state theory of Prigogine. Patterson and Rastogi [5] in their extension of the corresponding- state theory, dealt with the surface tension in terms of reduction parameters,

$$\sigma^{*} = k^{1/3} p^{*2/3} T^{*1/3} \tag{3}$$

The equation for excess volume according to Flory theory can be expressed as

$$\tilde{v} - \tilde{v}_0 = v^{E} = \frac{v^{E}}{x_1 v_1^{*} + x_2 v_2^{*} + x_3 v_3^{*}} \tag{4}$$

the ideal reduced volume ($\tilde{v}_0$) is related to

$$\tilde{v}_0 = \psi_1 \tilde{v}_1 + \psi_2 \tilde{v}_2 \tag{5}$$

and

$$V^{E} = (x_1 v_1^{*} + x_2 v_2^{*})[\tilde{v} - (\psi_1 \tilde{v}_1 + \psi_2 \tilde{v}_2)] \tag{6}$$

All the notations used in the above equations have their usual significance as detailed out by Flory.

The excess surface tension can be expressed as

$$\sigma^{E} = [\sigma_{cal} - \sigma_{idl}] \tag{7}$$

Results and Discussion

Surface tension, excess surface tension and excess molar volume for six cyclic polar-non polar liquid mixtures namely[1] (tetrahydrofuran+ 1,2,4-trimethyl benzene,[2] tetrahydrofuran+1,3,5- trimethyl benzene,[3] tetrachloromethane +1,2,4- trimethyl benzene, [4] tetrachloromethane +1,3,5- trimethyl benzene, [5] dimethyl solfoxide+ 1,2,4- trimethyl benzene and [6] dimethyl solfoxide+ 1,3,5- trimethyl benzene, have been predicted over the whole composition range at 298.15 K. All the necessary data have been taken from the work of P.Chuanrong et.al.[6]. The results of theoretical excess volume and surface tension are found fairly good both in magnitude and sign as compared with experiment. The results of V^{E}_{Cal} values shows positive for system [1], [6], [4] and [3] and negative values for system[5]and [2]. The values of excess surface tension are positive for systems [2] and [3] and negative for [6], [5], [4] and [2]. Since the theoretical results are very close to experimental finding it can be concluded that interactions are weak because 1,3,5 trimethyl benzene is a symmetrical non-polar molecule. Negative values of σ^{E} can be interpreted in terms of little stronger interactions which are dipolar-dipolar in nature. The positive value of V^{E} are possibly due to packing effect.

Conclusively it can be stated that Prigogine-Flory-Patterson model is very much suitable for the systems having weak molecular interactions particularly in nonpolar-polar cyclic liquid mixtures. Negative and Positive deviations in the values of V^{E} and σ^{E} are capable to decide the nature of solvent in the distillation process.

Mole Fractions (X_1), Excess Volume (V^E), Surface Tension (σ_{exp}), Surface Tension (σ_{theo}), and Density (ρ) of binary liquid mixtures at 298.15 K.

THF + 1,2,4-TMB

x_1	V^E / ccmol^{-1}	σ(exp)	σ_m(thr)	δσ / mNm^{-1}	ρ_m / g.cm^{-3}
0.1	0.0371	29.11	24.81	-0.01	0.8727
0.2	0.0698	29.00	24.62	-0.03	0.8737
0.3	0.0947	28.88	24.44	-0.04	0.8748
0.4	0.1125	28.73	24.26	-0.05	0.8758
0.5	0.1224	28.53	24.08	-0.06	0.8769
0.6	0.1228	28.29	23.91	-0.07	0.8779
0.7	0.1128	28.01	23.74	-0.07	0.8789
0.8	0.0901	27.68	23.58	-0.06	0.8800
0.9	0.0530	27.34	23.43	-0.04	0.8810

THF+1,3,5-TMB

x_1	V^E / ccmol^{-1}	σ(exp)	σ_m(thr)	δσ / mNm^{-1}	ρ_m / g.cm^{-3}
0.1	0.0305	27.88	24.01	-0.01	0.8631
0.2	0.0563	27.72	23.91	-0.03	0.8653
0.35	0.0840	27.57	23.77	-0.04	0.8684
0.4	0.0904	27.44	23.73	-0.05	0.8694
0.5	0.0980	27.32	23.64	-0.06	0.8716
0.6	0.0980	27.23	23.55	-0.07	0.8737
0.7	0.0895	27.15	23.47	-0.06	0.8758
0.8	0.0717	27.09	23.40	-0.06	0.8778
0.9	0.0421	27.06	23.34	-0.04	0.8800

TCM+1,2,4-TMB

x_1	V^E / ccmol^{-1}	σ(exp)	σ_m(thr)	δσ / mNm^{-1}	ρ_m / g.cm^{-3}
0.05	0.0135	29.13	24.89	-0.004	0.9069
0.1	0.0264	29.04	24.79	-0.009	0.9426
0.2	0.0498	28.89	24.60	-0.016	1.0131
0.3	0.0701	28.72	24.40	-0.024	1.0854
0.4	0.0857	28.50	24.20	-0.029	1.1569
0.6	0.0984	28.24	23.81	-0.035	1.2980
0.7	0.0927	27.89	23.62	-0.034	1.3692
0.8	0.0764	27.54	23.44	-0.028	1.4403
0.9	0.0459	27.13	23.25	-0.017	1.5134

TCM+ 1,3,5-TMB

x_1	V^E / ccmol^{-1}	σ(exp)	σ_m(thr)	δσ / mNm^{-1}	ρ_m / g.cm^{-3}
0.1	0.0858	27.77	23.944	-0.058	0.9340
0.2	0.1570	27.53	23.791	-0.108	1.0066
0.3	0.2114	27.29	23.648	-0.150	1.0774
0.4	0.2503	27.10	23.511	-0.184	1.1506
0.5	0.2697	26.99	23.389	-0.205	1.2223
0.6	0.2685	26.91	23.281	-0.211	1.2943
0.7	0.2443	26.86	23.191	-0.199	1.3661
0.8	0.1951	26.83	23.124	-0.166	1.4371
0.9	0.1120	26.81	23.084	-0.099	1.5124

DMSO + 1,2,4-TMB

x_1	V^E / ccmol^{-1}	σ(exp)	σ_m(thr)	δσ / mNm^{-1}	ρ_m / g.cm^{-3}
0.1	-0.0508	28.48	21.22	-4.735	0.8942
0.2	-0.0926	28.77	21.90	-5.014	0.9166
0.3	-0.1251	28.81	22.61	-5.272	0.9390
0.4	-0.1472	29.10	23.32	-5.503	0.9611
0.5	-0.1584	29.46	24.09	-5.710	0.9838
0.6	-0.1570	29.34	24.88	-5.877	1.0062
0.7	-0.1423	29.35	25.70	-5.998	1.0282
0.8	-0.1124	30.04	26.59	-6.067	1.0506
0.9	-0.0646	35.71	27.57	-6.066	1.0734

DMSO+ 1,3,5-TMB

x_1	V^E / ccmol^{-1}	σ(exp)	σ_m(thr)	δσ / mNm^{-1}	ρ_m / g.cm^{-3}
0.1	-0.0610	27.30	25.031	-0.146	0.8850
0.2	-0.1087	26.92	25.926	-0.261	0.9076
0.3	-0.1486	26.70	26.919	-0.359	0.9320
0.4	-0.1743	27.41	27.885	-0.423	0.9551
0.5	-0.1871	28.40	28.888	-0.457	0.9783
0.6	-0.1854	30.09	29.941	-0.456	1.0018
0.7	-0.1679	32.05	31.016	-0.416	1.0250
0.8	-0.1320	34.77	32.164	-0.330	1.0487
0.9	-0.0770	37.92	33.342	-0.195	1.0720

Figure :Variation of Excess molar Volume (V^E) with mole fraction(X^1)

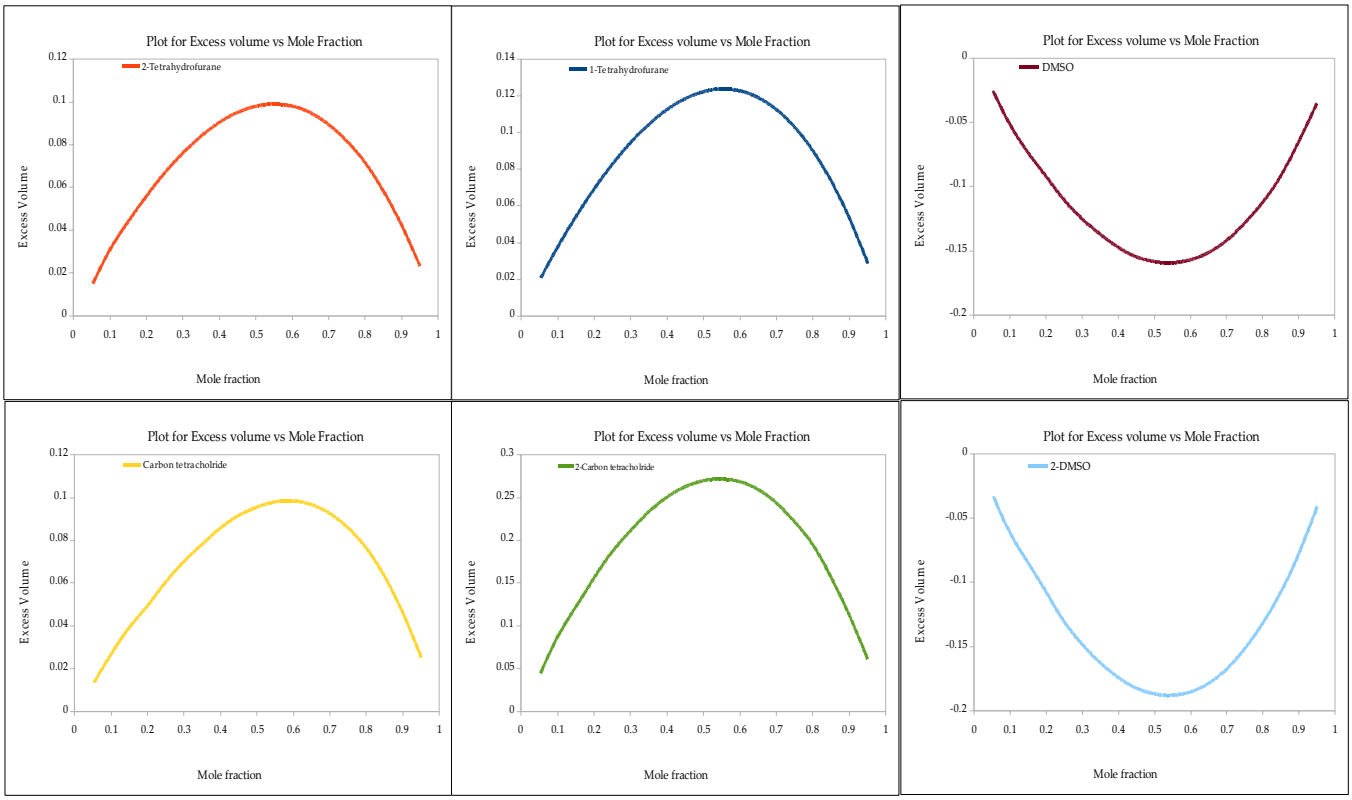

References

1. I.Prigogine, A.Bellemand and V.Mathot, "The Molecular Theory of Solutions," North-Holl and Pub. Co., Amsterdan, Chapter 17, Inc., New York, N.Y.1957.
2. J.D.Pandey, R.D.Rai and R.K.Shukla, J.Chem. Soc. Faradey Trans. I, 85(2), 331 (1989).
3. I.Prigogine and L.Saraga, J.Chem. Phys., 49, 399(1952).
4. (a) P.J.Flory, R.A.Orwall andA.Vrij, J. Amer. Chem. Soc. 86, 3507 (1964); (b) A.Abe and P.J.Flory, Ibid., 87, 1838 (1965).
5. D.Patterson and A.K.Rastogi, J.Phys. Chem., 48, 1067 (1970).
6. P.Chaunrong, Q.Ke, G.Quyang, X.Zhen,Y.Yang and Z.Huang, J.Chem. Eng. Data., 49, 1839 (2004).

Inhomogeneous density distributions of ideal gases in nano structures

Sisman A[1], Firat C[1,2] and Ozturk ZF[1,3]

[1]Energy Institute, Istanbul Technical University, 34469 Maslak, Istanbul, Turkey.
[2]San Diego State University, Center for Renewable Energy and Energy Efficiency, 5500 Campanile Drive San Diego, CA 92182 USA.
[3]Department of Photonics Engineering, Technical University of Denmark, DK-2800 Kongens Lyngby, Denmark.

e-mail: sismanal@itu.edu.tr

Abstract

Due to the wave nature of particles, density of an ideal gas is actually not homogenous even at thermodynamic equilibrium. Inhomogeneous region occurs near to the domain boundaries and it is called quantum boundary layer, QBL. Thickness of QBL is in the order of mean de Broglie wavelength of particles, $\overline{\lambda}$. Therefore inhomogeneity becomes important for the gases confined in nano structures although it is totally negligible in macro ones. The existence of QBL changes the thermodynamic behavior of gases considerably in nano scale. In this study, density distributions of ideal Maxwell, Fermi and Bose gases at thermodynamic equilibrium are examined by considering the wave nature of particles. Density profiles of Fermi and Bose are analyzed under quantum degeneracy conditions, namely low temperature and/or high density conditions. It is seen that there is a density oscillation in a degenerate Fermi gas. The magnitude of oscillations decreases with increasing distance to the boundaries and a flat distribution is recovered in the inner regions of the domain. In a degenerate Bose gas, QBL occupies the entire domain and there is no flat region in density distribution.

1. Introduction

In nano scale, thermodynamic behaviors of gases are considerably different than those in macro scale. The wave nature of gas particles causes some new effects which can be used to design and produce completely new cycles and devices. Design and fabrication of thermodynamic gas cycles in nano scale will soon be possible since today's technology makes the production of the mechanical structures in nano scale possible [1-4]. Consequently, quantum effects on thermodynamic behaviors of gases constitute an interesting research subject [5-14].

For an ideal gas consisting of N particles confined in a domain of volume V, classical thermodynamics predicts a homogenous density distribution in an equilibrium state and the density is given by $n_{cl} = N/V$. This result is actually based on the classical probability density, which considers the particle nature of gas atoms. The classical probability density is a homogenous quantity and it is equal to $1/V$. Therefore, the density is simply N/V in case of a particle representation of gas atoms. If the wave nature of gas atoms is considered, however, the probability density is given by the square of the absolute value of eigenfunction (wavefunction) the Schrödinger equation for a particle in quantum state r, $|\psi_r(\mathbf{x})|^2$. Therefore, the particle density of an ideal gas in thermodynamic equilibrium is expressed more precisely as follows,

$$n(\mathbf{x}) = \sum_r n_r(\mathbf{x}) = \sum_r \frac{|\psi_r(\mathbf{x})|^2}{\exp[(\varepsilon_r - \mu)/k_b T] \mp 1}, \tag{1}$$

where n_r is the density of particles in a specific quantum state r, ε_r is the energy eigenvalue of particles, k_b is the Boltzmann's constant, T is temperature, μ is the chemical potential, ψ_r is the eigenfunction of the single particle Schrödinger equation for a quantum state r and $\boldsymbol{x}$ is the position vector. Plus (mines) sign is used for a Fermi (Bose) gas. Domain integration of density equals to the total number of particles N in the domain. Since the domain integration of $|\psi_r(\mathbf{x})|^2$ is always equal to unity, dimensionless density can be defined by using Eq.(1) as

$$\tilde{n}(\mathbf{x}) = \frac{n(\mathbf{x})}{n_{cl}} = \frac{\sum_r \frac{|\psi_r(\mathbf{x})|^2}{\exp[(\varepsilon_r - \mu)/k_b T] \mp 1}}{\frac{1}{V}\sum_r \frac{1}{\exp[(\varepsilon_r - \mu)/k_b T] \mp 1}}. \tag{2}$$

Right hand side of Eq.(2) represents the ratio of ensemble average of quantum probability to that of the classical one. In other words, it is the dimensionless ensemble average of quantum probability. For high temperature and/or low density conditions, quantum distributions go to Maxwell-Boltzmann distribution and Eq.(2) simplifies as

$$\tilde{n}(\mathbf{x}) = \frac{n(\mathbf{x})}{n_{cl}} = \frac{\sum_r \exp\left[-\varepsilon_r / k_b T\right] \left|\psi_r(\mathbf{x})\right|^2}{\frac{1}{V}\sum_r \exp\left[-\varepsilon_r / k_b T\right]} \tag{3}$$

To calculate the dimensionless local density given by Eqs.(2) and (3), energy eigenvalues and eigenfunctions of a single particle Schrödinger equation are need to be known and the Poisson summation formula has to be used to calculate the summations precisely. Therefore it is necessary to solve the single particle Schrödinger equation by considering the boundary conditions of the domain. The exact analytical solutions for both eigenvalues and eigenfunctions are possible only for a rectangular domain.

In a recent study [5], density distribution of an ideal Maxwell gas, Eq.(3), has been analytically calculated for a rectangular domain. It has been shown that the density of an ideal Maxwellian gas confined in a rectangular domain is not homogeneous even in thermodynamic equilibrium and there is a boundary layer in which the density goes to zero. The thickness of this layer is in the order of mean de Broglie wave length and the layer has been called quantum boundary layer (QBL) since its thickness goes to zero when the Planck's constant goes to zero, $\hbar \to 0$. In the study here, density distributions of Fermi and Bose given by Eq.(2) are analyzed under quantum degeneracy conditions, namely low temperature and/or high density conditions. The results are compared with that of the ideal Maxwell gas.

2. Density distributions of ideal Fermi and Bose gases in thermodynamic equilibrium

$_2He^3$ and $_2He^4$ gases are considered here as ideal Fermi and Bose gases respectively. They are assumed to be confined in a domain bounded by an infinite potential, which represents the non penetrable boundaries. For a particle confined in an arbitrary domain bounded by an infinite potential, stationary Schrödinger equation can be written as

$$\nabla^2 \psi_k(\mathbf{x}) + k^2 \psi_k(\mathbf{x}) = 0 \text{ in D}, \ \psi_k\big|_{\partial \mathrm{D}} = 0 \tag{4}$$

where D represents the bounded domain of an arbitrary shape, $k = \sqrt{2m\varepsilon_r}/\hbar$ is the wave number. To make the results independent from the length units, it is necessary to define the problem in a dimensionless spatial coordinates. Therefore, Eq.(2) is written in a dimensionless form by using a length scale L_* as follows

$$\tilde{n}(\tilde{\mathbf{x}}) = \frac{\sum_{\tilde{k}} \dfrac{\left|\psi_{\tilde{k}}(\tilde{\mathbf{x}})\right|^2}{\exp\left[\left(\dfrac{\alpha}{\pi}\right)^2 \tilde{k}^2 - \dfrac{\mu}{k_b T}\right] \mp 1}}{\dfrac{1}{\tilde{V}} \sum_{\tilde{k}} \dfrac{1}{\exp\left[\left(\dfrac{\alpha}{\pi}\right)^2 \tilde{k}^2 - \dfrac{\mu}{k_b T}\right] \mp 1}} \tag{5}$$

where $\tilde{V} = V/L_*^3$, $\tilde{k} = kL_*$, $\alpha = L_c/L_*$, $\tilde{\mathbf{x}} = \mathbf{x}/L_*$, L_c is one half of the most probable de Broglie wavelength given by $L_c = h/2\sqrt{2mk_bT} = \sqrt{\pi}\lambda_T/2$. L_* can be any length. In this study, it is simply chosen as $L_* = 5L_c$ for the calculations, which means $\alpha = 0.2$.

For one dimensional domain bounded by infinite potential, both eigenvalues and eigenfunctions of Eq.(4) can analytically be obtained. If they are used in Eq.(5) and the summations are calculated precisely, the density distributions of degenerate Fermi and Bose gases confined in one dimensional domain are obtained as seen in figure 1. Density distribution of a Maxwell gas is also given to compare the results. It is seen that the particles stand away from the boundaries and density distribution of even an ideal gas is not homogenous. There is a boundary layer in which the density goes to zero. Thickness of this layer takes the largest value for Bose gas and the smallest value for Fermi gas. Wave nature of particles keeps the gas away from the boundaries and increases the density of inner region of the domain. Furthermore, Friedel-like oscillations appear in case of degenerate Fermi gas.

For a two dimensional rectangular domain, analytical solution of Eq.(4) is again possible and the results are shown in figure 2 and figure 3 for Fermi and Bose gases respectively. In figure 2, it is seen that the superposition of Friedel-like oscillations in each direction causes peaks at the corners. The results of Fermi and Bose gases are obtained for 10K, 1.000 atm and 10K, 80 atm respectively.

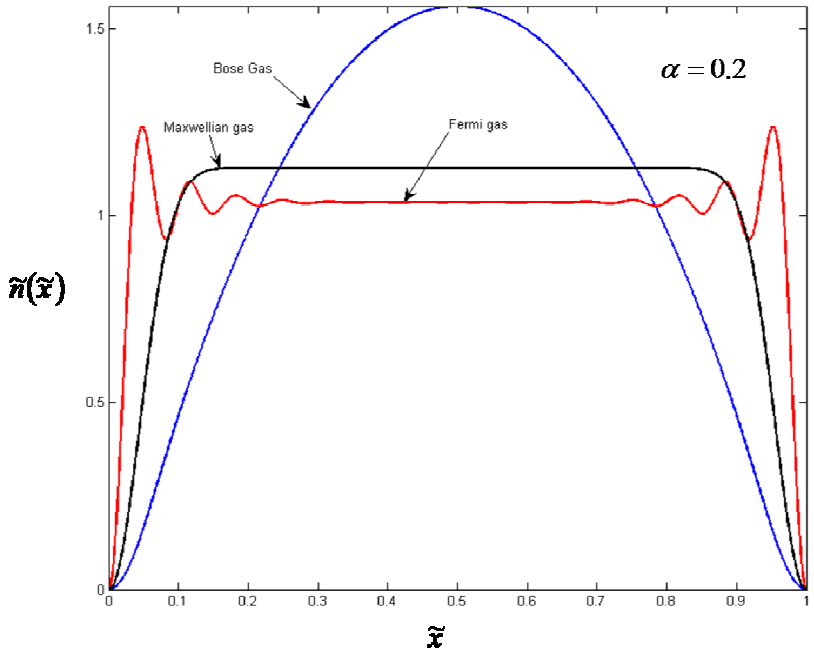

Figure 1. Density distributions of ideal Maxwellian, Fermi and Bose gases in 1D domain. $\Lambda = \mu / k_b T$ is chosen as $\Lambda = 5$ for Fermi gas and $\Lambda = -0.01$ for Bose gas while α is always considered as 0.2.

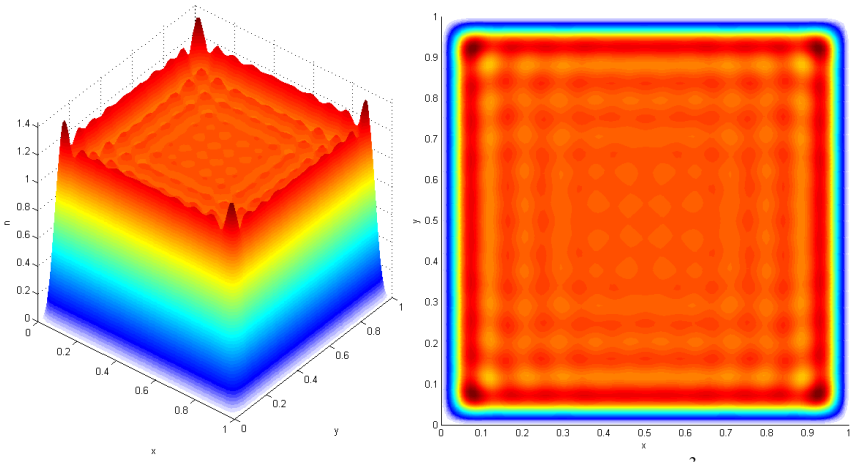

Figure 2. Friedel-like density oscillations in a degenerate Fermi gas, $_2He^3$, at 10K and 1.000 atm.

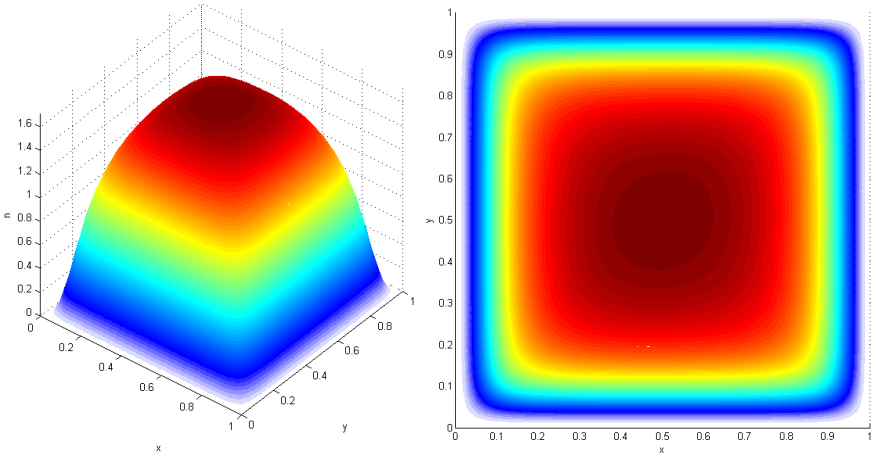

Figure 3. Density distribution of a degenerate Bose gas, $_2He^4$, at 10K and 80 atm.

3. Conclusion

Due to wave nature of particles, it is seen that there is boundary layer which makes density of a gas inhomogeneous even in thermodynamic equilibrium. Because of this layer, density increases in the rest part of the domain. In a degenerate Fermi gas, density even oscillates. On the other hand, oscillations are damped and a flat distribution occurs in the inner parts of the domain. In a degenerate Bose gas, density becomes completely inhomogeneous in the entire domain. These results show that the thermodynamic state functions, which depend on density, become complicated in nano scale. Therefore, thermodynamic behaviors of gases confined in nano structures are different those in macro ones. These interesting results observed in gas density can allow to design completely new devices based on these unusual behaviors.

Acknowledgements
This work is supported by The Scientific and Technological Research Council of Turkey, TUBITAK, under the contract number of 105T086 and Istanbul Technical University- Scientific Research Program.

References

[1] Goddard III W A, Brenner D W, Lyshevski S E and Iafrate G J (Editors) 2003 *Handbook of Nanoscience, Engineering, and Technology* (Boca Raton: CRC Press)
[2] Wolf E L 2004 *Nanophysics and Nanotechnology* (Weinheim:WILEY-VCH)
[3] Kang J W and Hwang H J 2004 *Nanotechnology* **15** 1633-38
[4] Hoummady M and Fujita H 1999 *Nanotechnology* **10** 29–33
[5] Sisman A, Ozturk Z F and Firat C 2007 *Phys. Lett.* A **362** 16-20
[6] Dai W S and Xie M 2007 *J. Math. Phys.* **48** 123302
[7] Dai W S and Xie M 2007 *Ann. Phys.* **322** 1771-75
[8] Pang H, Dai W S and Xie M 2006 *J. Phys.* A*: Math. Gen*. **39** 2563-71
[9] Sisman A 2004 *J.Phys.* A: *Math. Gen*. **37** 11353-61
[10] Sisman A and Müller I 2004 *Phys. Lett.* A **320** 360-6
[11] Dai W S and Xie M 2004 *Phys. Rev.* E **70** 016103-1
[12] Dai W S and Xie M 2003 *Phys. Lett.* A **311** 340-6
[13] Pathria R K 1998 *Am. J. Phys*. **66** 1080-85
[14] Molina M I 1996 *Am. J. Phys.* **64** 503-5

A Rigorous Formal Analogy between Gibbs-Tisza-Callen Thermodynamics and Microeconomic Consumer Theory

T. Sousa ∗ and T. Domingos∗

∗IN+ Center for Innovation, Technology and Policy Research - Environment and Energy Section, Instituto Superior Técnico, 1049-001 Lisbon, Portugal,
tdomingos@ist.utl.pt

Abstract

We develop a unified conceptual and mathematical structure for the use of concepts and tools of equilibrium thermodynamics in neoclassical microeconomics and vice versa, based on the analogy between entropy in thermodynamics and utility in consumer theory. With this analogy, we have obtained the following results in microeconomic theory: (1) the definition of irreversibility in economic behavior; (2) the clarification that the Engel curve and the offer curve are not descriptions of real processes dictated by the maximization of utility at constant endowment; (3) the derivation of a relation between elasticities proving that economic elasticities are not all independent; (4) the proof that Giffen goods do not exist in a stable equilibrium; (5) the derivation that 'economic integrability' is equivalent to the generalized Le Chatelier principle and (6) the definition of a first order phase transition, i.e., a transition between separate points in the utility function. In thermodynamics the results obtained are: (1) a relation between the non-dimensional isothermal and adiabatic compressibilities and the increase or decrease in the thermodynamic potentials; (2) the distinction between mathematical integrability and optimization behavior and (3) the generalization of the Clapeyron equation.

Entropy production as a metabolic quantifier in intra- and inter-species comparisons

T. Sousa ∗, J. D. Fernandes ∗, S. A. L. M. Kooijman †, and T. Domingos∗

∗IN+ Center for Innovation, Technology and Policy Research - Environment and Energy Section, Instituto Superior Técnico, 1049-001 Lisbon, Portugal,
†Department of Theoretical Biology, Vrije Universiteit, 1081 HV Amsterdam, Netherlands
taniasousa@ist.utl.pt

Abstract

The quantification of metabolic activity is usually done with mass or energy fluxes, e.g. dioxygen consumption or heat flux, that are not universal measures of metabolic activity. We propose the use of entropy production as a universal quantifier of metabolic activity, given its association with energy transformation, in order to unify the measurability and comparability of all types of metabolism.

For aerobic organisms, entropy production is correlated with the dissipated heat flux because the net entropy content of the mass fluxes is negligible. However, in general, entropy production is not directly measurable. We obtain it with the use of a general theory for organisms based on physical and chemical principles, the Dynamic Energy Budget theory, that provides quantification for biochemical activity at the individual level and across species.

Conceptually, metabolism is an aggregation of all reactions associated with a given organism, unifying analysis for all types of organisms and the way they relate to mass and energy flows. The problem of metabolic measurement is one of the most deep and recurrent questions in biology, given the variety of scales and types of metabolism. How can a deep sea chemolithoautotroph with a hankering for sulphur be compared to a plankton-sweeping dioxygen-using whale?

There have been two answers to this question: either quantify metabolism as proportional a) to a mass flux, such as dioxygen or b) to released heat via direct calorimetry. Although useful, these measurements are not universal. The dioxygen flux is not a universal measurement because some organisms do not use dioxygen consumptively, for example anaerobic bacteria. The heat flux is a misleading measurement for organisms that have both endothermic and exothermic chemical reactions because a given amount of dissipated heat cannot be linked unequivocally to a given metabolic activity. Autotrophic metabolisms also cannot be quantified by calorimetry, because non-absorbed light contributes towards generated heat.

In order to be universal, a given quantifier has to be applicable to all metabolisms and increase or decrease monotonically with the level of biochemical activity. We propose entropy production as a quantifier for metabolism. It is a universal measurement because all organisms are subject to the second law of thermodynamics, implying that all organisms produce entropy in their metabolic functioning and that this entropy production is always positive, being additive over all processes.

In order to quantify entropy production we use the Dynamic Energy Budget (DEB) theory and recent results obtained for the thermodynamics of organisms. DEB theory is a biological non-species-specific theory that aims to capture the quantitative aspects of the organization of metabolism at the organism level. This theory presents disaggregated mass and energy fluxes as functions of model parameters and state variables. Model parameters have to be obtained indirectly by statistically analyzing data but gain mechanistic relevance within this theoretical structure. Hence, quantities such as the dioxygen flux, the dissipated heat flux and entropy production can be mechanistically derived and explained.

Another strong feature of this theory is that differences between species can be reduced to differences in parameter values that are roughly predicted by DEB theory to be a function of the species maximum size, allowing for inter-species comparisons.

References

Kooijman S. A. L. M. (2009) *Dynamic energy and mass budgets in biological systems*, third edition (Cambridge Univ. Press, Cambrige, UK).

Sousa T., Domingos T., Kooijman S. A. L. M. (2008) From empirical patterns to theory: A formal metabolic theory of life. *Philos. Trans. R. Soc* London, Ser. B, 363:2453–2564.

Sousa T., Mota R., Domingos T., Kooijman S. A. L. M. (2006) Thermodynamics of organisms in the context of dynamic energy budget theory. *Phys. Rev. E*, 74:051901.

A Thermodynamic Approach to Computational Complexity: Tunneling as the Source of Intractability in *NP*-complete Problems

Donald Spector
Department of Physics
Hobart and William Smith Colleges
Geneva, NY 14456 USA
spector@hws.edu

1. Summary

One of the fundamental problems in computer science is to determine whether the complexity classes *P* and *NP* are in fact distinct from each other. In this paper, I offer an approach to this problem that involves recasting the essential computer science ideas into the language of physics, specifically that of thermodynamics. Specifically, the work described below suggests that the *NP* problems, the apparently intractable ones that take exponentially long to solve, correspond to systems that must undergo tunneling to reach their respective ground states. While this work is still speculative in many ways, it is fleshed out sufficiently to offer not only a potential road map for addressing the distinction between *P* and *NP* problems, but also to contribute new ideas for thinking about computational complexity, by invoking the ideas of physics.

2. Key Highlights of Computational Complexity

To understand this work, it is important to have some understanding of the necessary issues in computational complexity, before turning to the use of thermodynamics. A detailed discussion of these ideas is found in [1].

We focus here on measures of computational complexity based on how the time it takes to solve a problem depends on the size of the input. A typical problem is the Traveling Merchant Problem (more familiarly, the Traveling Salesman Problem), which entails, roughly speaking, finding the shortest path visiting *N* arbitrarily specified points in the plane or, to put it in its *NP*-complete form, to determine whether there is a path visiting all the cities of length less than a given length *L*.

Consider an algorithm **A** to solve some problem **P**. Let a given instance of the problem (e.g., in our example, a specific collection of points) be denoted *I*. The amount of information needed to specify the instance *I* is denoted $|I|$ (e.g., in our example, the number of coordinates needed to specify the cities). We denote the time it takes algorithm **A** to solve instance *I* of problem **P** by $\tau_A(I)$. We then define

$$T_A(N) = \operatorname*{Max}_{I\,:\,|I|=N} \tau_A(I)$$

This quantity uses the worst case scenario (i.e., the instance that takes the longest time to solve) to provide a measure of the efficacy of the algorithm **A** in solving the problem **P**.

We can now distinguish the complexity of the problem **P** overall by distinguishing two generic cases:

> Case 1: If there exists an algorithm **A** such that $T_A(N)$ has a polynomial dependence on *N* for large *N*, the problem is said to be in the class *P* of tractable problems.
>
> Case 2: If there exists no algorithm **A** such that $T_A(N)$ has a polynomial dependence on *N* for large *N*, the problem is said to be in the class of intractable problems.

There are, of course, problems known to be in the class *P*. There are other problems for which the best known algorithms are exponential in time. Among these, there is the class of those problems for which a potential solution can be checked in polynomial time; these for the class *NP* of computational problems. It is an open question as to whether this is because those problems are genuinely intractable ($P \neq NP$) or because the best algorithms are polynomial in time but have not yet been found (in which case $P=NP$). Within the class *NP* are the *NP*-complete problems; a rigorous proof that one of these problems can or cannot be solved in polynomial time is sufficient to determine whether the entire classes *P* and *NP* are equal or not.

3. Thermodynamics as a Framework for Understanding Computational Complexity

In this paper, I propose to understand the distinction between *P* and *NP* by recasting the computational problem in the language of statistical mechanics. Early versions of these ideas were presented in [2]. A specific instance in which the tools of physics can be used to draw a distinction between *P* and *NP* problems appears in [3].

Let us imagine solving some problem, such as the Traveling Merchant Problem, which can be phrased as a minimization problem. Finding the minimal length path through a list of points in the plane is, as far as is known, an intractable problem. (Strictly speaking, this problem is not an *NP* problem, as it is not a decision problem, but it has a closely related *NP*-complete version, namely to determine whether there is a path of length less than a given length *L* [1]. If the minimization problem can be solved in polynomial time, so can the decision problem; if the decision problem requires exponential time, so does the minization problem.) We focus on a minimization problem rather than a decision problem as this affords the clearest connection to thermodynamics. We use Q to denote the quantity to be minimized.

Suppose we have some algorithm **A** for solving this problem. The role of the algorithm is, over time, to take us from a situation in which any path is a possible solution, to one in which we have found the minimum path. The algorithm **A** thus can be understood as a time evolution operator, evolving the system from a situation in which a multitude of states is possible to a situation in which only one — the state of minimal Q — is possible. Certainly, one way to understand the process is to imagine one starts with a prospective path, and then the algorithm gradually acts on this path, changing the sequence of cities, to turn it into the optimal path. For the purposes of this abstract, we confine ourselves to such algorithms. (The analogous problem in one-dimension is to alphabetize a list of words, something which can easily be done in polynomial time.) In this framework, then, the algorithm **A** can be understood as the time evolution operator acting on the space of states, where each state corresponds to a particular path or sequence of cities. Thus the algorithm **A** plays the role of the Hamiltonian.

The algorithm **A** also plays another role. One path s is considered to be adjacent to another path s' if the algorithm will convert path s to path s' without an intermediate path being generated. (For example, an algorithm might search the space of states by interchanging two cities to turn one path into another.) Thus the algorithm **A** determines which configurations are adjacent to which other configurations, and thus how far apart any two configurations are. Thus **A** also serves to define the geometry on the space of configurations, implicitly placing a metric on this space.

The algorithm then must narrow down the possibilities so as to minimize the quantity Q. Consequently, Q plays the role of the free energy in a thermodynamic system. Of course, in thermodynamics, the Hamiltonian underlies the time evolution, but the Hamiltonian is hidden, and so we use thermodynamics rather than classical mechanics to analyze the system.

This insight from physics is the key insight to introduce to the study of computational complexity. Since the study of computational complexity involves examining the time behavior of algorithms for large $|I|$, we find ourselves in the computational analogue of the thermodynamic limit. With this in mind, we conjecture the following:

Conjecture: An algorithm **A** takes exponentially long to minimize a quantity Q if the function Q on the space of configurations has, with the metric determined by **A**, a local maximum, so that for at least some trial initial states, a Q-barrier must be overcome to reach the state of minimal Q.

The underlying concept here is that for the system reach the state of minimal Q, a barrier must be overcome. If the conjecture is true, it means that rather than understanding this process in terms of a step-like Hamiltonian evolution, we can rephrase the time evolution of algorithm **A** in the thermodynamic language of tunneling [4].

What does this mean for computational complexity, and what is necessary for this approach to work?

For computational complexity, this approach offers the following potential insights. A problem in the class P (such as alphabetizing a list of words) is one in which there is an algorithm **A** that places a metric on the space of states such that the function Q has no local maxima, and such that there is a path connecting each configuration to the optimal configuration that is monotonically decreasing in Q.

If a problem is such that for every algorithm **A** there are instances I of the problem for which there are local maxima in Q that must be overcome for the optimal configuration to be reached, then the problem will take at least exponentially long to solve, as the system will have to go undergo tunneling to reach the optimal state.

This reframing of these key concepts of computational complexity in the language of thermodynamics then allows the possible use of tools and results from physics to address the distinction between the classes P and NP.

Note that we have phrased things in terms of a particular kind of algorithm, one that, like a sorting algorithm, effects a time evolution in the space of configurations. While this makes the contact with physics clearer, the full application of these ideas requires that these ideas be generalized. The way to do this is to recognize that any algorithm is a time evolution operator acting on the states of the computer on which the algorithm is running. Raising the argument to this level of abstraction would provide the context for applying the above approach in a general context.

4. Outlook and Related Insights

In this section, I offer some varied insights that are germane to further progress with this approach.

Let us suppose, as most do, that $P \neq NP$. In the framework I have proposed, it would be necessary to show that every algorithm **A** leaves us with a metric, in at least some cases, that must have a local maximum. To do so, it would of course suffice to do so for a single NP-complete problem; I will have a bit more to say about the choice of the problem below. In order to show that a local maximum is unavoidable, a likely mathematical tool is Morse Theory, which can offer results as to whether extrema of various kinds can be eliminated under deformations of the parameters of a problem.

One might wonder how the transition from classical mechanics to thermodynamics/statistical mechanics can be achieved in the computational case. That is, the behavior of an algorithm looks very much like Hamiltonian time evolution, but how do we make the transition to the thermodynamic description for the computational problems? Here, there are some open questions but also some useful insights.

The fact that we are looking at the time behavior of algorithms for large instances of the problem brings us to the thermodynamic limit, and allows us to replace the discrete time evolution of the algorithm with the continuous time evolution of a something like a Hamiltonian. The fact that we *a priori* any path is a possible solution may play a role analogous to that of the ergodic hypothesis, but that is at the moment hard to establish.

Perhaps the biggest open question is what plays the role of energy in the computational problem. The appearance of exponential Boltzmann factors, which ultimately underlie the exponential time behavior required for tunneling processes, rests on conservation of energy and contact with a reservoir of some kind [4]. It seems that the analogy requires a conservation law in the quantity Q being minimized or some close related quantity, but it is not yet clear how to achieve this. An alternative possibility is that, just as information loss has to be associated with an increase in physical entropy, the tunneling required in intractable problems and algorithms that take exponential time may be associated with overcoming a barrier in physical energy.

A deeper question is how a deterministic system can be understood in a probabilistic language. This, of course, is a problem already apparent in the physical context (it is here that the ergodic hypothesis plays a critical role in the physical case), but if we are to apply thermodynamic reasoning to computational complexity, we must establish that a probabilistic description is accurate here, too. Of course, even in the physical context, this transition from deterministic to probabilistic description is not rigorously established. How might we do so?

The key insight here is that ignorance and stochasticity should be empirically indistinguishable from each other. Thus, before the algorithm has generated information, the behavior of the algorithm should, with regard to that information, behave in a way that is indistinguishable from stochastic. In this way, the identification of the computational problem with thermodynamic calculations should be possible. This insight may also offer a new to think about the transition from classical to statistical mechanics.

As mentioned above, it is possible to focus on particular problems (the *NP*-complete problems) and gain results that are more generally relevant. One useful exercise is to distinguish the Traveling Merchant Problem in two-dimensions from its one-dimensional version. Suppose we have an instance of the problem and gradually move one or more of the cities around to obtain a new instance; when will the optimal path change? In the one-dimensional case, this is easy to identify: whenever one city passes through another, and their locations overlap. In the two-dimensional case, however, there is no local indicator of when the configuration has changed sufficiently for there to be a new optimal path. This distinction is probably a key to understanding why tunneling is unavoidable in the two-dimensional case but not the one-dimensional case.

5. Final Observations

The approach suggested in this paper offers many insights, but still possesses significant gaps. However, the framework offers a compelling case that the ideas of thermodynamics and the relationship between classical and statistical mechanics can be fruitfully applied to notions of computational complexity. At best, the conjecture put forward here that intractability and tunneling are equivalent processes will be verified, and the question of whether *P* and *NP* are distinct will be resolved. But even without this, thermodynamics offers a new language and set of tools for analyzing computational complexity.

6. References

[1] M. Garey and D. Johnson, *Computers and Intractability* (1979) W H Freeman & Co.
[2] D. Spector, *A Statistical Mechanics Approach to P vs. NP*, presented at Quantum Information Workshop, Cambridge, 1999.
[3] J. Harwich, *A Study of Cooling Schedules in Simulated Annealing*, unpublished thesis, 1994.
[4] D. A. McQuarrie, *Statistical Mechanics* (1976) Addison-Wesley.

Mean Field Models and Finite-Time Thermodynamics: A Unified Framework for Low Order, Multi-Scale Galerkin Models of Fluid Flows

Gilead Tadmor[1], Bernd R. Noack[2], Michael Schlegel[2], Marek Morzyński[3] and Scott Kelley[1]

[1]*Communications & Digital Signal Proc. Center, Northeastern University, Boston, MA 02115, USA*
[2]*Dept. of Fluid Dynamics and Engineering Acoustics, Berlin Institute of Technology, D-10623 Berlin, Germany*
[3]*Inst. of Combustion Engines and Transportation, Poznań University of Technology, PL 60-965 Poznań, Poland*
tadmor@coe.neu.edu

Abstract

Galerkin models of fluid flow systems are focused on a limited range of spatio-temporal scales of dominant coherent structures. Neglecting the slow dynamics of large structures, and the fast dynamics of small scales and turbulence, have been shown to be able to severely distort the dynamics predicted by the model. Here we outline a cohesive framework that integrates into the Galerkin model least order representations of these neglected scales: Mean field models account for slow variations in the base flow, and of entailed linear stability corrections. And a recent framework of finite time thermodynamics in Galerkin systems is used as a basis for the representation of effects of smaller structures, in the aggregate. The proposed approach is illustrated by the cylinder wake benchmark.

1 Introduction

Model reduction is pursued in investigations of fluid flow systems, both as a means to encapsulate key dynamic properties of the system, and as an indispensable tool for model-based design of feedback control mechanisms. A mature and sophisticated theory of model reduction and system identification is available for linear systems [1, 2] and has been successfully applied to linearized flow models [3–5]. Yet despite very substantial efforts over many decades, results available today are rather restrictive and are either limited to local models (based on extensions of the linear theory) or to well defined classes of systems [6–9]. The difficulties to attain the generality, power and mathematical rigor of the linear theory therefore led to the evolution of alternative methods that rely heavily on physical insight and an accumulated experience. The inherent nonlinearity and complexity of the Navier-Stokes equation (NSE), the trusted model in fluid dynamics, is a case in point, leading to the massive use of Galerkin models, and among those, of empirical *proper orthogonal decomposition* (POD) models [10].

By design, Galerkin and spectral models of fluid flow systems are capable and intended to resolve a selected range of spatial and temporal scales. Ideally, these modes and scales represent the dominant coherent flow structures, in which one is interested, and the Galerkin approximation resolves most of the kinetic energy of the unsteadiness, in these structures. Yet, as was elaborated in [11] and demonstrated repeatedly, even when the kinematic approximation is excellent, neglecting both longer and shorter scales may lead to severe distortions in the dynamic predictions by the Galerkin model: The truncation of small scales, hence of the energy cascade to turbulent dissipation may lead to over-predicted states. Slowly varying larger flow structures represent mean field corrections. They are effected by time variations in the Reynolds stress and, in turn, modulate the linear growth rate of unsteady fluctuations. Their suppression too may lead to an unfortunate combination of attractor. Both these shortcomings are exacerbated with the reductions of the Galerkin model order. This article proposes a cohesive approach to address both these shortcomings. That approach integrates into a unified framework two previously introduced tools: A *finite time thermodynamics* (FTT) model [12, 13] is used to capture the effect of slow time variations of mean modal energies in small length and time scales. Tracing to the fundamentals of mean field theory [14], *shift mode(s)* [15, 16] represent the slow time variations of large structures and their effects on the linear term in the original Galerkin model. The added models are based on physical first principles and therefore aim to capture a physically meaningful tradeoff between model order and resolution level. In particular, unlike unsteady Reynolds-averaged Navier-Stokes models or Smagorinsky-type reductions of the Navier-Stokes equation, the reduced order model respects mathematically rigorous momentum and energy balance equations.

The resulting theory demonstrates how both the aggregated representations of the neglected long and short time and length scales provide a theoretically solid expansion of Landau's original amplitude20equations [17]. It is illustrated with the cylinder wake benchmark.

2 A generalized framework for Galerkin models

The Standard Galerkin Model for Dominant Fluctuations. The starting point is an affine approximation of the velocity field $\mathbf{u}(\mathbf{x},t)$ in terms of a base flow $\mathbf{u}_0(\mathbf{x})$ and an orthonormal set of modes $\{\mathbf{u}_i(\mathbf{x})\}_{i=1}^N$:

$$\mathbf{u}(\mathbf{x},t) = \mathbf{u}_0(\mathbf{x}) + \sum_{i=1}^{N} a_i(t)\,\mathbf{u}_i(\mathbf{x}). \tag{1}$$

The POD modes [10] maximize the norm resolution for the budgeted model order N. The standard Galerkin system is an ordinary differential equation, formed by the projection of Navier-Stokes equations on the approximation (1):

$$\dot{a}_i \;=\; c_i \;+\; \sum_{i=1}^{N} c_{ij} a_j \;+\; \sum_{i,j=1}^{N} c_{ijk} a_j\, a_k, \quad i = 1,\ldots,N \tag{2}$$

Postulating a completion of the expansion set, we shall next view (1)-(2) as exact and elaborate on subclasses of modes and the sought physics based order reduction in (2).

A Galerkin-Reynolds Decomposition. In complete analogy to the full flow field, the states a_i of (2) are associated with a *slowly varying* mean and fluctuation energy (TKE):

$$a_i \;=\; m_i + a_i', \quad m_i \;:=\; \langle a_i \rangle\,, \quad E_i \;:=\; \frac{1}{2}\,\left\langle \left(a_i'\right)^2 \right\rangle. \tag{3}$$

Finite Time Thermodynamics. The constitutive FTT equations for m_i and E_i are obtained from the modal pendants of the Reynolds and TKE equations in the Galerkin space. The unknown second and third moments are expressed in terms of E_i by energetic closure assumptions [13]. The resulting $2N$ equations for $2N$ unknowns read

$$0 \;=\; c_i + \sum_{j=1}^{N} c_{ij}\, m_j + \sum_{j,k=1}^{N} c_{ijk}\, m_j\, m_k + \sum_{j=1}^{N} 2\,(c_{ijj} + c_{iji})\, E_j, \tag{4a}$$

$$\dot{E}_i \;=\; Q_i + T_i, \quad Q_i = q_i\, E_i, \quad T_i = \sum_{j,k=1}^{N} T_{ijk} = \alpha\, \chi_{ijk}\, \sqrt{E_i\, E_j\, E_k}\, \left[1 - \frac{3E_i}{E_i + E_j + E_k}\right]. \tag{4b}$$

A detailed description and discussion of the FTT equations are detailed in the original paper [13]. Highlights include the distinction of states as either energy donors and recipients, depending on their linear growth or decay rates, and the existence of at least one of each, the postulation that, on average, the lossless triadic terms conduct energy flows from high-to low energy states, and that participating Galerkin states are assumed uncorrelated.

The fixed point of (4) corresponds to the steady or the post-transient Navier-Stokes solution. Numerically, the stability properties of the Navier-Stokes solution are observed to transfer to the FTT equations. Thus, plain forward integration of (4) eventually converges against the non-trivial fixed point associated with the unsteady attractor.

The standard representation (1)-(2) now will give way to three types of states and associated dynamics, using the conceptual framework of (3). The index set is partitioned as $\{1,\ldots,N\} = \mathcal{I}_A \cup \mathcal{I}_B \cap \mathcal{I}_C$ and their governing equations are:

A-Modes, $i \in \mathcal{I}_A$, dominant fluctuations:

$$\dot{a}_i \;=\; c_i + \sum_{j=1}^{N} c_{ij}\, a_j + \sum_{j,k=1}^{N} c_{ijk}\, a_j\, a_k + \kappa_i\,(a_i - m_i), \tag{5a}$$

$$\dot{m}_i \;=\; \frac{1}{\tau}\,\left[a_i - m_i\right], \tag{5b}$$

$$\dot{E}_i \;=\; \frac{1}{\tau}\,\left[(a_i - m_i)^2/2 - E_i\right], \quad \text{where } 2\,\kappa_i\, E_i = \sum_{j \vee k \notin \mathcal{I}_A} T_{ijk}. \tag{5c}$$

B-modes, $i \in \mathcal{I}_B$, capturing slow variations in the mean flow:

$$0 \;=\; c_i + \sum_{j=1}^{N} c_{ij}\, m_j + \sum_{j,k=1}^{N} c_{ijk}\, m_j\, m_k + \sum_{j=1}^{N} 2\,(c_{ijj} + c_{iji})\, E_j, \tag{6a}$$

$$m_i \;=\; a_i, \tag{6b}$$

$$E_i \;=\; 0. \tag{6c}$$

C-modes, $i \in \mathcal{I}_C$, turbulence represented by slowly varying energy levels:

$$\dot{E}_i = Q_i + T_i, \tag{7a}$$

$$m_i = 0. \tag{7b}$$

$$a_i = 0. \tag{7c}$$

Of these three types, energy producing modes are all of type A. Turbulence modes are energy dissipating and effect the dynamics of A-modes only through the time averaged energy consumption (the last term on the right hand side of (5a)). B-type, shift modes are driven by by quadratic terms, representing the Reynolds stress in the Galerkin system [15, 16]. In turn, B-modes adjust growth rates of A-modes from instability at the steady solution, to a marginal stability over an attractor.

A Unified Framework for Model Reduction. C-modes sacrifice phase-information on fast fluctuations and retain only pertinent energy levels. Additional compression is achieved as a single C-mode is used to capture multi-modal energy. Likewise, the slow mean field variations are effectively captured by a single or few shift modes.

The details of this well studied benchmark that are used here can be found in [15]. The unstable steady solution $\mathbf{u}_s(\mathbf{x})$ is chosen as base flow. The fluctuations are resolved with the first 8 POD modes of the periodic flow $\mathbf{u}_i$, $i = 1, \ldots, 8$. The mean-flow deformation is resolved with a shift-mode as 9th mode $\mathbf{u}_9$. All 9 modes constitute an orthonormal basis and the Galerkin expansion reads. As shown in [13], the FTT model, in which all 8 POD modes are treated as C-modes reproduces essentially the same energy levels as those produced by the standard Galerkin model, where all are treated as standard A-modes (see Fig. 1).

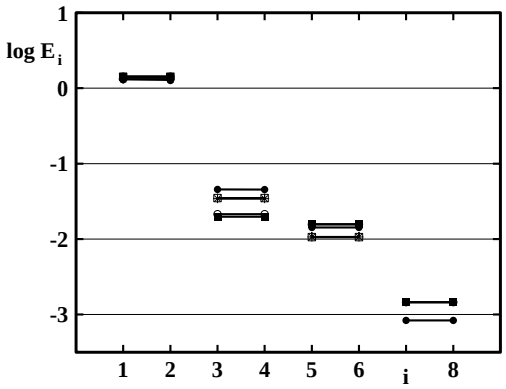

Figure 1: Modal energy distribution E_i, $i = 1, \ldots, 8$ of the Navier-Stokes attractor (•), of the Galerkin system (○), of the system with A-modes ($i \leq 8$ and one B-mode ($i = 9$) (■), of the system with C-modes ($i \leq 8$) and one B-mode) (□), and of the system with A-modes ($i \leq 2$), B-modes ($i = 3 \ldots 8$) and one C-mode ($i = 9$) ($*$).

3 Conclcusions and outlook

We have proposed a frame-work for reduction of a dynamic system with energy-preserving quadratic nonlinearity. Such dynamic systems arise, for instance, from the traditional Galerkin method or spectral method of incompressible fluid flow. The goal of system reduction is to reduce the dimension of the state space with associated time propagator (dynamics). This implies to eliminate dynamic degrees of freedoms or ordinary differential equations (ODE) by modeling their effect on the remaining dynamical system. The ODEs of slow modes associated with base-flow variations are replaced by algebraic equations defining a manifold in Galerkin space. The ODEs of fast modes associated with fine-scale fluctuations are modeled statistically by their energy distribution. The dynamics of the remaining dominant modes incorporates the effect of the slow and fast modes as inertial manifolds and energy flow terms.

Key enabler for a mathematically rigorous system reduction is a finite-time thermodynamic (FTT) formalism, representing a cumulant closure for the first and second moments. FTT yields approximate versions of the modal Reynolds and TKE equations. FTT allows to derive the interactions between slow, dominant and fast modes without heuristic assumptions beyond the validated FTT closure. The ensemble averaged equations for slow, dominant and fast modes including the interaction terms coincide with the FTT equations. For instance, the fast unresolved modes change the inertial manifolds and absorb energy from the dominant modes in a well-defined manner. Furthermore, the slow modes change the dynamics and the energy supplies of the fast modes. In short, FTT offers a design principle for interaction terms across resolved and unresolved flow components.

The proposed system reduction method has been applied to a 9-dimensional empirical wake model. The full system mimics a 'DNS', while the considered reduced systems include a RANS-type version with a completely statistical description and an LES-type version with a deterministic resolution of the first harmonics and stochastic model for the higher harmonics. The numerical accuracy of this proof-of-concept study are encouraging.

The proposed FTT-based system reduction accommodates mean-field models, inertial manifolds, a derivation of the eddy-viscosity term and the truncated Euler solution exhibiting thermal equilibrium. Thus, FTT and the proposed system reduction strategy offer a toolkit which reproduces current models of nonlinear dynamics and turbulence theory and allows to construct myriad of new models of potential relevance. The authors actively pursue the derivation of an alternative for unsteady RANS and VLES following the sketched path employing physical Galerkin models.

The authors acknowledge the funding and excellent working conditions of the Collaborative Research Centre (Sfb 557) "Control of complex turbulent shear flows" which is supported by the Deutsche Forschungsgemeinschaft (DFG) and hosted at the Berlin Institute of Technology. The work has been funded by the DFG under grants NO 258/1-1, NO 258/2-3, SCHL 586/1-1 and by the Centre National de la Recherche Scientifique (CNRS). The work of G. Tadmor was partially supported by NSF grants 0410246 and 0524070 and the US AFOSR grants FA9550-05-1-0399 and FA9550-06-1-0373. We are indebted to the *Bernd R. Noack Cybernetics Foundation*, the *Boye Ahlborn Turbulence Foundation* and Hermine Freienstein-Witt for generous additional resources. We appreciate valuable stimulating discussions with many friends and colleagues including Boye Ahlborn, Jean-Paul Bonnet, Remi Bourget, Laurent Cordier, Joël Delville, and Jose-Eduardo Wesfreid. We thank the local Berlin team as our very stimulating back office: Katarina Aleksic, Hans-Christian Hege, Ingrid Hotz, Jens Kasten, Rudibert King, Oliver Lehmann, Dirk M. Luchtenburg Nikolas Losse, Mark Pastoor, Jon Scouten, Tino Weinkauf and Olaf Wiederhold. We are grateful for outstanding hardware and software support by Lars Oergel and Martin Franke.

References

[1] A. Antoulas. *Approximation of Large-scale Dynamical Systems*. SIAM press, 2005.

[2] P. Benner, V. Mehrmann, and D. Sorensen, editors. *Dimension Reduction of Large-Scale Systems*, volume 45 of *Lecture Notes in Computational Science and Engineering (LNCSE)*. Springer Verlag, 2005.

[3] C.W. Rowley. Model reduction for fluids, using balanced proper orthogonal decomposition. *Int. J. on Bifurcation and Chaos*, 15:997–1013, 2005.

[4] E. Åkervik, J. Hœpffner, U. Ehrenstein, and D. S. Henningson. Optimal growth model reduction and control in a separated boundary-layer flow using global eigenmodes. *J. Fluid Mech.*, 579:305 – 314, 2007.

[5] J. Kim and T. R. Bewley. A linear systems approach to flow control. *Ann. Rev. Fluid Mech.*, 39:383 – 417, 2007.

[6] J. M. A. Scherpen. *Balancing for nonlinear systems*. PhD thesis, University of Twente, 1994.

[7] S. Lall, J. E. Marsden, and S. Glavaski. A subspace approach to balanced truncation for model reduction of nonlinear control systems. *Int. J. Robust and Nonlin. Control*, 12:519–535, 2002.

[8] A.N. Gorban, N. K. Kazantzis, I. G. Kevrekidis, H.C. Öttinger, and C. Theodoropoulos, editors. *Model Reduction and Coarse-Graining Approaches for Multiscale Phenomena*. Springer Verlag, 2006.

[9] J. A. Lee and M. Verleysen. *Nonlinear Dimensionality Reduction*. Springer Verlag, 2007.

[10] P. Holmes, J.L. Lumley, and G. Berkooz. *Turbulence, Coherent Structures, Dynamical Systems and Symmetry*. Cambridge University Press, Cambridge, 1998.

[11] N. Aubry, P. Holmes, J.L. Lumley, and E. Stone. The dynamics of coherent structures in the wall region of a turbulent boundary layer. *J. Fluid Mech.*, 192:115–173, 1988.

[12] B. Andresen, R. S. Berry, A. Nitzan, and P. Salamon. Thermodynamics in finite time. I. The step-Carnot cycle. II. Extremals for imperfect heat engines. *Phys. Rev. A*, 15:2086–2102, 1977.

[13] B.R. Noack, M. Schlegel, B. Ahlborn, G. Mutschke, M. Morzyński, P. Comte, and G. Tadmor. A finite-time thermodynamics of unsteady flows. *J. Nonequilibrium Thermodynamics*, 33:103 – 148, 2008.

[14] J.T. Stuart. Nonlinear stability theory. *Ann. Rev. Fluid Mech.*, 3:347–370, 1971.

[15] B.R. Noack, K. Afanasiev, M. Morzyński, G. Tadmor, and F. Thiele. A hierarchy of low-dimensional models for the transient and post-transient cylinder wake. *J. Fluid Mech.*, 497:335–363, 2003.

[16] G. Tadmor, O. Lehmann, B. R. Noack, and M. Morzyński. Mean field representation of the natural and actuated cylinder wake. *Phys. Fluids*, 2008. submitted.

[17] L.D. Landau and E.M. Lifshitz. *Fluid Mechanics*. Course of Theoretical Physics, Vol. 6. Pergamon Press, Oxford, 1987.

Use of thermodynamic entropy as thermal charge

Prof. Jean Thoma
Department of Systems Design
University of Waterloo
N2L3G1, Canada
www.jthoma.ch
jean@jthoma.ch

Dr. Gianni Mocellin
Straco consulting
15, rue du Diorama
1204-Geneva, Switzerland
www.straco.ch
gianni.mocellin@straco.ch

1. Introduction

Thermodynamics is considered a very difficult subject, expressed with so many letters and differentials. It becomes much simpler if one accepts the circuit thinking of electrical engineering. It is the purpose of this article to develop systematically the circuit and network thinking in thermodynamics and to go on from there. Instead of electric circuit elements, we use the Bondgraph (BG) formalism and we develop the BG symbols as needed. A pre-knowledge of BG is helpful, but not necessary to understand the definition of entropy in this article.

Here we shall develop the circuit thinking for thermodynamics and built the formalism from there. Circuit thinking was firstly developed in electrical engineering and for thermodynamics only slight modifications are required, as we shall develop.

The main point is to consider entropy as a substance, indeed as thermal charge. As such it has many similarities with electric charge, but also some differences. Entropy flow is connected to the transfer of heat power by the so-called Carnot's equation

$$\dot{Q} = T\dot{S} \quad or \quad \dot{S} = \dot{Q}T$$

To repeat, entropy flow is the more familiar heat flow divided by absolute temperature.

Entropy flow is very similar to the transmission of electric power, or simply electric conduction, which has the equation

$$\dot{E} = u\dot{q} = ui$$

With entropy as thermal charge, one can built circuits of thermodynamic installations, a little like electric circuits, but with slightly different properties. Here it is convenient to use the BG formalism and to show the difference to electric circuits by special BG elements. We will describe them, when we built the thermodynamic circuits.

2. Properties of entropy

Contrary to electric charge, which is always conserved is best to imagine entropy as a kind of substance, connected to heat flow by Carnot's equation, and produced by all kinds of frictions or irreversibilities. Under friction we understand not only mechanical and electric friction, but also heat conduction under finite temperature difference.

Further mechanisms to generate entropy are unopposed mixing of fluids, and also the resistance in chemical reactions. They exist but are in practice not important enough to justify treatment here. We use the Bondgraph (BG) formalism here, where all frictions are R-elements. To indicate properly the entropy generation, the R-element becomes saddled with a source element, becoming thus an RS-element.

Important is that the single R-element is a power sink, but does not exist as such. It becomes a power conserving RS-element: all absorbed power in the R-part appears again as heat, or as entropy times absolute temperature. This is illustrated by Fig. 1, with the simple R-element at top and the power conserving RS-element at bottom:

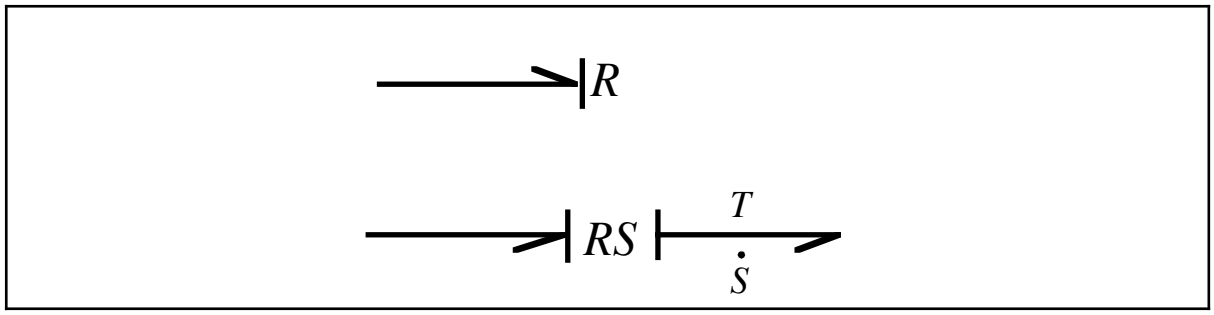

Fig. 1: Including thermics, the R element becomes an RS element.

Let us repeat: a simple R-element does not exist and becomes a power conserving RS-element by including thermal effects in our BG.

3. Thermodynamic circuits

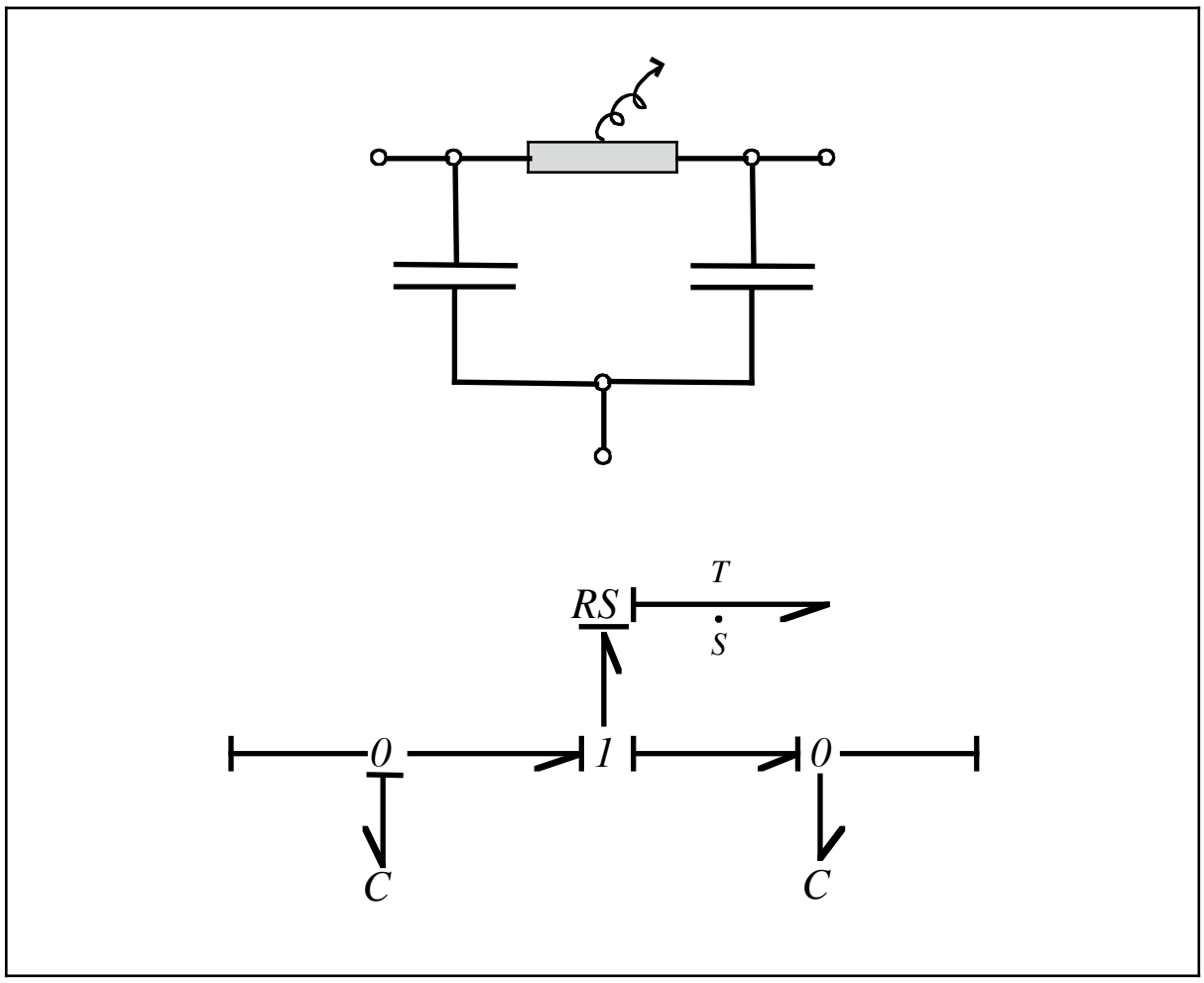

Fig. 2: Top: simple electric circuit with one resistor and two capacitors. Bottom: BG of this circuit.

One can built circuits for simple electric installations as on Fig. 2 with a resistor between two capacitors. As long as the voltages in the capacitors are different, there will flow a current through the resistor and we have

dissipation. It will appear in the thermal domain, as new entropy times absolute temperature as indicated below. Dissipation is a power flow that is always positive out from the resistor, even if the voltage changes sign. This is well shown by the equation

$$I = Ru \quad and \quad Dis = \frac{u^2}{R}$$

where one sees that the dissipation is always positive (even if the voltage u is negative).

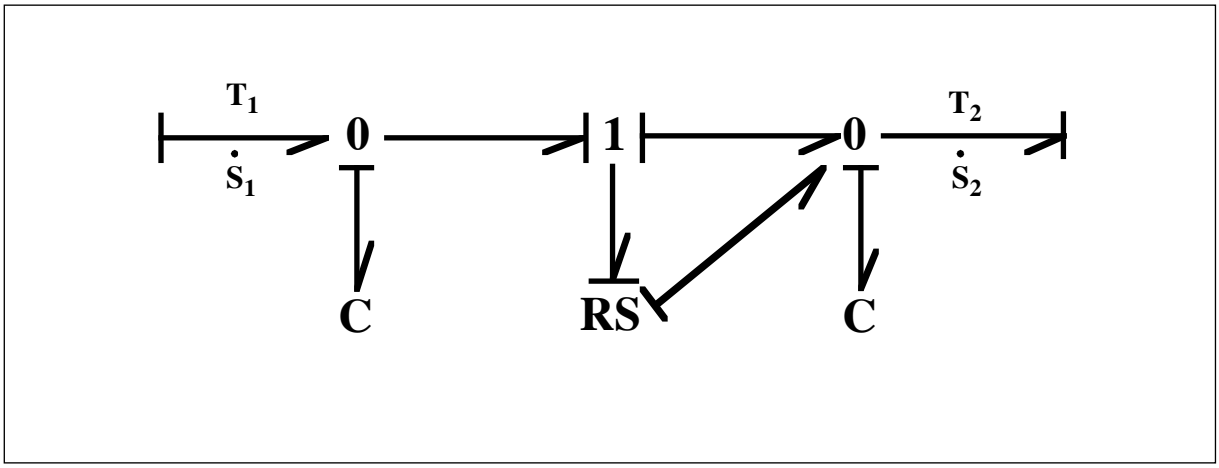

Fig. 3: BG for thermal conduction. Here the new entropy is injected to the C-element at lower temperature.

Thermal conduction is quite similar to electric conduction, with the dissipation in a thermal RS-element. Only its dissipation is thrown as entropy flow into the C-element having the lower temperature on the right of Fig. 3. Again, thermal dissipation is always positive. These electric dissipation and heat conduction are the two main mechanisms of generating entropy. If it is not clear which C-element is at lower temperature, a switch element SW can be interposed between the dissipating RS-field and both 0-junctions near to the C-elements. Such an element is quite easy to realize on a computer. It is notable that entropy has a semi-conservation property: it can never be destroyed, but is generated "out of nothing" by all kind of irreversibilities. To remove entropy from our field of interest, it must be transported away. Ultimately is must be disposed in stellar space around the earth.

Picture of Carnot cycle

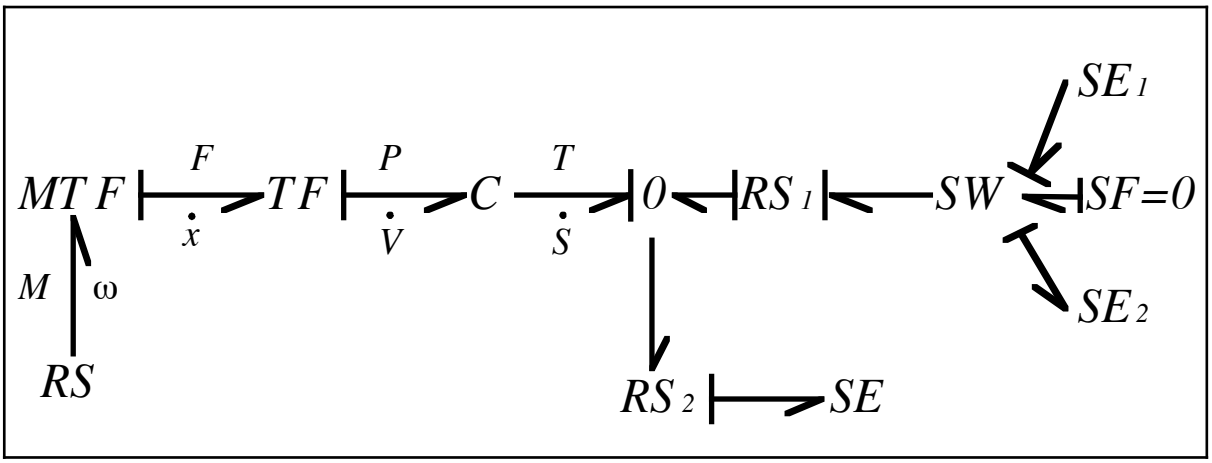

Fig. 4: BG of the famous Carnot cycle, where two adiabatics are interposed between the entropy spending and absorbing isothermals, one hot, the other cold.

The celebrated cycle of Carnot (1824) is represented in our formalism as follows: at left, we find a continuous flow source, driving a modulated transformer MTF, which converts the rotation into alternating movement in a cylinder. The working gas is contained in a 2-port C-field -C- . The switch SW has 3 positions:

1. connecting to the high temperature in SE1;
2. connecting to the low temperature in SE2;
3. connecting to nothing, the so called adiabatics of Carnot.

As Thoma has explained in [THOMA 2009], to interpose the 2 adiabatics between the isothermals was a great invention by Carnot. It avoids thermal short circuit when switching from high temperature to low temperature and vice versa. In practice, the Carnot cycle is not used because too much of the power gained in the expansion is needed to drive the compression. In other words, the power ratio, also called work ratio, is too small, especially if the working medium is an ideal gas. Therefore, historically one used a two phases working medium, water and steam, where the feeding pump with water used only negligible power. This is called the steam engine, with its heavy boiler, which dominated the world. Later, it was superseded by the more efficient internal combustion engine with its burning of gas inside the working cylinders.

Origins of entropy and heat

All tables of hot matter or water and steam give only incremental values, which are from a certain reference. In a water-steam mixture, one assigns the origin to water just at freezing as the most stable state and counts the values from there. Entropy is given only in incremental values by the formula

$$S_1 - S_2 = \int \frac{dQ}{T} \approx \int \frac{dQ_1}{T_1} - \int \frac{dQ_2}{T_2}$$

There is also the Nernst theorem which says that at zero temperature the entropy content of all matter is zero. We hold that this is only a theoretical law, and that entropy content, especially at low temperature, is unknown: we don't know the modifications of structure at cryogenic temperatures.

4. Conclusion

We care at the end of our trip through classical thermodynamics, which is simple and beautiful, if we take entropy as something fundamental, as thermal charge. It has special conservation properties: it can be generated "out of nothing" by frictions but it can never be destroyed and has ultimately to be disposed of in the stellar space around the earth. The important point is that all tables are giving only increments and leave the question of absolute entropy undecided. It would be good to give more thought to the absolute values of entropy.

References

[THOMA-MOCELLIN 2006]
Simulation with Entropy in Engineering Thermodynamics
J. Thoma and G. Mocellin
Springer, Heidelberg, 2006
"Thermodynamics using Bondgraphs and entropy as thermal charge. New standard work of the authors."

[THOMA 2009]
Carnot and his Cycle
J. Thoma - To be published in the series Thermodynamics and the Natural World, M. W. Collins, Editor
WITT Press, Southampton, 2009
"Comprehensive introduction to the Carnot cycle and its motivation, followed by a 15 page introduction to BG. This can also be downloaded from Thoma's home page www.jthoma.ch."

Stability conditions and Le Chatelier – Braun principle: links between equilibrium and non-equilibrium thermodynamics

Alexander Toikka
Department of Chemical Thermodynamics and Kinetics, Saint-Petersburg State University, Faculty of Chemistry, Universitetsky prospect 26, Petrodvoretz, 198504 Saint-Petersburg, Russia
E-mail: toikka@yandex.ru

Stability conditions in thermodynamics could be considered as a statement based on the positivity of entropy production. Simultaneous processes accompanying by the entropy production are the sign of non-equilibrium systems. On the other hand in classical thermodynamics stability conditions are usually related to equilibrium states. Le Chatelier – Braun principle is one of the basic rules that determines the direction of the processes and also should be regarded to the statement resulting from both the law of entropy increasing and stability criteria. In classical thermodynamics the applications of Le Chatelier – Braun principle mostly concerned the shifting of equilibrium. Such applications of originally non-equilibrium results (stability conditions and Le Chatelier – Braun principle) to the equilibrium thermodynamic theory could be considered as some link (or bridge) between equilibrium and non-equilibrium thermodynamics. In this paper we discuss some aspects of these basic thermodynamic statements.

Firstly we consider the alternative approaches to stability criteria and Le Chatelier – Braun principle. New variants of formulations of these statements are proposed. For example the interconnection between non-conjugated thermodynamic parameters is discussed on the base of Le Chatelier – Braun principle. Respective thermodynamic relationships could be considered as a special case of theorems of moderation. Various transformations of the stability matrix are presented as variants of mathematical formulations of stability conditions. Particularly the transformations of stability matrix to diagonal form are discussed. In both cases (stability criteria and Le Chatelier – Braun principle) the approach of Gibbs and Prigogine – de Donde method are considered, also in comparison. Elements of axiomatic of thermodynamics (Caratheodory and Afanassjewa-Ehrenfest) had been involved in consideration too.

Then we consider the general system of thermodynamic inequalities as a base of stability theory in equilibrium thermodynamics. The concept of affinity is used both for chemical and for phase processes. The possibility of the description of different types of physical-chemical processes on the base of generalized affinity is discussed. The illustration of the application of thermodynamic inequalities to various physical-chemical systems and processes will be presented. For example the problem of the shifting of phase and chemical equilibrium in the system under different external conditions is discussed.

In conclusion we present some relationships that illustrate the possibility to use the criteria of stability of the equilibrium to characterise the non-equilibrium process. These relationships could be also considered as results from Le Chatelier – Braun principle. Inequalities for second derivatives of thermodynamic potentials give opportunity to compare the changes of thermodynamic parameters in equilibrium and non-equilibrium processes. Processes in homogeneous and heterogeneous systems are discussed. Particularly the processes accompanied by generation of new phases are considered. The interpretation of so-called jumps in the values of second derivatives of thermodynamic potentials is presented.

Acknowledgment. This work was supported by Russian Foundation for Basic Research (grant 09-03-00812).

Truth, Belief and Knowledge in Statistical Physics

Flemming Topsøe
University of Copenhagen, Department of Mathematical Sciences
Universitetsparken 5, 2100 Copenhagen, Denmark
topsoe@math.ku.dk

1 Introduction, Overview

It is our goal to isolate the truly important notions of entropy for statistical physics. Until not that long ago, the one and only notion, *classical entropy*, was the one rooted in works of Boltzmann and Gibbs and consistent with the later theory developed by Shannon. A multitude of other notions have been suggested by mathematicians since the fifties. In 1971 the first suggestion of new entropies for statistical physics were presented by Lindhard and Nielsen. This was met by little interest. It was not until 1988 when Tsallis, unaware of previous research, pointed to the same entropy measures, that the development gained momentum. Since then, more than 2500 publications have studied the new entropies now bearing Tsallis' name and also referred to as *q-entropies* with q a real parameter. Classical entropy is obtained when $q = 1$.

Tsallis' success in promoting the q-entropies seems to be due to his direct and pragmatic approach, as well as the demonstration by Tsallis and followers that for a long list of phenomena, q-entropies lead to a better match with data than classical entropy. As another attractive feature, it turns out that the popular power-laws appear naturally when applying Jaynes *maximum entropy principle* (MaxEnt) with q-entropy in place of classical entropy.

In spite of the attraction to many, the new theory has also been met with pronounced scepticism due, especially, to the deviation from standard physical theory. What is missing in order for Tsallis theory to win general recognition appears to be a convincing interpretation of the "mysterious" q-entropies. This is where the present research claims to contribute.

Our approach involves a focus on the concepts *truth, belief* and *knowledge*, with knowledge conceived as the synthesis of extended *experience*. We appeal to game theoretical thinking involving two "players", *nature* and the

physicist. The physicist seeks the truth, held by nature, but is restricted by his beliefs. After extensive observations, knowledge is gained. The physicist attempts to minimize *description cost*, whereas nature, following thoughts going back to Jaynes, has the opposite goal. *Entropy* is defined as the minimal achievable description cost.

There are two main ingredients of our approach. Firstly, considerations related to nature, and outside the control of the physicist, identifies the *world* the physicist operates in. Secondly, we focus on *description* which is controlled by the physicist. As to the first element, it rests on the assumption that there is an *interaction* which, given truth (x) and belief (y), determines knowledge (z). If the interaction is given by $z = x$, we operate in the *classical world*, whereas the interaction $z = y$ is taken to define a *black hole*. In a black hole, you can only get out what you yourself put in. Interactions which lie between these extremes are taken to define *Tsallis worlds*.

Regarding description, it is assumed that every observation is connected with a *cost*. Based on a natural variational principle, it is possible to determine this cost and Tsallis entropy emerges as minimal expected description cost.

Though our approach provides a reasonable interpretation, there are many outstanding issues. These concern the physics behind interaction and more concrete notions of description, ideally in terms of coding as known from the classical case.

2 Technical sketch

Truth- and belief elements are taken to be probability distributions over some discrete set, respectively $x = (x_i)$ and $y = (y_i)$ with i varying over some discrete *alphabet*. Interaction is given by an *interactor* which is a function π defined on $[0, 1] \times [0, 1]$. It is assumed that π is *sound*, i.e. that $\pi(s, s) = s$. The interpretation is that $\pi(s, t)$ represents the "force" with which an event will be presented to the physicist in case the true probability of the event is s and the believed probability is t. We assume that π is *consistent*, i.e. that $\sum_i z_i = 1$ if x and y are probability vectors and $z_i = \pi(x_i, y_i)$. Simple considerations then show that there exists $q \in \mathbb{R}$ such that $\pi = \pi_q$ with

$$\pi_q(s, t) = qs + (1 - q)t\,. \tag{1}$$

By a *descriptor* we understand a non-negative function κ defined on [0,1] for which $\kappa(1) = 0$ and $\kappa'(1) = -1$. The latter condition serves to fix the unit used which we shall refer to as *nats*. Given t, $\kappa(t)$ represents

the effort by the physicist, measured in nats, which is needed in order to describe an event with probability t. The *total description cost* associated with observations in a situation governed by the truth vector $x = (x_i)$ and the belief vector $y = (y_i)$ is the quantity

$$\Phi(x, y) = \sum_i \pi(x_i, y_i)\kappa(y_i)\,. \tag{2}$$

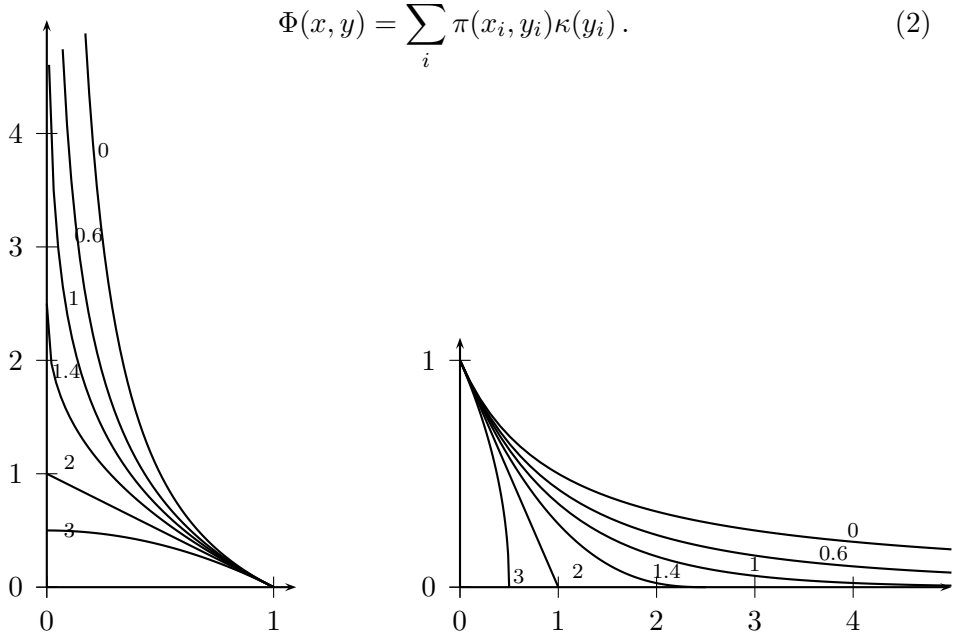

descriptors inverse functions (pr-checkers)

Figure 1: Descriptors and their inverses for selected values of q

Though x is unknown, the physicist can argue as follows in attempts to assign a descriptor which is best suited in the world, he is operating in: Surely, given any truth vector x, the total description cost is minimal when there is a *perfect match* between belief and truth, i.e. when $y_i = x_i$ for all i. This principle is the *perfect match principle* (PMP). It dictates that the general inequality $\Phi(x, y) \geq \Phi(x, x)$ holds. Thus the entropy of x is $S(x) = \Phi(x, x)$. It is found that PMP can only be satisfied if $q \geq 0$ and that then the descriptor is given by the formula

$$\kappa_q(t) = \ln_q \frac{1}{t} \tag{3}$$

with the *q-logarithm* defined as the usual natural logarithm when $q = 1$ and

otherwise as

$$\ln_q t = \frac{1}{1-q}(t^{1-q} - 1)\,. \tag{4}$$

Inserting $\pi = \pi_q$ and $\kappa = \kappa_q$ in (2), the *q-description cost* $\Phi(x, y)$ is obtained; the associated Tsallis q-entropy is found to be

$$S_q(x) = \Phi_q(x, x) = \frac{1}{1-q}\Big(\sum_i x_i^q - 1\Big)\,. \tag{5}$$

Also q- *divergence*, defined as $\mathrm{D}_q(x, y) = \Phi_q(x, y) - S_q(x)$ is important. It may be written as

$$\mathrm{D}_q(x, y) = \sum_i \Big(\frac{q}{1-q} x y^{q-1} + y^q - \frac{1}{1-q} x^q\Big)\,. \tag{6}$$

The descriptors κ_q and their inverses, called *pr-checkers* (pr for "probability") and denoted ε_q play a central role, especially for the smooth technical handling of MaxEnt (details in [3] and [4]). As to the interpretation of the pr-checkers, $\varepsilon(a)$ determines the smallest probability an event can have in order that it can be described by a nats. The figure is meant to give an impression of the descriptors and pr-checkers in the Tsallis family.

Acknowledgments: Stig Steenstrup pointed me to [2] and discussions with Peter Harremoës and Jan Caesar helped to fix the terminology.

References

[1] E. T. Jaynes. Information theory and statistical mechanics, I and II. *Physical Reviews*, 106 and 108:620–630 and 171–190, 1957.

[2] J. Lindhard and V. Nielsen. Studies in Statistical Dynamics. *Mat. Fys. Medd. Dan. Vid. Selsk.*, 38(9):1–42, 1971.

[3] J. Naudts. Generalised exponential families and associated entropy functions. *Entropy*, 10:131–149, 2008.

[4] F. Topsøe. Exponential Families and MaxEnt Calculations for Entropy Measures of Statistical Physics. In Qurati et al, editors, vol. 965 of *AIP Conference Proceedings*, pp 104–113, 2007.

[5] C. Tsallis. Possible generalization of Boltzmann-Gibbs statistics. *J. Stat. Physics*, 52:479–487, 1988. See http://tsallis.cat.cbpf.br/biblio.htm for a comprehensive and updated bibliography.

Thermodynamical estimation of the limiting potential of irreversible binary distillation

A. M. Tsirlin and I. N. Grigorevsky

Abstract

The limiting potential of binary distillation is considered for conventional heat supply to the column bottom and heat removal from the refluxer and for heat supply and removal distributed over the column height. For either case, the limiting column capacity and the minimum heat consumption are related to the external stream compositions and to the heat and mass transfer coefficients.

1 INTRODUCTION

The problem of optimal distillation design has been the subject of numerous studies [1 – 8]. The irreversibility of the process in the column has been taken into account by correcting its reversible characteristics (by passing from the minimum reflux rate to the working reflux rate, from theoretical separation stages to real trays, and so on) through introduction of time-proved experimental coefficients. Some of the studies suggest design improvements to the process in order to reduce its cost and, accordingly, enhance its economic effi- ciency. However, the following questions arise here: What is the highest potential of such improvements? What advantages can they offer over the conventional organization of the process? What form should the optimal operating line have, and how this line can be realized without radically complicating the process? These problems are far from being solved completely. In our earlier works [9,10], based on results reported in [11], we determined the "ideal" form of the operating line, for which the irreversibility of the process, characterized by entropy production, is the lowest at a given column capacity and integrated heat and mass transfer coefficients. Below, we make

an attempt to take into account the irreversibility of the process in terms of heat and mass transfer kinetics in order to elucidate the effect of the kinetic factors on the limiting performance parameters of the column (capacity and heat consumption). Since it is required to obtain an upper-bound estimate of the potential of the column, the assumptions simplifying the computational procedure and extending the applicability domain of the results will be made so that none of them adds to the irreversibility of the process. Only in this case can we claim that the performance parameters of a real column will not exceed the estimated upper bound. These assumptions lead to estimates biased upward, but these estimates are, nevertheless, much closer to the true values than the estimates based on consideration of reversible processes. Furthermore, the limiting capacity of the column can by no means be derived from reversible estimates.

Here are the basic assumptions we make: mass exchange is equimolar; in each cross section along the column height, the vapor and liquid flows have similar temperatures and pressures (which vary from one cross section to another); the effects of diffusion between adjacent cross sections are negligible, and the phases move in nearly plug-flow regimes; the heat of the exiting streams is transferred to the entering streams, and the irreversibility of this heat transfer can be neglected; the mixture to be separated, as a liquid heated to its boiling point, is fed into that cross section of the column in which it has the same composition as the reflux.

Thus, we will consider an "idealized" column, taking into account two sources of irreversibility, namely, heat transfer associated with heat supply to the exhausting section of the column and heat removal from the rectifying section and mass transfer between the vapor and the reflux along the column height. Note that, if the mass transfer coefficient is derived from data for an operating column, it indirectly allows for the deviation from the plug flow pattern, mixing on trays, and diffusion between cross sections. In the next section, using thermodynamic balance equations for a binary distillation column, we will correlate the compositions and flow rates of the external streams

with heat consumption in the case of heat supply to the column bottom and heat removal from the refluxer. The limiting performance parameters of this column will be estimated. In the last section, we will investigate the limiting performance of the column with the ideal operating line and report the laws of heat supply and removal along the column height that make it possible to effect this operating line.

2 COLUMN IN WHICH HEAT IS SUPPLIED TO THE BOTTOM AND IS REMOVED FROM THE REFLUXER

Consider the steady-state operation of a two-section binary distillation column. The mole fractions of the lower boiling component in the feed stream ($x_{_F}$) and in the steams drawn from the refluxer ($x_{_D}$) and bottom ($x_{_B}$), as well as the related liquid temperatures at the bottom ($T_{_B}$) and in the refluxer ($T_{_D}$), will be fixed. The draw-off ratio is completely determined by the compositions of the entering and exiting streams. From the material balance for the lower boiling component, we derive

$$\varepsilon = \frac{x_F - x_B}{x_D - x_B}. \tag{1}$$

Under the assumption that the liquid phase is similar in properties to ideal solutions and the vapor phase is similar to ideal gases, the equilibrium concentrations of the lower boiling component in the vapor and in the liquid are related as follows [1]:

$$y^0(x) = \frac{\alpha x}{1 + (\alpha - 1)x}, \tag{2}$$

where y^0 is the concentration of the lower boiling component in the vapor phase, $\alpha = \dfrac{P_1^0(T)}{P_2^0(T)} > 1$ is the relative volatility, and P_i^0 is the saturation

vapor pressure over the pure ith component ($i = 1$ for the lower boiling component).

Thermodynamic balances for binary distillation and the reversible estimate of energy consumption.

Let us write the thermodynamic (energy and entropy) balance equations under the assumption that the mixtures are similar to ideal solutions and the heat of mixing can be neglected:

$$q_+ - q_- + g_{_F} h_{_F} - g_{_F}\varepsilon h_{_D} - g_{_F}(1-\varepsilon)h_{_B} = 0, \tag{3}$$

$$g_{_F} s_{_F} - g_{_F}\varepsilon s_{_D} - g_{_F}(1-\varepsilon)s_{_B} + \frac{q_+}{T_B} - \frac{q_-}{T_D} + \sigma = 0. \tag{4}$$

From conditions (3) and (4), by eliminating q_-, we obtain

$$q_+ = g_{_F}\frac{T_B}{T_B - T_D}\Big[(s_{_F}T_D - h_{_F}) - \varepsilon(s_{_D}T_D - h_{_D}) - \\ - (1-\varepsilon)(s_{_B}T_D - h_{_B})\Big] + \sigma\frac{T_B T_D}{T_B - T_D} = q_+^0 + \sigma\frac{T_B T_D}{T_B - T_D}. \tag{5}$$

The first term on the right-hand side of this equation, designated q_+^0 is the heat consumption in the reversible process, when the heat and mass transfer coefficients (column dimensions) are arbitrarily large. It depends only on the parameters of the entering and exiting streams and is proportional to the feed flow rate g_F.

The second term accounts for the dissipative loss of energy. The external streams entering and exiting the column usually pass through heat exchangers, in which the hot streams are cooled and the feed streams are heated to the feed tray temperature. We will include these heat exchangers in the system and assume that the irreversible losses there are low. It will then be possible to assume that all external streams have the same temperature and that this temperature is close to T_D. These assumptions lead to some underestimation of the energy spent on separation, but they substantially simplify the analysis of the system. In particular, under these assumptions $q_+ = q_- = q$.

Taking into account the fact that the difference $((h - T_D s))$ for each stream is equal to the molar free energy, i.e., to the chemical potential μ of the mixture at $T = T_D$, we obtain the following relationship between the heat flux and the feed flow rate:

$$q = g_{_F} \frac{T_B}{T_B - T_D} \Big[\varepsilon \mu(T_D, x_D) + (1-\varepsilon)\mu(T_D, x_B) - \mu(T_D, x_F) \Big] + \sigma \frac{T_B T_D}{T_B - T_D}. \quad (6)$$

For mixtures similar to ideal solutions, the chemical potentials are written as

$$\mu_i(T, P, x_i) = \mu_{i0}(P, T) + RT \ln x_i, \quad i = D, B, F. \quad (7)$$

Because the chemical potentials in each particular cross section refer to the same temperature and pressure, we can write the following differences:

$$\mu_1(T, y^0) - \mu_1(T, y) = RT \ln \frac{y^0}{y},$$
$$\mu_2(T, 1-y) - \mu_2(T, 1-y^0) = RT \ln \frac{1-y}{1-y^0}.$$

The right-hand side of equality (6) can be expressed in terms of stream compositions:

$$q = g_{_F} \frac{T_B}{T_B - T_D} \Big[A_F - \varepsilon A_D - (1-\varepsilon) A_B \Big] + \frac{\sigma T_D T_B}{T_B - T_D} = \frac{p_0}{\eta_{\mathrm{K}}} + \frac{\sigma T_D}{\eta_{\mathrm{K}}}. \quad (8)$$

Here, $A_i = -RT_D \Big[x_i ln x_i + (1-x_i) ln(1-x_i) \Big] (i = F, D, B)$ is the reversible work of the separation of 1 mol of the ith stream into pure components. The right-hand side of this equality is equal to the power of separation of the feed flow $g_{_F}$ with the lower boiling component concentration $x_{_F}$ into streams with the lower boiling component concentrations $x_{_B}$ and $x_{_D}$ at the temperature $T_{_D}$ divided by $\eta_{\mathrm{K}} = (1 - T_D/T_B)$. By equating the entropy production in (8) to zero, we obtain the reversible estimate $q^0 = \dfrac{p_0}{\eta_{\mathrm{K}}}$ for heat consumption in the distillation process.

Expression (8) means that reversible distillation can be represented as a reversible heat engine operating between reservoirs having the temperatures T_B and T_D and producing the reversible separation power p^0.

Since the heat flux q can be expressed as the product of the vapor flow rate in the column (V) and the latent heat of evaporation (r),

$$q = Vr, \tag{9}$$

and the entropy production depends on the feed flow rate g_F, the vapor flow rate, and the transfer coefficients k, condition (8) relates the variables g_F, V, and k through thermodynamic balances. Expression (8) will be called *the thermodynamic relationship.*

Irreversible losses of energy.

According to (5), the energy consumption includes both q^0 and an irreversible component proportional to the entropy production σ. The main source of irreversibility in the column is mass transfer between the vapor and the liquid, during which the lower boiling component passes from the liquid to the vapor and the higher boiling component passes from the vapor to the liquid.

In order to calculate the entropy production associated with mass transfer, we will use a packed column model in which the vapor and liquid move countercurrently in a near-plug-flow regime and mass transfer is equimolar. The vapor flow rate V in the case of equimolar mass transfer is invariable and is related to the reflux flow rate L by the following equalities:

for the column top,

$$L_{_D} = V - g_D, \tag{10}$$

for the column bottom,

$$L_{_B} = V + g_{_B}. \tag{11}$$

In binary distillation, the concentration of the higher boiling component in the liquid and vapor streams is $1 - x$ and $1 - y$, respectively, and the

driving force of the process is determined by the difference between the current concentration y and the equilibrium concentration $y^0(x)$; therefore, the entropy production associated with mass transfer can be expressed in terms of flow rates and chemical potentials as

$$\sigma_g = \int_{x_B}^{x_D} \frac{1}{T(x)} \{g_1(y, y^0)[\mu_1(T, y^0) \; -$$

$$-\mu_1(T, y)] + g_2(1-y, 1-y^0)[\mu_2(T, 1-y) - \mu_2(T, 1-y^0)]\} \, dx, \qquad (12)$$

where g_j and μ_j (j = 1, 2) are the mass transfer fluxes and chemical potentials of the components. Taking into account the expression for the chemical potentials (7) and the equimolarity of mass transfer ($g_1(y, y^0) = -g_2(1-y, 1-y^0) = g,$), expression (12) can be rewritten as

$$\sigma_g = R \int_{x_B}^{x_D} g(y, y^0) \ln \frac{y^0(1-y)}{y(1-y^0)} \, dx. \qquad (13)$$

Here, it is accepted that the liquid feed to be separated, whose flow rate is $g_{_F}$, is at its boiling point and is entered into that column cross section in which its composition coincides with the reflux composition.

Thus, the mass transfer component of the entropy production is determined by the forms of the equilibrium and operating lines. The former depends on the properties of the mixture to be separated (relative volatility α; see Eq. (2)), and the latter depends on V. From the material balance equations for the lower boiling component at the column top and bottom, we obtain

$$Vy(x) - g_{_D} x_{_D} - x L_{_D} = 0, \qquad (14)$$

$$L_{_B} x - V y(x) - g_{_B} x_{_B} = 0. \qquad (15)$$

In view of (10) and (11),

$$y^{_D}(x, V, g_{_D}) = \left(1 - \frac{g_{_D}}{V}\right) x + \frac{x_{_D} g_{_D}}{V}, \qquad (16)$$

$$y^{B}(x, V, g_{D}) = \left(1 + \frac{g_{B}}{V}\right) x - \frac{x_{B} g_{B}}{V}. \tag{17}$$

It follows from these equalities that $y^{D}(x_D) = x_D$, $y^{B}(x_B) = x_B$, $y^{D}(x_F) = y^{B}(x_F) = y_F$, and $y_F - x_F = \frac{g_D}{V}(x_D - x_F)$.

Substituting expressions (16) and (17) into equality (13) and expressing the exit flow rates in terms of the feed flow rate g_F and ε makes it possible to determine $\sigma_g(V, g_{F})$ for the given mass transfer law. The integral in (13) should be calculated as the sum of integrals over the intervals between x_B and x_{F}, where $y(x) = y^{B}(x, V)$, and between x_{F} and x_D, where $y(x) = y^{D}(x, V)$.

When passing from x to another variable depending monotonically on x, it is necessary to recalculate the effective mass transfer coefficient. For example, when passing to integration over the column height, the mass transfer coefficient per unit height, $\bar{k}$, is obtained from the mass transfer coefficient per unit change in the lower boiling component concentration, k, by dividing it by the column height and multiplying it by the length of the concentration interval:

$$\bar{k} = \frac{k(x_D - x_B)}{H}. \tag{18}$$

Let us establish a relationship between the vapor flow rate V and the column capacity. To do this, we will take into account that the total amount of the lower boiling component passing from the liquid into the vapor phase in the top and bottom sections of the column is

$$\int_{x_B}^{x_{F}} g(y^{B}(x, V, g_{F}), y^{0}(x))dx + \int_{x_{F}}^{x_D} g(y^{D}(x, V, g_{F}), y^{0}(x))dx = V[y^{D}(x_D) - y^{B}(x_B)]. \tag{19}$$

Condition (19) relates the vapor flow rate V to the feed flow rate g_{F}. This relationship will be designated $V(g_{F})$. The substitution of this relationship into (16) and (17) demonstrates that the dissipative losses and, accordingly, the heat consumption q are completely determined by flow parameters and the feed flow rate. The distillation column has a limited capacity, like any heat-driven separation system. Let the mass transfer flux be proportional

to the difference between the working and equilibrium concentrations of the lower boiling component. Equality (19) will then take the following form:

$$\int_{x_B}^{x_F} k(y^0(x) - y^B(x))dx + \int_{x_F}^{x_D} k(y^0(x) - y^D(x))dx = V[y^D(x_D) - y^B(x_B)], \tag{20}$$

where $y^0(x, \alpha), y^D(x)$, and $y^B(x)$ are defined by expressions (2), (16), and (17), respectively, and depend on the compositions of the entering and exiting streams (x_F, x_B, and x_D), on the vapor flow rate V, and on the feed flow rate g_F.

In the widespread case of $y^D(x_D) = x_D$ and $y^B(x_B) = x_B$, after taking the integrals we obtain an expression relating the vapor flow rate to the feed flow rate g_F and the compositions x_F, x_B, and x_D:

$$b(x_B, x_D, x_F)g_F = a(x_B, x_D, \alpha)V - \frac{x_D - x_B}{k}V^2. \tag{21}$$

Here, ε is defined by expression (1) and the following designations are introduced:

$$a(x_B, x_D, \alpha) = \frac{\alpha(x_D - x_B)}{\alpha - 1} - \frac{\alpha}{(\alpha - 1)^2}\ln\left(\frac{1 + x_D(\alpha - 1)}{1 + x_B(\alpha - 1)}\right) - \frac{(x_D^2 - x_B^2)}{2},$$

and

$$b(x_B, x_D, x_F) = 0,5\left[\varepsilon(x_D - x_F)^2 + (1 - \varepsilon)(x_F - x_B)^2\right]$$

are complexes depending on the compositions of the exiting streams and on the relative volatility. In the general case, we have, instead of Eq. (21),

$$b(x_B, x_D, x_F)g_F = a(x_B, x_D, \alpha)\frac{y^D(x_D) - y^B(x_B)}{x_D - x_B}V - \frac{(y^D(x_D) - y^B(x_B))^2}{k(x_D - x_B)}V^2. \tag{22}$$

Equalities (21) and (22) relate the variables V, g_F, and k through mass transfer kinetics. They will be called the *kinetic relationships*.

From condition (21), we will derive an expression for the effective mass transfer coefficient. This coefficient depends on the vapor flow rate as

$$k = \frac{V^2(x_D - x_B)}{aV - g_F b}. \tag{23}$$

After the determination of the k value that is necessary for achieving the required column capacity and stream compositions, knowing the $\bar{k}$ value, we can estimate the column dimensions using equality (18). Formula (23) can also be used to calculate the effective mass transfer coefficient in an operating column because, in this case, all the variables appearing on its right-hand side are known.

The maximum of expression (21) with respect to V determines the limiting capacity of the column at a fixed mass transfer coefficient. The limiting capacity is attained at the vapor flow rate

$$V^{max} = \frac{ka(x_B, x_D, \alpha)}{2(x_D - x_B)} \tag{24}$$

and is

$$g_F^{max} = \frac{ka^2(x_B, x_D, \alpha)}{4(x_D - x_B)b(x_B, x_D, x_F)}. \tag{25}$$

Further raising the vapor flow rate will reduce the column capacity. The maximum appropriate vapor flow rate V^{max} determines the maximum appropriate heat flux $q^* = V^{max}r$. Use of Eq. (22) implies more tedious computations. However, the computational experience has demonstrated that Eq. (22) leads to only slightly different results.

The stream compositions satisfy the inequalities

$$x_D > y^0(x_F), \quad x_F > y^0(x_B),$$

And the equilibrium curve should be above the operating line. The operating line ordinate corresponding to x_F is the closest to the equilibrium curve. From the inequality $y^0(x_F) \geq y_F$ and expression (16), it follows that the vapor flow rate is

$$V > g_F \varepsilon \frac{x_D - x_F}{y^0(x_F) - x_F}. \tag{26}$$

Condition (23) also imposes the constraint $V > \dfrac{g_F b}{a}$ on the vapor flow rate since its denominator must be positive. Figure 1 plots the dependence

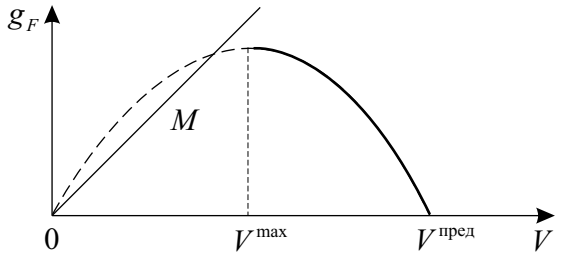

Fig. 1. Column capacity as a function of the vapor flow rate. The dashed line shows the nonoperating region. V^{lim} is the vapor flow rate limit.

of the column capacity g_F on the vapor flow rate. The line M represents inequality (26).

The kinetic and thermodynamic relationships (8) and (21) at given heat transfer coefficients at the column bottom and in the refluxer provide two links, one thermodynamic and the other kinetic, between the three variables g_F, V, and k. At a give value of k, which indirectly characterizes the column dimensions, these links allow one to determine the g_F and V values that would ensure the desired stream compositions. At a given feed flow rate g_F, they make it possible to determine the vapor flow rate V and k (heat consumption). The feed flow rate cannot exceed its maximum possible value, which is given by expression (25).

Computational procedure.

We will assume that the column capacity g_F and the bottom and refluxer temperatures are known. Simultaneously solving the thermodynamic and kinetic relationships (8) and (21), in which the heat consumption is expressed in terms of the vapor flow rate, makes it possible to determine k and V. The V value is determined by numerically solving the thermodynamic equation (8), which can be rewritten as

$$rV = q^0(g_F) + \frac{T_D}{\eta_k}\sigma(V, g_F). \tag{27}$$

The reversible component q^0 of the heat consumption depends on the feed

flow rate g_F, and the irreversible component is proportional to the entropy production σ and is determined via taking integral (13) in which the mass transfer coefficient $k(V)$ is expressed through the feed flow rate and the vapor flow rate (see expression (23)). The integration interval of (13) should be divided into the two intervals corresponding to the rectifying and exhausting sections of the column because the operating lines in these sections are different. For the linear law of mass transfer, the entropy production will take the following form (see (13)):

$$\sigma(V) = R\left[\int_{x_B}^{x_F} g(y^B, y^0) \ln \frac{y^0(1-y^B)}{y^B(1-y^0)} dx + \int_{x_F}^{x_D} g(y^D, y^0) \ln \frac{y^0(1-y^D)}{y^D(1-y^0)} dx\right]. \tag{28}$$

Here,

$$g(y^B, y^0) = k(V)(y^0(x) - y^B(x)), \tag{29}$$

$$g(y^D, y^0) = k(V)(y^0(x) - y^D(x)). \tag{30}$$

After solving Eq. (27), it is possible to determine the corresponding value of k and, from it, the necessary column height.

Relationships (8) and (21) between the basic variables characterizing the column make it possible to solve technical and economic problems in which the heat transfer coefficient, the column size, and the column capacity are sought variables. The optimality criterion in these problems should reach its extremum within the tolerance region of the variables, which is given by these relationships.

Irreversibility of heat transfer. For heat fluxes proportional to the temperature drop, the entropy production due to the thermal process in the bottom section and refluxer is given by

$$\sigma_q = q^2\Big[\frac{1}{\beta_{_B} T_B T_+} + \frac{1}{\beta_{_D} T_D T_-}\Big], \tag{31}$$

where $\beta_{_B}$ and $\beta_{_D}$ are the heat transfer coefficients and T_B and T_D are the liquid temperatures at the bottom and in the refluxer, which are assumed to

be known. The heat flux is expressed as

$$q = rV = \beta_{_B}(T_+ - T_B) = \beta_{_D}(T_D - T_-). \tag{32}$$

The temperatures T_B and T_D are determined by the properties of the components being separated, and the pressure in the column is set to satisfy the condition that T_- is equal to the ambient temperature. The distribution of heart transfer surface areas between the bottom and the refluxer should minimize σ_q under dome constraints.

3 OPTIMAL ORGANIZATION OF BINARY DISTILLATION

As was shown above, the energy consumption includes both q_+^0, and an irreversible component proportional to the entropy production σ. At a fixed feed flow rate and column dimensions, the entropy production cannot be zero. Let us determine the minimum possible value of irreversibility and the corresponding design of the column.

Mass transfer with minimum irreversibility and the ideal form of the operating line. As distinct from the entropy production associated with heat supply and removal, the entropy production in mass transfer depends on the forms of the equilibrium and operating lines because the driving force of mass transfer is determined by the difference between the current concentration $y(x)$ and the equilibrium concentration $y^0(x)$. The entropy production associated with mass transfer is given by expression (12). The functions y and y^0 depend on x, but this variable ia not involved explicitly in the expression for σ. Since y^0 is a single-valued and monotonic function of x, the entropy production in the column for x varying between x_B and x_D can be calculated using expression (13):

$$\sigma = R \int\limits_{y^0(x_B)}^{y^0(x_D)} g(y, y^0) \ln \frac{y^0(1-y)}{y(1-y^0)}\, dy^0. \tag{33}$$

The operating line should be optimized to minimize σ at a given integrated mass transfer flux $\bar{g}$:

$$\int_{y^0(x_B)}^{y^0(x_D)} g(y, y^0)\, dy^0 = \bar{g}. \tag{34}$$

The value of $\bar{g}$ which characterizes the intensity of mass transfer, depends on the compositions of the entering and exiting streams and the feed flow rate g_F.

For a mass transfer flux proportional to its driving force,

$$g(y, y^0) = s \ln \frac{y^0(1-y)}{y(1-y^0)}$$

problem (33), (34) was solved in [11]. The optimum form of the operating line is given by

$$y(y^0) = \frac{y^0}{\gamma - (\gamma - 1)y^0}, \tag{35}$$

and the total mass transfer flux in the optimal column is constant throughout the column height and is equal to $s \ln \gamma$. To find the constant γ, it is necessary to express $\bar{g}$ in expression (34) in terms of the feed flow rate and the compositions of the external streams.

For the relationship $y^0(x)$ in the form of Eq. (2), the ideal operating line equation for the binary distillation column appears as

$$y(x) = \frac{\alpha x}{\gamma + (\alpha - \gamma)x}. \tag{36}$$

Since $y(x) > x$, the following equality is true for the parameter γ:

$$1 < \gamma < \alpha. \tag{37}$$

For realization of the optimal operating line, it is necessary to determine the corresponding laws of heat supply (removal) along the column height. The changes in the vapor and reflux flow rates along the column height for all $l \neq l_F$ satisfy the condition

$$\frac{dV}{dL} = 1, \tag{38}$$

Therefore, for any form of the operating line, equalities (10) and (11) are valid for the exhausting and rectifying sections of the column. The variation of the vapor and liquid flow rates along the height of a column with intermediate heat supply is shown in Fig. 2.

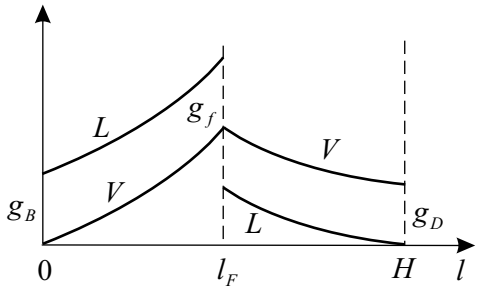

Fig. 2. Variation of the vapor and liquid flow rates along the height of the column with intermediate heat supply (removal).

The vapor flow rate for any cross section of the column and, accordingly, for the x value corresponding to this cross section can be derived from the material balance for the lower boiling component. For the rectifying section of the column,

$$V_D(x)y(x) - g_D x_D - xL_D(x) = 0.$$

Hence, taking into account that $x < x_D \quad L_D = V_D - g_D$, we obtain

$$V_D(x) = g_D \frac{x_D - x}{y(x) - x}, \quad x_F \le x < x_D, \quad V_D(x_D) = g_D, \quad y(x_D) = x_D. \quad (39)$$

Likewise, for the exhausting section of the column,

$$V_B(x) = g_B \frac{x - x_B}{y(x) - x}, \quad x_F \ge x > x_B, \quad L(x_B) = g_B. \quad (40)$$

The flow rate of the lower boiling component passing from the liquid into the vapor phase is equal to the feed rate of this component ($g_F x_F$) minus the withdrawal rate of this component as bottoms ($g_B x_B$). Since the equivalent mass transfer flux is constant, we obtain the following equation for γ:

$$\bar{g} = s(y^0(x_D) - y^0(x_B)) \ln \gamma = 2(g_F x_F - g_B x_B) = 2g_F(x_F - x_B(1 - \varepsilon)). \quad (41)$$

The doubling of the flow rate is due to the fact the countercurrent flow of the higher boiling component is equimolar to the flow of the lower boiling component. From (41), we obtain

$$\gamma = exp\Big[2g_F \frac{(x_F - x_B(1-\varepsilon))}{s(y^0(x_D) - y^0(x_B))}\Big]. \tag{42}$$

The minimum possible entropy production associated with the irreversibility of mass transfer is as follows (see (33)):

$$\begin{aligned} \sigma^{min} = R\bar{g}(y^0(x_D) - y^0(x_B)) \ln\gamma = \frac{R\bar{g}^2}{s(y^0(x_D) - y^0(x_B))} = \\ = g_F^2 R \frac{4(x_F - x_B(1-\varepsilon))^2}{s(y^0(x_D) - y^0(x_B))}. \end{aligned} \tag{43}$$

The substitution of σ^{min} into the above expressions for the heat consumption and limiting column capacity provides lower and upper estimates of these quantities, respectively. The desired heat supply (removal) laws and heat transfer area distribution correspond to these estimates.

Distributed heat supply and the corresponding minimum irreversibility. The above relationships make it possible to understand how the heat removal and supply along the column height should be organized so as to effect the ideal operating line $y(x)$. In the case of heat removal and vapor condensation in the rectifying section of the column, the removed heat flux $q_{_D}(x) < 0$ is

$$q_{_D}(x) = r\frac{dV_{_D}}{dx} = rg_{_D}\frac{(1 - \frac{dy}{dx})(x_{_D} - x) - (y - x)}{(y(x) - x)^2}. \tag{44}$$

Here, r is the specific heat of evaporation (condensation). In the general case, it depends on the feed composition. Likewise, for the exhausting section of the column, the supplied heat flux $q_{_B}(x) > 0$ that causes reflux evaporation is

$$q_{_B}(x) = r\frac{dV_{_B}}{dx} = rg_{_B}\frac{(y - x) - (\frac{dy}{dx} - 1)(x - x_{_B})}{(y(x) - x)^2}. \tag{45}$$

In order to determine, using these formulas, the distribution of the heat fluxes over the column height, it is necessary to calculate $x(l)$. The heat flux is expressed as

$$q(l) = r\frac{dV}{dl} = r\frac{dV}{dx}\frac{dx}{dl}. \tag{46}$$

Let us write the material balance equation for the lower boiling component, taking into account that, in the optimal column, the mass transfer flux per unit height is constant, being equal to $g_l = \bar{g}/H$, and is given by expression (41). So, we obtain

$$\frac{d}{dl}[V_{_D} y] = g_l - \frac{q_D y}{r} = g_l - \frac{dV_{_D}}{dl} y \Rightarrow \frac{dx_{_D}}{dl} = \frac{g_l}{\frac{dy}{dx} V_{_D}(x)}, \quad x_{_D}(l_F) = x_F. \tag{47}$$

Substituting the solution $x_{_D}(l)$ of this equation into (44) yields the optimal heat removal law $q_{_D}(l)$ for the rectifying section of the column.

For the exhausting section, similar expressions are valid, with the only difference that the subscript D is replaced with the subscript B and the boundary condition for $x_{_B}(l)$ is written as $x_{_B}(0) = x_{_B}$.

Let us estimate the minimum entropy production associated with heat supply to the liquid phase in the exhausting section and with heat removal from the vapor phase in the rectifying section. We will assume that the heat flux is proportional to the temperature difference and to the heat transfer coefficient $\beta(x)$. The integrated value of this coefficient, $\bar{\beta}$, is definite since it is related to the heat transfer area:

$$\int_{x_B}^{x_D} \beta(x) dx = \bar{\beta}. \tag{48}$$

The entropy production in heat removal from the *rectifying section* is given by

$$\sigma_{_{Dq}} = \int_{x_D}^{x_F} \frac{q_D^2(x) dx}{\beta_{_D}(x) T_{_D}(x) u(x)}. \tag{49}$$

Here, $u(x)$ stands for the absolute temperature of the coolant (usually, water at the initial temperature T_0) and $\beta_{_D}(x)$ is the heat transfer coefficient distribution.

The temperature T in the column as a function of the lower boiling component concentration x can be determined via the mass flux, taking into account the expressions for the chemical potentials. In view of the equimolarity of mass transfer, the flux of the lower boiling component from the liquid to the vapor is half the total flux $\bar{g}$; therefore,

$$kRT(x)\ln\frac{y^0(x)}{y(x)} = \bar{g}/2 = \frac{k}{2}\ln\gamma. \tag{50}$$

Hence,

$$T(x) = \frac{\ln\gamma}{2R\ln\frac{y^0(x)}{y(x)}} = \frac{\ln\gamma}{2R\ln\frac{\gamma+x(\alpha-\gamma)}{1+x(\alpha-1)}}, \quad x_{_B} \le x \le x_{_D}. \tag{51}$$

The relationship $q_{_D}(x)$ is known (see (44)). The coolant temperature $u(x)$ and the heat transfer coefficient $\beta_{_D}(x)$ can be derived from the heat balance in the heat exchanger and heat transfer kinetic equation:

$$(u(x) - T_0)W = rV_{_D}(x) \Rightarrow u(x) = \frac{rV_{_D}(x)}{W} + T_0, \tag{52}$$

$$\beta_{_D}(x) = \frac{q_{_D}(x)}{T_{_D}(x) - u(x)}. \tag{53}$$

Here, W is the water equivalent of the coolant flow rate and $V_{_D}(x)$ is given by expression (39).

In turn, the water equivalent depends on the fraction of the total heat transfer coefficient associated with the rectifying section, μ, because

$$\int_{x_{_F}}^{x_{_D}} \beta_{_D}(x) = \int_{x_{_F}}^{x_{_D}} \frac{q_{_D}(x)Wdx}{T_{_D}(x) - rV_{_D}(x) - WT_0} = \mu\bar{\beta}. \tag{54}$$

The solution of Eq. (54) determines $W(\mu)$. By substituting this relationship into (52) and (53) and substituting the result into (49), we determine $\beta_{_D}(x,\mu)$ and $\sigma_{_{Dq}}(\mu)$.

In the exhausting section, the partial evaporation of the liquid stream is usually due the supply of a vapor at a temperature T_+, which condenses on going from $x_{_B}$ to $x_{_F}$. This temperature and the supplied heat flux $q_B(x)$ will

be considered to be known (see (45)). The entropy production will appear as

$$\sigma_{Bq} = \frac{1}{T_+} \int_{x_B}^{x_F} \frac{q_B^2(x)dx}{\beta_B(x)T_B(x)}. \tag{55}$$

The heat transfer coefficient distribution here is determined by a formula similar to the formula used for the rectifying section:

$$\beta_B(x) = \frac{q_B(x)}{T_+ - T_B(x)}. \tag{56}$$

The choice of temperature depends on the distribution of the heat transfer area between the sections because

$$\int_{x_B}^{x_F} \beta_B(x) = \int_{x_B}^{x_F} \frac{q_B(x)dx}{T_+ - T_B(x)} = (1-\mu)\bar{\beta}. \tag{57}$$

By determining the relationship $T_+(\mu)$ from condition (57) and substituting it into expression (55), we obtain $\sigma_{Bq}(\mu)$. The distribution of the heat transfer area between the sections must satisfy the condition

$$\sigma_q(\mu) = (\sigma_{Bq}(\mu) + \sigma_{Dq}(\mu)) \to min. \tag{58}$$

4 CONCLUSIONS

In this work, we have set up computational relationships directly taking into account the irreversibility effects in terms of heat and mass transfer kinetics and thermodynamic balances. Based on these relationships, we suggest a computational procedure for determining the parameters of a binary distillation column using the conventional heat supply (removal) scheme and a column height-distributed one. In the latter case, the column performance parameters can be used to assess the thermodynamic perfection of the distillation process and find a way of reducing the irreversible losses.

NOTATION

g — flow rate, mol/s;
$\bar{g}$ — total mass transfer flux throughout the column height, mol/s;
H — column height, m;
h — molar enthalpy, J/mol;
k — mass transfer coefficient per unit change in the lower boiling component concentration, mol/s;
$\bar{k}$ — effective mass transfer coefficient per unit height of the column, mol/(s m);
L — liquid flow rate, mol/s;
l — coordinate characterizing position along the column height, m;
P — pressure, Pa;
p — power, W;
q, q^0 — total heat consumption and heat consumption in the reversible process, W;
q_+, q_- — heat fluxes supplied to the column bottom and removed from the refluxer, W;
R — universal gas constant, J/(mol K);
r — molar heat of evaporation, J/mol;
s — coefficient of proportionality between the mass transfer flux and the driving force, mol/s;
s_D, s_B, s_F — molar entropies in the refluxer, bottom, and feed stream, J/(mol K);
T_+, T_- — temperatures of the vapor heating the bottom and of the water cooling the refluxer, respectively, K;
V — vapor flow rate, nol/s;
W — water equivalent of the coolant flow rate, kg/s;
x — molar concentration of the lower boiling component in the liquid phase, mol/l;
y — molar concentration of the lower boiling component in the vapor phase,

mol/l;
y^0 — equilibrium concentration of the lower boiling component in the vapor phase, mol/mol;
α — relative volatility;
β — heat transfer coefficient, W/K;
$\bar{\beta}$ — total heat transfer coefficient, W/K;
γ — parameter in the ideal operating line equation;
ϵ — draw-off ratio;
μ — chemical potential, J/mol;
σ — entropy production, W/K.

SUBSCRIPTS AND SUPERSCRIPTS

B — bottom;
D — refluxer;
F — feed;
i — flow number;
q — heat transfer;
g — mass transfer;
j — component number;
lim — limiting value.

REFERENCES

1. *Planovskii, A.N. and Nikolaev, P.I.* Protsessy i apparaty khimicheskoi i neftekhimicheskoi tekhnologii. Uchebnik dlya vuzov (Petrochemical Engineering: A Students' Textbook), Moscow: Khimiya, 1987.

2. *Boshnyakovich, F.* Tekhnicheskaya termodinamika (Technical Thermodynamics), Moscow: Gosenergoizdat, 1956, vol. 2.

3. *Aleksandrov, I.A.* Rektifikatsionnye i absorbtsionnye apparaty (Distillation and Absorption Apparatuses), Moscow: Khimiya, 1978.

4. *Aleksandrov, I. A.* Tochnaya kriometriya organicheskikh soedinenii (Precision Cryometry of Organic Compounds), Moscow: Khimiya, 1975.

5. *Pavlov, K.F., Romankov, P.G., and Noskov, A.A.* Primery i zadachi po kursu protsessov i apparatov khimicheskoi tekhnologii (Chemical Engineering: Examples and Exercises), Leningrad: Khimiya, 1976.

6. *Berry R.S., Kasakov V.A., Sieniutycz S. et al.* Thermodynamic Optimization of Finite Time Processes. // Chichester: John Wiley and Sons, 1999.

7. *Naka Y., Terashita M.* An intermediate heating and cooling method for a distillation column // J. Chrem. Eng. Jap. 1980. Vol.11, N2.

8. *Amel'kin, S.A., Burtsler, I.M., Khoffman, K.Kh., and Tsirlin, A.M.* Evaluating the Efficiency Frontier of Separation Processes, Theor. Found. Chem. Eng., vol. 35, no. 3, p. 217.

9. *Tsirlin A. M., Kazakov V.A.,* Irreversible work of separation and heat-driven separation // J.Phys.Chem. B 2004. V.108. P 6035–6042.

10. *Tsirlin, A.M.* Neobratimye otsenki predel'nykh vozmozhnostei termodinamicheskikh i mikroekonomicheskikh sistem (Irreversible Estimates of the Limiting Performance of Thermodynamic and Microeconomic Systems), Moscow: Nauka, 2003.

11. *Tsirlin, A.M., Zubov, D.A., and Barbot, A.V.* Consideration of Irreversibility Factors for Binary Distillation, Theor. Found. Chem. Eng. , vol. 40, no. 3, p. 245.

Modeling the Complex Hydrogen Bonding Behavior of Mixtures with Glycols

Ioannis Tsivintzelis* and Georgios M. Kontogeorgis

Center for Phase Equilibria and Separation Processes (IVC-SEP), Department of Chemical and Biochemical Engineering, Technical University of Denmark, DK-2800 Lyngby, Denmark,
*Email: it@kt.dtu.dk

The thermodynamic properties of highly non-ideal mixtures of associated or hydrogen-bonded fluids and their correlation/analysis in terms of molecular thermodynamic models are not only of academic interest but also of importance for the rational design of industrial chemical processes involving such systems. Hydrogen bonding may be one of the most important interactions in these mixtures and such types of interactions may appear between molecules of the same and/or different kind. Moreover, hydrogen bonding interactions may appear between two different functional groups in the same molecule.

Glycols are important compounds for the gas production and the chemical industry. Monoethylene glycol (MEG) is mainly used as antifreeze and gas hydrate inhibitor of natural gas, while diethylene glycole (DEG) and triethylene glycol (TEG) are used as drying agents. Other compounds, such as tetraethylene glycol (TeEG) and propylene glycol (PG) are mainly used as solvents in numerous applications. On the other hand, higher molecular weight polyglycols, such as poly(ethylene glycol) (PEG) and poly(propylene glycol) (PPG) are used in many biomedical applications.

However, the modeling of glycol containing mixtures is a challenging task due to the strong specific inter- and intra- molecular interactions that are observed in such mixtures. Glycol molecules can form inter- and intra- molecular hydrogen bonds, due to the $-OH....OH-$ and $-OH....-O-$ association. Moreover, in their solutions with other associating fluids, such as water or alcohols, they also form cross- hydrogen bonds with solvent molecules. This complex hydrogen bonding behavior has a great impact on the properties and the phase equilibria of such mixtures.

In this study the phase behavior of mixtures with glycols is modeled using the Non Random Hydrogen Bonding Theory (NRHB) [1, 2]. This is an advanced equation of state model, based on statistical thermodynamics, which is able to account for the various hydrogen bonding interactions. The vapor – liquid equilibria of binary systems containing glycols or polyclycols with other hydrogen bonding fluids such as water, alcohols or amines was investigated. Effort has been made to explicitly account for all hydrogen bonding interactions. The results reveal that the NRHB model offers a flexible approach to account for various self- or cross associating interactions. In most cases model's predictions (using no binary interaction parameter $kij=0$) and model's correlations (using one temperature independent binary interaction parameter, $kij\neq0$) are in very satisfactory

agreement with the experimental data, despite the complexity of the examined systems. Representative results are presented in Figures 1 and 2

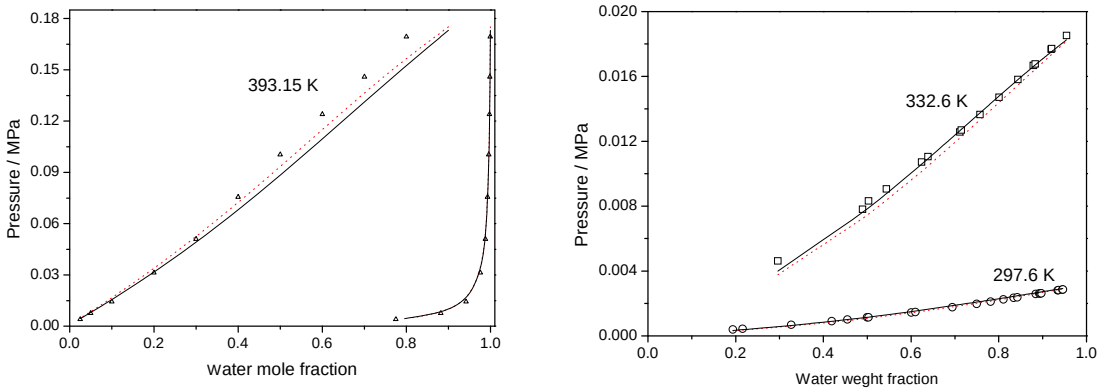

Figure 1. Experimental data (points), NRHB predictions (dotted lines, *kij*=0) and correlations (solid lines, *kij*≠0) for Water – DEG (left) and Water – TEG (right) systems.

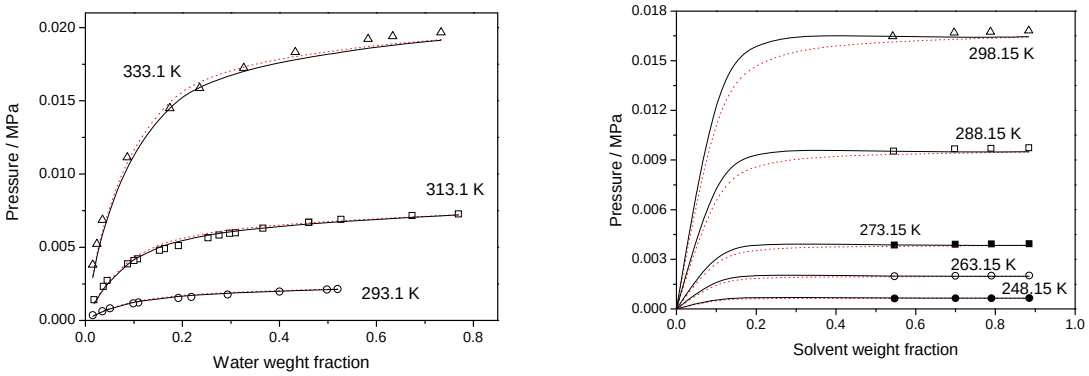

Figure 2. Experimental data (points), NRHB predictions (dotted lines, *kij*=0) and correlations (solid lines, *kij*≠0) for water – PEG (Mw= 600 g mol^{-1}, left) and methanol - PPG (Mw= 3350 g mol^{-1}, right)

References

[1] Panayiotou C, Tsivintzelis I, Economou IG. Nonrandom Hydrogen-Bonding Model of Fluids and their Mixtures. 2. Multicomponent Mixtures. Ind. Eng. Chem. Res. 2007;46:2628-2636.

[2] Tsivintzelis I., Kontogeorgis G.M. Modeling the Vapor – Liquid Equilibria of Polymer – Solvent Mixtures: Systems with Complex – Hydrogen Bonding Behavior. Fluid Phase Equilib. Submitted for publication.

The magnetism as the main factor for increasing of irradiation stability of transition element alloys: bcc –in Fe –Cr and fcc- in Ni-Cr systems

A.Udovsky[1)], V.Kolotushkin[2)]
[1)]Baikov Institute of Metallurgy and Materials Science of RAS
[2)] Joint Stock Company «A.A. Bochvar High-technology Research Institute of Inorganic Materials»
udovsky@imet.ac.ru

Introduction

The Fe-base alloys of the Fe-Cr system stimulated interest during recent years because of high radiation stability at temperatures between 600-900K. So it is interesting for better understanding of physical nature of material stability to compare the behaviour under irradiation of BCC- Fe-base alloys and FCC-alloys of the Ni-Cr system. It has been established that the high radiation stability of FCC Ni-Cr - alloys depends mainly on position of configurational point of alloy composition. With increasing the Cr-content in Ni-Cr alloys from stoichiometrical composition of the Ni_2Cr – compound the enthalpy of formation (ΔH) increases from negative values through zero (at $x_{Cr} \approx 0{,}41$ and T=723K) up to the positive values. It is possible to formulate the hypothesis: the alloys with compositions arranged near the configurational point with the zero value of ΔH have high radiation stability at the low temperature. At higher temperatures it is necessary to take into account the behaviour of concentration dependences of mixing Gibbs energy and their singularities, namely inflection points.
The published results of experimental investigations of the BCC- Fe-base alloys on the Fe-Cr system in compositions about 9-12 at.% Cr demonstrated high radiation stability in comparison with austenitic steels [1-2]. At the same time ab-initio calculated results [3-7] showed the *sign-change* concentration dependence of mixing enthalpy $\Delta H(x_{Cr})$ for BCC –alloys in the Fe-Cr system under 0 K in a ferromagnetic state. It was proved by modeling as ab-initio as far as physical-empirical models that between different contributions (configurational, magnetic, vibrating, electronic and elastic energy accounted for the elastic distortions of crystal lattice of the solid solution induced by the static displacements of ionic cores) of a total free Gibbs energy mixing of BCC – *ferromagnetic* solutions of the Fe-Cr system has demonstrated that magnetic part of free energy is a dominant contribution on stabilization of Fe-rich BCC – alloys in the range of low and medium temperatures. It must be note that the Fe-Cr and Ni-Cr systems have the same behavior as magnetic properties for as *sign-change* concentration dependences of mixing enthalpy $\Delta H(x_{Cr})$ for BCC –alloys in the Fe-Cr system and FCC Ni-Cr – alloys. For the Ni-Cr system $\Delta H(x_{Cr})$ for FCC –phase was obtained by experimental investigations while for the Fe-Cr system ferromagnetic BCC-phase the results on $\Delta H(x_{Cr})$ were obtained by ab-initio calculations only. So the FCC-alloys of the Ni-Cr system will be discussed in the next section in the beginning and then we will return to BCC-alloys of the Fe-Cr system.

The experimental results

Non-equilibrium state in the Ni-Cr alloys` system, created by quenching from the temperature of 1050-1100 °C, begins to show itself at the temperatures corresponding to the working temperatures (above 350 °C). At the process of aging at the temperature of 450 °C after quenching from monophase γ - region of the state diagram (fig. 1a) the long ordering is developed in the structure of alloys near a stoichiometrical composition (alloy No. 1).

In the alloy No. 1 the domains of the Ni_2Cr phase as large as 4-10 nm with number density $7 \cdot 10^{21}$ m^{-3} separated by the antiphase boundaries are formed (fig. 1b). In the alloys with 38-41wt % Cr concentration development of long order Ni_2Cr - phase occurs more slowly. In the alloy No.4 in the process of aging is formed short ordering only, which is demonstrated as tweed contrast – fig.1 c.

In the alloys more 41wt % Cr concentration (alloy No. 6) during the aging the Cr –base α – phase is formed as lamellae of cellular dissociation (fig.1 d), then in the fields between α - phase lamellae the Ni_2Cr – precipitates are formed. The Ni-42Cr-1Mo and Ni-47Cr-1Mo alloys (types No. 4 and 6) have been neutron irradiated in BOR – 60 reactor up to 32 dpa at 350 °C, which microscopic structures are presented in figs. 1e and 1f. In the short ordered Ni-42Cr-1Mo alloy (type No. 4) the dislocation loops of number density equal $4{,}5 \cdot 10^{21} m^{-3}$, with diameter 14 nm are formed. In the Ni-47Cr-1Mo alloy (type No. 6) without short ordered structure the dislocation loops of number density equal $3 \cdot 10^{22}$ m^{-3}, with diameter 7 nm are formed. The total elongation of short ordered irradiated alloy was three times more respectively [11]. Let us examine results obtained by X-ray and pycnometric studies, which prove the existence of short ordering in crystal structure of alloys of the Ni-Cr system. The formation of short and/or long ordering under temperature influence reduce decreases the lattice period of crystal structure of alloys of the Ni-Cr system (fig. 2) and increases the density of alloys (fig. 3). The formation of the Ni_2Cr phase increases the density of alloys, but the formation of the α - phase decreases the density. It may be seen in the density increase of alloy No. 4,

that there is in the vicinity of the Ni_2Cr/ (Ni_2Cr +α) phase boundary and in the density decrease of alloys with Cr concentration more than 44 at. %.

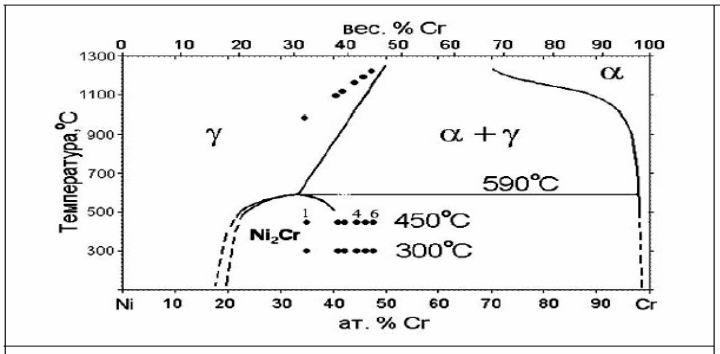

a

Figure 1a: The fragment of the phase diagram of the Ni-Cr system, the numerals 1 -6 shows different compositions of alloys treatment at 300 and 450 C.

Figures 1b-1d present microstructures of alloys № 1, №4 and №6 treatment at 450 C before irradiation.

Figures 1e-1f present microstructures of alloys № 4 and №6 after neutron irradiation at 350 C 32 dpa.

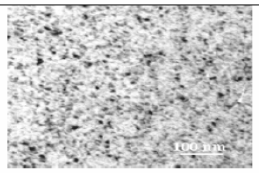

b

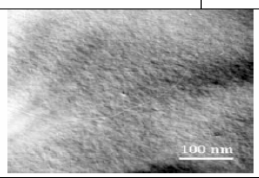

c

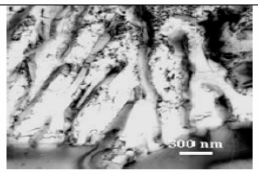

d

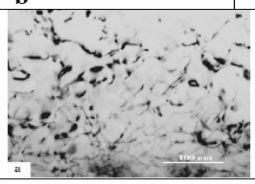

e

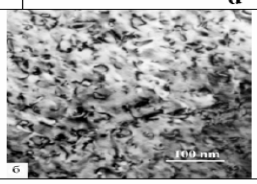

f

The density of these alloys decreases owing to increasing α - phase fraction. Accordingly to equilibrium phase diagram (fig. 1a) in temperature range from 300 up to 450°C these compositions alloys must be in equilibrium state having two Ni_2Cr - and α - phases.

But sluggishness of diffusion processes at above mentioned temperatures reduces to the α- phase precipitates firstly and Ni_2Cr – phase precipitates from metastable γ- phase secondly. So there are three phases in alloys, namely stable α- and Ni_2Cr – phases and metastable γ- phase. After aging at 450 C the X-ray pictures of alloys does not found the X-ray reflections of the α- phase owing to its small fraction, but the measurements of alloy density (fig.3) and metallography (fig.1d) show it.

The comparison of Bragg reflections (331)- types of the Ni-41Cr alloy, aged at 300 and 450 C, demonstrates decreasing of lattice period ($\Delta d/d \approx 4x10^{-4}$) and increasing width of reflections which equals ~20 %, that proves the existence of short ordering.

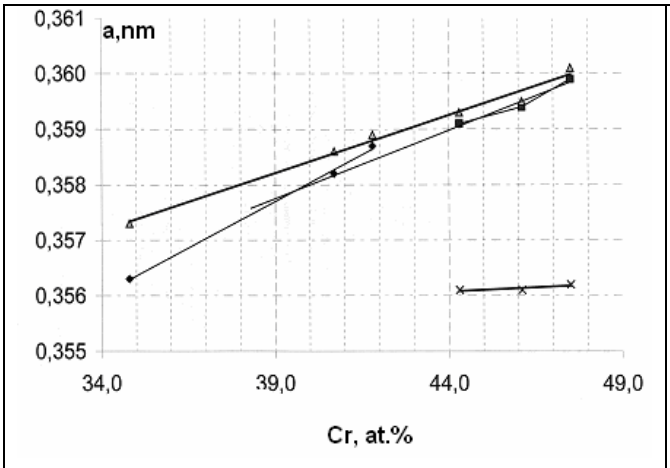

Fig.2. The lattice parameters of crystal structure of Ni-Cr alloys: ▲ – matrix, aging at 300 °C; ◆,■ – matrix, aging at 450 °C; × - the ordered Ni_2Cr – phase at 450 °C

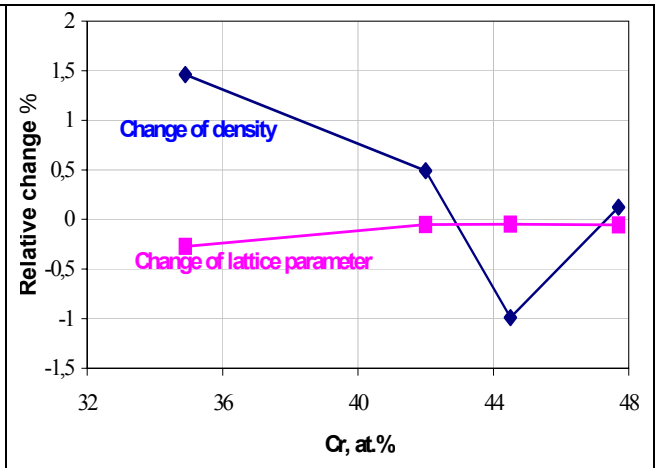

Fig.3. The relative change of lattice parameters of crystal structure and density of aging alloys of the Ni-Cr system at increasing temperature aging from 300 to 450 °C during 40000 h.

The assessment of influence of short ordering in Ni-Cr alloys on recombination of vacancies and interstitials was realized by using positron annihilation method. The change of photon distribution spectrum at capture of positrons by vacancies we assessed by using changing the S- parameter, that proportional to vacancy concentration. When vacancy concentration increases then the probability of annihilation of positrons with conduction electrons and value of the S- parameter increase also. The Ni-32Cr-1Mo alloy in state of short ordering (aging at 300°C during 40000 h) and long ordering (aging at 450°C during 40000 h) was irradiated by 5 MeV electrons at 200°C [8]. Fig. No. 5 demonstrates the increasing vacancy concentration when the electron fluence increases. When electron fluence equals ~1,8x10^{22} m^{-2} the value of S- parameter for short ordered alloy reaches the saturation. It means that all new vacancies recombine with interstitials. The Ni-32Cr-1Mo alloy after aging at 450°C during 40000 h in irradiation process continues to accumulate non-recombined vacancies.

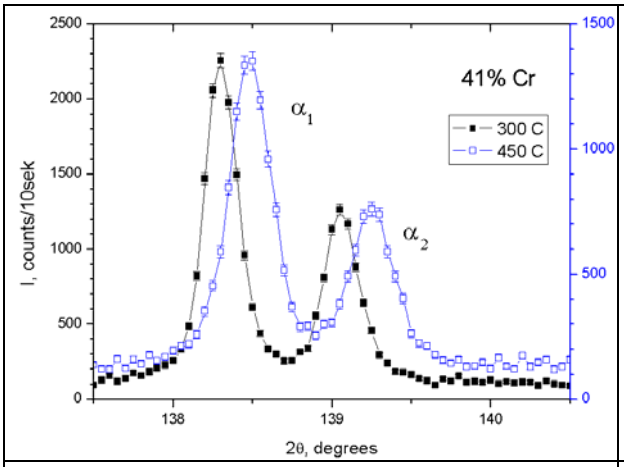

Fig. 4 The comparison of X-ray (331) -reflections of Ni-41Cr alloy after aging at 300 and 450°C during 40000 h.

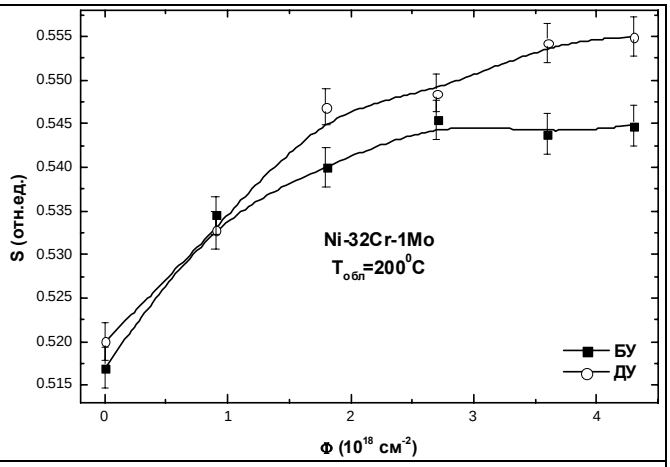

Fig. 5 The dependencies of the S- parameter on electron fluence of Ni-32Cr-1Mo irradiated alloy at 200°C after aging at 300 (open circles) and 450°C (dark squares) during 40000 h.[8]

So the experimental results demonstrate the small influence of neutron irradiation on the short ordered alloys properties, particularly the Ni-42Cr-1Mo alloy. It is necessary to note the importance of obtained results, because the short order in crystal structure of alloys increase the recombination of vacancies and interstitials, which are formed under neutron irradiation.

Discussion

It has been established significantly higher stability of mechanical properties of the Ni-Cr base alloys with the comparison austenitic stainless steels after neutron irradiation. It has been shown that fcc - Ni-Cr - alloys (points from 4 up to 6 on Fig.1) have demonstrated the high irradiation stability depending on position of configurational point of alloy composition. The alloys numbers from1 up to 6 (Fig.1) after quenching from 1000-1200 C were aged at 300 and 450 C during 40,000 hours. The microstructures of these alloys before irradiation are shown on Figures 1 b - 1d. You can see that the alloy №1 has the long-range ordering structure, the alloy № 4 - short-range ordering structure whereas the alloy № 6 – disintegration structure.

The alloys № 4 and № 6 were investigated after irradiationat the temperature of ~350 °C in the reactor БОР-60 up to ~32 dpa. The total elongation of the alloy № 4 was three times more then the alloy № 6. So the existence of short-range ordering structure in alloy stabilized the mechanical properties under irradiation while two-phase structure of alloys destabilized theirs. On the other hand it is known that in the Ni-Cr system with increasing the Cr-content from the Ni through stoichiometric composition of the Ni_2Cr compound and further the enthalpy of formation (ΔH) of FCC –phase increases from negative values (which is beginning the long-range order structure evolution) through zero (at x_{Cr}≈0,4 and T=723 K) up to positive values (which is beginning the formation of two-phase structure) -(Fig. 7).

Recently the sign-changing concentration dependence of the ΔH(x) at 0 K for ferromagnetic BCC - alloys of the Fe-Cr system have been obtained by different scientific groups [3-4] using the ab-initio calculations – Fig.6. It is necessary to note that calculated results for ferromagnetic alloys show substantial deviations from experimental data obtained by Muller and Kubashevski for BCC-alloys in paramagnetic state (blue curve on Fig.7). Thus, the calculated formation energy ΔEf is negative for alloys of the Fe-Cr system for Fe-rich BCC - alloys, but it is positive at higher Cr concentrations. It is necessary to underline the cymbate concentration behavior of the mixing enthalpies dependences at 0 K for ferromagnetic states as the BCC- phase of the Fe-Cr for as the FCC-phase of the Ni-Cr systems**.** In other words in the both systems there are as composition fields with short-range ordering structure, which have irradiation stability, for as with two-phase structure, which have irradiation instability.

So it is possible to formulate a hypothesis: the alloys of the compositions arranged near configurational point with the zero value of ΔH have a higher irradiation stability at moderate temperatures. It is important to underline that a optimal composition of high temperature irradiation stable alloy it is necessary estimate by coupling experimental and simulated research.

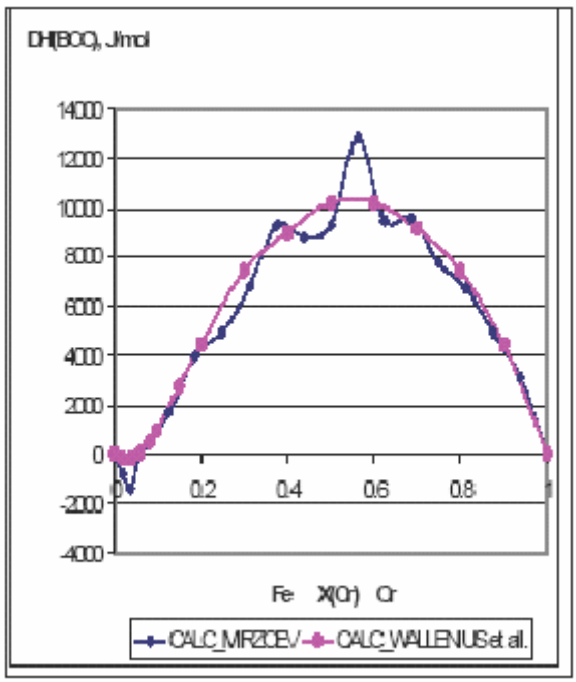

Fig.6. The comparison ab-initio results obtained by asm Mirzoev et all. (2003) – blue points for as Olsson et all. (2003) and Wallenius et all. (2004) – rose points enthalpy of mixing for ferromagnetic state BCC –phase of the Fe-Cr system at 0 K

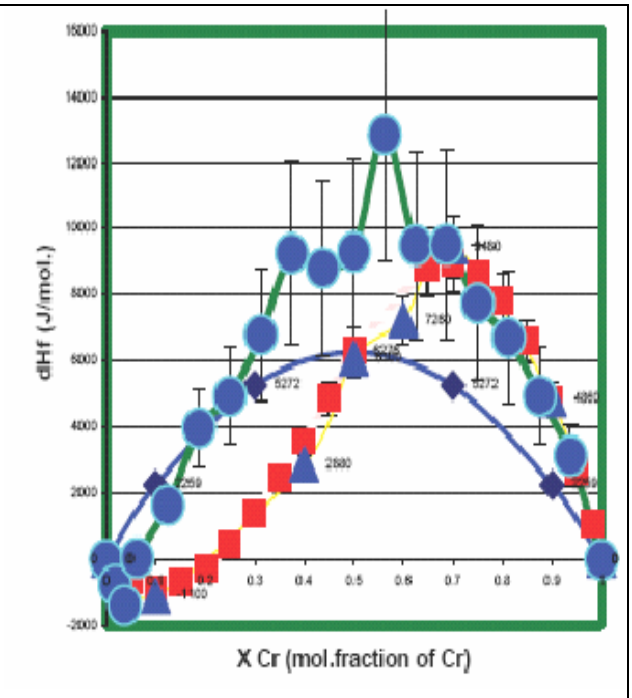

Fig. 7. The experimental data

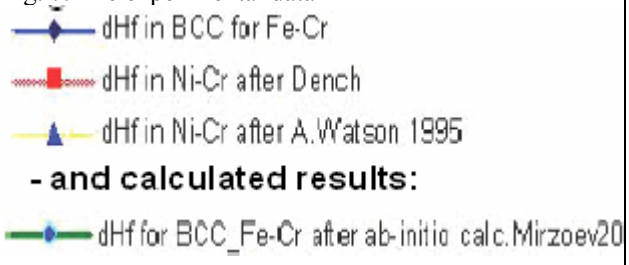

Conclusion

In work [7] was installed that anomalous stability (the part of curve ΔH(x), where ΔH(x)<0) the Fe-rich BCC solutions in Fe-Cr system is conditioned by influence of the magnetism on interatomic interactions Fe and Cr atoms. The research [12] was shown that with increasing the temperature relative part from magnetism on the total free mixing energy of BCC alloys of the Fe-Cr system decreases. Thereby, for development stable Fe-base alloys under irradiation follows to take into consideration that magnetism as the main factor for increasing of irradiation stability of alloys.

References

[1]. A.M. Dvoriashin, S.I. Porollo, Yu.V. Konobeev et al., J. Nucl. Mater. Vol. 367-370, Part 1 (2007), p. 92-96.
[2]. C. Petersen, A. Povstyanko, V. Prokhorov, et al., J. Nucl. Mater. Vol. 367-370, Part 1 (2007), p. 544-549
[3] P.Olsson, I.A.Abrikosov, L.Vitos, J.Wallenius. J.Nuclear Materials 321 (2003) 84-90.
[4 A.A.Mirzoev, M.M.Yalalov, D.A.Mirzaev. Phys. Met. Metallogr. 97, 336 (2004)
[5] J.Wallenius, P.Olsson, C.Lagerstedt, N.Sadberg, R.Chakarova, V.Pontikis. Phys.Rev. B 69, 094103 (2004).
[6] A.L. Udovsky, A.A. Mirzoev, M.M. Yalalov. CALPHAD XXXIV,May 22-27,2005 Maastricht,The Netherlands.
[7] A.E.Kissavos,S.I.Simak,P.Olsson,L.Vitos, I.A.Abrikosov. Comp.Mater.Sci., 2006, v.35, p.1-5.
[8] A.P. Druzhkov, V.P. Kolotushkin, V.L.Arbuzov, S.E. Danilov, and D.A. Perminov. The Physics of Metals and Metallography, 2006, Vol. 101, No. 4, pp. 369-378.
[9] I.Ya.Dekhtyar. Doklady of Academy Science of USSR, 1952, v. 85, № 3 (in Russian).
[10] Yu.Bagaryatskii and Yu.D.Tyapkin. Doklady of Academy Science of USSR. 1958.V 122, № 5, p. 806-809 (in Russian).
[10] V.P. Kolotushkin, A.A.Chernyshev, A.A. Veligzhanin. //Materials science No 1, 2006 (in Russian).
[11] V.P. Kolotushkin, The Physics of Metals and Metallography, Vol. 97. No. 2, 2004, pp.177-187.
[12] A.L.Udovsky, D.A.Vasilyev. Abstracts of the SCTE2008. July 26-31, 2008. Dresden, Germany.

Calculations and analysis of thermodynamics functions of BCC- alloys of the Fe-Cr system by physical-empirical model

A.L. Udovsky, D.A. Vasilyev
Baikov Institute of Metallurgy and Materials Science of RAS, Moscow, Russia
udovsky@imet.ac.ru

Introduction

Development of new generation of nuclear reactors entailed need in new materials for the reactors. For example, materials for fuel cladding of the reactors must be more stable and withheld higher temperatures than Zr-based materials used in existing VVER reactors. Correspondingly, thermodynamic properties of the materials, and BCC – alloys in the Fe-Cr system particularly, became of significant interest. Experimental data for mixing enthalpy for BCC –alloys in the Fe-Cr system were obtained under 1600 K temperature, when the alloys are paramagnetic. Unfortunately, such experiments are not feasible under lower temperature because diffusion slows down drastically as temperature is lowered. Thus, new approaches to obtain the thermodynamic parameters in range of temperatures applicable to the real world have to be found. Recently, numerous scientific works focused on modeling of BCC – alloys in the Fe-Cr system. For BCC –alloys of the Fe-Cr system in a ferromagnetic state, the sign-change concentration dependency of mixing enthalpy under 0 K have been obtained by quantum-mechanical calculations [1-5]. Although presently quantum mechanical calculations are a sole mean to compute thermodynamic properties of metastable phases, they can be performed for equilibrium properties for 0 K temperature only. Use of these results to compute thermodynamic properties and phase diagrams of multi-component systems under higher temperature is quite problematic. To circumvent these limitations of ab-initio results, we have tried to integrate ab-initio results into physical-empirical models. For example, the model links harmonic and anharmonic properties (in quasiharmonic approximation) to energetic characteristics of alloys calculated at 0K, that allows to calculate vibration part of thermodynamic properties of alloys under medium and higher temperatures. Our research applies developed early physical-empirical models to analysis and computation of thermodynamic properties of BCC – alloys in ferromagnetic state of the Fe-Cr system under wide range of temperatures and compositions.

The short description of using physical-empirical models

Solid solutions with BCC crystal lattice of the Fe-Cr system could be modeled as a system of non-interacting subsystems from point of view of statistic thermodynamic. Then, a statistic sum of the modeled system is equal to a product of statistic sums of non-interacting subsystems. This approach leads to equality between total free energy of the system and sums of free energies of various subsystems.

We assume that this system could be modeled as a combination of independent subsystems, including: 1) a configuration part of free energy which describes an ion-subsystem, 2) the elastic part of free energy, which describes static distortion of crystal lattice of the solid solution induced by static displacement of ion-cores, 3) thermal contribution of an electron subsystem, 4) thermal contribution of a spin subsystem, 5) a vibration subsystem which includes harmonic and anharmonic constituents. Every of these subsystems contributes to the free energy of the system. Values of various contributions to free energy of the system could be calculated by means of experimental data for appropriate physical properties which are input characteristic of the model.

The method for calculation of thermodynamic function of disordered solutions at paramagnetic state was suggested in work [6]. On basis of this method and adding in a thermal contribution of a spin subsystem to description of thermodynamic properties of BCC solutions of the Fe-Cr system at ferromagnetic state, we can describe the free energy of BCC solution as a function of composition (concentration of the second component - Cr) and temperature by formula (1).

$$\Delta G(x,T) = \Delta H_{chem}(x,0) + \Delta G_{vibr}(x,T) + \Delta G_{el}(x,T) + \Delta G_{mag}(x,T) + \Delta G_{elast}(x,T) - TS_{conf}(x,0). \qquad (1)$$

Here $\Delta H_{chem}(x,0)$ is chemical interaction energy of average size atoms under condition of alloy formation at 0 K; $\Delta G_{vibr}(x,T)$ is free energy of crystal lattice vibrations; $\Delta G_{el}(x,T)$ is free energy of thermally excited electrons; $\Delta G_{mag}(x,T)$ is the thermal term of free energy which takes magnetic subsystems into account; $\Delta G_{elast}(x,T)$ is the energy of elastic distortions of crystal lattice of the solid solution induced by the static displacements of ionic cores; $S_{conf}(x)$ is a configurational entropy of completely disordered solid solution that is described by a model of ideal solution.

To describe both thermodynamic of alloys and phase equilibrium in binary systems, we can, keeping with our general approach, turn from the free energy of solutions to free energy of mixing by virtue of an invariance of system of equilibrium equations in relation to linear transformation on composition at T=const.

The vibration contribution to free energy was calculated as a sum of harmonic and anharmonic contributions. Harmonic contribution was described by Debye model, whereas anharmonic contribution was described by

quasiharmonic approximation. To approximate anharmonic contribution, we took into account that Debye temperature depends on volume through Gruneisen parameter, and the volume, in its own turn, depends on temperature through a volumetric thermal expansion coefficient.

Thermal part of magnetic contribution to the free energy of the system was modeled by the Inden-Hillert-Jarl model, using Curie temperature and average value of magnetic moment as input parameters of the model [7-8]. Contribution of thermally exited electrons was accounted by a well-known expression using experimental data for electron specific heat coefficient. It should be noted, in principle the data can be obtained by quantum-mechanical calculations as well.

In order to calculate the free Gibbs energy of BCC alloys, we collected experimental data for physical properties being parameters of our physical - empirical models from literature. Graphics of the properties (Debye temperature, electron specific heat coefficient [9-10], Curie temperature, average value of magnetic moment, volumetric thermal expansion coefficient, Gruneisen parameter) are shown in fig. 1- fig 2.

Then, these approximated dependences on the composition of the physic properties were calculated. Then, some contributions and dependency of total free energy on the function of composition to BCC solutions of the Fe-Cr system for different temperatures were calculated. Analysis of contributions like $\Delta H(x,0)$, $G_{harm}(x,T)$, $G_{magn}(x,T)$, $G_{anharn}(x,T)$, $G_{el}(x,T)$, $G_{elast}(x,T)$ and their influence on a stability of BCC solutions of the Fe-Cr system was accomplished.

The description of physical properties as input data for physical-empirical models

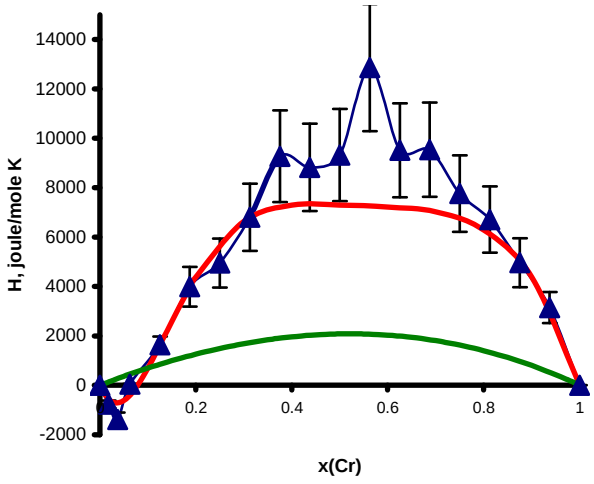

*Fig. 1a. The ab-initio **ΔH(x,0)** according to [2]; calculated **$\Delta G_{elast}(x,0)$** and **$\Delta H_{chem.}(x,0)$**.*

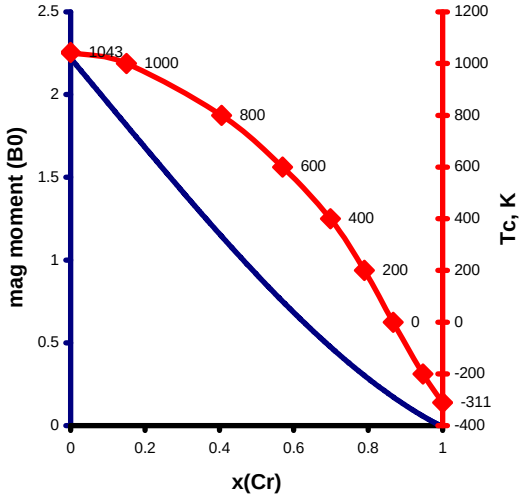

*Fig. 1b. The Curie temperature **(Tc)** and average value of magnetic moment **(B0)** of BCC phase.*

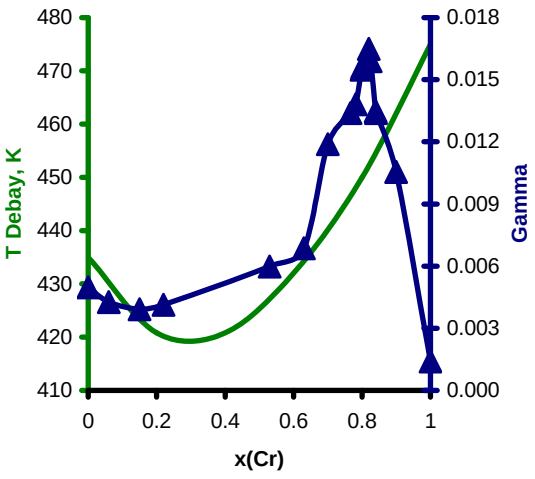

a

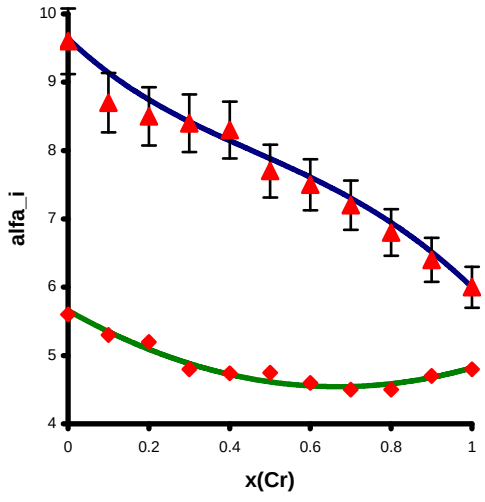

b

*Fig.2. Concentration dependencies: (a) Debye temperature (**θ_D**) and electron heart capacity coefficient (**Gamma**); (b) Linearly thermal expansion coefficients of BCC alloys for the Fe-Cr system (**$alfa=alfa_0+alfa_1T$**).*

When we attempted to input contributions to the free energy of BCC solution obtained by quantum mechanic calculations to our model, we obtained results that differ from experimental data. Calculated the critical point of immiscibility gap of BCC- phase reached the melting temperature that contradicts experimental phase diagram of the Fe-Cr system. Future analysis of results shown that this discrepancy appears because of large value of ab-initio calculated mixing enthalpy of ferromagnetic BCC solution at 0K [1-2,4]. Therefore, we made an assumption that $\Delta H(x,0)$ can be modeled as a sum of the chemical energy of formation of the alloy at 0K - $\Delta H_{chem}(x,0)$ and elastic energy $\Delta G_{elast}(x,0)$, see fig. 1a.

Concentration dependence of Debye temperature (see fig. 2a) was calculated using assessment values which were calculated by Lendeman's criteria for the melting of BCC- solution of the Fe-Cr system. The concentration dependence of electron specific heat coefficient was approximated using experimental data from [9-10]. The linear thermal expansion coefficients of the BCC-solution of Fe-Cr alloys accounting for its thermal dependence were approximated using experimental data from [11-14], see fig. 2b. Concentration dependence of Curie temperature and average value of magnetic moment for BCC alloys of the Fe-Cr system (see fig. 1b) were taken from [15-17].

The computational results

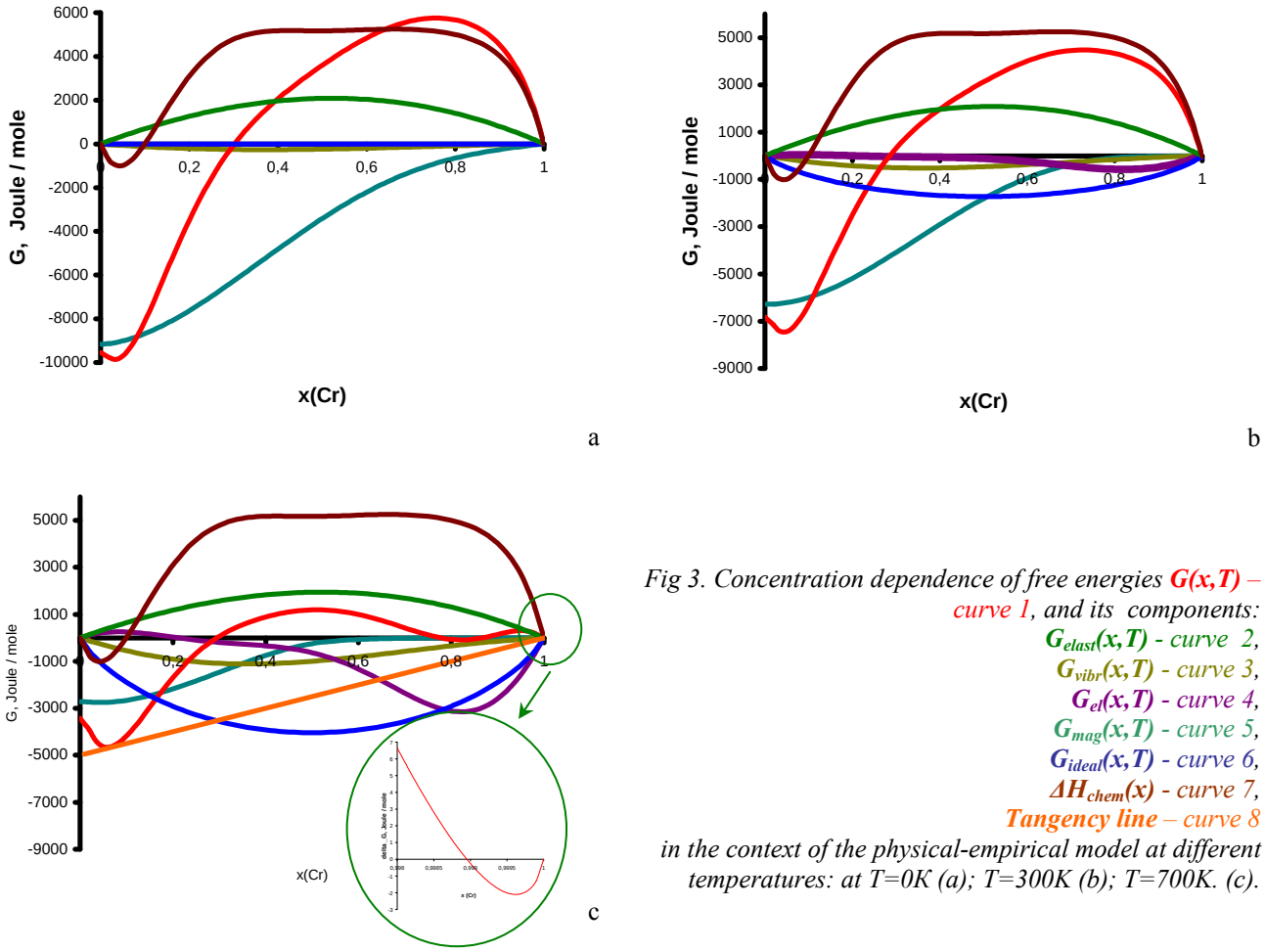

Fig 3. Concentration dependence of free energies ***G(x,T)*** *– curve 1, and its components:*
$G_{elast}(x,T)$ *- curve 2,*
$G_{vibr}(x,T)$ *- curve 3,*
$G_{el}(x,T)$ *- curve 4,*
$G_{mag}(x,T)$ *- curve 5,*
$G_{ideal}(x,T)$ *- curve 6,*
$\Delta H_{chem}(x)$ *- curve 7,*
Tangency line *– curve 8*
in the context of the physical-empirical model at different temperatures: at T=0K (a); T=300K (b); T=700K. (c).

All components of total Gibbs energy of ferromagnetic BCC- solutions of the Fe-Cr system (see formula (1)) were calculated on basis of the above mentioned physical–empirical models. They are shown on fig. 3a, 3b and 3c for temperatures 0K, 300K and 700K correspondingly. The phase immiscibility gap evolution of the BCC- solution of the Fe-Cr system can be quality estimated by those graphs.

Conclusion

The analysis of calculated results of different parts of total free Gibbs mixing energy of BCC – ferromagnetic solutions of the Fe-Cr system demonstrated that magnetic part of free energy plays dominant role in stabilization of Fe-rich BCC – alloys in the range of low and medium temperatures, whereas electronic part of free energy plays dominant role in stabilization of Cr-rich BCC – alloys in the range of high temperatures.

The research was support by RFBR Project No. 06–03–33152a.

References

[1] P.Olsson, I.A.Abrikosov, L.Vitos, J.Wallenius. J.Nuclear Materials 321 (2003) 84-90.
[2] A.A.Mirzoev, M.M.Yalalov, D.A.Mirzaev. Phys. Met. Metallogr. 97, 336 (2004)
[3] J.Wallenius, P.Olsson, C.Lagerstedt, N.Sadberg, R.Chakarova, V.Pontikis. Phys.Rev. B 69, 094103 (2004).
[4] A.L. Udovsky, A.A. Mirzoev, M. M. Yalalov. CALPHAD XXXIV, May 22-27, 2005 Maastricht, The Netherlands.
[5] A.E.Kissavos,S.I.Simak,P.Olsson,L.Vitos, I.A.Abrikosov. Comp.Mater.Sci., 2006, v.35, p.1-5.
[6] A.L. Udovsky, O.S. Ivanov. J. of Nucl. Mater. 46 (1973) 192-206.
[7] G. Inden. Proc. CALPHAD Conf. Dusseldorf, 1976, III, 4-1.
[8] M. Hillert, M. Jarl. CALPHAD 2 (1978) 227.
[9] C.H. Cheng, C.T. Wei, P.A. Beck. Phys. Rev. 1960. V. 120, No. 2. P. 426–436.
[10] K. Schroeder. Phys. Rev. 1962. V. 125, No. 4. 1209–1212.
[11] T.I. Babuk, G.P. Kushta, S.A. Chornei. FMM, 1973, т. 35, № 4, с. 851–853.
[12] Ja.I. Dutchak, V.G.Cheh. Phys.-chem. material mechanical , 1980, т. 16, № 2, с. 116–118.
[13] Ja.I. Dutchak, V.G.Cheh. Phys.-chem. material mechanical 1982, т. 18, № 5, с. 116–119.
[14] S.I. Novikova. Heat expansion of solids. M. Nauka. 1974.
[15] J.C. Lin, Y.Y. Chuang,K.C. Hsien, Y.A.Chang. CALPHAD 11 (1987) 73-81.
[16] J.O. Andersson, B. Sundman. CALPHAD 11 (1987) 83-92.
[17] S.Hertzman, B.Sundman. CALPHAD 6 (1982) 67-80.

Generalized Erenfest's relationships as continuity condition for determinants of Hessian matrix from equilibrium Gibbs potential and its algebraic cofactors on one/ two-phase boundaries of the phase diagrams of multicomponent systems

Alexander Udovsky

Baikov Institute of Metallurgy and Materials Science of the Russian Academy of Sciences
The Moscow Engineer-Physical Institute (State University)

udovsky@imet.ac.ru ; al-udovsky1@yandex.ru

Introduction

In paper [1] were received general equations between the second derivatives to equilibrium Gibbs energy (G_E) of multi-component of the closed systems on one/two-phase boundaries of the α⁄α+β–type of phase diagram (PD). Later in [2-3] were derived relationships for jumps of all second derivatives of G_E of binary systems on one/two-phase boundary of the α⁄α+β type, as follows, namely, specific heat, the thermal expansion coefficient, partial enthalpies and entropies of components, isothermal compressibility, concentration slope of the volume (the partial volumes of the first and second components), as well as the second derivative of Gibbs energy of α-phase on composition for the T-P-x PD, where x – mole fraction of the second component, T is temperature and P – pressure. In [4] was shown that between jumps of some derivatives of second order to EGE (specific heat, compressibility and the thermal expansion coefficient) on one/two-phase type boundaries of binary systems exists intercoupling, which was is earlier received by P. Erenfest [5]. Recently in works [6-7] was shown that determinant of the Hessian matrix of G_E on with respect to all arguments (T-P-x) is an continuous function on the α⁄α+β type of phase boundaries of T-P-x PDs though all elements of matrix are an discontinuous functions on the α⁄α+β – type of phase boundaries T-P-x phase diagram.

In the persisting work have been proved that determinants of as Hessian matrix all algebraic minors of the Hessian matrix of G_E with respect to its arguments are an continuous functions on the α⁄α+β –type of phase boundaries of the T-P-x PDs. Proved equivalence of the generalized Erenfest's equations and relationships to continuity of the determinant of the Hessian matrix of G_E of two-component systems on one/two-phase boundaries of T-P-x PDs and its determinants of the algebraic adjuncts.

The continuity of determinants of Hessian matrix from equilibrium Gibbs potential and its algebraic cofactors

Let us take down difference of values for determinant the Hessian matrix of G_E of binary system between two-phase and single-phase states of the alloys, located on different sides of α⁄α+β –type of phase boundaries of the T-P-x PDs

$$\det\{Ges(G^{\alpha+\beta}(x^{\alpha}(T,P)) - Ges(G^{\alpha}(x^{\alpha}(T,P))\} =$$

$$= \det\begin{Bmatrix} -\dfrac{[C_P]_{x^\alpha}^{\alpha\to\alpha+\beta}}{T} & V^{\alpha}(x^{\alpha})[\alpha_V]_{x^\alpha}^{\alpha\to\alpha+\beta} & -\left[\dfrac{\partial S}{\partial x}\right]_{x^\alpha}^{\alpha\to\alpha+\beta} \\ V^{\alpha}(x^{\alpha})[\alpha_V]_{x^\alpha}^{\alpha\to\alpha+\beta} & -V^{\alpha}(x^{\alpha})[\chi_T]_{x^\alpha}^{\alpha\to\alpha+\beta} & \left[\dfrac{\partial V}{\partial x}\right]_{x^\alpha}^{\alpha\to\alpha+\beta} \\ -\left[\dfrac{\partial S}{\partial x}\right]_{x^\alpha}^{\alpha\to\alpha+\beta} & .\left[\dfrac{\partial V}{\partial x}\right]_{x^\alpha}^{\alpha\to\alpha+\beta} & -\left.\dfrac{\partial^2 G^{\alpha}}{\partial x^2}\right|_{x^\alpha} \end{Bmatrix}. \qquad (1)$$

In relationship (1) element matrixes are a values, for instance, the first element

$$-\frac{[C_P]_{x^\alpha}^{\alpha\to\alpha+\beta}}{T} = -\lim_{\varepsilon\to 0}\left\{\frac{C_P^{\alpha+\beta}(x^{\alpha}+\varepsilon) - C_P^{\alpha}(x^{\alpha}-\varepsilon)}{T}\right\} \qquad (2)$$

equals difference corresponding to functions (for instance, isobaric specific heat) taken in two-phase area in vicinities one/two-phase boundary of the T-P-x phase diagrams and subtracted similar function computable in vicinities of the same boundary, but on the part of single-phase area. Account got in [2-4] relationships for jumps of specific heat

$\left[C_P\right]_{x^\alpha}^{\alpha\to\alpha+\beta}$, of the volume termal expansion coefficient $\left[\alpha_V\right]_{x^\alpha}^{\alpha\to\alpha+\beta}$, isothermal compressibility $\left[\chi_T\right]_{x^\alpha}^{\alpha\to\alpha+\beta}$, concentration inclinations of entropy $\left[\frac{\partial S}{\partial x}\right]_{x^\alpha}^{\alpha\to\alpha+\beta}$ as for as volume $\left[\frac{\partial V}{\partial x}\right]_{x^\alpha}^{\alpha\to\alpha+\beta}$

$$-\frac{\left[\frac{\partial S}{\partial x}\right]_{x^\alpha}^{\alpha\to\alpha+\beta}}{\left(\frac{\partial x^\alpha}{\partial T}\right)_P}=\frac{\left[S_A\right]_{x^\alpha}^{\alpha\to\alpha+\beta}}{\left(\frac{\partial x^\alpha}{\partial T}\right)_P x^\alpha}=-\frac{\left[S_B\right]_{x^\alpha}^{\alpha\to\alpha+\beta}}{\left(\frac{\partial x^\alpha}{\partial T}\right)_P (1-x^\alpha)}=\frac{\left[C_P\right]_{x^\alpha}^{\alpha\to\alpha+\beta}}{\left(\frac{\partial x^\alpha}{\partial T}\right)_P^2 T^{\alpha/\alpha+\beta}}=\frac{\left[\frac{\partial V}{\partial x}\right]_{x^\alpha}^{\alpha\to\alpha+\beta}}{\left(\frac{\partial x^\alpha}{\partial P}\right)_T}=$$

$$=-\frac{\left[V_A\right]_{x^\alpha}^{\alpha\to\alpha+\beta}}{\left(\frac{\partial x^\alpha}{\partial P}\right)_T x^\alpha}=\frac{\left[V_B\right]_{x^\alpha}^{\alpha\to\alpha+\beta}}{\left(\frac{\partial x^\alpha}{\partial P}\right)_T (1-x^\alpha)}=\frac{V^\alpha(x^\alpha)\left[\chi_T\right]_{x^\alpha}^{\alpha\to\alpha+\beta}}{\left(\frac{\partial x^\alpha}{\partial P}\right)_T^2}=-\frac{V^\alpha(x^\alpha)\left[\alpha_V\right]_{x^\alpha}^{\alpha\to\alpha+\beta}}{\left(\frac{\partial x^\alpha}{\partial T}\right)_P\left(\frac{\partial x^\alpha}{\partial P}\right)_T}= \quad (3)$$

$$=-\frac{1}{x^\alpha}\left(\frac{\partial G_A^\alpha}{\partial x}\right)\Bigg|_{x^\alpha}=\frac{1}{(1-x^\alpha)}\left(\frac{\partial G_B^\alpha}{\partial x}\right)\Bigg|_{x^\alpha}=\frac{\partial^2 G^\alpha}{\partial x^2}\Bigg|_{x^\alpha}>0.$$

As example on Fig.1 optimized PD of the Al-Si system are presented, got at using CALPHAD - method, as well as fragment this PD for Si-rich alloys. Besides the temperature dependencies of specific heat for alloys, compositions which equal 99,98 at.% Si and 99,99 at.% Si, are presented on Fig.1 c and d. From analysis these dependencies follows that values of jumps for specific heat on liquidus equal the giant of values, approximately on 3 orders exceeding 3R!
Let as shall substitute equations (3) instead of elements of the matrix (1), as a result of calculations we shall get

$$\det\left[GesG(x^\alpha(T,P))\right]^{\alpha\to\alpha+\beta}=\left(\frac{\partial^2 G^\alpha}{\partial x^\alpha}\right)^3\left(\frac{\partial x^\alpha}{\partial T}\right)_P^2\left(\frac{\partial x^\alpha}{\partial P}\right)_T^2\det\begin{pmatrix}-1\ldots-1\ldots.1\\-1\ldots-1\ldots.1\\1\ldots\ldots1\ldots-1\end{pmatrix}=0. \quad (4)$$

Thereby, the relationship (4) proves continuity of the determinant of the Hessian matrix from equilibrium of the Gibbs potential of two-phase binary systems on one/two-phase boundary of the T-P-x phase diagram.
Let as calculate determinants a main algebraic additions of the Hessian matrix

$$\det\{A_{11}^{\alpha+\beta}-A_{11}^{\alpha}\}=\det\begin{Vmatrix}-V^\alpha\left[\chi_T^\alpha\right]_{x^\alpha}^{\alpha\to\alpha+\beta} & \left[\frac{\partial V}{\partial x}\right]_{x^\alpha}^{\alpha\to\alpha+\beta}\\ \left[\frac{\partial V}{\partial x}\right]_{x^\alpha}^{\alpha\to\alpha+\beta} & \frac{\partial^2 G^\alpha}{\partial x^2}\Big|_{x^\alpha}\end{Vmatrix}=0, \quad (5)$$

$$\det\{A_{22}^{\alpha+\beta}-A_{22}^{\alpha}\}=\det\begin{Vmatrix}-\left[C_P\right]_{x^\alpha}^{\alpha\to\alpha+\beta}/T & -\left[\frac{\partial S}{\partial x}\right]_{x^\alpha}^{\alpha\to\alpha+\beta}\\ -\left[\frac{\partial S}{\partial x}\right]_{x^\alpha}^{\alpha\to\alpha+\beta} & \frac{\partial^2 G^\alpha}{\partial x^2}\Big|_{x^\alpha}\end{Vmatrix}=0, \quad (6)$$

$$\det\{A_{33}^{\alpha+\beta}-A_{33}^{\alpha}\}=\det\begin{Vmatrix}-\left[C_P\right]_{x^\alpha}^{\alpha\to\alpha+\beta}/T & V^\alpha(x^\alpha)\left[\alpha_V\right]_{x^\alpha}^{\alpha\to\alpha+\beta}\\ V^\alpha(x^\alpha)\left[\alpha_V\right]_{x^\alpha}^{\alpha\to\alpha+\beta} & -V^\alpha(x^\alpha)\left[\chi_T\right]_{x^\alpha}^{\alpha\to\alpha+\beta}\end{Vmatrix}=0. \quad (7)$$

Generalized Erenfest relationships

From equation (7) we directly get Erenfest equation (8)

$$\left[C_P\right]_{x^\alpha}^{\alpha\to\alpha+\beta}\left[\chi_T\right]_{x^\alpha}^{\alpha\to\alpha+\beta}=TV^\alpha(x^\alpha)\left\{\left[\alpha_V\right]_{x^\alpha}^{\alpha\to\alpha+\beta}\right\}^2 \quad (8)$$

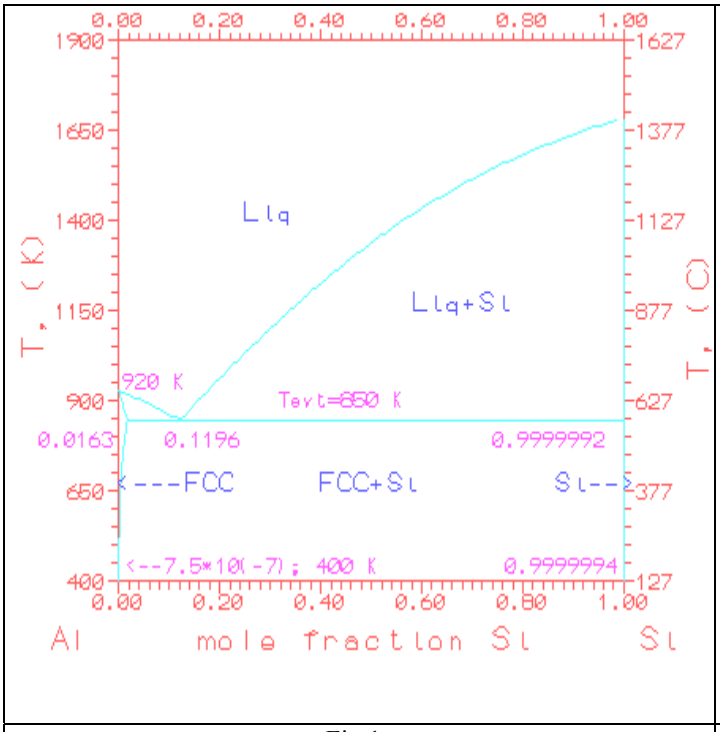

Fig.1a

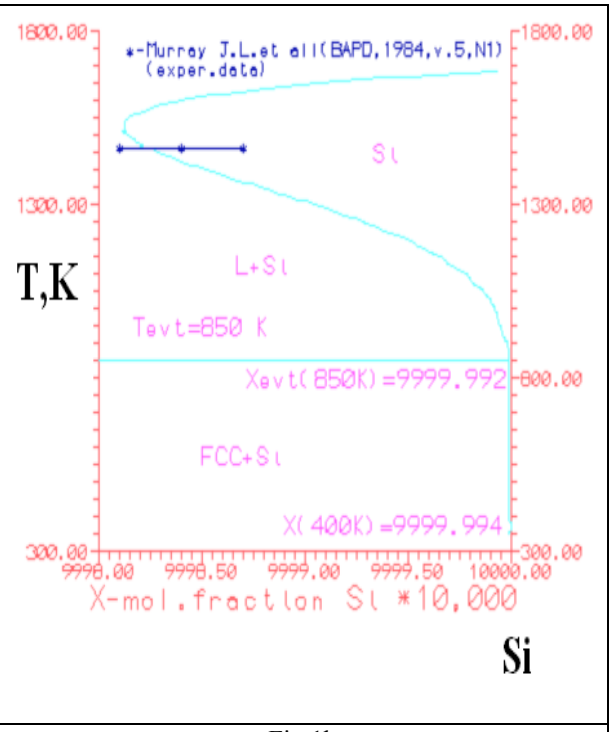

Fig.1b

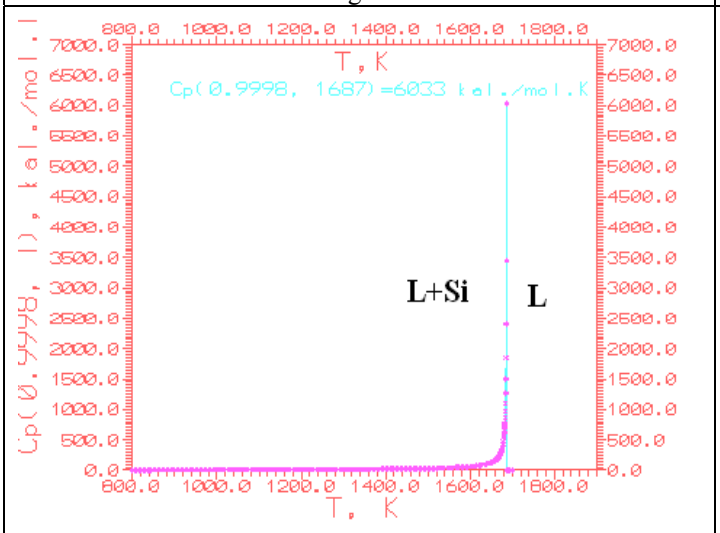

Fig.1c

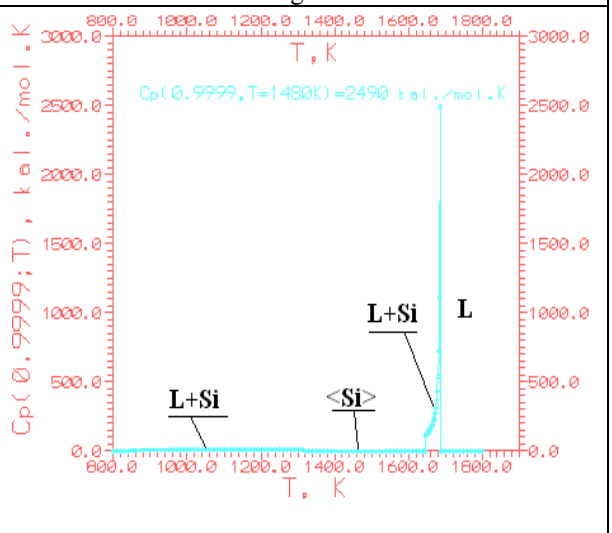

Fig.1d

Fig.1. The optimised phase diagram of the Al-Si system (fig.1a and b) and predicted calculated temperature dependensies of specific heat for alloys with copositions equals 99,98 at.%Si as for as 99,99 at.%Si (Fig.1c and d)

which links the jumps of isobaric specific heat, isothermic compressibility and the volume thermal expansion coefficient. The first equation (8) was obtained by Erenfest [5], but under postulation that he considered phase the transition second mode. Then as in [2-4, 7] and here this equation follows from condition of continuity of the determinant of one of the algebraic additions (7) of the Hessian matrix from equilibrium of the Gibbs energy on $\alpha/\alpha+\beta$ –type of phase boundary of T-P-x phase diagram.

Other similar relationships followed from conditions of continuity determinant cofactors (6) and (7)

$$V^{\alpha}\left[\chi_T^{\alpha}\right]_{x^{\alpha}}^{\alpha\to\alpha+\beta} * \left.\frac{\partial^2 G^{\alpha}}{\partial x^2}\right|_{x^{\alpha}} = \left\{\left[\frac{\partial V}{\partial x}\right]_{x^{\alpha}}^{\alpha\to\alpha+\beta}\right\}^2 , \quad (9)$$

$$\left[\frac{\partial V}{\partial x}\right]_{x^{\alpha}}^{\alpha\to\alpha+\beta} \left.\frac{\partial^2 G^{\alpha}}{\partial x^2}\right|_{x^{\alpha}} = T\left\{\left[\frac{\partial S}{\partial x}\right]_{x^{\alpha}}^{\alpha\to\alpha+\beta}\right\}^2 . \quad (10)$$

Relationships (8) - (10) we shall name as generalised Erenfest equations on α/α+β –type of phase boundaries of the T-P-x phase diagrams of the binary systems. The similar relationships we can be received from equality zero remained three determinants of the differences of the algebraic cofactors of the Hessian matrix between two-phase and single-phase states alloys on on α/α+β –type of phase boundary T-P-x phase diagram

$$\det\{\mathrm{A}_{12}^{\alpha+\beta} - \mathrm{A}_{12}^{\alpha}\} = 0, \ \det\{\mathrm{A}_{23}^{\alpha+\beta} - \mathrm{A}_{23}^{\alpha}\} = 0, \ \det\{\mathrm{A}_{31}^{\alpha+\beta} - \mathrm{A}_{31}^{\alpha}\} = 0. \quad (11)$$

From here follow three additional generalised Erenfest equations

$$V^{\alpha}(x^{\alpha})\left[\alpha_V\right]_{x^{\alpha}}^{\alpha\to\alpha+\beta}\left\{\left.\frac{\partial^2 G^{\alpha}}{\partial x^2}\right|_{x^{\alpha}}\right\} = -\left[\frac{\partial S}{\partial x}\right]_{x^{\alpha}}^{\alpha\to\alpha+\beta}\left[\frac{\partial V}{\partial x}\right]_{x^{\alpha}}^{\alpha\to\alpha+\beta} , \quad (12)$$

$$\left[C_P\right]_{x^{\alpha}}^{\alpha\to\alpha+\beta}\left[\frac{\partial V}{\partial x}\right]_{x^{\alpha}}^{\alpha\to\alpha+\beta} = TV^{\alpha}(x^{\alpha})\left[\alpha_V\right]_{x^{\alpha}}^{\alpha\to\alpha+\beta}\left[\frac{\partial S}{\partial x}\right]_{x^{\alpha}}^{\alpha\to\alpha+\beta} , \quad (13)$$

$$\left[\alpha_V\right]_{x^{\alpha}}^{\alpha\to\alpha+\beta}\left[\frac{\partial V}{\partial x}\right]_{x^{\alpha}}^{\alpha\to\alpha+\beta} = \left[\chi_T^{\alpha}\right]_{x^{\alpha}}^{\alpha\to\alpha+\beta}\left[\frac{\partial S}{\partial x}\right]_{x^{\alpha}}^{\alpha\to\alpha+\beta} . \quad (14)$$

Conclusion

Thereby, we have proved the continuity of the determinant of the Hessian matrix from equilibrium of the Gibbs potential on α/α+β –type of phase boundaries of the T-P-x phase diagrams of the binary systems and all its algebraic cofactors on one/two-phase boundary of the T-P-x PD. All generalised Erenfest's equations (8)-(10), (12)-(14) are immediate from conditions of continuity determinant of the Hessian matrix and its algebraic cofactors on α/α+β –type of phase boundary of the T-P-x PD of closed binary systems.

The last statement demonstrates equivalence of the generalised relationships Erenfest's equations and continuity of the determinant of the Hessian matrix from equilibrium of the Gibbs potential on α/α+β –type of phase boundaries of the T-P-x phase diagrams of the binary systems and its algebraic cofactors. However, stated method, unlike Erenfest's derivation [5], is directly generalised on event the n-component systems at n>2. Herewith considering that partial derivatives on composition from entropy, volume for binary system are changed on gradients on vector of compositions, but the second derivatives from Gibbs energy replace by square matrix, which element are all second derivatives from Gibbs energy on independent concentrations of components of the n-component closed system. Herewith independent concentrations of components of the n-component closed system are an contravariant rectangular components of covariant basis, basis vectors which coincident with ribs of (n-1) - dimensional regular simplex of compositions for closed n-component system.

The work in part has been supported by RFBR N 06-03-33152-a grant.

References

[1] A.L.Udovsky, A.M.Gaidukov, O.S.Ivanov. // Phys. Letters. 1979. V.72A. N 1. P. 1.
[2] A.L.Udovsky. In book: Phase diagrams in materials science. Kiev. Naukova Dumka. 1984. C.112(in Russian).
[3] A.L.Udovsky. Russian Metally .1990 N 2. P.136 (in Russian).
[4] A.L.Udovsky. Russian Metally .1991 N 4. P. 34 (in Russian).
[5] P.Erenfest. Proc. Koningklijke Akad.Watenschappen. Amsterdam. 1933. V. XXXVI. № 2. S.153
[6] A.L.Udovsky. Physical base of computer design materials. Great Novgorod. 2005. 88 p. (in Russian).
[7] A.L.Udovsky. The Physical base of computer design materials. In: Physical Materials Science. Textbook in 6 volumes. Under general editing Prof.B.A.Kalin. The vol. 4, Chapter 15. MEPhI, 2008 (in Russian).

Modeling of structural and thermodynamic properties of the sigma–phase in the Fe-Cr system

Alexander Udovsky and Mikhail Kupavtsev

Baikov Institute of Metallurgy and Materials Science, Russian Academy of Sciences,
Leninsky Prospect, 49, Moscow 119991, Russia, e-mail: udovsky@imet.ac.ru; kmv@imet.ac.ru

Introduction

The σ– phase is present in 43 binary systems and also many three- and more component systems. Sigma- phase is generated between various transient elements (Cr, V, Fe, Ni, Mn and etc.). The σ–phase is thermodynamic stable only for one pure component – uranium (β– phase) and metastable for β–Ta. The lattice of σ– phase is consisting from 5 sub-lattices (thirty of atoms, which are having different of coordination numbers 12, 14 and 15). At last ten years a σ–phase was subject of modeling by quantum-mechanical calculations (Havrankova et all. [1], Houserova et all [2]).). It was applied for calculation of energy cohesion and mixing enthalpy at 0°K for order complexes. And only in work [3] was obtained calculation for influence temperature on distribution atoms of components for σ–phase in the Re-W system by using Gorsky – Bragg – Williams approximation.

In this paper was obtained three- sublattice model (3SLM) for description of equilibrium distribution of atoms of the components into σ–phase depending on composition and temperature and modeling of σ–phase in the Fe-Cr system.

The formulation of the three sublattice model

According to 3SLM for the real structure of σ–phase $\mathbf{A_2^{12}B_4^{15}C_8^{14}D_8^{12}E_8^{14}}$ (including 5 sublattice) was approximated by 3 sublattices. Every from model sublattices are filling atoms of two components with coordination numbers (12, 14 and 15).

$$\begin{aligned} a^{(12)} &= a^{(A)} + a^{(D)} = 10 \qquad & \alpha^{(12)} &= a^{(12)}/(a^{(12)} + a^{(14)} + a^{(15)}) \\ a^{(14)} &= a^{(C)} + a^{(E)} = 16\ , \qquad & \alpha^{(14)} &= a^{(14)}/(a^{(12)} + a^{(14)} + a^{(15)}) \\ a^{(15)} &= a^{(B)} = 4 & \alpha^{(15)} &= a^{(15)}/(a^{(12)} + a^{(14)} + a^{(15)}) \end{aligned}$$

The functional of mixing Gibbs energy of the σ– phase relatively of both components in σ– phases according to 3SLM is

$$\begin{aligned} {}^{\sigma}\Delta^{\sigma}G^{\sigma}(x, y_2^{12}, y_2^{15}, T) &= y_1^{12}\cdot y_2^{12}\cdot\delta E_{12}^{12} + y_1^{12}\cdot y_2^{14}\cdot\delta E_{12}^{14} + y_1^{12}\cdot y_2^{15}\cdot\delta E_{12}^{15} \\ &+ y_1^{14}\cdot y_2^{12}\cdot\delta E_{14}^{12} + y_1^{14}\cdot y_2^{14}\cdot\delta E_{14}^{14} + y_1^{14}\cdot y_2^{15}\cdot\delta E_{14}^{15} + \\ &y_1^{15}\cdot y_2^{12}\cdot\delta E_{12}^{15} + y_1^{15}\cdot y_2^{14}\cdot\delta E_{14}^{15} + y_1^{15}\cdot y_2^{15}\cdot\delta E_{15}^{15} + \\ &R\cdot T\cdot\begin{bmatrix} \alpha^{12}\left(y_1^{12}\cdot\ln(y_1^{12}) + y_2^{12}\cdot\ln(y_2^{12})\right) + \\ \alpha^{14}\left(y_1^{14}\cdot\ln(y_1^{14}) + y_2^{14}\cdot\ln(y_2^{14})\right) + \\ \alpha^{15}\left(y_1^{15}\cdot\ln(y_1^{15}) + y_2^{15}\cdot\ln(y_2^{15})\right) \end{bmatrix} \end{aligned} \quad , \quad (1)$$

where energetic parameters 3SLM are equal

$\delta E_{12}^{12} = 6\cdot(a^{12})^2\left[\delta E_1^{12,12} + \delta E_2^{12,12}\right]$, $\delta E_{12}^{14} = 12\cdot(a^{12})^2\delta E_1^{12,14} + 9\cdot(a^{14})^2\delta E_2^{14,12}$, $\delta E_{12}^{15} = 6\cdot(a^{12})^2\delta E_1^{12,15} + 6\cdot(a^{15})^2\delta E_2^{15,12}$,

$\delta E_{14}^{12} = 9\cdot(a^{14})^2\delta E_1^{14,12} + 12\cdot(a^{12})^2\delta E_2^{12,14}$, $\delta E_{14}^{14} = 15\cdot(a^{14})^2\left[\delta E_1^{14,14} + \delta E_2^{14,14}\right]$, $\delta E_{14}^{15} = 4\cdot(a^{14})^2\delta E_1^{14,15} + 8\cdot(a^{15})^2\delta E_2^{15,14}$,

$\delta E_{15}^{12} = 6\cdot(a^{15})^2\delta E_1^{15,12} + 6\cdot(a^{12})^2\delta E_2^{12,15}$, $\delta E_{15}^{14} = 8\cdot(a^{15})^2\delta E_1^{15,14} + 4\cdot(a^{14})^2\delta E_2^{14,15}$, $\delta E_{15}^{15} = (a^{15})^2\left[\delta E_1^{15,15} + \delta E_2^{15,15}\right]$.

The materials balance condition described by equation (2)

$$a^{12}y_2^{12} + a^{14}y_2^{14} + a^{15}y_2^{15} = 30\cdot x, \qquad (2)$$

where x is total composition of second component of the Fe-Cr binary system. y_1^i, y_2^i - (i =12,14,15) are fraction of the first or second components in different model sublatties for the σ– phase.

Methodology.

Account equation (2) the functional of mixing Gibbs energy of σ– phase dependence on external arguments (total composition of second component and temperature) and independent intrinsic degrees of freedom (y_1^{12}, y_2^{15}). The equilibrium values of independent intrinsic degrees of freedom are the roots of set of equation of state (SES) – (3a) when the local stability criterion (3b) is fulfill:

$$\begin{cases} \dfrac{d^{\sigma}\Delta^{\sigma}G^{\sigma}(x,T)}{dy_2^{12}} = 0 \\ \dfrac{d^{\sigma}\Delta^{\sigma}G^{\sigma}(x,T)}{dy_2^{15}} = 0 \end{cases} \quad (3a) \qquad \det \begin{Vmatrix} \dfrac{d^2\Delta^{\sigma}G^{\sigma}(x,T)}{dy_2^{(12)2}} & \dfrac{d^2\Delta^{\sigma}G^{\sigma}(x,T)}{dy_2^{(15)}dy_2^{(12)}} \\ \dfrac{d^2\Delta^{\sigma}G^{\sigma}(x,T)}{dy_2^{(12)}dy_2^{(15)}} & \dfrac{d^2\Delta^{\sigma}G^{\sigma}(x,T)}{dy_2^{(15)2}} \end{Vmatrix} > 0 \quad (3b)$$

- at fixing total composition of second component and temperature.

When total composition of second element is changed at fixing value of temperature then solution of equations set – (3a) describe the concentration dependences of distribution atoms of second component between model sub-lattices of σ– phase. It is necessary note the first that equations in set (3a) are transcendental equations, the second it is not general mathematic methods for solution transcendental equations. So original method for solution transcendental equations set (3a) was been created. The computer program for numerical realization of original method solution of SES (3a) was been developed. The development 3SLM, algorithm and computer program was applied for modeling distribution of the Fe and Cr atoms between model sublattice of σ–phase depending on composition and temperature.

The selection of starting energy parameters of model.

For calculation of parameters energy of 3SLM was constitute set of equations for free mixing Gibbs energies of the σ–phase (relatively of metastable σ–phases of pure components) for compositions of σ–phase – base solution, which equals with compositions ordered complexes $\mathbf{A_2^{12}B_4^{15}C_8^{14}D_8^{12}E_8^{14}}$ **–** type for σ– phase (see table 1). In the result there was obtained the set of relationships (2) between energetic parameters of 3SLM and results obtained by ab-initio calculations of energies of formation for $\mathbf{A_2^{12}B_4^{15}C_8^{14}D_8^{12}E_8^{14}}$ – type of ordered complexes [1]. Thus was to get out of limitations as quantum-mechanical calculations of formation energy for full ordered complexes only at 0°K for as phenomenological models (many number of energetic parameters, impossibility of description atoms of components for sublattice of σ–phase) for description of thermodynamic properties of alloy with σ–phase structure.

Table. №1 The data of quantum-mechanical calculations for 0 K of Cr-Fe system [1].

The types of ordered complexes	The values of fractions of the first and second components in different model sublattices for the σ– phase	X(Fe)	${}^{\sigma}\Delta^{\sigma}E^{\sigma}\left(\frac{mRy}{at}\right)$
CrFeCr	$y_1^{12}=1,\ y_2^{12}=0,\ y_1^{15}=0,\ y_2^{15}=1,\ y_1^{14}=1,\ y_2^{14}=0$	0.133	0.8
FeCrCr	$y_1^{12}=0,\ y_2^{12}=1,\ y_1^{15}=1,\ y_2^{15}=0,\ y_1^{14}=1,\ y_2^{14}=0$	0.333	-10.8
FeFeCr	$y_1^{12}=0,\ y_2^{12}=1,\ y_1^{15}=0,\ y_2^{15}=1,\ y_1^{14}=1,\ y_2^{14}=0$	0.467	-9.2
CrCrFe	$y_1^{12}=1,\ y_2^{12}=0,\ y_1^{15}=1,\ y_2^{15}=0,\ y_1^{14}=0,\ y_2^{14}=1$	0.533	-7.8
CrFeFe	$y_1^{12}=1,\ y_2^{12}=0,\ y_1^{15}=0,\ y_2^{15}=1,\ y_1^{14}=0,\ y_2^{14}=1$	0.667	-5.0
FeCrFe	$y_1^{12}=0,\ y_2^{12}=1,\ y_1^{15}=1,\ y_2^{15}=0,\ y_1^{14}=0,\ y_2^{14}=1$	0.867	-4.0
(CrFe)FeFe	$y_1^{12}=1/5,\ y_2^{12}=4/5,\ y_1^{15}=0,\ y_2^{15}=1,\ y_1^{14}=1/2,\ y_2^{14}=1/2$	0.933	-1.8
FeCr(FeCr)	$y_1^{12}=0,\ y_2^{12}=1,\ y_1^{15}=1,\ y_2^{15}=0,\ y_1^{14}=1/2,\ y_2^{14}=1/2$	0.6	-10.0

According table № 1 was obtained system of equation for searching of starting parameters of σ– phase model (for 0 K)

$$\begin{cases} {}^{\sigma}\Delta^{\sigma}E^{\sigma}(x=0.133) = \delta E_{12}^{14} + \delta E_{12}^{15} + \delta E_{14}^{15} = 0.8 \\ {}^{\sigma}\Delta^{\sigma}E^{\sigma}(x=0.333) = \delta E_{14}^{12} + \delta E_{15}^{12} = -10.8 \\ {}^{\sigma}\Delta^{\sigma}E^{\sigma}(x=0.467) = \delta E_{14}^{12} + \delta E_{14}^{15} = -9.2 \\ {}^{\sigma}\Delta^{\sigma}E^{\sigma}(x=0.533) = \delta E_{12}^{14} + \delta E_{15}^{14} = -7.8 \\ {}^{\sigma}\Delta^{\sigma}E^{\sigma}(x=0.667) = \delta E_{12}^{14} + \delta E_{12}^{15} = -5.0 \\ {}^{\sigma}\Delta^{\sigma}E^{\sigma}(x=0.867) = \delta E_{15}^{12} + \delta E_{15}^{14} = -4.0 \\ {}^{\sigma}\Delta^{\sigma}E^{\sigma}(x=) = \dfrac{4}{25}\cdot\delta E_{12}^{12} + \dfrac{1}{5}\cdot\delta E_{12}^{14} + \dfrac{1}{5}\cdot\delta E_{12}^{15} = -1.8 \\ {}^{\sigma}\Delta^{\sigma}E^{\sigma}(x=) = \dfrac{1}{2}\cdot\delta E_{14}^{12} + \dfrac{1}{4}\cdot\delta E_{14}^{14} + \delta E_{15}^{12} + \dfrac{1}{2}\cdot\delta E_{15}^{14} = -10.0 \end{cases} \quad (4)$$

Solving of linear equations set (4) relatively energetic parameters of 3SLM was obtained the next value (see table 2)

Accordingly 3SLM – equation (1) the number of energetic parameters equals nine. Obviously that solution of linear equations set (4) let us obtained eight energetic parameters of 3SLM. So the nine of unknown energetic parameter was been calculates by fitting to critical point of metastable part of miscibility gap of BCC-solid solutions of the Fe-Cr system [5]. The calculated values of energetic parameters of 3SLM for σ– phase were presented in table 2.

Table № 2 The data of energies parameters of model for σ–phase (Joule/mole)

$\Delta E_{12}^{12} = -6500$	$\Delta E_{12}^{14} = 520$	$\Delta E_{12}^{15} = -7020$
$\Delta E_{14}^{12} = -19500$	$\Delta E_{14}^{14} = -13520$	$\Delta E_{14}^{15} = 7540$
$\Delta E_{15}^{12} = 5460$	$\Delta E_{15}^{14} = -10660$	$\Delta E_{15}^{15} = -26000$

Results.

There were obtained the distribution of iron atoms in the Cr-Fe system between model sub-lattices of σ-phase at different values of temperatures (see fig.1) into T=300÷1100 K. Comparison between calculated results and experiment data was shown a good agreement.There was obtained a satisfactory agreement between calculation and experimental data for 300, 700, 1000 and 1100°K (see fig.1).

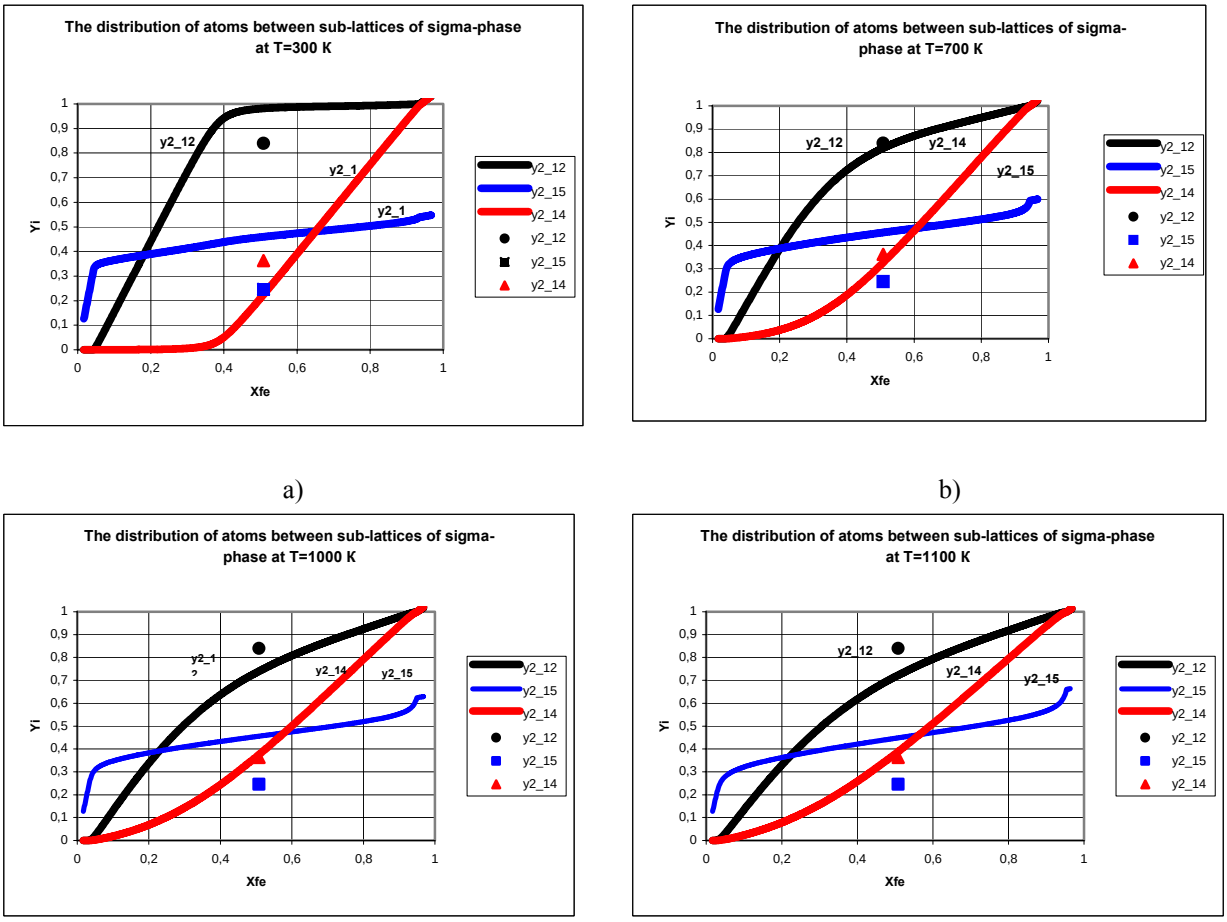

Fig. 1 The distribution of atoms between sub-lattices of σ-phase of Cr-Fe system at T=300 K (a), 700 K (b), 1000 K (c), 1100 K (d).

After calculated equilibrium distribution atom of component between model sub-lattices of σ– phase we obtained minimizing free Gibbs mixing energies of intrinsic degree of freedom as concentration functions of composition at different values of temperature. For example calculated free Gibbs energies mixing of intrinsic degree of freedom as concentration functions for σ– phase as for as BCC – phase at T=300 and 1000 K were presented on Fig.2.In the next step the phase equilibrium between σ- and BCC- phases of the Fe-Cr system was calculated in to 800-1100 K – Fig. 3. It is necessary note that calculated σ-phase has homogeneity field limited by blue triangles (fig. 3). The calculated phase equilibrium between σ- BCC- phases we used stability parameters for pure Fe and Cr obtained by Sluter [5].

Conclusion.

Developed model was allowed coupling two scientific levels: namely the creation of bridge between ab-initio results for ordered complexes with σ- crystal structure at 0 K and statistical thermodynamic model for σ-phase into wide field

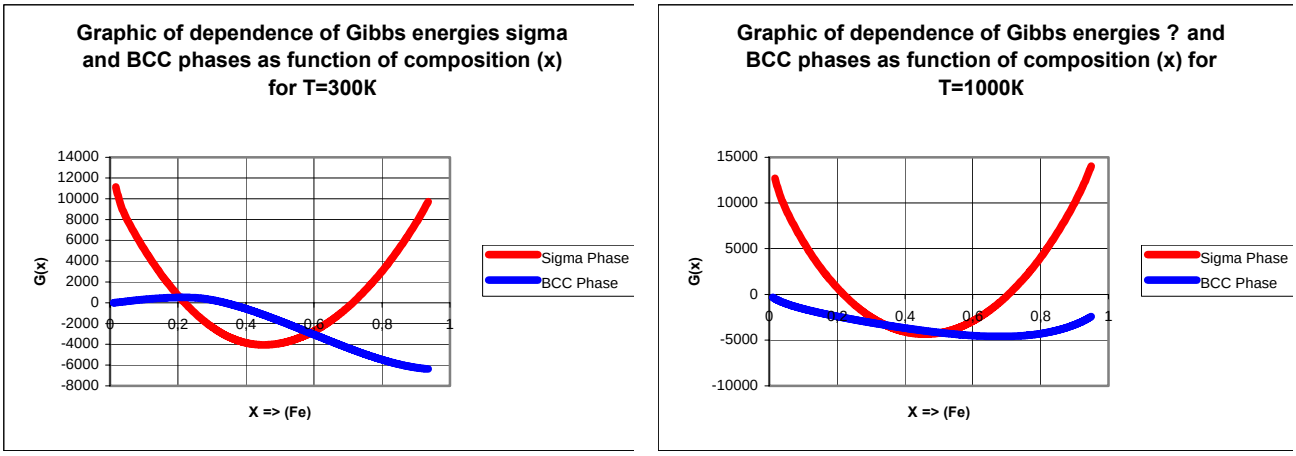

Fig.2 Concentration dependences of free Gibbs energy mixing for BCC (blue curve) and Sigma (red curve) phases of the Cr-Fe system at T=300 K (left) and 1000 K (right).

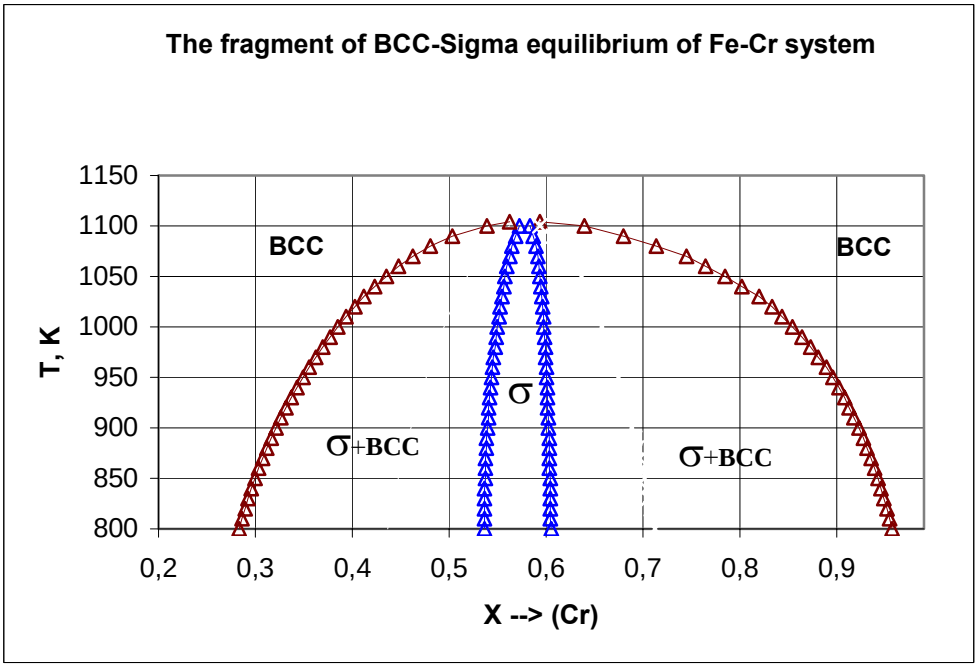

Fig. 3 The fragment of BCC-Sigma equilibrium of Fe-Cr system

composition and temperature. That approach was allowed to link three different kinds of experimental data:

1) Structural data obtained by neutron and X-ray investigations (occupied different sublattices of crystal structure of chemical compounds with homogeneity field);
2) Thermodynamic properties for solution on base chemical compounds with crystal structure consisting many sublattices as function composition and/or temperature;
3) Phase equilibriums between different phases as disordered solution for as chemical compounds (with crystal structure include many sublattices) with homogeneity field.

The work has been supported by RFBR N 06-03-33152-a grant.

Reference.

1. J. Havrankova, J. Vrest'al, L. G. Wang, M. Sob. Ab initio analysis of energetics of σ-phase formation in Cr-based systems, Phys.Rev. B 63, 174104 (2001)

2. J. Houserova, M. Friak, M. Sob, J. Vrestal. Ab initio calculations of lattice stability of sigma-phase and phase diagram in the Cr–Fe system, Comp. Mater.Science 25, 562 (2002)

3.S.G.Fries, Bo. Sundman. Using Re-W σ-phase first-principles results in the Bragg-Williams approximation to calculate finite-temperature thermodynamic properties. Phys.Rev. B 66, 012203 (2002)

4.M.Yu. Lavrentiev, R. Drautz, D. Nguyen-Manh, T.P.C. Klaver, S.L. Dudarev. Monte Carlo study of thermodynamic properties and clustering in the bcc Fe-Cr system, Phys. Rev. B 75, 014208 (2007).

5. M.Sluiter. Ab initio lattice stabilities of some elemental complex structures. CALPHAD, 30 (2006) 357-366.

Exergy evolution of the mineral capital on Earth

Alicia Valero Delgado
CIRCE – University of Zaragoza (Spain)
aliciavd@unizar.es

The greatest success of Thermodynamics throughout the 20th century has been in its concepts and equality equations. Inequalities are apparently less practical than equalities. The former only talks about limits and limits in evolution show tendencies. There is no certainty about the final state. On the contrary, considering systems in equilibrium, as Classical thermodynamics do, is quite comfortable. We become pretty sure about the properties of the system. All intensive properties of the system are homogeneously well defined in any part of it. The departure of equilibrium means that everything becomes ill defined and insecurity in the analysis is intrinsic. Therefore, the Thermodynamics of irreversible processes (Prigogine, 1947) started from linear systems at steady non-equilibrium states instead of from systems far from equilibrium. Ecosystems are among the most complex energy systems. Those systems use energy to survive far from thermodynamic equilibrium and organize themselves in a way that yields the highest flux of useful energy and the most exergy stored in the system, (Jorgensen, 2000). The complexity of these systems is so great that the laws of observed behaviour are only tentative and provisional.

In other words, scientists needed long time to understand the Second Law inequality that Clausius formulated hundred and sixty years ago as the "Die Entropie der Welt strebt einem Maximum zu". First they exploited the equilibrium properties of entropy and related magnitudes, and then used the Second Law to see the limits and the direction of processes. With that, they envisaged the arrow of time and irreversibility as a philosophical message of death and destiny. The first steps of analyses of departures from equilibrium gave birth to new ideas about evolution, stability, attractors, evolutive bifurcations and dissipative structures. Now, scientists working on systems far from equilibrium, try to explain concepts such us development, growth, behaviour, ascendency and self-organization to maximize the degradation of exergy.

Thermodynamics is a phenomenological science, i.e. a black box theory. It does not describe the mechanisms by which systems behave. It only advises about tendency. It tells us which states are allowed and which are not. This analysis is close to Economics, it only precisely predicts what already happened. Prediction is not determinism. It is a selection of possible scenarios and the discarding of impossible ones. Consider, for instance, the evolution of the planet because of human action. It is impossible to predict neither the state of the atmosphere, hydrosphere nor of the lithosphere in the next hundred years. We can only do models and guess what is likely to happen if tendencies maintain as they are. And these models will never be purely thermodynamic.

However Thermodynamics has not been sufficiently exploited at the planetary level. The planet evolution can be considered as a complex evolutionary ecosystem. We must recognize that mineral resources like forests or glaciers have exergy and their state should be assessed for a careful husbandry of the planet. In other words, and as prof. Andresen says “Thermodynamics is far from being a complete polished subject, useful only as a tool to evaluate chemical and thermal processes. On the contrary, Thermodynamics is vibrant with new ideas and methods, receiving inspiration from other fields of science as well as providing inspiration to such other fields, e.g. general optimization theory, fluid dynamics, and ecological modelling.”

The main message of this paper is that Second law analysis can be universally applied to evaluate the mineral endowment of the Earth’s crust. Exergy is a tool that can be applied no matter if dealing with materials, fossil fuels, water, gases or air. This fact has been recognized by a significant number of ecological economists, such as Georgescu-Roegen (1971), but very few scientists have dared to put real numbers on it and no one at a global scale. Recognition should be also owed to Ayres and Nair (1974), Szargut (2005), Odum (1996) or Wall (2005), among others.

The irreversibility concept tells us that sooner or later everything will be degraded with the maximum possible generated entropy. And the Second Law is present in all natural processes fixing their limits and

direction. Even life, which looks completely antientropic, is a consistently dissipative process. Human beings can accelerate or slow down those irreversible and unavoidable processes. However, the irreversibility concept assures that we are approaching a degraded planet of maximum entropy and hence with the absence of resources essential for life. This simple fact allows us to understand better Nature. The knowledge of the "end of the planet" is fundamental for managing efficiently the finite amount of the Earth's non-renewable resources. This will play a key role in understanding the Thermodynamics of far from equilibrium systems.

Irreversibility plays another important key role for understanding the degradation processes of Nature: it is the root of the physical cost and thus it connects Thermodynamics with Economics. To such an extent that a new science has been created: Thermoeconomics (see a historical overview in Valero, 2004). Most analysts agree that exergy is an adequate thermodynamic property to which allocate cost because it accounts for energy quality. Once the reference environment is defined, exergy is the thermodynamic function of state which makes possible to formulate the equivalence between different energy and/or matter flow streams of a system. Thermoeconomic analysis allows to value resources with a single unit of measure (the exergy costs) and in an objective way far removed from market distortions or currency speculation.

Joining the model of a degraded Earth's crust with the exergy resource accountability system based on the thermoeconomic analysis, immediately leads to the "exergy countdown" proposed in this paper. The exergy countdown is based on the fact that there is a measurable amount of exergy resources on Earth, which are being depleted by human action. Furthermore, as demonstrated in the study, using exegy, mineral extraction behaves similar to the well known King Hubbert's peak for fossil fuel resources. This way, the exergy countdown of the planet allows visualizing and monitoring the exergy evolution of mineral resources of the Earth and estimating when each resource will reach the maximum level of degradation. Since the accounting unit is exergy, the analysis can be performed to single or aggregated resources. Furthermore, all studied substances can be represented in a single diagram. The results are striking: at the actual rates of extraction, most of the strategic metal resources will reach the peak before this century and in some cases even before fossil fuels (see Fig. 1).

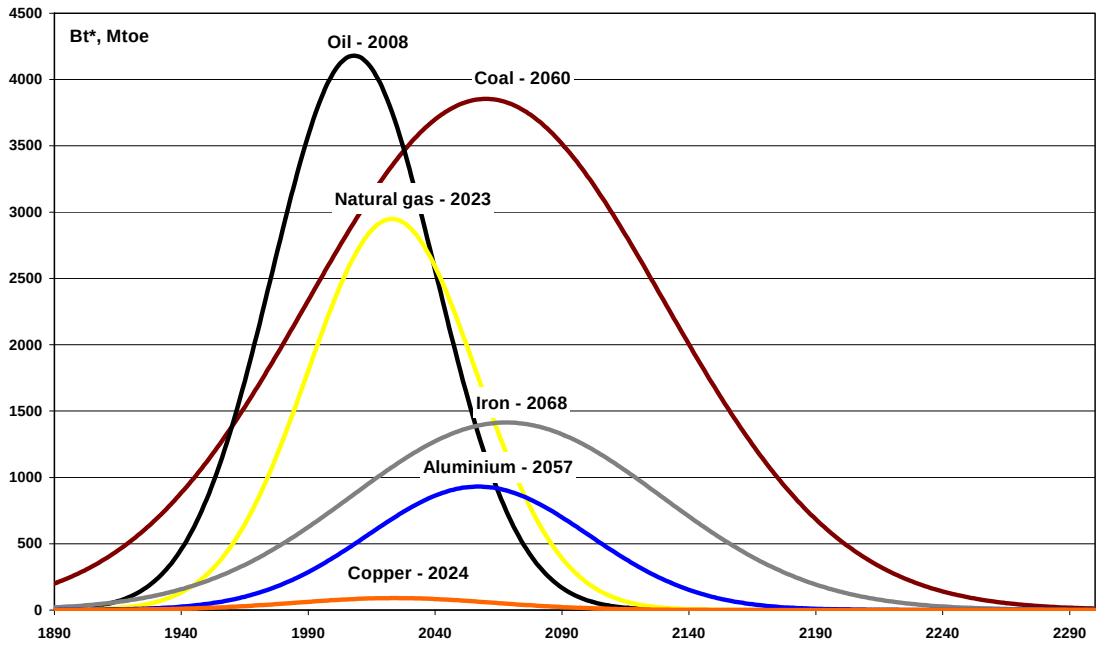

Fig. 1: Exergy countdown of the main minerals extracted on Earth

This paper demonstrates that Thermodynamics can play a key role in the management of natural resources and in the awareness that we are quickly approaching a crepuscular planet. The latter will never be determined exactly, but it can be gradually better delimited just by applying the second law

evolutionary theories. In short, it is not the same to perceive that time passes than to have a watch and measure exactly how many minutes are left until the end of the day. The aim of this study is to pave the way to precisely account the time to reach a degraded planet.

References

Ayres, R. and Nair, I. (1984). Thermodynamics and Economics Physics Today, 35, 62-71.

Georgescu-Roegen, N. (1971). The Entropy Law and the Economic Process Harvard University Press.

Jorgensen, S. E. (2000). Thermodynamics and Ecological Modelling CRC

Odum, H. T. (1996) Environmental Accounting. Emergy and Environmental Decision Making. John Wiley & Sons, inc.

Prigogine, I. (1947) Etude thermodynamique des phénomènes irréversibles. Thèse d'agrégation présentée en 1945 à l'Université Libre de Bruxelles. Desoer, Liège.

Szargut, J. (2005). Exergy method: technical and ecological applications. WIT-press.

Valero V. and Torres C. (2005). Thermoeconomic Analysis. Exergy, Energy System Analysis, and Optimization, from Encyclopedia of Life Support Systems (EOLSS), Developed under the Auspices of the UNESCO. Eolss Publishers, Oxford, UK; Online encyclopedia: http://www.eolss.net, Retrieved May 19, 2005.

Wall, G. (2005). Exergetics. Exergy, Energy System Analysis, and Optimization, from Encyclopedia of Life Support Systems (EOLSS), Developed under the Auspices of the UNESCO. Eolss Publishers, Oxford, UK; Online encyclopedia: http://www.eolss.net, Retrieved May 19, 2005.

Relativistic temperature and the generic stability of relativistic fluids

P. Ván*

*Department of Theoretical Physics, KFKI, RMKI
1525 Budapest, Konkoly Thege Miklós u. 29-33., Hungary and
Department of Energy Engineering, BUTE
1111 Budapest, Bertalan Lajos u. 4-6., Hungary
vpet@rmki.kfki.hu

ABSTRACT

There are two old paradoxical issues in relativistic generalisations of thermodynamics. The first one is related to the relativistic interpretation of the thermodynamic quantities and is related to the hypothetical transformation properties of the temperature. According to the three most important opinions the temperature of a moving body can appear colder (Einstein-Planck), appear hotter (Ott) or is the same (Landsberg) as the temperature measured by an inertial observer.

The second important problem is related to heat conducting and dissipative fluids. There the first and most straightforward generalization of the Navier-Stokes-Fourier system is due to Eckart (1940). But the homogeneous equilibrium of an Eckart fluid is violently unstable (Hiscock and Lindblom, 1985) due to the relativistic modification of the Fourier heat conduction law, that contains the acceleration of the fluid. The suggested extensions (the most popular is the Müller-Israel-Stewart theory) can suppress this generic instability. However, the price we pay is a set of additional material parameters, that should depend on the thermodynamic state in a very particular way according to the stability conditions.

We argue that the two problems are not independent. An investigation of the fluid equations by rigorous thermodynamic methods - Liu procedure for first-order weakly nonlocal constitutive state space - leads to a modified simple form of the internal energy ϵ of relativistic fluids [1, 2], that can be expressed by the local rest frame energy density e and momentum density q^a as:

$$\epsilon = \sqrt{u_a T^{ab} T_{bc} u^c} = \sqrt{e^2 - q_a q^a}.$$

Here T^{ab} is the energy-momentum density and u^a is the velocity field of the fluid. One can show that the homogeneous equilibrium of the corresponding relativistic dissipative fluid is linearly stable due to the concavity of the entropy and the positivity of the heat conduction and diffusion coefficients and the viscosities [3] .

In the presentation we will show, that due to the corresponding equilibrium thermodynamic relations the meaning of different thermodynamic temperatures (Enstein-Planck, Ott and Landsberg) can be well interpreted and understood. Causality and hyperbolicity questions will be mentioned, too.

References

[1] Ván P., Internal energy in dissipative relativistic fluids, *Journal of Mechanics of Materials and Structures*, **3**/6, 1161-1169, 2008.

[2] Ván, P. and Bíró, T. S., Relativistic hydrodynamics - causality and stability, *The European Physical Journal - Special Topics*, **155**, 201-212, 2008, (arXiv:0704.2039v2).

[3] Ván, P., Generic stability of dissipative non-relativistic and relativistic fluids, *under publication in Journal of Statistical Physics*, 2009, (arXiv:0811.0257).

Heat transfer in quantum devices at low temperatures: a classical field theory approach*

F. Vázquez[1,3], F. Márkus[1] and K. Gambár[2]
[1] Physics Department, Budapest University of Technology and Economics, Budafoki út 8, H-1521, Budapest, Hungary.
[2] Department of Atomic Physics, Roland Eötvös University, Pázmány Péter sétány 1/A, H-1117, Budapest, Hungary.
E-mail address: vazquez@uaem.mx

In this contribution we show the canonical quantization procedure of a class of nonlinear transport equations to describe heat transfer in nano-scaled conductors. Non-linearity is considered through the assumption that the thermal conductivity depends on the size of the system. The Lagrangian density function is written in terms of a potential field which gives all the physical information on the measurable temperature. The potential field together with the thermal conductivity is expanded in Fourier series. The quantization procedure is then carried out in the Fourier coefficients space and creation, annihilation and number operators with their commutation properties are introduced. This allows us to study the energy level structure of heat conductors at low temperature. We illustrate the formalism with the example of a 1-D conductor with size lengths in the scale of nano-meters. This formalism constitutes a complementary point of view of heat transfer in quantum devices which may be useful in nano-devices at low temperatures.

*Work supported by the National Office of Research and Technology (NKTH, Hungary) and the National Council of Science and Technology (CONACYT, México) under contract MX-20/2007 (OMFB-00960/2008). FV acknowledges CONACYT and PROMEP (México) for financial support.

[3] On sabbatical leave from Facultad de Ciencias, Universidad Autónoma del Estado de Morelos, México.

Dilemma of Heat or Work.

József Verhás
Budapest University of Technology and Economy,
H-1521 Budapest, Hungary
verhas@phy.bme.hu

The modern results of thermodynamics are often difficult to get widely accepted because in teaching thermodynamics a number of ideas not firmly established are taught, even spiced up with contradictions or patterns of thinking leading to contradictions sooner or later. One important circumstance is that heat is poorly defined. And usually all other ideas are introduced basing on it. The most widespread idea of heat applies for processes starting and ending in equilibriums and are used as if it were of general validity. It is worth studying if the separation of energy transfer into heat and work has been established with a satisfactory certainty. The answer is not. On a simple example, we show that the uncertainty of the idea of heat and work does not cause any severe problem in non-equilibrium thermodynamics; proper modeling can lead to a correct model even if modeling heat is completely spoiled.

We have been taught the idea of heat and work since the early years of school. The theory of heat was based on hotness and coldness of every day bodies; the temperature was established and the amount of heat was explained by the equation of calorimetry. The work was introduced in mechanics and was generalized in electricity. The definition of energy was the ability to perform work.

We had no problem when the idea of energy was generalized; the heat was involved into energy; and the first law of thermodynamics was based. We did not take care of the consequence of the generalization that the energy was not the ability to perform work any longer. The conservation rule has been paid for with the original definition. The above would have caused no problem if the definition of heat and work had been exact. In some textbooks of thermodynamics the heat is defined with the part of the transferred energy that is not work. But what is work? I elucidate the question on the example of electric work. We have known for long that the electric work equals the product of the voltage and the electric charge having passed; and the time integral of the product of voltage and current if the voltage is changing;

$$w = \int V(t)J(t)dt \tag{1}$$

The formula is valid for both direct and alternating current. If the voltage changes arbitrarily we are faced with some difficulty. We suspect and a detailed analysis also shows that the above integral is rather heat if the voltage is Nyquist noise. If a hot conductor is attached to an ideal transmission line the work obtainable with a bridge obeys Carnot's formula. Nevertheless, noise is usually treated with statistical methods, the phenomena were discovered and are detected with macroscopic observations.

Another puzzling example is the electromagnetic radiation. A monochromatic wave performs work — e.g. on the aerial of a TV receiver — but a real wave is

never strictly monochromatic. On the other hand, the thermal radiation is obviously heat even if it is within a narrow frequency band cut by a monochromator. The same uncertainty emerges when the internal energy balance is established.

Assume an electrical conductor in an electromagnetic field. The equation usually reads

$$\rho\frac{dU}{dt} + \operatorname{div}\mathbf{J}_q = \mathbf{Ej} + r, \tag{2}$$

where rho is the density, U the specific internal energy, $\mathbf{J}q$ the heat current density, **E** the electric field strength, **j** the electric current density, and r is the so called heat supply. No mechanical motion is assumed. The source terms on the right hand side are the power of the field and the heat given the body by the field of thermal radiation in unit volume, respectively. Keep in mind that the heat radiation is an electromagnetic field, consequently, the term **Ej** contains the absorbed heat; the appearance of the heat supply on the right hand side is an explicit error unless **E** and **j** are interpreted as apart from the radiation field. The separation of the thermal and non-thermal parts of the electric field strength and the current is not without arbitrariness. The above form of the internal energy balance includes the separation of the field and the material staying at the same place, which may be problematic again. Regarding the volume elements of the reality — material and field together — the form

$$\rho\frac{dU}{dt} + \operatorname{div}(\mathbf{J}_q + \mathbf{S}) = 0 \tag{3}$$

is more correct, in which **S** is Poynting's vector;

$$\mathbf{S} = \mathbf{E} \times \mathbf{H}. \tag{4}$$

The dilemma of what is heat is also present. The quantity **Jq** has to be declared as heat flow apart from the radiating part or **E** and **H** as apart from the radiation? We can not help but concluding to that the distinction between heat and work is not always clear at all.

Nevertheless, one of the foundation stones seems loose, removing it does not destroy the building of non-equilibrium thermodynamics as you can see in the book of Giftopoulos and Beretta. On the other hand, even if the definition of heat fails sometimes and the heat flow in the energy balance may be wrong, proper modeling of the entropy current and the constitutive equations are able to lead to correct results.

ETA-Graphics – An Interface to Endoreversible Thermodynamics

Katharina Wagner and Karl Heinz Hoffmann
Institute of Physics, Chemnitz University of Technology, Germany
katharina.wagner@physik.tu-chemnitz.de

Endoreversible Thermodynamics

Endoreversible thermodynamics is a powerfull tool for the optimization of irreversible thermodynamic processes. Because of its well defined structure consisting of only few different elements it is possible to break down complex irreversible thermodynamical systems into subsystems for which calculations are much simpler.

In general endoreversible systems are networks of reversible subsystems that exchange energy. All the irreversibilities of the system are located at the interactions between the subsystems. Thus the reversible subsystems can be treated with equilibrium thermodynamics. Another aspect of endoreversible systems is that each interaction consists of two fluxes, since the energy flux is always accompanied by a flux of an extensive quantity (extensity), e.g. entropy or particle flux, that acts as a carrier of the energy.

The reversible subsystems can be divided into two main categories: reservoirs and engines. While reservoirs store energy and therefore act as sources or sinks, engines only transform energy, for instance from thermal into mechanical energy. Thus, for engines a set of balance equations can be set up. The sum of all energy fluxes entering and leaving an engine has to equal zero and for each extensity the sum of all extensity fluxes has to equal zero as well.

The interactions between the engines and reservoirs are characterized by transport equations for energy and the accompanying extensity. The two fluxes are related by a corresponding intensive quantity.

ETA-Graphics

ETA-Graphics (where ETA is an acronym for Endoreversible Thermodynamics Application) is a graphic based interface to endoreversible thermodynamics that uses the fact that endoreversible systems have such a well defined structure. It enables the user to construct endoreversible systems using engines and reservoirs and defining the interactions between these subsystems by entering transfer equations. The application guides the user with dialogs and lists from which certain properties can be chosen.

The logic of endoreversible systems is implemented, i.e. the application is capable of setting

up the balance equations and solving the resulting equation system. To do so Wolfram Mathematica is used. Furthermore the efficiency and power output of engines can be calculated and plotted.

ETA-Graphics is meant to support the user in creating endoreversible representations of systems and analyzing them especially with regards to efficiency and power output.

Rigorous and General Definition of Thermodynamic Entropy. Part I: Basic Concepts and Energy

Enzo Zanchini* and Gian Paolo Beretta†

INTRODUCTION

In traditional expositions of thermodynamics, entropy is defined in terms of the concept of heat, which in turn is introduced at the outset of the logical development in terms of heuristic illustrations based on mechanics. For example, in his lectures on physics, Feynman [1] describes heat as one of several different forms of energy related to the jiggling motion of particles, a form of energy which really is just kinetic energy. Tisza [2] argues that such slogans as "heat is motion," in spite of their fuzzy meaning, convey intuitive images of pedagogical and heuristic value.

There are at least three problems with these illustrations. First, work and heat are not stored in a system: each is a mode of transfer of energy from one system to another. Second, concepts of mechanics are used to justify and make plausible a notion—that of heat—which is beyond the realm of mechanics. Indeed, as pointed out by Hatsopoulos and Keenan [3], without the Second Law heat and work would be indistinguishable. Third, heat is a mode of energy transfer between systems that are very close to thermodynamic equilibrium, so that any definition of entropy based on heat is bound to be valid only at thermodynamic equilibrium.

The first problem is addressed in some expositions. Landau and Lifshitz [4] define heat as the part of an energy change of a body that is not due to work done on it. Guggenheim [5] defines heat as an exchange of energy that differs from work and is determined by a temperature difference. Keenan [6] defines heat as that which transfers from one system to a second system at lower temperature, by virtue of the temperature difference, when the two are brought into communication. Following Guggenheim it would be possible to state a rigorous definition of heat, with reference to a very special kind of interaction between two systems, and to employ the concept of heat in the definition of entropy [5]. However, Gyftopoulos and Beretta [7, 8] have shown that the concept of heat is unnecessarily restrictive for the definition of entropy, as it would confine it to the equilibrium domain. Therefore, in agreement with Ref. [7], we will present and discuss a definition of entropy where the concept of heat is not employed.

Other problems are present in the traditional scheme for the definition of entropy [5, 6, 9]: many basic concepts, such as those of system, state, property, isolated system, environment of a system, adiabatic process are not defined rigorously; the unnecessary concept of *quasistatic process* is employed; it is assumed implicitly that the quantity of heat exchanged in a cycle between a source and a reversible cyclic engine is independent of the initial state of the source.

In this paper, a rigorous and general definition of entropy is presented, which is based on operative definitions of all the concepts employed and involves neither the concept of heat nor that of quasistatic process; it applies to both equilibrium and nonequilibrium states and considers also systems with movable internal walls and/or semipermeable walls, with chemical reactions and/or external force fields, with small numbers of particles. In Part I, the definitions of the basic concepts and of energy are presented. In part II, entropy and thermodynamic temperature are defined and the principle of entropy non-decrease is proved.

BASIC DEFINITIONS

Constituents, amounts of constituents. We call *constituents* the material particles chosen to describe the matter contained in any region of space R, at a time instant t. Examples of constituents are: atoms, molecules, ions, protons, neutrons, electrons. Constituents may combine and/or transform into other constituents according to a set of model-specific *reaction mechanisms*. We call *amount of constituent* i in any region of space R, at a time instant t, the number of particles of constituent i contained in R, at time t.

Region of space which contains particles of the i-th **constituent**. We will call region of space which contains particles of the i-th constituent a connected region R_i of physical space (the three-dimensional Euclidean space) in which particles of the i-th constituent are contained. The boundary surface of R_i may be a patchwork

*Università di Bologna, Italy, enzo.zanchini@unibo.it
†Università di Brescia, Italy, beretta@ing.unibs.it

of *walls*, i.e., surfaces impermeable to particles of the i-th constituent, and ideal surfaces (permeable to particles of the i-th constituent). The geometry of the boundary surface of R_i and its permeability topology nature (walls, ideal surfaces) can vary in time, as well as the number of particles contained in R_i.

Collection of matter, composition. We call *collection of matter*, denoted by C^A, a set of particles of one or more constituents which is described by specifying the allowed reaction mechanisms between different constituents and, at any time instant t, the set of r connected regions of space, $\boldsymbol{\mathsf{R}}^A = \mathsf{R}_1^A, \ldots, \mathsf{R}_i^A, \ldots, \mathsf{R}_r^A$, each of which contains n_i^A particles of a single kind of constituent. The regions of space $\boldsymbol{\mathsf{R}}^A$ can vary in time and overlap. Two regions of space may contain the same kind of constituent provided that they do not overlap. Thus, the *i-th* constituent could be identical with the *j-th* constituent, provided that R_i^A and R_j^A are disjoint.

Comment. This method of description allows to consider the presence of internal walls and/or internal *semipermeable* membranes, *i.e.*, surfaces which can be crossed only by some kinds of constituents and not others. In the simplest case of a collection of matter without internal partitions, the regions of space $\boldsymbol{\mathsf{R}}^A$ coincide at every time instant. The amount n_i of the constituent in the i-th region of space can vary in time for two reasons: matter exchange; reaction mechanisms.

Compatible compositions, set of compatible compositions. We say that two compositions, $\boldsymbol{n}^{1A}$ and $\boldsymbol{n}^{2A}$ of a given collection of matter C^A are *compatible* if the change between $\boldsymbol{n}^{1A}$ and $\boldsymbol{n}^{2A}$ or viceversa can take place as a consequence of the allowed reaction mechanisms without matter exchange. We will call *set of compatible compositions* for a system A the set of all the compositions of A which are compatible with a given one, $\boldsymbol{n}^{0A}$. We will denote a set of compatible compositions by the symbol $(\boldsymbol{n}^{0A}, \boldsymbol{\nu}^A)$, where $\boldsymbol{\nu}^A$ is the matrix of the stoichiometric coefficients.

External force field. Let us denote by $\mathbf{F}$ a force field given by the superposition of the gravitational field $\mathbf{G}$, the electric field $\mathbf{E}$ and the magnetic field $\mathbf{H}$. Let us denote by Σ_t^A the union of the regions of space R_t^A in which the constituents of C^A are contained, at a time instant t, which will also be called region of space occupied by C^A at time t. We call *external force field* for C^A at time t, denoted by $\mathbf{F}_{e,t}^A$, the spatial distribution of $\mathbf{F}$ which is measured at time t in Σ_t^A if all the constituents and the walls of C^A are removed and placed far away from Σ_t^A.

System, properties of a system. We will call *system* A a collection of matter C^A defined by the initial composition $\boldsymbol{n}^{0A}$, the stoichiometric coefficients $\boldsymbol{\nu}^A$ of the allowed reaction mechanisms, and the possibly time-dependent specification, *over the entire time interval of interest*, of:

- the geometrical variables and the nature of the boundary surfaces that define the regions of space $\boldsymbol{\mathsf{R}}_t^A$,
- the rates $\dot{\boldsymbol{n}}_t^{A\leftarrow}$ at which particles are transferred in or out of the regions of space, and
- the external force field distribution $\mathbf{F}_{e,t}^A$ for C^A,

provided that the following conditions apply:

1. an ensemble of identically prepared replicas of C^A can be obtained at any instant of time t, according to a specified set of instructions or preparation scheme;
2. a set of measurement procedures, $P_1^A, \ldots, P_n^A$, exists, such that when each P_i^A is applied on replicas of C^A at any given instant of time t, the arithmetic mean $\langle P_i^A \rangle_t$ of the numerical outcomes of repeated applications of P_i^A is a value which is the same for every subensemble of replicas of C^A (the latter condition guarantees the so-called statistical *homogeneity* of the ensemble); $\langle P_i^A \rangle_t$ is called the *value of* P_i^A for C^A at time t;
3. the set of measurement procedures, $P_1^A, \ldots, P_n^A$, is *complete* in the sense that the set of values $\{\langle P_1^A \rangle_t, \ldots, \langle P_n^A \rangle_t\}$ allows to predict the value of any other measurement procedure satisfying conditions 2 and 3.

Then, each measurement procedure satisfying conditions 2 and 3 is called a *property* of system A, and the set $P_1^A, \ldots, P_n^A$ a *complete set of properties* of system A.

State of a system. Given a system A as just defined, we call *state of system A at time t*, denoted by A_t, the set of the values *at time t* of

- all the properties of the system or, equivalently, of a complete set of properties, $\{\langle P_1 \rangle_t, \ldots, \langle P_n \rangle_t\}$,
- the amounts of constituents, $\boldsymbol{n}_t^A$,
- the geometrical variables and the nature of the boundary surfaces of the regions of space $\boldsymbol{\mathsf{R}}_t^A$,
- the rates $\dot{\boldsymbol{n}}_t^{A\leftarrow}$ of particle transfer in or out of the regions of space, and
- the external force field distribution in the region of space Σ_t^A occupied by A at time t, $\mathbf{F}_{e,t}^A$.

Closed system, open system. A system A is called a *closed system* if, at every time instant t, the boundary surface of every region of space R_{it}^A is a wall. Otherwise, A is called an *open system*.

Comment. For a closed system, in each region of space R_i^A, the number of particles of the i-th constituent can change only as a consequence of allowed reaction mechanisms.

Composite system, subsystems. If systems A and B, defined in the same time interval, are such that no region of space R_i^A overlaps with any region of space R_j^B, we will say that that the system C whose regions of

space of are $\boldsymbol{R}^C = R_1^A, \ldots, R_i^A, \ldots, R_{r_A}^A, R_1^B, \ldots, R_j^B, \ldots, R_{r_B}^B$ is the *composite* of systems A and B, and that A and B are *subsystems* of C. Then, we write $C = AB$ and denote its state at time t by $C_t = (AB)_t$.

Isolated system. We say that a closed system I is an isolated system in the stationary external force field $\mathbf{F}_e^I$, or simply an *isolated system*, if during the whole time evolution of I: (a)I is surrounded by a region of space in which no material particle is present, and (b) the external force field $\mathbf{F}_e^I$ is stationary, *i.e.*, time independent.

Separable closed systems. Consider a composite system AB, with A and B closed subsystems. We say that systems A and B are *separable* at time t if:

- the force field external to A coincides (where defined) with the force field external to AB, i.e., $\mathbf{F}_{e,t}^A = \mathbf{F}_{e,t}^{AB}$;
- the force field external to B coincides (where defined) with the force field external to AB, i.e. $\mathbf{F}_{e,t}^B = \mathbf{F}_{e,t}^{AB}$.

Subsystems in uncorrelated states. Consider a composite system AB such that at time t the states A_t and B_t of the two subsystems fully determine the state $(AB)_t$, *i.e.*, the values of all the properties of AB can be determined by *local* measurements of properties of systems A and B. Then, at time t, we say that the states of subsystems A and B are *uncorrelated from each other*, and we write the state of AB as $(AB)_t = A_t B_t$. We also say, for brevity, that A and B are *systems uncorrelated from each other* at time t.

Environment of a system, scenario. If a system A is a subsystem of an isolated system $I = AB$, we can choose AB as the isolated system to be studied. Then, we call B the *environment* of A, and we call AB the *scenario* under which A is studied.

Comment. The chosen scenario AB contains as subsystems all and only the systems that are allowed to interact with A; all the remaining systems in the universe are considered as not available for interaction.

Process, cycle. We call *process* for a system A from state A_1 to state A_2 in the scenario AB, denoted by $(AB)_1 \to (AB)_2$, the change of state from $(AB)_1$ to $(AB)_2$ of the isolated system AB which defines the scenario.

Restriction. In the following (for brevity) we will consider only *closed systems* and only states of a closed system A in which A is separable and uncorrelated from its environment. Moreover, for a composite system AB, we will consider only states such that the subsystems A and B are separable and uncorrelated from each other.

Reversible process, reverse of a reversible process. A process for A in the scenario AB, $(AB)_1 \to (AB)_2$, is called a *reversible process* if there exists a process $(AB)_2 \to (AB)_1$ which restores the initial state of the isolated system AB. The process $(AB)_2 \to (AB)_1$ is called *reverse* of process $(AB)_1 \to (AB)_2$.

Comment. A reversible process need not be slow. In the general framework we are setting up, it is noteworthy that nowhere we state nor we need the concept that a process to be reversible needs to be *slow* in some sense.

Weight. We call *weight* a system M always separable and uncorrelated from its environment, such that:

- M is closed, it has a single constituent, with fixed number of particles and mass m, contained in a single region of space whose shape and volume are fixed;
- in any process, the difference between the initial and the final state of M is determined uniquely by the change in the position z of the center of mass of M, which can move only along a straight line whose direction coincides with that of a uniform stationary external gravitational force field $\mathbf{G}_e = -g\mathbf{k}$, where g is a constant gravitational acceleration.

Weight process, work in a weight process. A process of a system A is called a *weight process*, denoted by $(A_1 \to A_2)_W$, if the only effect external to A is the displacement of the center of mass of a weight M between two positions z_1 and z_2. We call *work performed by A in the weight process*, denoted by the symbol $W_{12}^{A\to}$, the quantity

$$W_{12}^{A\to} = mg(z_2 - z_1) \ . \tag{1}$$

We will say that the work is *done* by A if $z_2 > z_1$ or is *received* by A if $z_2 < z_1$. Two equivalent symbols for the opposite of this work are $-W_{12}^{A\to} = W_{12}^{A\leftarrow}$.

Equilibrium state of a closed system. A state A_t of a system A, with environment B, is called an *equilibrium state* if:

- state A_t does not change with time;
- state A_t can be reproduced while A is an isolated system in the external force field $\mathbf{F}_e^A$, which coincides with $\mathbf{F}_e^{AB}$.

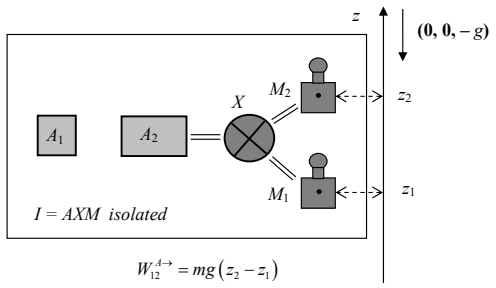

Figure 1: Schematic illustration of a weight process for system A.

Stable equilibrium state of a closed system. An equilibrium state of a closed system A is called a *stable equilibrium state* if it cannot be modified in any process such that neither the geometrical configuration of the walls which bound the regions of space $\boldsymbol{R}^A$ nor the state of the environment B of A have net changes.

DEFINITION OF ENERGY FOR A CLOSED SYSTEM

First Law. Every pair of states $(A_1,\, A_2)$ of a system A can be interconnected by means of a weight process for A. The works performed by the system in any two weight processes between the same initial and final states are identical.

Definition of energy for a closed system. Proof that it is a property. Let $(A_1,\, A_2)$ be any pair of states of a system A. We call *energy difference* between states A_2 and A_1 either the work $W_{12}^{A\leftarrow}$ received by A in any weight process from A_1 to A_2 or the work $W_{21}^{A\rightarrow}$ done by A in any weight process from A_2 to A_1; in symbols:

$$E_2^A - E_1^A = W_{12}^{A\leftarrow} \quad \text{or} \quad E_2^A - E_1^A = W_{21}^{A\rightarrow}. \tag{2}$$

The first law guarantees that at least one of the weight processes considered in Eq. 2 exists. Moreover, it yields the following consequences:
(a) if both weight processes $(A_1 \rightarrow A_2)_W$ and $(A_2 \rightarrow A_1)_W$ exist, the two forms of Eq. 2 yield the same result $(W_{12}^{A\leftarrow} = W_{21}^{A\rightarrow})$;
(b) the energy difference between two states A_2 and A_1 depends only on the states A_1 and A_2;
(c) (*additivity of energy differences*) consider a pair of states A_1B_1 and A_2B_2 of a composite system AB; then

$$E_2^{AB} - E_1^{AB} = E_2^A - E_1^A + E_2^B - E_1^B \;; \tag{3}$$

(d) (*energy is a property*) let A_0 be a reference state of a system A, to which we assign an arbitrarily chosen value of energy E_0^A; the value of the energy of A in any other state A_1 is determined uniquely by the equation

$$E_1^A = E_0^A + W_{01}^{A\leftarrow} \quad \text{or} \quad E_1^A = E_0^A + W_{10}^{A\rightarrow} \tag{4}$$

where $W_{01}^{A\leftarrow}$ or $W_{10}^{A\rightarrow}$ is the work in any weight process for A either from A_0 to A_1 or from A_1 to A_0.
Rigorous proofs of these consequences can be found in Refs. [7, 10], and will not be repeated here.

References

[1] R. Feynmann, *Lectures on Physics*, Vol. 1, Addison-Welsey, 1963.
[2] L. Tisza, *Generalized Thermodynamics*, MIT Press, 1966, p. 16.
[3] G.N. Hatsopoulos and J.H. Keenan, *Principles of General Thermodynamics*, Wiley, 1965, p. xxiii.
[4] L.D. Landau and E.M. Lifshitz, *Statistical Physics*, Part I, 3rd Ed., Revised by E.M. Lifshitz and L.P. Pitaevskii, Translated by J.B. Sykes and M.J.Kearsley, Pergamon Press, 1980, p. 45.
[5] E.A. Guggenheim, *Thermodynamics*, North-Holland, 7th Ed., 1967, p. 10.
[6] J.H. Keenan, *Thermodynamics*, Wiley, 1941, p. 6.
[7] E.P. Gyftopoulos and G.P. Beretta, *Thermodynamics. Foundations and Applications*, Dover, Mineola, 2005 (first edition, Macmillan, 1991).
[8] G.P. Beretta and E.P. Gyftopoulos, Teaching energy and entropy before temperature and heat, in *Proceedings of the 1991 Taormina Conference on Thermodynamics*, Accademia Peloritana dei Pericolanti, Messina, Vol. LXX-1, pp. 331-340 (1992); G.P. Beretta and E.P. Gyftopoulos, A novel sequence of exposition of engineering thermodynamics, in *Thermodynamics and the Design, Analysis, and Improvement of Energy Systems*, ASME Book AES-Vol. 30, HTD-Vol. 266, pp. 209-219 (1993).
[9] E. Fermi, *Thermodynamics*, Prentice-Hall, 1937.
[10] E. Zanchini, Thermodynamics: Energy of nonsimple systems and second postulate, *Il Nuovo Cimento B* **107 A**, pp. 123–139 (1992); E. Zanchini, On the definition of extensive property energy by the first postulate of thermodynamics, *Foundations of Physics* **16**, pp. 923–935 (1986).